

Porous Network Concrete

**a bio-inspired building component to make
concrete structures self-healing**

Porous Network Concrete

a bio-inspired building component to make concrete structures self-healing

Proefschrift

ter verkrijging van de graad van doctor
aan de Technische Universiteit Delft,
op gezag van de Rector Magnificus Prof. ir. K.C.A.M. Luyben,
voorzitter van het College voor Promoties,
in het openbaar te verdedigen op 2 Maart 2015 om 10.00 uur

door

Senot SANGADJI

Magister Teknik in Civil Engineering,
Institut Teknologi Bandung, Indonesië
geboren te Banyuwangi, Indonesië

Dit proefschrift is goedgekeurd door de promotor:
Prof. dr. ir. E. Schlangen

Samenstelling promotiecommissie:

Rector Magnificus,	Technische Universiteit Delft, voorzitter
Prof. dr. ir. E. Schlangen,	Technische Universiteit Delft, promotor
Prof. dr. ir. K. van Breugel,	Technische Universiteit Delft
Dr. H. Jonkers,	Technische Universiteit Delft
Prof. dr. ir. S. van der Zwaag,	Technische Universiteit Delft
Prof. dr. ir. N. De Belie,	Universiteit Gent
Prof. Dr. R.J. Lark,	Cardiff University
Prof. S. A. Kristiawan ST, MSc, PhD	Universitas Sebelas Maret, Indonesia

Prof.dr. R.B. Polder, Technische Universiteit Delft, Reservelid

ISBN: 978-94-6186-439-0

Keywords: Concrete, Porous Concrete, Porous Network Concrete, Self-healing concrete, Biomimetic, Bio-inspired engineering, Closed-loop feedback, Autonomous healing mechanism, Autogeneous healing mechanism.

Copyright © 2015 by Senot Sangadji
Email: senot.sangadji@gmail.com

All rights reserved. This copy of the thesis has been supplied on condition that anyone who consults it is understood to recognize that its copyright rests with its author and that no quotation from the thesis and no information derived from it may be published without the author's prior consent.

Cover page designed by Stevie Heru Prabowo
Printed by Haveka B.V. in the Netherlands

*To my beloved late mother,
To 'Diajeng Pingku', for the constant love,
To 'Quanta', the reason I did this.*

Acknowledgements

The multidisciplinary nature of this sort of project turns an individual into a team player. You collect ideas, thoughts and information voraciously, formulate your own and ask feedback and after a bit you can no longer remember you might did particular act of intellectual larceny. Fortunately the team of scholars and technicians that I work with are astonishingly generous with their time, ideas and energy. Quite often they even asked me to be the ‘team manager’ as well.

Prof. Erik Schlangen, the idea generator, supervisor, promotor and benefactor, is the one who is responsible introducing me to the exciting ‘playing field’ of self-healing concrete at Microlab. Erik, you taught me many necessary knowledge and skills. You helped me through difficult searching in the first year until one serendipitous ‘A-ha’ moment made me comfortable to ‘play’ in the field on my own. As you have given me (almost) total freedom, you’re very patient to my constant annoyance. Most of all, thanks for believing that I can do it. Dank je wel, Erik!

Dr. Henk Jonkers played his role not only mentoring me but in rekindling my ‘love’ to (micro)biology. You always have time for discussing and answering every question I asked. Thanks for pushing me to be a better scientist. Bedankt, Henk! Dr. Virginie Wiktor was, is and always my greatest collaborator and mentor. Virginie, when you designed your remarkable ‘solution’, you allowed me to be among the first few users. And together we found the ‘nice things’ under the microscope. I will always remember our excitement when, ‘...it works!’ This thesis could not find its shape without your help. Merci beaucoup, Virginie!

Ger, Kees and Arjan are the ‘pro player in the team’ to whom I extremely grateful. When I was tinkering ‘the mechanics and electronics’ in my design, Ger and Kees were always ready with good idea to execute and made a ‘goal’. Arjan skilfully helped me to ‘see’ what is ‘inside’ my concrete.

In doing the PhD project, I have benefited the generosity particularly from three institutions; Materials and Environment Section, CiTG, TU Delft, Directorate General of Higher Education, Ministry of Education, Indonesia and Civil Engineering Department, Faculty of Engineering, UNS, Indonesia. To Prof. Klaas van Breugel, the head of M&E section, I would like to thank for giving me the chance to tackle this job. To all colleagues at JTS FT UNS, I would like to thank for your kind supports.

I am very grateful to all members of my doctoral committee for thoroughly reviewing the draft of my thesis. Their suggestions and comments have helped me improve this work greatly. Special thanks to ‘Pak Iwan’ for also being my good fellow.

Without a single doubt, the group of people at Microlab, have contributed to my academic and personal development. To Oguzhan, big thanks for the wonderful CMC and many valuable discussions which help me sharpen my mind. To Guang Ye, thanks for the short but very good course. To the secretaries: Claudia, thanks for

showing me the beautiful side of humanity; Nynke, big thanks for the cheerful days, and Iris, thanks for the trolley. To the member of bioteam; Lupita, Renee (thanks for doing the translation), Damian, Eirini, Balqis, thanks for all discussion, debate, and the wonderful lunch. To Rob, Dessi, Jeannete, John, Natalie, Jiayi, Zhipei, Hua, Peng, Xuliang, Hao, Josepha, Tianshi, Mladena, Ma Xu, Marija, Xiaowei, Jose, Zichao, Farhad, Lourdes, Rene, Bei, Zhengxian, Zhuqing, Yong, Yun, Yibing, Jure. Thanks to all of you for your contributions directly in some of the work of this thesis or indirectly by making my time in the Microlab so enjoyable. Caner and Branko, you have helped me a lot, thanks! In the past, Ayda Agar, Zhao Jie, Wang Ying, Haoliang, Zhiwei Qian, Quantao Liu, Yuwei Ma, has helped me a lot during my years in the lab. To Alvaro, *what a wonderful coincidence.., thanks for showing me the way!* Thanks to Agus Susanto, '*kawan seperjuangan*', for the nice moments we can talk in our mother tongue and sharing frustration of living so far from home. You all have made Microlab, probably, the best place to learn and 'play'. To Dr. Ayke, those flash exchanges were so remarkable.

In the personal side of my life, I would like to thanks to the friends turn-to-brother and -sister; Julian, Andre, Thomas, Yuli. It has been my pleasure to know you and to learn the bright side of life from you. '*Afbalen zonder betalen*' is an amazing concept. To Stevie, friend and amazing designer, thanks for making my ideas manifested in the beautiful illustration and animation. To the Indonesian community in the Netherlands; Cisca, Tya, Sandra, Iyus, Alma, Dwi, Xander, Piet, Awi, Sayuta, Caesar, Asti, Gladys (in many good times), Sinar, Iwa, Sam and Lukas, Pia, Eka, Enny and Juan, thanks for being the comforter when we miss the place we call home. Super special thanks to Mbak Ida, Bang Jun, Jihan and Falah, who guided us on the very first day and over many years. Fossy, Rizal and the *kerucik*, thanks for many good times together. To Yazdi, Budi, Dieky, Adhi, Isnaeni, Ajeng and their families, Bu Lasmini, Mbak Ochi, Mas Agung, Mas Andri, Fiona, Ronald Halim, Sonny, Yudha, Karina, Ernestasia and many more friends member of PPI, thank you for letting me learn a lot of good things in life from you. To ISC, the home away from home community; Fr. Avin, Rev. Waltraut, Ruben, Oom Henk, choir members, thanks for many nice things and for letting me play the 'jembe'. To Marco Poot, thank you for always be there when I need help to better understand this beautiful country.

It is hard to express my gratitude to the Pirngadi and Prayogo family, since words can never be enough. Though we started from a humble beginning, your never ending support is what makes me able to reach this point. Thanks for Ibu, Mas, Mbakyu, Keponakan, for the support and prayers. Rm. Sad Budi, thank you! I can never tell where your influence to me stops.

And last but absolutely not least, to my loving wife and my boy. Pungky, thanks for being here with me. This join force of doing PhD together would have been a very tough journey without your constant inspiration and perseverance,... and for sure the delicious *sambel tempe penyot* you cook. Quanta, thanks for being presence in our life, for posing many hard questions, and for exploring and experimenting together with 'snow, gravity, fracture mechanics, games, robotics, and music'. I do hope Diajeng and Adji will think of this book as a gift from me (only a small gift I suppose...) in return for the gift of being present every single day in my life for many years.

Summary

The high energy consumption, its corresponding emission of CO₂ and financial losses due to premature failure are the pressing sustainability issues which must be tackled by the concrete infrastructure industry. Enhancement of concrete materials and durability of structures (designing new infrastructures for longer service life) is one solution to overcome the dilemma.

Concrete is a quasi-brittle material with properties that are high in compression but weak in tension, therefore concrete is prone to cracking. In the case that a continuous network of cracks is formed, the permeability of concrete will increase and the reinforcement bars may be open to the ambient atmosphere. This opening provides easy means for aggressive substances to enter into concrete and reach rebars which may start to corrode. Further cracks may threaten the tightness of the retaining structures, e.g. liquid containing structures tank wall, aqueducts, underground spaces, tunnels, etc., which undergo tensile forces. In these cases cracks may facilitate the flow of fluid – liquid or gas – into and out of the structures which considerably alters its serviceability, leads to unhealthy environments within a structure, and diminishes its *functionality*. In case the container or reservoir contains waste, highly toxic materials or radioactive materials, leakage through the concrete is catastrophic and unacceptable.

One promising concept *to design new concrete structures to achieve higher durability* is incorporating self-healing mechanisms that are found in nature into the cement-based materials or the concrete structural element. If unavoidable cracks due to inherent brittleness in concrete could be self-sealed/healed/repared, concrete will certainly serve longer and be more durable and sustainable.

In general, on attempting to solve engineering problems, one can (always) seek inspiration from biology (nature). Though, borrowing nature's idea to enhance our living environment is as old as humankind, the post-industrial technical advent makes the process more systematic and deliberate, hence makes use of *bio-mimicry* to solve problems and inspire innovation.

Observing the domain of biology, there are several wound healing mechanisms found in nature: cut skin and bone fracture healing in human and animal, and plant response to injury. The present work takes inspiration from studies on bones of present-day mammals and birds and its healing mechanism. Two of appropriate principles that might be constructive are identified; (1) *bone morphology* comprises of cortical (solid) bone and trabecular (spongy) bone and (2) a *feedback loop process* is present in the remodelling and healing process.

These two principles formed the basis for the development of a healable concrete material and for a method for healing it with healing agents. The idea behind this is that cortical bone may be mimicked with solid concrete and trabecular bone may be imitated by porous concrete. The combination of the two types of concrete resembles *Porous Network Concrete*, a bone-like concrete able to self-heal by the mechanism of feedback loop. These are the points addressed in the chapter 1 which

explores the success story of concrete in serving society and civilization for millennia, the present challenge to make modern concrete more durable, and the bio-inspired solution of self-healing concrete

Porous Network Concrete (PNC) is a hybrid system in which high permeability porous concrete is embedded in the interior or exterior of normal dense concrete. The porous network core constitutes alternate means for [1] channelling temporary or permanent materials to form a dense layer in the later stage and [2] distributing healing agent from the point of injection to cracks in the concrete main body. In chapter 2 the concept of the PNC is elaborated by setting up criteria and realized by creating a fabrication procedure. The production process – *the making of the PNC* – follows the current standard for both of the main and porous part and seemingly there is no complicated fabrication procedure. PNC characterization was carried out to study its pore and mechanical properties.

The *autonomous* healing mechanism in the PNC is designed by incorporating the feedback mechanism; once a certain crack width is sensed, an action to heal takes place. As a proof-of-concept, in chapter 3, a simple and intuitive approach to design a feedback system for PNC self-healing mechanism has been carried out. When a concrete structure receives loads and builds up internal stress, it deflects, cracks and deforms. Once the crack mouth opening reaches a certain prescribed value the healing agent is injected automatically. The proposed working principle is verified by mechanical and leakage (permeability, infiltration) testing.

The solidification process of the self-healing agent is important and even critical for the success of the healing strategy and mechanism designed. Instead of developing new healing agent and investigating its behaviour, this present study aims to examine the effectiveness and efficiency of the healing process in the Porous Network Concrete with different classes of agents. Three groups of healing agents are then studied and its healing efficiency is tested by leakage and mechanical testing.

The *first* type of agent is a single- and double-component chemical based which mostly works through poly-condensation or cross-link polymerization upon contact with the atmosphere, with the concrete matrix or within the reactants. In this case, epoxy resin is used. The *second* healing agent used is grout material made of a cementitious powder mix. Cementitious grout material can be thought of as healing agent for concrete structures since it functions as crack sealant and void filler with the objective to restore structural integrity. The use and healing performance of PNC by both healing agents is discussed in chapter 4.

The third agent is bacteria-based repair solution. It contains alkaliphilic bacteria able to facilitate bio-mineralization, nutrients and transport solution. It was originally developed as a bio-based repair material for cracked concrete. This is discussed in the dedicated chapter 5.

It has been demonstrated in this thesis that the Porous Network Concrete has a good prospect in making concrete structural elements self-healing. This is the concluding point presented in the final chapter. Some recommendations for improving the work are presented such as; modelling work, larger and realistic experimental campaign and improved damage sensing.

Table of content

Acknowledgement	i
Summary	iii
Table of content	v
List of figure	ix
List of table	xiii
Chapter 1. Concrete: its success, issues, and bio-inspired solution	1
1.1. The success of concrete	1
1.2. What are the issues at stake	3
1.2.1. Sustainability issue; environment under pressure	3
1.2.2. Concrete cracks; challenge to durability, functionality, and cost of repair	4
1.2.3. Durable, therefore, sustainable concrete materials and structures; resolving complex problem	5
1.3. Bio-inspired engineering	7
1.3.1. Brief story and modern design process and strategy	7
1.3.2. Brief study of bone physiology and its healing principles	11
1.4. Self-healing materials; synthetic approach to healing	15
1.5. Self-healing concrete; concepts and strategies	16
1.5.1. Evolution of concepts and definitions	16
1.5.2. Strategies and state of the art 1; autogeneous healing	17
1.5.3. Strategies and state of the art 2; autonomous healing	19
1.5.4. Strategies and state of the art 3; self-healing by means of microbes	20
1.6. Remaining challenges; ideas development	20
1.6.1. Problem and goal definition	21
1.6.2. Biological domain and abstraction of biological model	22
1.6.3. Idea development	23
1.7. Scheme of this thesis	24
Chapter 2. Porous Network Concrete: design, production and characterization	27
2.1. Introduction; motivation, ideas and goals	27
2.2. Materials; combination of two concrete, <i>normal (dense) concrete</i> and <i>porous concrete</i>	29
2.2.1. Mix design and characterization of self-compacting concrete	32
2.2.2. Mix design of porous concrete	35
2.2.3. Characterization of porous concrete	38
2.3. Porous Network Concrete	45
2.3.1. Mix design and production of Porous Network Concrete	45
2.3.2. Characterization of Porous Network Concrete	51
2.4. Findings: PNC	55

Chapter 3. Development of automatic healing system and test method	57
3.1. Manual repairing vs. Engineered healing	58
3.2. Automatic repair system	59
3.3. Mechanical test	61
3.3.1. Tension test for cylinder specimen	61
3.3.2. Three-point bending test for prism specimen	62
3.4. Evaluation of the feedback mechanism efficacy	64
3.5. Evaluation of healing efficiency	65
3.5.1. Mechanical properties regain by reloading	68
3.5.2. Permeability or leakage test	69
3.5.3. Visual confirmation; light and electron microscopy	71
3.6. Concluding remarks	71
Chapter 4. Crack healing by means of chemical and cementitious grouting	73
4.1. Introduction; the choice of healing agents	74
4.2. Materials	75
4.2.1. Three types of healing agent	76
4.2.2. Specimen type	77
4.3. Test 1; Porous Network Concrete cylinder with epoxy resin	78
4.3.1. Manual healing of the PNC cylinder	78
4.3.2. Autonomous healing of the PNC cylinder	81
4.4. Test 2; Prism with epoxy resin injection	84
4.4.1. Manual injection healing	85
4.4.2. Autonomous healing	90
4.5. Test 3; PNC prism cementitious grout injection	94
4.6. Evaluation of crack repair	98
Chapter 5. Porous Network Concrete healing by means of bacteria based repair solution	101
5.1. Introduction; working principle of bacteria based self-healing concrete and the success story	103
5.1.1. Urea hydrolysis	103
5.1.2. Metabolic conversion of nutrient	104
5.1.3. Bacteria based repair solution	107
5.2. Test 1: Feasibility of the bacteria-based repair solution for the PNC	111
5.2.1. Materials; the PNC and solution preparation	111
5.2.2. Testing cycle	115
5.2.3. Results of injection bacteria-based solution to the PNC	115
5.3. Test 2: Optimization of the solution by injecting it into porous core	116
5.3.1. Rationalization and approach to experiment	117
5.3.2. Material and specimen preparation	118
5.3.3. Methods and evaluation techniques	119
5.3.4. Results and discussion	122
5.3.5. Findings	131
5.4. Test 3: Healing efficiency of the PNC prism	132
5.4.1. Experimental program	132
5.4.2. Materials	132
5.4.3. Optimum solution	132
5.4.4. Testing methods	133
5.4.5. Results and discussion	134
5.4.6. Findings	140

5.5.	Conclusion of healing efficiency of the PNC primers by means of bacteria	140
Chapter 6. Conclusions and outlook		145
6.1.	Fundamental approach	145
6.2.	Design and Performance of Porous Network Concrete	146
6.2.1.	Porous Network Concrete	146
6.2.2.	Healing efficiency upon different healing agent	147
6.3.	What we need to improve: outlook	149
Appendix 1. Development of automatic on-off control system		141
References		157
Samenvatting		167
Ringkasan		169
About the author		171

List of figure

1.1.	Pont du Gard and Pantheon Dome.	2
1.2.	Cracks in concrete structures lead into unacceptable leakage and costly repair	5
1.3.	Conceptual diagram of infrastructure performance over its service life	7
1.4.	Sketches of Culmann's crane with stress trajectories in the left part and trabecular architecture of long femur [42].	8
1.5.	Diagram of inverse design approach	9
1.6.	Coined as forward design process by Jenkins, the diagram shows that 'engineering question' is the starting point in the design process	10
1.7.	DesignLens g.10 is a design spiral proposed by The Biomimicry 3.8 Institute (www.biomimicry.net) which includes design evaluation process by means of life's principle	11
1.8.	Hierarchical level of bone (<i>redrawn from</i> [68, 69, 71]).	12
1.9.	Section of bone showing cortical (solid) bone comprises of concentric lamellae called osteon at the exterior of the long femur and trabecular bone in the interior region showing interconnected struts that make up porous layer. (<i>Captured from www.bonebiology.amgen.com; accessed 15 January 2014; all rights reserved</i> [71]).	13
1.10.	Simplified feedback loop mechanism of biomechanical and mechanotransduction regulation of bone remodelling.	14
1.11.	Fracture healing cascade overlapping process (adapted from [80]).	15
1.12.	[A]Self-healing classification proposed by TC-075B JCI depicted in Venn diagram. [B] Interpretation by Mihashi and Nishiwaki [90] to the definition of self-healing materials proposed by RILEM TC-221 SHC (adapted from [80, 90]).	17
1.13.	Classification of most possible causes of autogenic self-healing mechanism of concrete.	18
1.14.	Ideas transformation of Porous Network Concrete following forward design approach by selecting bone as biological model of healing process [62, 142].	22
1.15.	Flow of information in Porous Network Concrete.	23
1.16.	Several possible application of the proposed system.	24
1.17.	Roadmap of research and development of Porous Network Concrete.	24
2.1.	Artists render of the conceptual working principle of healing agent transport in the Porous Network Concrete.	28
2.2.	Cross section of porous concrete.	32
2.3.	Diagram of mixing steps used in producing concrete batches	34
2.4.	Strength (N/mm ²) and slump flow (mm) of self-compacting concrete designed for main body of Porous Network Concrete	35
2.5.	Three porous concrete prisms 40 × 40 × 160 mm were made with different aggregate size, from left to right; 4-8 mm, 2-4 mm, and 1-2 mm.	36
2.6.	(i) Three porous concrete cylinders Ø56 – 120 were enveloped with plastic membrane for measuring volumetric porosity, (ii) specimen was weighed on a scale.	40
2.7.	(a) An cross sectional image of epoxy impregnated porous concrete cylinders, (b) Image segmentation, (c) Binary image on which the pore fraction was calculated.	41
2.8.	(a) Working principle of X-ray micro computed tomographic (CT) scan, (b) Image segmentation process, (c) 3D reconstruction image is colour-coded on which void fraction may be distinguished and calculated. Frames (a) and (b) are taken from Landis and Keane [52].	41
2.9.	Series of images of individual porous concrete pore structure taken with micro CT-scan.	43
2.10.	Setup of falling head permeability (hydraulic conductivity) test	43
2.11.	Artist render of Porous Network Concrete specimen.	46

2.12.	Porous Network Concrete prism specimen with prism porous core in the centre utilized for 3-point bending test.	47
2.13.	(a) shows the porous core cylinder after the PVC mould was cut open longitudinally at 3 days and figure (b) exhibits the PVA film covered porous core ready to be placed in the mould for PNC production.	47
2.14.	Production and preparation of the Porous Network Concrete cylinder.	48
2.15.	Cross section of the PNC specimen	50
2.16.	Production of PNC prism	50
2.17.	PNC prisms specimen	51
2.18.	PNC cylinder specimen failure mode under compression	52
2.19.	3D image reconstruction of PNC	52
2.20.	Series of images showing the centre of PNC using different aggregate size	53
3.1.	Method of injecting materials to repair cracks in concrete. Image (1) and (2) were adapted from FHWA report [201].	59
3.2.	Block diagram showing a rudimentary feedback with its elemental components.	59
3.3.	Conceptual block diagram of feedback mechanism implemented in the self-healing of Porous Network Concrete.	60
3.4.	The rendering of the Porous Network Concrete cylinder $\varnothing 56-120$ mm specimen used for tension test	61
3.5.	The tension test setup for cylinder PNC specimen with the hanger	62
3.6.	The rendering of the Porous Network Concrete prisms	63
3.7.	Rendering of the basic setup of three-point bending tests (TPBT) where a Porous Network Concrete (PNC) is loaded in the mid-span	64
3.8.	The tension test with the autonomous healing mechanism by means of on-off control	65
3.9.	Graph of the load versus crack width of the tension test of cylinder specimen and the signals of automatic healing system	66
3.10.	The close up cylindrical PNC specimen reveals the healing agent flow from inside-out through the crack opening	67
3.11.	The expected load versus crack width graph of virgin and healed specimen and determination of strength and stiffness for self-healing efficiency	68
3.12.	Basic setup of leakage (permeability/infiltration) test	69
4.1.	Crack opening width matched with the injection materials classes correspond to the void portion unable to fill	76
4.2.	The cylinder PNC after crack formation	79
4.3.	The load versus displacement of Cylinder specimen injected manually with epoxy resin	79
4.4.	(1) The crack formation in the notch, (2) the new crack formation after the first was healed, and (3) the new crack face	80
4.5.	Longitudinal section of the cylinder portrayed under UV light showing the crack path filled with epoxy	81
4.6.	Setup of autonomous healing of the PNC	82
4.7.	The composites graphs of load versus CMOD and signal of actuator of specimen injected automatically with epoxy resin	83
4.8.	The PNC cylinder healed autonomously with epoxy resin	84
4.9.	A water leakage (permeability) test for the PNC test	85
4.10.	Three-point-bending test setup for (1) plain concrete, (2) reinforced concrete, and (3) Porous Network Concrete	86
4.11.	Load versus displacement curve of plain prism	86
4.12.	Injection of the epoxy resin into the porous concrete	87
4.13.	Load versus displacement curve of RC prism healed by direct injection into the crack face	88
4.14.	Load versus displacement curve of PNC prism healed by manual injection through porous core	88
4.15.	Permeability curve representing the weight of water discharged as function of time for initial condition, pre- and post-healing for the PNC with manual injection	89
4.16.	The cross and longitudinal section of the healed PNC specimen showing the filling of the porous core and the crack	90

4.17.	Test setup of the autonomous healing of PNC prism	91
4.18.	The load versus crack mouth opening displacement of PNC healed with epoxy resin autonomous injection	92
4.19.	The Porous Network Concrete specimen; (1) right after injection where epoxy resin flew out and wetted the crack surface, and (2) after several hours of polymerization has formed portrayed under UV light	93
4.20.	The Porous Network Concrete specimen; (1) right after failure where the second crack formed in the weaker plane, and (2) formation of the healed crack and the flexural failure portrayed under UV light	93
4.21.	Permeability curve representing the weight of water discharged as function of time for initial condition, pre- and post-healing for the PNC with autonomous healing mechanism	94
4.22.	The clogging of the cement grout close to the port of injection	96
4.23.	The 2-4 mm aggregate size porous core was replaced with the porous core that has aggregate size of 4-8 mm	96
4.24.	Permeability curve representing the weight of water discharged as function of time for initial condition, pre- and post-healing for the PNC with manual injection of cement grout	97
4.25.	Load versus displacement curve of PNC prism healed by manual injection of cement grout	98
4.26.	Longitudinal section of the PNC injected with cement grout	98
5.1.	Working mechanism of bio-based concrete healing developed at Microlab, Faculty of Civil Engineering and Geosciences	105
5.2.	The principle and components of the bacteria-based repair system	108
5.3.	Observation under ESEM of specimens treated with Na-gluconate NaS + bacteria. The figure is of courtesy of Wiktor and Jonkers [147].	109
5.4.	Roadmap of the test campaign implementing bacteria based repair system as self-healing agent in the Porous Network Concrete	111
5.5.	Testing procedure 1-2-3	113
5.6.	Testing procedure 4-5	113
5.7.	Three-point bending test was performed to introduce the crack into the PNC specimen	114
5.8.	Testing procedure 6-7	114
5.9.	Graph of leakage (permeability) test of the prism over time and the histogram representing the healing efficiency	115
5.10.	Load versus crack opening displacement graph of three-point bending test of the prisms injected by bacteria-based solution	116
5.11.	Experimental approach in optimizing the healing capacity of the bacteria-based solution	117
5.12.	Specimen prepared by covering porous concrete core with plastic film and adhesive tape	118
5.13.	Experimental test cycle showing six steps from preparation of specimen up to the eventual polished section for ESEM observation	119
5.14.	Setup of Injection test and permeability test	120
5.15.	A) Surface of polished section marked with points where in-depth ESEM observation will be spotted. (B) The image taken at the top surface of the specimen point 1	121
5.16.	Histogram of permeability value in the porous cores before and after healing with bacteria-based solution	122
5.17.	Images of pre- and post-injection specimen were taken by x-ray micro CT scan showing the newly formed materials suspected as Ca-based mineral	124
5.18.	histogram of volume of new material in the porous core after injection of bacteria-based solution as calculated from x-ray micro CT scan 3D tomographic model	125
5.19.	ESEM pictures of polished sections of Control series at top surface of the specimen, at surface of the aggregate and pore, 14, and 28 days	126
5.20.	ESEM pictures of polished sections of series A at 7, 14, 21, and 28 days. De-bonding of epoxy-matrix is obviously seen and small crystals is observed in the specimen at 21 days where elemental mapping confirms the Ca-based mineral	127
5.21.	ESEM pictures of polished sections of series B showing globular Ca-based mineral	128

5.22.	FT-IR spectra of the precipitates showing indication of Ca-carbonate peaks among Ca-lactate	128
5.23.	Bacteria imprints in the globule Ca-based mineral of series B indicating that bacteria were active, metabolically converted nutrients, produced layers of mineral and entombed it selves	128
5.24.	ESEM pictures of polished sections of series A in comparisons to series C where more obvious cavity appear in the specimen series 'C'	129
5.25.	Massive bacteria imprints have been found in different spot in the series C indicating high activity due to the layering of solution in the system	130
5.26.	Layer of crystal observed in the surface of void of porous concrete core in series D	131
5.27.	Testing procedure; [1] initial permeability test, [2] crack formation by three-point bending test, and [3] pre-healing permeability test of cracked specimen	134
5.28.	Injection of bacteria based repair solution; [1] specimens are prepared and [2] solution leaks out from crack opening	134
5.29.	Graphic of output flow weight (water permeability) over time for control specimen	135
5.30.	Bottom surface flexural crack of the control PNC specimen	136
5.31.	Graphic of output flow weight (water permeability) over time for specimen treated by bacteria-based solution injection	136
5.32.	Bottom surface flexural crack of the PNC specimen injected with bacteria-based solution (1) at day 1 and (2) after dry cured for 28 days	137
5.33.	Graphic load versus crack mouth opening displacement (CMOD, μm) after three-point bending test	138
5.34.	Histogram of the bacteria-based healing efficiency test in the PNC prism	139
5.35.	ESEM images of the crack reopened	139
5.36.	Diagram of the crack sealing performance over time by means of bacteria based repair solution into Porous Network Concrete	142
A.1.	Custom built on top of aluminium plate, the automatic injector is used to pump healing agent through porous core in the PNC	151
A.2.	The box' is used to regulate the actuator by sending voltage signal	152
A.3.	Block diagram showing the flow of electronic signal in the system	155
A.4.	Block diagram showing the communication between data acquisition (DAQ) system and measurement software	154
A.5.	Representation of on-off controller input-output feature	155
A.6.	State machine diagram represents the logic allowing the script to generate event-driven action	155

List of table

1.18.	Typical permeability regimes, intrinsic permeability and hydraulic conductivity values of geologic (natural) materials. Table has been modified from Bear [150].	29
1.19.	Physical property of cement and fly ash.	33
1.20.	Composition of concrete mixture	34
1.21.	Design experiment for porous concrete	36
1.22.	Composition of porous concrete mixture	36
1.23.	Mechanical and transport properties of porous (pervious) concrete; compressive strength (N/mm ²), porosity (%) measured by water displacement and image analysis, and hydraulic conductivity (cm/sec).	45
1.24.	Design experiment for Porous Network Concrete (PNC)	49
1.25.	a. Mechanical and transport properties of Porous Network Concrete without PVA film; compressive strength capacity (N/mm ²), porosity (%) measured by 3D image analysis, and hydraulic conductivity (cm/sec).	54
	b. Mechanical and transport properties of Porous Network Concrete with PVA film covering the porous core.	54
1.26.	Mechanical and transport properties of Porous Network Concrete porous core having 2-4 mm aggregate and main body high strength SCC.	55
4.1.	Experimental program for assessing healing efficiency of PNC prism. Note; n.a = not available, TPBT = three-point bending test, T = temperature; RH = relative humidity.	85
4.2.	Recapitulation of the healing efficiency of Porous Network Concrete beam	99
5.1.	The composition of solution A where Na-silicate solution provides the alkaline environment (pH 10.5 after mixing with solution B) fit for the bacteria to grow.	112
5.2.	The composition of solution B where Ca-lactate is provided to feed bacteria and bring a calcium source to the system. The pH of this solution is neutral.	113
5.3.	Experimental matrix for assessing and optimizing the bacteria-based repair solution	117
5.4.	Matrix of experimental program of healing efficiency of the PNC prism	132
5.5.	Recapitulation of the PNC prisms healing efficiency test result	138

1.

Concrete: its success, issues, and bio-inspired solution

'...And of all the remarkable properties of natural materials, one is truly exceptional – that of the ability for self-repair.'

- Mike Ashby

The chapter starts by exploring why concrete is such a successful engineering material. This triumph, however, is not without dilemmatic issues of current unsustainable practice in meeting the need of infrastructures development for the society advancement. The challenge for engineers, then, is to develop sustainable concrete by making it more durable. One particular solution posited is to bio-mimic nature and make concrete materials and structures self-healing achieving longer service life. Surveying the state of the art of self-healing concrete and adopting the problem-driven bio-inspired engineering design methodology, the chapter studies bone – its multi-scale structures and healing processes –, which then inspires the novel design concepts of porous network concrete.

1.1. The success of concrete

Concrete has been achieving a historic success as construction materials and may be seen as either old or new materials. This cementitious material had served society where a mortar floor consisting of several layers of CaCO_3 dated back nine millennia ago was discovered in Yiftah El by archaeologists in 1985 [1-3]. About 300 B.C. concrete had been utilized intensively in the ancient Egyptian civilization where later on it was adopted by the Greeks and then the Romans. The previous mere hydrated lime fabricated by burning limestone and slaking thereafter was improved by mixing it with volcanic ash (called Pozzolana as it was found near Pozzuoli at Naples) by the Romans. Vitruvius (13 B.C) observed the material hardened in air and when it is mixed with water leading to the load bearing solid concrete [1, 4]. Romans then recognised compaction as an important factor to create dense durable material. During the period between 300 B.C and 200 A.D. this material had already been used in constructing many large scale structures such as theatres, sewers and aqueducts, for instance Pont du Gard in the south of France [5-7], see figure 1.1. A lightweight concrete material incorporated by pumice aggregate obtained from porous volcanic rock had been used in the making of Pantheon Dome in Rome [1]. Together with the knowledge that the material available works best under compression, the Roman engineers chose the right shape and proportioned the structure accordingly.

Therefore the unreinforced dome preserved under compression load and survives two thousand years.

These successful techniques were lost during the middle Ages which saw the declining of cementing material quality of inferior mortars hardened by carbonation of lime. The modern concrete was mainly started by the invention of patented Portland Cement by Joseph Aspdin leading to the economic up-scaling of cement production after industrial revolution [4]. Cement plants with capacity of 1 million tonnes annually are very common nowadays.



Figure 1.1. Pont du Gard and Pantheon Dome. Both of them have been surviving for two millennia proving engineering sustainability. The master builder design and built based on the knowledge that concrete is good in compression. Resisting solely compression, the dome needs no steel reinforcement which means no corrosion taken into account.

It is hard to imagine the progress of modern civilization without concrete serving as major engineering material. Concrete will continue to be of great and increasing importance for infrastructure development throughout the world. Concrete can be found above ground, in residential buildings, hospitals, public and commercial buildings, industrial plants, military installations, stadiums, storage facilities, and bridges etc., on the ground in roads, parking facilities, industrial floors, airport runways, etc., under the ground in foundation, drainage systems, sewers, tunnels, etc., and in water in rivers, canals, dams, harbour works and offshore structures.

One may mix cement, water, sand, gravel in a bucket, pour it in the mould and let it harden, and one gets concrete. The simplicity of the concrete making process helps the large acceptance of this material. Apparently, the reasons why concrete is so successful as construction material comes from the fact that, firstly, its principal components namely aggregate – coarse and fine –, Portland cement, and water, are available broadly in term of geography and inexpensive in production cost. These make concrete the most readily available material in the construction site. Secondly, these low cost components can be easily prepared and mixed with water to obtain flow-able and cast-able slurry in the dormant period. Afterwards, with the help of hydration reactions fresh concrete is transformed into hardened solid concrete with great variety of sizes and shapes giving the engineers a broad design space. Thirdly, this load bearing rock-like material has attractive engineering properties such as excellent water resistance makes it able to withstand water action with no rapid and serious deterioration. Concrete also has high corrosion resistance, therefore can protects less resistant metal embedded in it. In corrosion prone sites this protection

makes it requires less maintenance for reinforcement provided there is sufficient thickness of concrete cover. Concrete possesses high resistance to fire and cyclic loading making it even acceptable for infrastructure construction.

Concrete achieves its full performance in *reinforced concrete* which is designed to have steel bars acting in composite action to carry multiple load action, e.g. compression, tension, bending and torsion. In *prestressed concrete* a pre-compression is introduced using steel tendons to counteract larger tensile forces. Large amounts of concrete serves as reinforced or prestressed structural elements [8].

The success of concrete might also be justified by the claim that concrete is currently the most used man-made material. As the second largest volume material utilized by human – water is the first – concrete is virtually irreplaceable for innumerable large infrastructure developments from the point of view of economy and ecology [9, 10]. Data support the claim that the amount of concrete used for construction worldwide exceeds 12 billion tonnes annually, approximately 2 metric tonnes per person per year. In addition, one may imagine a clear area of 1 x 1 km on the ground and on top of it concrete is poured and casted until it reaches Tropopause, a boundary layer between troposphere and stratosphere, a kilo meter above Mt. Everest. This is the volume of concrete produced, reaching presently about 10 km³ per annum [11, 12]. For comparison, the amount of fired clay, timber, and steel used in construction represent, respectively about 2, 1.3, and 0.1 km³ [11].

1.2. What are the issues at stake

1.2.1. Sustainability issue; environment under pressure

When addressing the socio-economic activity, infrastructure is the vital backbone while its development encourages productivity and growth. Primarily in developing countries infrastructure expansion and investment is an important government expenditure to elevate economic development and influence income distribution despite the fact in the variation of the infrastructure performance [13]. On the other side, the construction, maintenance, refurbishment and demolition of these infrastructure requires huge amount of material and intense energy demand leading into high ecological impact. Further, there is a concern to the unsustainable interaction between built and natural environment globally.

For the concrete related production alone, significant environmental – thereby also societal – impact has been reported by several researchers and agencies. Portland cement, the primary hydraulic binder of concrete, is produced typically requiring 3 to 6 million Btu (3.2 to 6.3 GJ) of energy. 1.7 tonnes raw material per ton clinker is accompanied by emissions of mostly 1 ton of CO₂, primarily from calcination of limestone [14, 15]. This accounts 5% of global CO₂ emissions from cement industry as it ‘side effect’ [16, 17]. While cement consumption is growing at 2.5% annually, CO₂ emissions from the cement industry are expected to rise from 2.297 million tonnes in 2005 to 3.486 Mt by 2020 at current technological levels and efficiency rates [18].

Concrete which is mostly used in its own right and *Mortar* which is used to ‘glue’ together bricks in masonry-type structures are both chiefly important construction material. They heavily rely on hydraulic (Portland) cement binders to gain their

strength and durability even though only 10% to 12% of the mixture is dry cement. Concrete is mostly mixed of 65% to 80% fine and coarse aggregate, water about 15% to 20% and small portion of air (0.5% to 8%), while the combination of cement and water is called cement paste. Mortar differs from concrete because it has no coarse aggregate in the mixture. Typically 1 ton cement is required to make 3-4 m³ concrete of about 7 – 9 metric tonnes in weight [14].

From the extraction, production process, and distribution to its place for use, concrete (in proportion of 1:2:3 for general purpose) ‘embodies’ energy and carbon emission of about 0.95 MJ/kg and 0.35 kg C/kg, respectively. This embodied energy (energy required from raw material extraction up to the material ready to use) is much lower than for many other common construction materials [19]. However, due to high rate of consumption above mentioned, cement and concrete still demonstrates total high energy demand and carbon emissions. These facts imply that efficient use of cement, concrete, and mortars will certainly save the total energy and reduce environmental impact in the life time of the infrastructure.

1.2.2. Concrete cracks; challenge to durability, functionality, and cost of repair

Another challenge the concrete confronts is the fact that concrete is quasi-brittle material with properties strong in compression but weak in tension. This inherent brittleness leads into concrete cracks under tension or bending action. This is the reason of the instalment of steel reinforcement bar (rebar) which then creates the reinforced concrete composite action. In this case cracks may be attributed as innate aspect, since its formation may activate the reinforcement to carry the tensile stresses of the concrete structures. Within the prescribed crack width, the crack opening as such may not damage or fail the structure or hamper the overall safety, although it may expose the reinforcement bar to corrosive action.

Aside of the visible macrocracks, microcracks are practically inevitable to the normal concrete. In the event when continuous network of microcracks is formed, concrete permeability will increase and the reinforcement bar may be open to ambient atmosphere. This corresponds to the concrete’s vulnerability to ingress of aggressive substances. Technically speaking, concrete can succeed a 50 years – or even longer – of life time even though it encounters several degradation processes, e.g. chemical ingress, freeze-thaw cycle, carbonation, etc. However, the presence of cracks triggers more serious problems and limits the concrete capacity to be *durable*, e.g. premature failure or decrease of safety level due to reinforcement corrosion [20, 21].

In concrete structure designed cracks may be acceptable, but in many other cases are not desirable. Cracks may threaten the tightness of the retaining structures, e.g. liquid containing structures tank wall, aqueducts, underground spaces, tunnels, etc., which undergo tensile forces. In these cases cracks may facilitate the flow of fluid – liquid or gas – into and out of the structures which considerably alters its serviceability, leads to unhealthy environments within a structure, and diminishes its *functionality*. In case of waste, highly toxic materials and radioactive disposal container, the leakage through concrete is catastrophic and unacceptable.



Figure 1.2. Cracks in concrete structures lead into unacceptable leakage and costly repair.

The unexpected premature deterioration and fracture of concrete structures not only limit its service life, but also leads into another issue concerning huge inspection, maintenance and repair cost. Tougher issue emerges when the cracks are invisible and or inaccessible, such as in the underground waste container structures which may impractical to repair. To get a deeper view of this economic pressure, consider few examples. The total amount of money for repairing and upgrading 10% of the US bridges which are considered functionally obsolete and structurally deficient is estimated at \$ 140 billion. In the UK, 45% of its construction and building industry activity is related to the repair and maintenance. In the Netherlands, one third of the yearly budget for large civil engineering works must be spent on monitoring, maintenance, repair and upgrading. It is estimated that the indirect cost and loss of productivity of traffic congestion caused by bridge (and tunnel) maintenance interruption is ten times higher than the direct maintenance cost, which may reach \$ 63 billion per annum in the US [22].

1.2.3. Durable, therefore, sustainable concrete materials and structures; resolving complex problem

The high energy consumption, its corresponding emission of CO₂ and financial losses due to premature failure are the pressing sustainability issues which must be tackled by concrete infrastructures industry. However on the other hand, public demand for housing and infrastructures is high level of service and performance, high durability and minimum negative ecological impact. Today the building industry can no longer ignore these issues. Minimizing consumption of non-renewable resources and maximizing the life-span of infrastructure are among the sustainable actions that must be taken.

Many technological measures already happen to resolve the problem; additives, replacement materials, and Supplementary Cementitious Materials (SCM) were successfully applied to enhance durability of concrete end-products. Some industrial by-products: e.g. fly ash, blast furnace slag, and silica fume, used currently in blended cements are proven to improve concrete durability therefore its sustainability and environmental friendliness. These materials also improve concrete's mechanical properties. It is proven by many studies on the chemical and physical characteristics, reactivity of blended cements, and impact of SCMs on the concrete performance [23, 24].

For tomorrow's concrete, from a materials perspective, Flatt and co-workers [11] identify several alternative solutions as follows:

1. Partial cement (clinker) replacement by supplementary cementitious materials
2. Development of alternative binders
3. Broader use of concrete mix designs that limit cement content
4. Recycling of demolished concrete in new concretes
5. Enhancement of durability (designing new infrastructures for longer service life)
6. Rehabilitation of existing infrastructures (extending the service life of existing infrastructures)

Pointing to durability enhancement, as van Breugel [20] argues durable concrete increase infrastructure sustainability and in turn will positively affect biosphere stability, this work focuses more on *how to design new concrete structures to achieve higher durability*. One promising concept is incorporating self-healing mechanism found in nature into cement-based materials. If those unavoidable cracks due to its inherent brittleness could be self-sealed/healed/repared, concrete will certainly serve longer, more durable and sustainable.

Conceptually, the approach to make concrete structures – and structural (engineering) material in general – self-healing can be justified by studying both design strategy and philosophy. The prevailing concepts of making structures better is by making them stronger and stiffer. This can be achieved by making stronger and stiffer (structural/engineering) material or combination of materials. Within this philosophy, designers focus on preventing damage by increasing the strength of the material and therefore the load bearing capacity of the overall structures. This may adjourn the event when the first fracture develops. This philosophy is termed as *Damage Prevention* paradigm [25]. Development of high and ultra-high strength material is the result of this productive and useful design philosophy.

As the damage formation is unavoidable during structures service life, damage monitoring is needed. Sooner or later any damage discovered requires repair and expenditure. A novel paradigm of managing or controlling damage is proposed as an alternative philosophy. As van der Zwaag argues, a certain level of damage “*is not problematic as long as it is counteracted by a subsequent autonomous process of “removing” or “healing” the damage*” [25]. Klaas van Breugel adds, that this certain limit of damage in structures may be acceptable as a trigger for the inherent healing or repairing mechanism to start [26]. Borrowed from nature, this pro-active *Damage Management* paradigm philosophy is the basis of emerging self-healing materials technology.

Figure 1.3 shows conceptual diagram of performance of infrastructure and its cost over time. Once cracks formed, a degradation process starts until (expensive) repair raises the structure to its initial performance level. Applying damage prevention principle, longer service life of infrastructure can be achieved by using higher strength material, by which longer maintenance free period is achieved. As the initial investment is higher, however the total cost may be lower compare to ‘normal’ material which requires several repair actions for the same period of service. On the other side, by applying self-healing materials, damage is allowed and even triggers the *autogeneous* or *autonomous* self-healing mechanism. As there will be ‘no’ or very limited repair cost during service life the total cost may be competitive compared to normal and high strength material application.

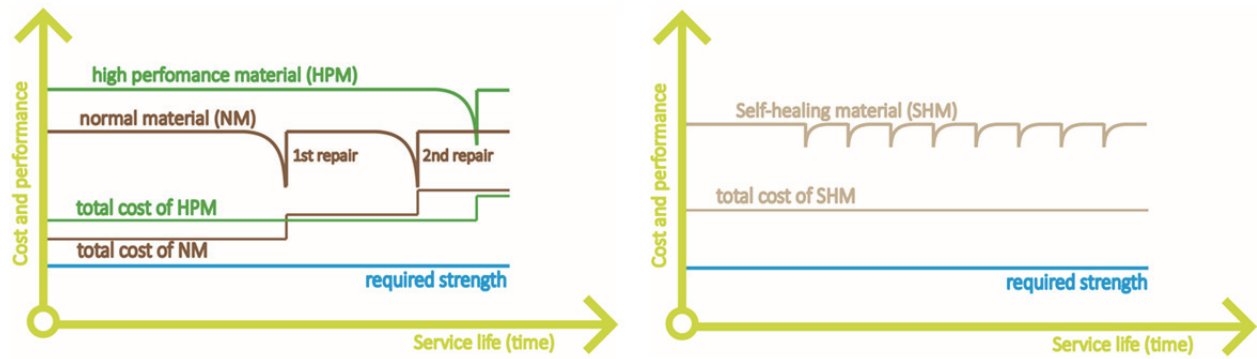


Figure 1.3. Conceptual diagram of infrastructure performance over its service life in which: [a] the application of damage prevention principle results in applying high performance material (HPM) instead of normal materials (NM) and [b] self-healing material (SHM) with replicable healing mechanism helps infrastructure to achieve longer maintenance free period and overall service life . (figure redrawn from van Breugel [20])

Therefore, technically speaking, in order to keep concrete infrastructure durable, it would be of benefit to implement self-healing, overcoming the inevitable concrete cracking. Moreover to function properly in preventing leakage, this *healing property will not only control the crack width but also self-sealing the crack making it impenetrable for fluid.*

1.3. Bio-inspired engineering

1.3.1. Brief story and modern design process and strategy

Steven Vogel points out human built mechanical devices and apparatus generally simulate what is found in nature, regardless the method of fabrication and material used [27]. Conceivably this applies in self-healing materials concepts. Self-healing of man-made material is inspired by nature [28, 29].

In general, on attempting to solve engineering problem, one can (always) seek inspiration from biology (nature). Though borrowing nature's idea to enhance our living environment is as old as humankind history, the post-industrial technical advent makes the process more systematic and deliberate. Hence, it makes use of *bio-mimicry* to solve problem and inspire innovation [30-36]. *Biomimetic*, the term coined by polymath Otto Schmitt in 1957, and *bionic*, coined by Jack Steele in 1960 [34, 35], attempts to take *inspiration, adaptation, derivation* and *abstraction* of a biological model¹, with cautionary advice that careful study of the nature's lessons may not lead to a blind 'close imitation' [37-39].

The history of scientist, engineer and inventor capturing inspiration from nature is long and rich with many inspiring successful examples. Architects and designers in the nineteenth century did biomimetic for aesthetical purpose, but other scientists and engineers recognized the ingenuity, efficiency and robust engineering of nature's materials and structures [40]. Nonetheless, those many successful applications were the fruit of serendipity and creative random thought. They were not the result of

¹ Janine Benyus – author and co-founder of then The Biomimicry 3.8 Institutes – defines *Biomimicry* as 'learning from and then emulating natural form, processes, and ecosystems to create more sustainable designs'. *Biomimetic* is portmanteau derived from the Greek word *bio-* and *-mimesis* which means imitation, while *bio-* and *-technics* is then combined into *bionics*. In general both words essentially, as Speck *et al.* articulates, is "the realization of technical applications based on insights resulting from fundamental biological research". Other essentially similar is Bio-inspired Design, Biologically Inspired Design, Bio-design, Bionik. This thesis accepts all the terms and use it without rigor precedent, merely to help reader grasp the essential idea.

deliberate systematic process as it is recently implemented such as Russia-born TRIZ (Theory of Inventive Problem Solving) and CAI (Computer Aided Innovation) [41].

The story of how George de Meestral invented Velcro is perhaps one of illustrious achievements of bio-inspired design. In 1940 after hunting with his dog in the mountains of Switzerland, de Meestral became curious about the burrs (burdock seeds) method of dispersal hitchhiked to his clothing and his dog's fur. Examined under microscope, he saw the tips of the burrs were shaped as hooks which easily stick to the fur of animal or clothes fabric. After laborious work in his workshop he eventually marketed 'Velcro' which becomes famous when NASA uses it as 'hook and loop' fastener for their astronauts space suits.

D'Arcy Thompson reveals the story how Zurich prominent engineer, Carl Culmann, while designing his new crane on 1866, gained inspiration from bone trabecular structure after wandering in the laboratory of anatomist Hermann von Meyer, who at the moment was studying cross section of femur [40]. Figure 1.4 shows the similarity between von Meyer's sketches of cancellous bone in a frontal cross section of proximal femur and the stress trajectories of the crane-like curved bar designed by Prof. Culmann [42].

Natural form, structure, and process have inspired many architects, scientists and engineers. Plants and trees inspired Antonio Gaudi in designing Sagrada Familia Church. Hierarchical nano-structure of Lotus leaf surface inspired innovation of super hydrophobic self-cleaning coatings [43]. Photosynthesis has inspired design of a dye-sensitised solar cell [44] which generates electricity as it is printed onto buildings. *Strelitzia reginea* flower has inspired the design of flectofin® which can move its fin up to 90 degrees by bending stress induced in its spine [45, 46]. More recently, physiology and morphological function of the human heart inspires the design of an 'artificial heartbeat' actuator [47]. Not only tangible products, life evolutionary processes, genetics, function of neurons and animal colony social interaction inspires many computational algorithms. Many new discoveries in biology will lead to many more applications which seemingly may be limited only by human creativity and ingenuity [48-50].

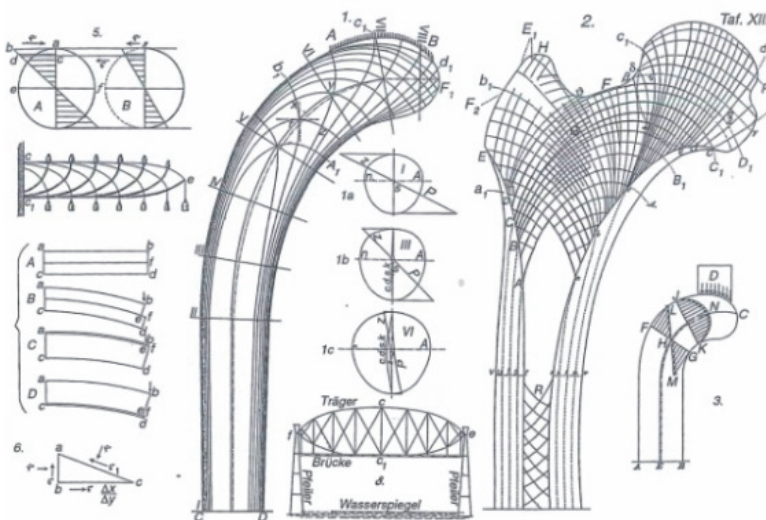


Figure 1.4. Sketches of Culmann's crane with stress trajectories in the left part and trabecular architecture of long femur [42].

Taking benefit from its evolution process, nature demonstrates myriad multi scale adaptation processes and strategies in various natural objects. Abundant natural objects provide examples which can be thought as data base for scientist, engineer, and designer to implement biomimetic.

However, the success of bio-inspired design is a function of several factors [51]:

1. Selection of nature appropriate system and strategy which involves large number of input data,
2. Scale of operation, e.g. strategies which perform well at nano-scale might not work at micro or macro-scale and vice versa, and
3. Resolution of paradoxical design requirements, e.g. the conflict between toughness, stiffness and strength.

In modern days, the field of biomimetic is highly interdisciplinary. It involves comprehension of biological structures, process and functions and bio-inspired design and fabrication of various commercial end-products. It draws interest of biologists, physicists, chemists, computer scientists, material scientists, engineers, architects, and product designers.

In tackling this challenging design program and innovation, several research groups and agencies develop systematic approaches to implement biomimetic [51]. Few of them are: The Biomimicry 3.8 Institute; BioTriz; Design and Intelligence lab, School of Interactive Computing and the Center for Biologically Inspired Design, Georgia Tech; Plant Biomechanics Group, University of Freiburg. The approaches developed may be classified into two different classes based on the starting point.

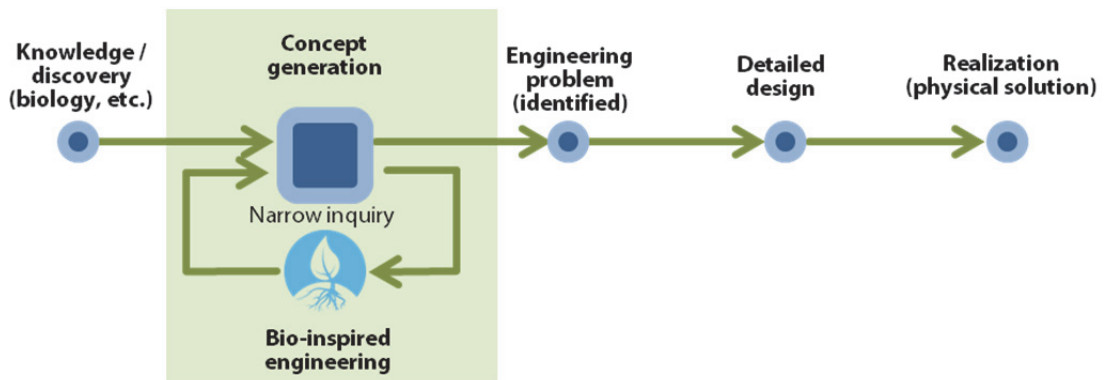


Figure 1.5. Diagram of inverse design approach which started from biological discovery through abstraction which involves studying in depth the biological principles of the chosen object and then selection of application as proposed by Jenkins (*redrawn from* [52]). Though depicted linear however in the design process iteration might occur.

The first approach is inspired by nature observation and discovery which is then expanded by concept generation and finding an area of application sketched as figure 1.5. This approach requires detailed understanding of biomechanics and functional morphology which lead to abstraction of biological insights [53]. Describing the process, several terminologies are used in the literature: *bottom-up process* [53], *solution-driven biologically inspired design* [54], *biology to design* [55], *biomimetic by induction* [56], and *inverse design* [52]. The story of development of Velcro from observation of burdocks

seed sticking to clothes until its implementation is perhaps one of the best example [51].

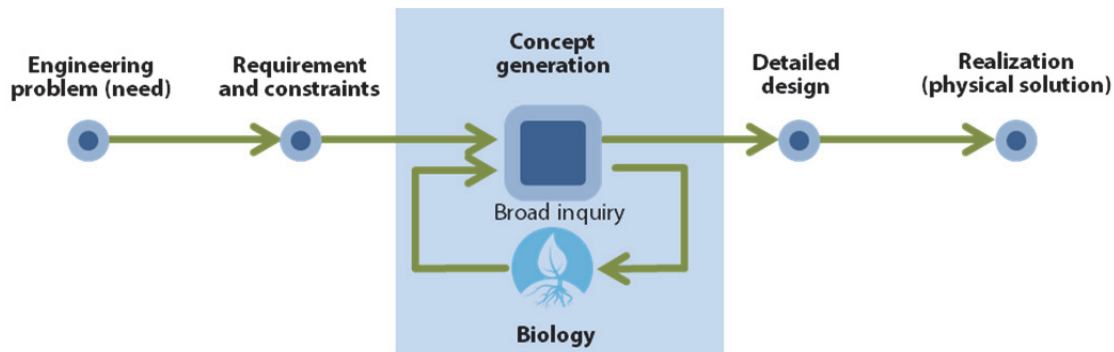


Figure 1.6. Coined as forward design process by Jenkins, the diagram shows that ‘engineering question’ is the starting point in the design process. After determining design criteria, designer and scientist seek the biological objects which might provide insights and proceed with detail study of one particular aspect which answers the questions posed (*redrawn from [52]*).

The second approach starts by (engineering) problem identification and then followed by selection of biological objects for that particular problem. The process in general can be sketched as in figure 1.6. Various terms have been found in literature for the design process e.g.; *top-down process* [53], *problem-driven biologically inspired design* [54], *challenge to biology* [55], *biomimetic by analogy* [56] and *forward design process* [52]. Posing question, ‘how to reduce swimmer’s drag?’, scientist and engineer evaluate fish swimming biomechanics and functional morphology and examine in detail shark skin. The banned hi-tech Olympic record breaking swimsuit is the example of the end product of this design process [51].

In both approaches, The Biomimicry 3.8 Institute advocates and includes Life’s Principle in their methodology to evaluate the success of design process. Life’s principle may be thought as ‘design lessons from nature’, a set of principles proven from 3.8 Giga years life evolution. They claim this principle can and must be used as the goal, strategy, and benchmark for the innovation process. The two aforementioned design processes then might be enhanced with more detailed design phases illustrated on figure 1.7.

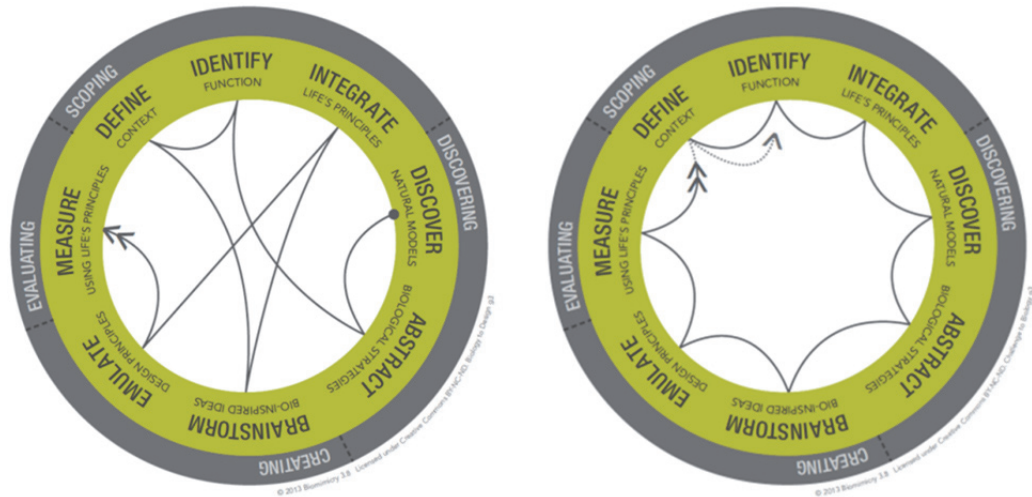


Figure 1.7. DesignLens g.10 is a design spiral proposed by The Biomimicry 3.8 Institute (www.biomimicry.net) which includes design evaluation process by means of life's principle – a set of life's basic operating condition emulated into design lessons which serve as sustainable benchmarks – emphasizing sustainability and condition conducive for life in designing end-product. Spiral A; Biology to design starts from natural models (biology), and Spiral B; Challenge to Biology starts by identification of problem [51, 55].

1.3.2. Brief study of bone physiology and its healing principles

Adhering to the forward design approach this thesis raises the question *how to develop a self-healing concrete material and structure that might seal the crack autonomously*. Observing the domain of biology, there are several wound healing mechanism found in nature: cut skin [57] and bone fracture healing in human and animal [58-62], and plant response to injury [63].

The present work studies bone of present-day mammals and birds and its healing mechanism. An elucidation of bone physiology and adaptation process might then provide the knowledge to develop new type 'synthetic/artificial' self-healing concrete. Inspiration gained from bone study later on will be utilized in this chapter.

Bone, a typical examples of biomaterials, have developed to have complex hierarchical structures owing to the 3.8 billion years of evolution [64]. To provide structural support, bone has to be strong and stiff whilst it must be as light as possible [65]. This superior feature has been optimized by different mechanisms of adaptation. A distinction then must be made between the long term Darwinian *evolutionary process* within a species which involves genetic modification inheritance and the *adaptive growth* and *remodelling* which materializes within individual lifetime. In adaptive growth, cells accommodate local growth by sensing local mechanical loading stimuli therefore deposits a new material depending on the environment. In remodelling a tissue might be restored by a process constituted of deposition and removal of (bio)material through metabolic activity in the living cells [66].

Bone may be defined as a stiff skeletal inorganic-organic bio composite consisting mainly of soft *collagen protein* and mineral *hydroxyapatite* – $\text{Ca}_{10}(\text{PO}_4)_6(\text{OH})_2$ – (a crystalline form of calcium phosphate). For the individual, bone is not only providing body structures supports and protecting vital organs, but also producing blood cells from its marrow and serving stocks of inorganic chemicals, i.e calcium and

phosphorus. On material level, bone demonstrates a hierarchical structure [64, 66-70].

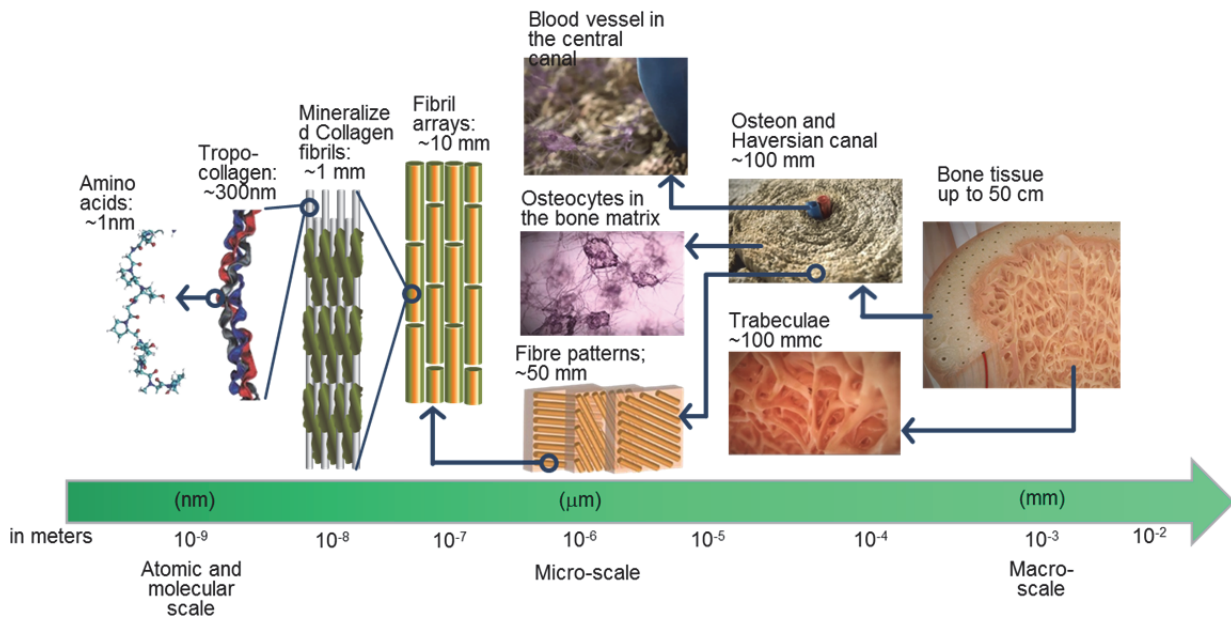


Figure 1.8. Hierarchical level of bone (redrawn from [68, 69, 71]).

In the *nanoscale*, during bone formation collagen protein molecules assemble into soft fibrils of aligned protein helices which are then impregnated by the formation of 10-50 nm in length stiffer hydroxyapatite crystal. This nanostructures size and orientation follows collagen template and the relation between two components is critical for bone mechanical properties, where the salt mineral crystals provide hardness and carry stress up to four times higher than flexible collagen fibril that is more responsible for responding deformation [67]. This extracellular collagen-apatite matrix is the basic building block which can be found throughout different type of bone and species.

As bone is produced inside the body, at *microscale* standpoint, it is usually covered with cells and certainly contains living cells. Bones contains blood vessels within it, by which all changes in bone shape lay on its surface. These living cells are *osteogenic* precursor cells, osteoblasts, osteocytes, osteoclasts, and bone marrow. *Osteoblasts*, metabolically active bone forming cells, deposit bone extracellular matrix in thin *lamellae* forming concentric mineralized wall around longitudinal capillary tubes called *Haversian canals* or *canals* in short. Then entrapped osteoblasts in the lacunae within the matrix differentiate into *osteocytes*. This osteocytes and the extracellular matrix is assembled surrounding a *central canal (Haversian system)* in which blood vessel for nutrient transport is located and form a cylindrical unit called *osteon* which is then cemented together to form bone. Further, tiny tubes for cytoplasmic process called *canaliculi* extend outward of each osteocyte within bone matrix to form a cellular network. On the other hand, *Osteoclasts*, multinuclear bone resorbing cells, remove bone mineral by releasing powerful acid and enzyme. These cells work in groups which attach onto the bone surface. The hydrolytic enzyme released will then dissolve the mineral in the bone matrix causing a shallow cavity on the surface.

At *macroscale*, osteons form bone in two distinct shapes and morphologies. *Trabecular (Spongy / Cancellous)* bone is a very porous, created as sponge like open network in interior region. It has porosity up to $\sim 85\%$ comprising bone marrow. This is where *hematopoiesis* process takes place. *Cortical (Compact / Lamellar)* bone is generally solid found in exterior region which has approximate porosity 3-5% for blood vessel and osteocytes. This type of bone makes up 90% of bone mass and serves multiple functions; locomotion, organ protection, and inorganic mineral stockpile.

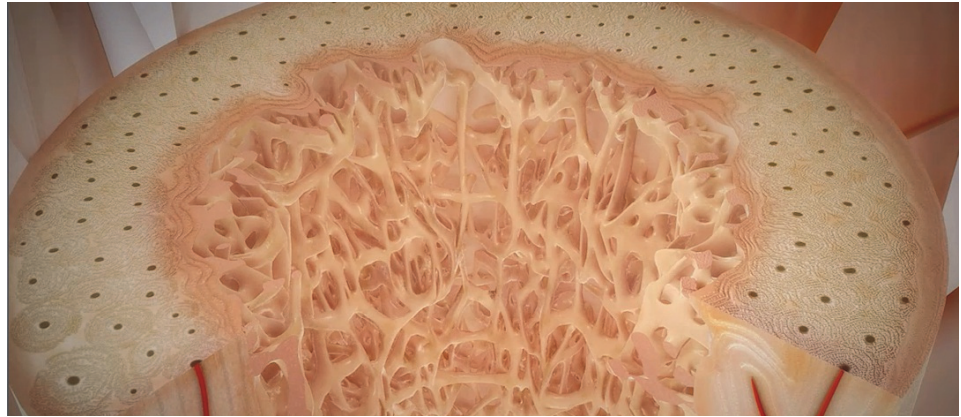


Figure 1.9. Section of bone showing cortical (solid) bone comprises of concentric lamellae called osteon at the exterior of the long femur and trabecular bone in the interior region showing interconnected struts that make up porous layer. (Captured from www.bonebiology.amgen.com; accessed 15 January 2014; all rights reserved[71]).

Bone may be seen as complex, dynamic, metabolically active living tissue which exhibits constant adaptation to its physical environment throughout its life cycle. This makes bone able to operate subject to damaging high stresses and strains which may lead into failure in short time if not repaired. It is believed that bone is constantly sensing the mechanical stimulus, checking the occurrence of microcracks and reinstating the new material into the damage zone. In this mechanotransduction process three aspects namely; sensing – transmitting – activating, play the role as such bone tissue can sense and response physical *stimuli* leading into changes in shape, composition and mass. The process cycle may be sketched in figure 1.10 as: [1] in macroscale, the body receives a physical stimulus which is then [2] transferred via bone tissue in term of poroelastic strain induced bone flow, [3] and then osteocytes sense the signal of large deformation and [4] via cellular interaction trigger signal to, [5] actuate osteoclasts by resorbing old bone tissue and osteoblasts by forming the new one, [6] eventually, it reshapes the macroscopic properties of the organ [59-61, 72, 73]. Owing to adaptive growth and – *more effective* – remodelling process bone has a property of being self-repaired.

Fratzl and Weinkamer [66] suggest three levels of bone self-repair mechanism. The first level is *reversible bond at molecular level*. When bone is loaded the hard mineralized bone is the responsible part to provide the stiffness and to bear the stresses. However this material is also quite brittle. Therefore, it is protected by a reversible mechanism by breaking up ‘sacrificial’ molecular bonds and closing in at soft collagenous substance leading to plastic deformation [74]. The second level is of *close loop feedback process at cellular level* when local damage is detected by osteocytes which then trigger action signal to effector cell; osteoblasts to develops bone materials and

osteoclasts to remove unused bone. In this bone remodelling process osteocytes are acting as dedicated sensors sensing strain deformation and triggering bone repair via cell-to-cell signalling [73].

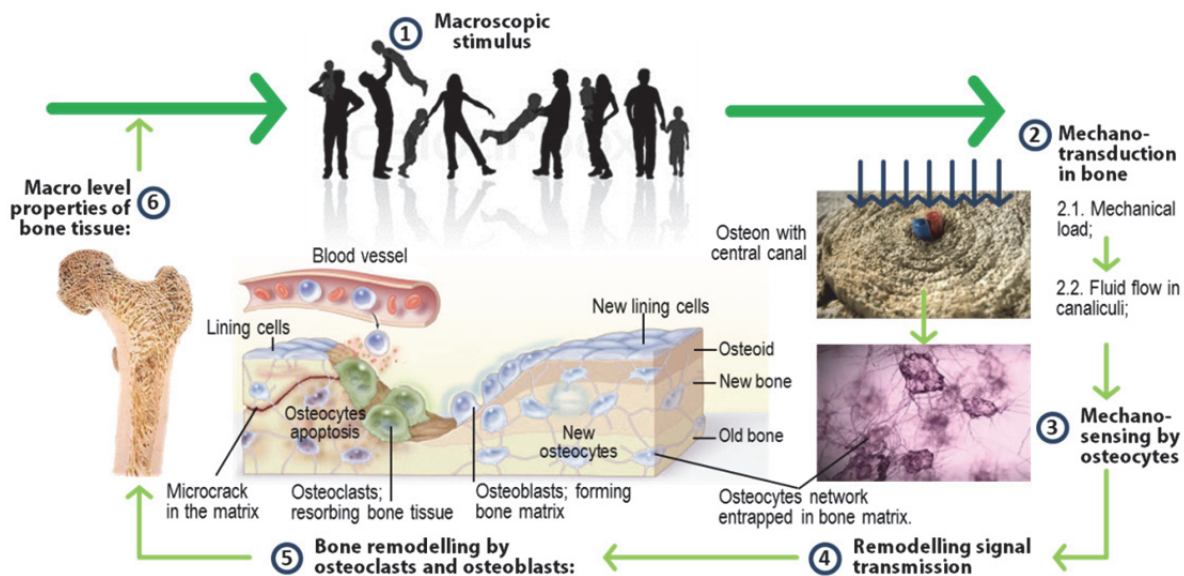


Figure 1.10. Simplified feedback loop mechanism of biomechanical and mechanotransduction regulation of bone remodelling. Microscopic process of bone remodelling may be seen in point 5 of the figure. (a) Osteoblasts anchor themselves creating microenvironment underneath its contact surface while releasing powerful acid eroding bone matrix – what is so called *Howship's lacunae*. Then hydrolytic enzymes removes remaining collagenous matrix. (b) Osteoblasts then move to the region depositing organic matrix (osteoid) – predominantly collagen – which later on scaffold inorganic matrix (crystallized calcium and phosphate) creating a new bone matrix. Entrapped osteoclasts transform into osteocytes while in the outer layer transform into lining cells. Graphs is adapted from [71-73, 75]. In depth information of signal transduction and regulation in molecular lever can be found in the literature, i.e. [76-79]

The next level is *bone fracture healing process*. When the bone fracture – often because of excessive loading associated with trauma or bone dislocation – is large enough to be remodelled by cellular remodelling process, more complex healing process takes place. Kalfas articulates three specific overlapping steps appear in the bone fracture healing process (figure 1.11); [1] inflammatory in the first hour and days, [2] repair mechanisms, and [3] remodelling process in the later stage [60, 80].

Right after fracture events occur, a hematoma develops in the inflammatory stage. The blood vessel rupture causing dilation and swelling of tissue and inflammatory cells permeate the fracture location causing tissue granulation. After few days osteoblast rapidly develops bony structure meanwhile fibroblasts produce fibrocartilage and bridge the gap between broken bones.

During the repair stage, the cartilage developed between two ends of broken bone supports the blood vessels growth by process of angiogenesis. A collagen matrix is then formed by osteoblast followed by secretion of osteoid which is the mineralized. This process leads into the formation of bony soft callus surrounding fracture site. Kalfas indicate this mineral is formed during first one to two months and quite weak

due to unsettled merger therefore need immobilization [60]. Eventually, callus is ossified by mineral crystallization caused by osteoclasts which are invading the area.

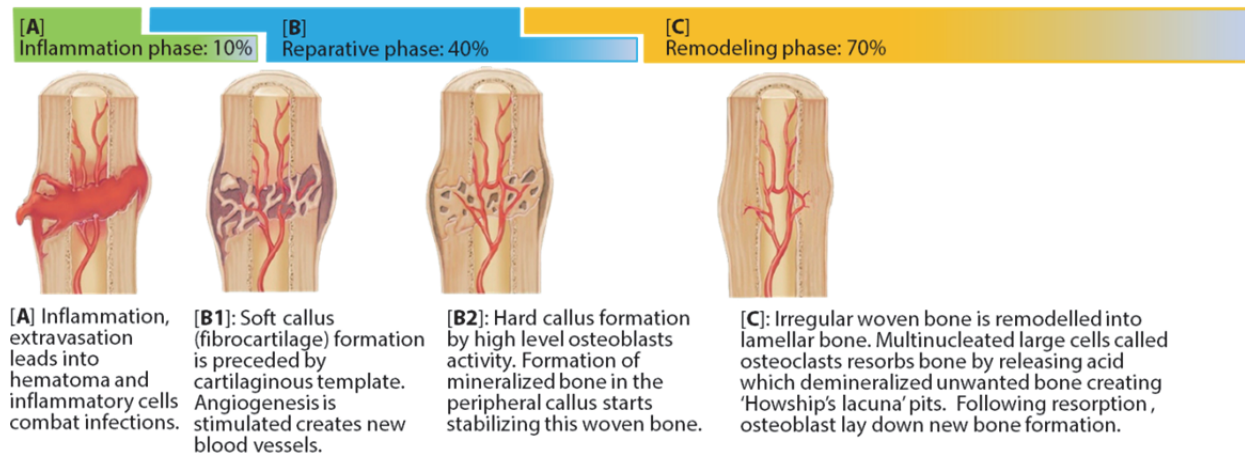


Figure 1.11. Fracture healing cascade overlapping process (adapted from [80]).

Typically, in replacing broken bone, more bone matrix is produced than what is necessary. Therefore, in the later steps, bone healing process is completed by remodelling process. Osteoblasts remove the excess bone matrix restoring the bone into its original shape and mechanical strength. This process develops over long term period as such months or years as function of the size of damage, fixation during healing, and mechanical stress enhancing bone healing. It is reported that proper axial loading force generates bone matrix formation where it is required and resorption from where it is unused.

1.4. Self-healing materials; synthetic approach to healing

Healing in hard or soft tissue triggered by injury follows in general three overlapping steps in time; inflammatory response, cell proliferation, and tissue remodelling. Mimicking its biological counterparts, self-healing materials are designed to possess the ability and perform self-repair and self-recovery of the pre-assigned materials properties and functionalities using built-in resources in the material [81]. It follows deliberately accelerated artificial route in equally similar three steps after damage is formed in the material: *actuation* (triggering actions), *transport of healing agents* into fracture zone, and *chemical repair*. Blaiszik and co-workers suggest that timescale and kinetic of this overall response is critical to the success of healing. However it is not independent to how the healing agents hardened e.g. polymerization, entanglement, reversible cross-linking. Inside of material, the rate of healing can be tailored by designing reaction kinetic of healing agent to respond the outside stimulus (damage, fracture, scratch, etc.) which is as a function of loading, stress and strain rate. Therefore self-healing material process might be thought as 'material-stasis' stabilizing rate of damage with the rate of healing which in turn determines the efficiency of healing [81].

After pioneering studies by several material scientists [82-84], a great deal of research has been carried out in the field of self-healing material after the landmark paper on self-healing polymer by White *et al.*, [85] was published in Nature in 2001. Further,

Blaiszik *et al.* categorizes development approaches to designing self-healing material typically based on the healing mechanism; *intrinsic (autogenic)* healing in which material shows inherent capacity to heal itself with or without stimulation, e.g. heat induction, etc., and *extrinsic (autonomic)* healing in which some ‘*intelligence feature*’ is embedded into material to have autonomous healing mechanism [81, 86, 87]. Autonomic healing mechanism developed may be further classified into *capsule based system* or *vascular based system*.

The state of the arts in self-healing materials shows the concept is currently implemented across the materials classes [88]. It includes self-healing in polymer, fibre reinforced matrix, metals and alloys, ceramics, bituminous material, and cement based material with various mechanisms. Some of them reach field operation while many are still in the lab phase.

1.5. Self-healing concrete; concepts and strategies

1.5.1. Evolution of concepts and definitions

Explosion in number of literature studies and development of self-healing concrete have been seen recently. Van Tittelboom provides an exhaustive literature review of concrete autogenic and autonomic healing in her PhD thesis. In it systematic in-depth analysis can be found on the different type of concrete healing mechanism, efficiency of various healing agents, suitable encapsulation techniques, triggering mechanism for autonomic action, and evaluation of recovered properties [86, 87]. State of the Art Report of RILEM TC-221 SHC entitled Self-Healing Phenomena in Cement-based Materials published in 2013 also provides extensive overview of the most recent progress.

In guiding advancement of this emerging field, attempts to set-up general framework and definition were carried out by technical committee TC-075B from Japan Concrete Institute (JCI), RILEM committee TC-221 SHC [89], and Mihashi and Nishiwaki [90], see figure 1.12.

RILEM TC-221 SHC suggests a definition which adopts a more general point of view of self-healing [89]. The committee defines **self-healing** as ‘*any process by the material itself involving the recovery and hence improvement of a performance after an earlier action that had reduced the performance of the material*’. Further, **autogenic healing** is attributed to the self-healing process, “*when the recovery process uses materials components that could otherwise also be present when not specifically designed for self-healing (own generic materials)*”. Meanwhile **autonomic healing** is defined as the process, “*when the recovery process uses materials components that would otherwise not be found in the material (engineered additions)*”.

For the field like self-healing which is still immature, the discrepancy of definitions for the same process may be seen as inevitable. However, dispute may be resolved by taking emphasis on the actual triggering mechanism of self-healing process implemented. Furthermore RILEM TC-221 SHC presumes the level of intelligence – basic, smart, and intelligent – of the materials for assessing healing mechanism. Smart material is engineered to demonstrate useful response for particular stimulus in its vicinity. Meanwhile, intelligent materials sense and respond external stimuli as well as regulate its own response which is achieved by integrating its multi functions.

These materials collect and process information and adjust its behaviour accordingly [89].

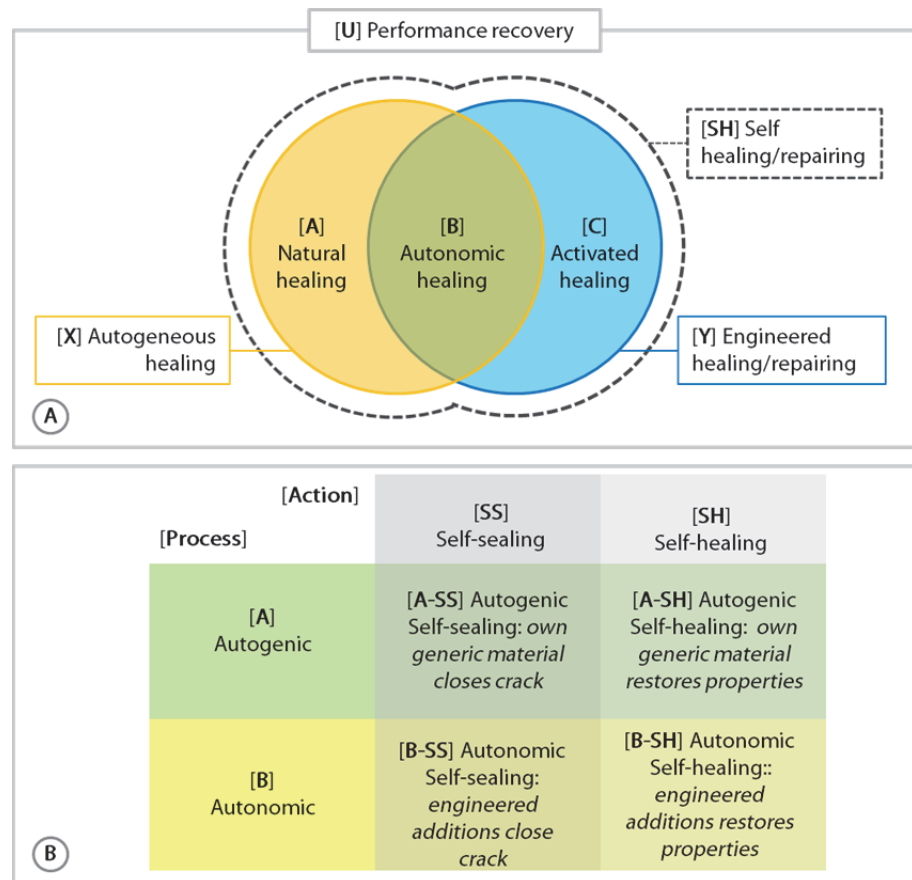


Figure 1.12. [A] Self-healing classification proposed by TC-075B JCI depicted in Venn diagram. [B] Interpretation by Mihashi and Nishiwaki [90] to the definition of self-healing materials proposed by RILEM TC-221 SHC (adapted from [80, 90]).

1.5.2. Strategies and state of the art 1; autogeneous healing

It is well known that cement-based materials have inherent autogenic self-healing capacity [91]. According to Hearn, French Academy of Science had observed autogeneous healing of cracks in fractured culverts, pipes, and water retaining concrete structures in 1836, and Hyde had already studied the phenomenon at the end of the nineteenth century [92, 93]. Van Breugel reports that Glanville in 1926 conducted research about these phenomena and at that time a distinction between *self-sealing* and *self-healing* was discussed which was then followed by Soroker *et al.* in 1926 and research of cracks in bridges by Brandeis in 1937[26].

A systematic study of concrete autogenic self-healing was carried out by Hearn [92, 93]. It turns out that crack opening in concrete diminishes in time by means of several processes with a great number of literature demonstrating the evidence [94, 95]. Four mechanisms show important contribution. (1) Swelling of the cement matrix in proximity of crack tip due to absorbed water into hydrated cement paste. (2) Continuing hydration of unreacted cement particles due to lack of water during hydration process which in turn occupy crack void. This is the second important contribution to healing mechanism which is more pronounced in young concrete. (3)

Dissolution of calcium ions (Ca^{2+}) which reacts with carbonate ions (CO_3^{2-}) from ambient environments and forms calcium carbonate (CaCO_3) which then precipitates at the crack faces. The mechanism, studied in great details by Edvardsen [96], is believed to be the most important contribution to the autogenous healing [93]. (4) Physical clogging of small particles crumbled from crack surface or carried by ambient water. According to RILEM TC-221 SHC this recovery processes are classified into three causes [94] as depicted in figure 1.13.

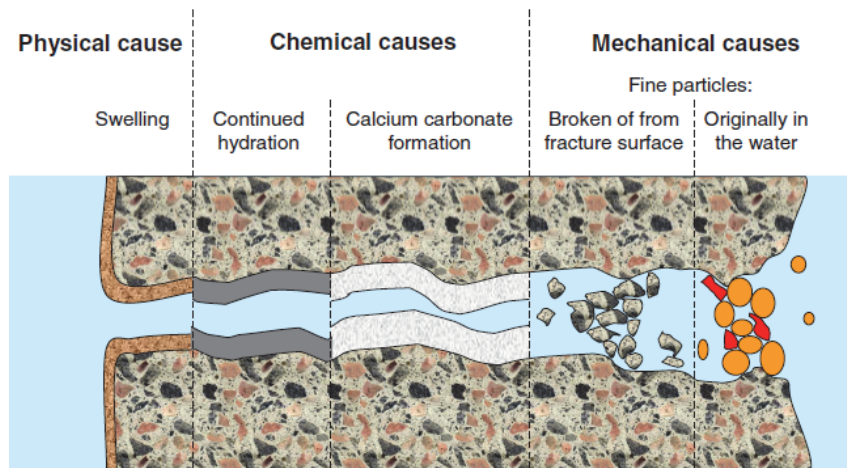


Figure 1.13. Classification of most possible causes of autogenic self-healing mechanism of concrete. The scheme appears in the thesis (pp. 4) of Nynke ter Heide [97] illustrating the mechanisms which is promote self-healing. The figure used in this work can be found in pp.65 RILEM State-of-the-art Reports TC 221-SHC Self-Healing Phenomena in Cement-Based Materials [89].

The efficiency of concrete autogenous self-healing capacity is influenced by environmental action (e.g. the presence of water), temperature [95], mix composition [86] and is deemed higher with higher cement content promoting continued hydration. The later may be thought as in contrast with the demand of low cement content concrete to satisfy sustainability criteria.

On the other hand, autogenous self-healing might be the reason for decreasing chloride ingress through the concrete cover and preventing corrosion of rebar. Klaas van Breugel suggests this innate ‘*immune system*’ makes concrete a material with high resistance. This beneficial feature may in turn promote longer concrete service life, though concrete structure was not designed taking into account its inherent autogenous healing capacity [26]. The reason is because the probability of occurrence of the process and necessary conditions are not fully understood therefore possess low reliability to be taken into account in the design explicitly. However a limited crack width is allowed in the design of watertight container with respect to pressure and crack stability. Van Breugel asserts, “*This in fact demonstrates that the self-healing capacity of ordinary concretes is considered a by-product of the material rather than a feature that could be manipulated by a sophisticated design of the mixture*” [26].

Studies show provisions to elevate the success rate of autogenous self-healing are crack width, water availability, and crack closure. Smaller cracks have a better chance to heal. The presence of ambient water helps un-hydrated cement particles to form hydration product and seal the cracks. Re-closing the crack opening promotes higher rate of healing mechanism afore-mentioned.

Autogeneous healing in concrete is restricted to small crack width (up to 200 μm), presence of water and crack closure by means of compression [86, 98, 99]. Many research and developments have been dedicated to improve concrete inherent healing capacity [86]. Several strategies and its combinations involve:

- (1) restricting crack width by embedding fibres in the concrete which takes form as: *fibre-reinforced concrete* (FRC) or *strain hardening cementitious composites* (SHCC)[100-103]. One successful example of SHCC is ECC (Engineered Cementitious Composites) developed by Li *et al.* which shows high ductility while ensuring that crack widths remain typically around 50 μm ;
- (2) closing crack opening by incorporating shape memory alloys [104-106] or shrinkable polymer tendons [107, 108];
- (3) providing additional water by means of super absorbent polymers (SAP) [109, 110] or water capsules; and
- (4) adding agents e.g. sodium monofluorophosphate [111, 112], microbes [113-116], to promote crystallization, precipitation of calcium carbonate and/or hydration.

1.5.3. Strategies and state of the art 2; autonomous healing

In order to have better ‘control’ on self-healing mechanisms, researchers purposefully develop ‘engineered healing’. Approaches in this autonomous healing mostly can be described by means of embedding (micro)capsule [84, 117, 118] or long brittle pipes containing healing agents [119, 120]. Heat evolution devices might be applied to promote accelerated reaction kinetics of healing agents [121]. Quite often these approaches are combined with some ‘health monitoring’ techniques.

Dispersing capsules containing healing agents was proposed by Dry [83, 84, 122-126] in the early nineties of the 20th century and successfully implemented in self-healing polymers by White *et al.* [85]. When the crack hits the capsule, its shell ruptures and healing agent is released and hardened upon contact with atmosphere or with polymeric crosslinking catalyst.

For implementation in cement based materials several examples may be presented. Yang *et al.* [117] successfully developed microcapsules with oil core and silica gel shell. Inside the shell, Yang and co-workers used commercially available methylmethacrylate (MMA) monomer as the healing agent and triethylborane as the catalyst. Upon releasing the agent, polymerization of methylmethacrylate initiated by the catalyst may be achieved at room temperature and seal micro cracks decreasing permeability by approximately 66%. Van Tittelboom used brittle borosilicate glass and ceramic cylindrical capsules with internal diameter about 1.71 to 3.00 mm containing polyurethane with accelerator, epoxy resins, polyacrylates, polyurethane and MMA. In case of using two compound agent, the capsules were connected two by two and placed manually in the concrete specimens.

Joseph [119, 120] used brittle borosilicate glass tubes containing cyanoacrylate (CA) cured in air in which one end of the tube is bent up and open to the air to supply the agent. This allowing continuous supply of the glue. Nishiwaki *et al.* [90, 121] developed a system where they embed organic film pipe containing healing agent and heating device made of ceramic fibre and conductive matrix. Upon crack formation the conductivity is reduced and the resistivity close to the crack increased therefore

selectively induced heating and melt the thermoplastic film and released the healing agent.

Despite the promising results, some issues arise regarding the most efficient healing process and appropriate healing agent used in the concrete. The issues are:

- (1) vulnerability of the capsules during mixing,
- (2) placing and curing of concrete, and
- (3) number and aspect ratio of capsules sufficient enough to ensure the random crack formation hit the capsules [26].

Extensive information and discussion upon these issues may be found in literature [86, 89].

1.5.4. Strategies and state of the art 3; self-healing by means of microbes

The discovery of deep sea hydrothermal vents in 1977 may revolutionize our view towards life. Firstly, life does not always depend on the photosynthetic organism in the base of the food chain. Secondly, quite number of microbes live in the extreme [127]. Chemotrophic bacteria, for instance, live in mutualistic symbiosis with other organism in the no-sun light underwater [127-130]. Many other bacteria thrive in desert [131], rock [132], extreme dry and cold regions in Antarctica [133], and hyper-alkaline environment [134].

On the other hand, bacteria have been used in developing ecological engineered process or product. Bacteria were applied in pollutant removal, soil bioremediation, and greenhouses gas removal of landfills. Special type of ureolytic bacteria were used in soil improvement and consolidation [135, 136], repair degraded limestone [137], and filling concrete pores and microcracks [115, 138-140].

These provisions may promote a leap forward ambition, to implement bio-based materials and processes for improving quality of materials as well as enhancing civil infrastructures sustainability [141]. In doing so, several scientists have proposed and developed ideas around enhancing concrete durability by introducing bacteria to promote self-healing to seal crack.

Jonkers *et al.* [138] has developed and tested the concepts in which bacteria start to be activated in contact with ambient water present in cracked concrete, consume nutrients, and precipitate calcium carbonate which in turn fill the voids and seal the cracks. Wiktor and Jonkers [110] encapsulated bacteria strain and nutrients into porous expanded clay to ensure viability and functionality of the bacteria after the concrete mixing. The in depth working principle of the bio-based self-healing concrete will be discussed in chapter 5.

1.6. Remaining challenges; ideas development

A new point of view of material design is introduced by self-healing materials concept. Damage in structural materials should not be something to worry about, however may be seen as presupposition to the healing mechanism. Throughout its service life this mechanism therefore is dynamic and adaptive to respond to the (damaging) external action.

In case of concrete, healing capacity is inherent to the material. It can heal itself via formation of Ca based mineral, continuation of hydration of un-hydrated cement, or via physical clogging or cement matrix swelling. There is no clear indication whether single or mixed mode process takes place and even harder to ascertain when the process started in the real structures.

This autogenous healing, therefore, remained unreliable. This may be attributed to the fact that concrete is highly variable with respect to the composition of its ingredients. Certain compositions may promote healing while the other mixtures proportion might raise questions upon its healing capacity. As the presence of water is the prerequisite for certain autogenous healing mechanism to happen, for instance continued hydration, its highly improbable the healing will occur in the element with limited contact to the ambient moisture. It is also hard to determine and to quantify the sort of healing mechanism taking place in the structure over a certain period. Moreover, although there is no agreement upon certain values, autogenous healing might occur only to very limited crack width. Additionally, in *quasibrittle* concrete, crack are hard to control. (Cracks tend to continue to increase once the critical value/characteristic length/crack thickness is reached, even in the decrease of tensile stress.) Even worse is when the tensile crack is actively opening up and propagating due to constant (local) tensile stress, autogenous healing might be inadequate.

Overcoming this dubious healing capacity, implementation of self-healing should be preferably through autonomous self-healing concepts. Several developed methods are based on embedded capsule or embedded vessel (tube) by which healing agent flows out upon shell breakage by the crack. In spherical capsules, however, there is tendency the crack surround the capsule instead of hit and break the capsule shell, by which scientists proposed elongated capsule or tube. Yet, some limitation of capsule and vascular based systems (or methods) occur due to the fact that; brittle hollow capsule and tube can become damaged during mixing and curing and dispersing long brittle tube in the concrete is laborious [87].

1.6.1. Problem and goal definition

It is believed applying *engineered (autonomic) self-healing mechanism* in concrete will be beneficial for enhancing its durability in general. However in the thesis the proposed engineered self-healing mechanism must also show greater advantage in tackling problems of fluid tightness and preventing leakage, especially in the locations that are less accessible or inaccessible to repair.

The goal, therefore, is to create a self-healing material or rather a self-healing component in a concrete structure which can tackle the problems described above. The proposed self-healing should not only applicable to the material level but also can be up-scaled to the structural level.

1.6.2. Biological domain and abstraction of biological model

Resolving the limitation of capsule and vascular based self-healing mechanisms, bone physiology and its healing process is revisited. It is clear that bone has superior mechanical properties which are derived from its functionally adaptive capacity

throughout its material hierarchical spectrum. It also demonstrates highly complex process to remodel in its life time and to perform scar-less self-healing. It is admittedly hard to mimic the process completely in the concrete.

However, two of appropriate principles that might be constructive are identified; *bone morphology* in macro level comprises of cortical (solid) bone and trabecular (spongy) bone and *feedback loop process* in the remodelling and healing process. From these two principles, abstraction was prompted into the development of a healable concrete material and to the method for healing it with healing agents.

The first aspect is development of porous network concrete emulating bone morphology as shown in figure 1.14. The idea behind this abstraction is cortical bone may be mimicked with solid concrete and trabecular bone may be imitated by porous concrete. Combination of the two types of concrete resembles the *Porous Network Concrete*, a bone-like concrete able to self-heal by the mechanism of feedback loop as depicted in figure 1.15.

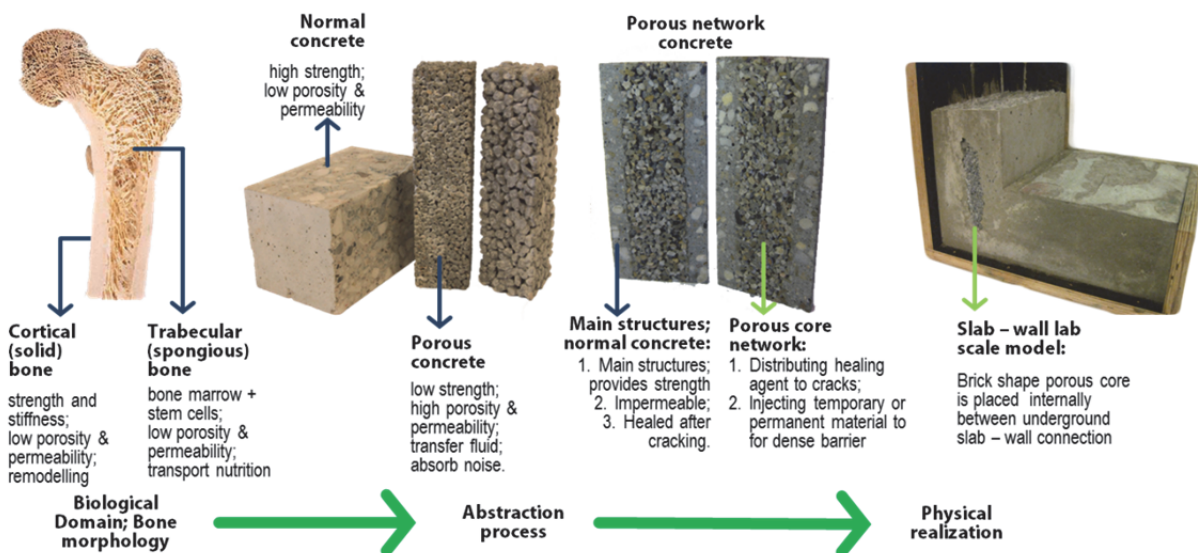


Figure 1.14. Ideas transformation of Porous Network Concrete following forward design approach by selecting bone as biological model of healing process [62, 142].

1.6.3. Idea development

This study will develop a new self-healing technique that makes use of the Porous Network Concrete. The porous concretes will be prefabricated e.g. cylinder, rectangular bar or thin brick, which are placed at the interior or surface of the concrete structure. Depending on the application, this layer of porous concrete will be filled by temporary or permanent materials that form a dense layer of even contains a self-healing agent and sensors for detecting damage, liquid, chlorides or corrosion products. This filling of the prefabricated porous concrete layer can be done before or after the concrete structure is poured and hardened. It even can be filled much later when for instance most of the initial shrinkage or settlement of a structure has taken place. The porous layer can also be filled with a material like gels containing sensors that detect if the condition of the concrete structure changes. At that moment the gel can be replaced by another material that takes care of the healing or fills the porous layer permanently.

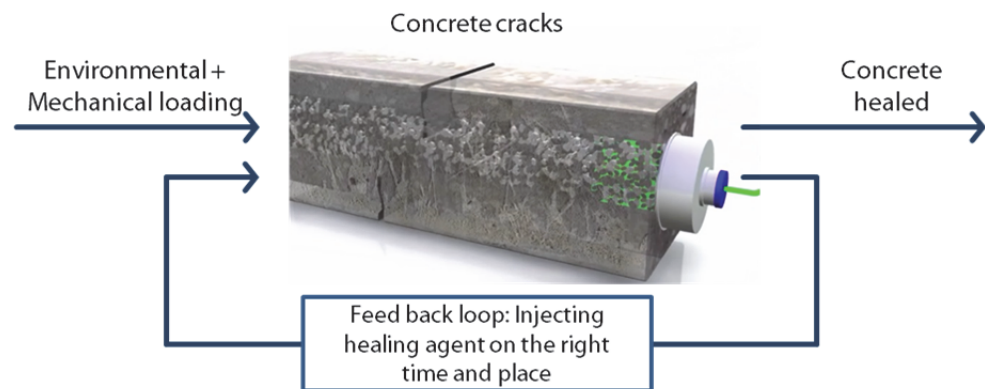


Figure 1.15. Flow of information in Porous Network Concrete.

In general the proposed self-healing mechanism concept which makes use of this porous network concrete will be carried out with minimum – *even without* – human intervention. This effort can be tackled using intelligent materials or structures technology concepts which have three basic requirements of capabilities; sensing, processing/controlling, and actuating. In addition, the performance of the structures and or material should be controlled actively using adaptive control algorithm and in an autonomous manner.

Figure 1.16 shows the flow of information in this proposed self-healing concrete. Damages in the concrete which may be inaccessible to human observation are detected using sensors, such as self-powered embedded fibre optic. Then data will be collected and calculated by a controller which sends triggering signal to the actuators. This actuator will switch on a pump that injects healing agent in the reservoir through the porous network concrete layer. This injection process will be stopped automatically using an algorithm which compares measured parameters with the designed values [143].

Having this idea in mind, several possible applications of the proposed system are shown in Figure 1.16. For instance, for water retaining structures, e.g. storage tanks, basement-walls, industrial floors, tunnels or aqueducts it shall keep the structures watertight. It shall form a water-tight connection between the classical wall and slab problem, in which the slab is old and the wall is young concrete. It can create a dense layer/barrier next to the reinforcement to stop ingress of aggressive substances. It can form a protective dense layer at the surface of concrete structures, which can also be used as architectural material.

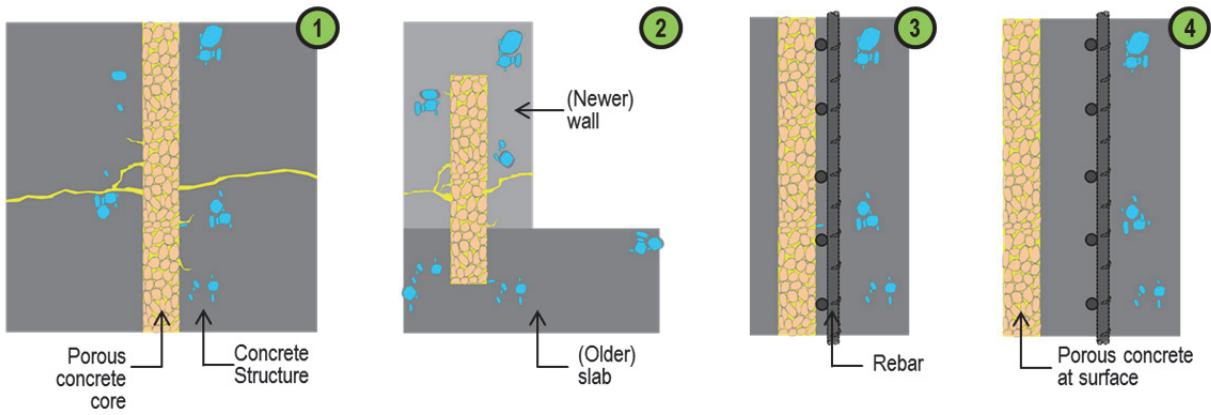


Figure 1.16. Several possible application of the proposed system. (1) Liquid retaining structures where porous network is placed in the centre (or the side) of the structure. (2) Liquid-tight connection for the classical problem between (older) wall and (newer) slab. (3) Porous barrier/layer next to the rebar to stop chloride ingress. (4) Porous network at the surface of concrete structure which may be used as architectural material as well. For (3) and (4) the porous layer may be filled later on with material to make it dense.

1.7. Scheme of this thesis

The research carried out is fundamental research to develop the porous material, fill that with self-healing agent, and study the efficiency of the self-healing mechanism proposed. In general the research consists of two parts; (1) development phase and (2) technical testing phase as depicted in the roadmap figure 1.17.

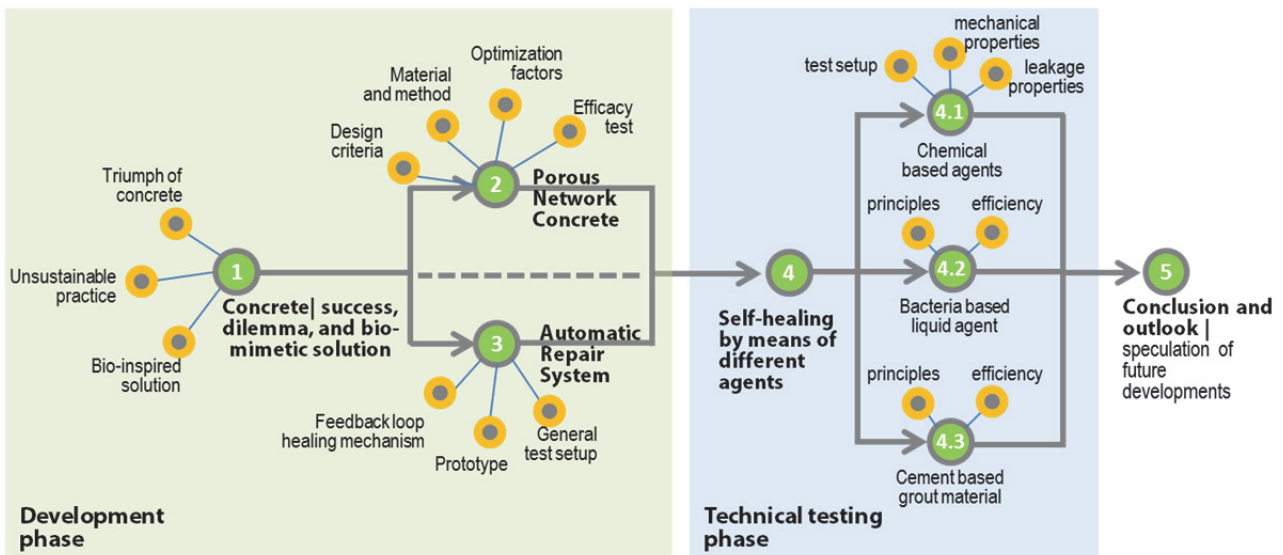


Figure 1.17. Roadmap of research and development of Porous Network Concrete. This roadmap visualizes the thinking and working flow process to be used to present the ideas and the thesis.

It has been shown in the chapter 1 (point 1 in the roadmap) that concrete is strong, easy to make, durable, and cheap therefore obtain its current success. However some problematic ecological issues need to be resolved by making concrete more durable. To address this problem three questions are posed and answered subsequently.

How to design new concrete structures to achieve higher durability? Technically speaking there are many ways to design highly durable concrete. The precondition, however, is to create concrete as dense as possible so it will not allow any ingress of deleterious substance. Denser concrete possesses higher strength to resist any mechanical loads which in turn tend to make concrete crack. Optimizing composition of concrete mixture, improving packing density of constituents, adding admixtures are among the conventional but popular methods which gain recent success. However, where the inevitable continuous interconnected crack coupled with problem of its inaccessibility to repair does occur in concrete, self-healing concrete is one of the promising methods to obtain durable concrete.

Further, in reinforced concrete (RC) structure, rebar will do the work to carry tensile stress when concrete in the tension area cracks. This is the reason why reinforced concrete is designed to allow certain prescribe crack width. However, the if cracks occur, the rebar will be exposed to atmosphere with the risk of corrosion. Responding to this case, self-healing provide sealing to the crack and further protect the rebar from external aggressive substance.

What natural objects demonstrate self-healing capability? What principles can be learned from the object and emulated into self-healing concrete? The process of abstraction in this thesis is based on bone. It has been chosen because it shows remarkable shape and healing capacity. As it is shown in the section 1.3.2., bone shape and its healing process is highly complex. Admittedly it is hard to ‘translate (total or partial mimicry)’ this shape and process to design self-healing concrete. However, by abstraction two principles may be drawn from this object. Firstly, bones macro morphology comprises of cortical and trabecular. Secondly, living bone has self-healing capacity by feedback loop mechanism and remodelling.

How to develop a self-healing concrete at material and structural level that might seal cracks autonomously and make it impenetrable for fluid? Studies show concrete has inherent (autogenous) healing capacity. In addition, several advances in self-healing concrete have been developed based on improved autogenous healing, dispersed capsule containing healing agent, and vascular based system. Deemed for improving current methods and providing alternate healing mechanisms, learning from bone morphology and healing processes, and guided by the definition of self-healing concrete abovementioned, the concept of Porous Network Concrete (PNC) is proposed, developed and tested in the thesis. This work proposed autonomous self-healing concrete which can sense its damage and trigger healing process accordingly.

What are the characteristics Porous Network Concrete should possess in order to be successfully used in self-healing concrete? How is PNC produced? Which tests and how should these tests be performed to check the characteristics and properties of PNC? How can this material be optimized? What is the evidence, if any, that PNC is effective for self-healing concrete? Chapter 2 will demonstrates in detail the production process of PNC and discuss which properties of this novel type of material may be optimized. Some tests will be conducted to characterize material properties and identify its effectiveness, e.g. strength of the material, porosity and permeability which in turn determine how efficient healing agent flows through the porous core.

Development and working principles of automatic healing mechanism will be discussed in detail in chapter 3. It will answer some questions; *How the system is built? How does the proposed automatic / autonomous healing mechanism work? Which test is designed and how should this test be carried out to measure the efficiency of the system?* Started by defining design criteria for autonomous system, different components; i.e. sensor, controller and actuator, to regulate the flow of information in the autonomous system will be described. Furthermore, the general test setup to evaluate the concept will be specified.

By having this setup ready, the development phase is transitioned into technical testing phase, where the proof-of-concept is further evaluated. Consequently, questions may arise; *What type of healing agent may be suitable to transfer into the crack(s) through porous core? How concrete healing efficiency will be evaluated?*

Point 4 in the figure 1.17 will report the test of porous network concrete autonomous healing mechanism with different healing agents. Three materials are chosen representing different classes; two compound epoxy resins as *chemical based agent* [142, 144], cement paste as *grout material* [149], and bacteria based solutions developed at Microlab [145-148], Faculty of Civil Engineering Geosciences, TU Delft as *bio-based agent*. Healing performance is measured by comparing properties of cracked (pre-healing) and healed (post-healing) specimen.

Conclusion will be drawn and presented at the last point of the roadmap. The primary questions and goals of this fundamental research will be re-addressed and possible future research will also be presented.

2.

Porous Network Concrete: design, production and characterization

'...What is design? It's where you stand with a foot in two worlds - the world of technology and the world of people and human purposes - and you try to bring the two together.'

- Mitchell Kapoor

The transformation from inspiration to conceptualization of the Porous Network Concrete (PNC) has been explained in the first chapter. This chapter describes in more detail the realization of the concept. It starts by identifying the goals of the design and what features the PNC should possess. This will be the performance requirement for the product. The study of the properties of both normal and porous concrete will elucidate the principles which in turn will guide the next production steps. It will then describe the production process of PNC. Further, the chapter elaborates on the test to evaluate the pore structure and mechanical properties of the PNC and discusses the results.

2.1. Introduction; motivation, ideas and goals

Damage may be seen as the necessary condition to start the self-healing process. One essential element for the process to work is the transport of healing agent into the damage i.e. *fracture or crack zone*. In living organisms transport of nutrients and ingredients appear at micro level in cellular signalling and transport and at macro level via vascular system, i.e. *organized networks* of xylem and phloem in trees and circulatory blood vessels in animal and human.

The transport process in concrete – which may be thought as porous material – takes place in the pore system. Through the pores, concrete absorbs and releases moisture and ingress of substance is made possible. Gradients of temperature, pressure, humidity, or solution concentration may influence the transport of the substance in the concrete. However, this driving force might not be enough to trigger healing agent transport into fractured sites without any *additional external force* and or *adequate channel* within the concrete.

In this work, *Porous Network Concrete* (henceforth PNC) is a hybrid system in which high permeability porous concrete is embedded in the interior or exterior of normal dense concrete. The porous network core constitutes alternate means for [142] channelling temporary or permanent materials to form a dense layer in the later stage and [62] distributing healing agent from point of injection to cracks in the concrete main body [62, 142].

Porous network in the interior (or exterior depending on the requirement) of the concrete main body is made of prefabricated porous/pervious concrete. Meanwhile concrete structure main body can be designed and produced using self-compacting concrete (SCC). This deliberate design and choice of material will *increase the survivability of the core as transport medium* during concrete structure (in-situ or prefabricated) casting.

Figure 2.1 renders the concept how healing agent is injected through the interconnected pores. Frame 1 of the figure shows the concrete beam (exterior main body) with injection port. In practice this main body might be a concrete underground wall, or container (liquid) tank structures which suffer from cracking. In the frame number 2 of figure 2.1, a semi-transparent picture describes the system showing how healing agent starts flowing into the porous core which eventually will reach the crack and sealing it inside out as it is depicted in the frame 3.

Creating a porous layer in a concrete structure to change that layer at a later stage into a dense layer seems at a first instance not logical. However, it is known that it takes some time for a concrete material to build up its properties and material structure, during which it deforms, settles, shrinks, swells and cracks. So it might be wiser to start the healing or formation of a dense layer at a later stage. Autonomous action will ensure healing intervention at the right time and location.

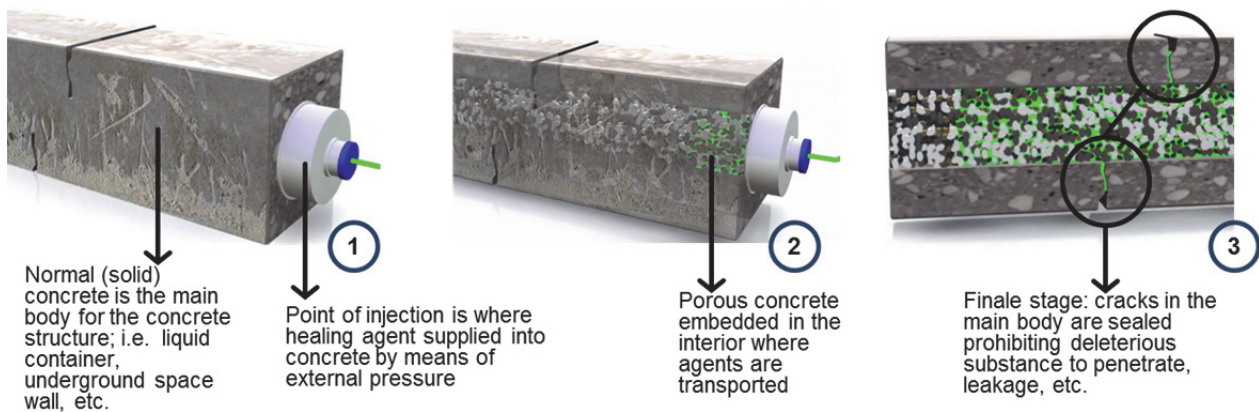


Figure 2.1. Artist render of the conceptual working principle of healing agent transport in the Porous Network Concrete.

Porous Network Concrete establishes a new category of concrete of which its high performance is not only associated with (high) strength as commonly accepted, but with its ability to meet performance criteria for particular conditions where conventional concrete would not be adequate.

In the developmental phase, acceptance criteria were set to evaluate the success of PNC. As the porous network core function is for transporting (liquid) healing

materials, it is logical to attain *permeability and interconnected pore diameter large enough* to channel healing agent from point of injection to the crack zone. Moreover the prefabricated porous core *should stay porous during and after casting the concrete main body* in order to be able to transport healing agent on the right time. However, common rationale argues the larger the concrete porosity the weaker the concrete. Therefore, PNC should sustain the *overall strength* prior to and after healing action to be efficiently implemented as concrete structures. Furthermore, the porous part in PNC will be small compared to the size of the concrete element. So there will hardly be any influence on strength.

The key performance criteria have been set for the development, namely:

1. The *porosity* or void fraction of the Porous Network Concrete should be higher than 0.2 or 20%. Relative permeability of the material should be in the *pervious regime* indicated in the table 2.1 whereas *intrinsic permeability* and *hydraulic conductivity* may be obtained from the evaluation test.
2. The minimum static compressive strength of the porous concrete should be higher than 15 N/mm² while the static compressive strength of normal dense concrete should be greater than 35 N/mm². As the Porous Network Concrete is composed of two different material constituents, the combination of both strength values may be reasonable for structural application. However, there are several other factors that will influence the overall strength of the Porous Network Concrete structures; quality of concrete main body, amount of reinforcement bar, configuration and geometry of the structure, etc. Continued research and development on PNC may yield to the enhancement of the specification.

Table 2.1. Typical permeability regimes, intrinsic permeability and hydraulic conductivity values of geologic (natural) materials. Table has been modified from Bear [150].

Relative permeability	Pervious				Semi pervious				Impervious				
Intrinsic permeability κ (cm ²)	0.001	10 ⁻⁴	10 ⁻⁵	10 ⁻⁶	10 ⁻⁷	10 ⁻⁸	10 ⁻⁹	10 ⁻¹⁰	10 ⁻¹¹	10 ⁻¹²	10 ⁻¹³	10 ⁻¹⁴	10 ⁻¹⁵
Intrinsic permeability κ (mildarcy)	10 ⁸	10 ⁷	10 ⁶	10 ⁵	10 ⁴	10 ³	100	10	1	0.1	0.01	0.001	10 ⁻⁴
Hydraulic conductivity K (cm/s)	10 ²	10 ¹	1	10 ⁻¹	10 ⁻²	10 ⁻³	10 ⁻⁴	10 ⁻⁵	10 ⁻⁶	10 ⁻⁷	10 ⁻⁸	10 ⁻⁹	10 ⁻¹⁰
Unconsolidated Sand & Gravel	Well sorted gravel		Well sorted sand or sand & gravel		Very fine sand, silt, loess, loam								
Consolidated Rock	Highly fractured rocks				Oil reservoir rocks		Fresh sandstone		Fresh limestone, dolomite		Fresh granite		

2.2. Materials; combination of two concretes, *normal (dense) concrete* and *porous concrete*

PNC consists of two types of concrete; normal (dense) concrete and pervious concrete (henceforth POC). Both concretes are made from cement, water, and aggregate where some admixtures may be added to achieve specified criteria. In pervious concrete, fine aggregate is not used and narrow distribution of coarse aggregate is employed.

An immense number of literatures have been written about normal concrete indicating its maturity as scientific subject even though many more aspects of concrete materials and structures still requires in depth study. On the other hand a considerable amount of effort has been devoted to study and develop contemporary porous/pervious concrete. The goal of this thesis is not towards studying and improving the inherent features of each of PNC's constituents, but rather to implement combination of engineering properties of both class of concrete to yield a novel approach for self-healing of concrete. Normal concrete which has strength properties from normal to ultra-high strength (± 30 to >200 N/mm²) *provides structural strength and stiffness* into the system. Meanwhile, porous concrete has porosity about 15% to 30% and *acts as internal channel*.

This present work utilizes *self-compacting concrete* (SCC). This special type of concrete – also known as *self-consolidating concrete* – being able to flow under its own weight will fill the mould with ease around the porous core in the interior and reinforcement bar. SCC achieves full consolidation without vibration (*passing ability* and *filling ability*) while completely filling formwork without segregation (*stability/resistance to segregation*) [151-154].

To achieve high flowability *high-range water reducer* (HRWR) admixture – also known as *superplasticizer* (SP) – is used while keeping the water cement (w/c) ratio low. *Viscosity enhancing* admixture – *anti-washout* admixture – is often used along with superplasticizer to maintain the materials cohesion [155]. This will attain highly workable concrete with sufficient level of viscosity to prevent aggregate obstruction while concrete is flowing. To maintain stability of SCC mixture in its plastic state higher amount of fine particle and limited amount of coarse aggregate is adopted. This will reduce internal collision among aggregates, decreasing internal contact stresses and reducing internal strain energy when the mixture flow [151].

Several fundamental studies of SCC rheology/workability, mechanical and physical properties, composition of constituents and admixtures, and SCC flow modelling have been performed [154]. Methods to design the SCC mixture have been developed leading to standardization [152-156]. In addition to these standards, several attempts have been made to produce SCC which demonstrates excellence in one or multiple engineering properties, such as; lightweight [157], high to ultra-high strength [158-161], durable and sustainable [160, 162]. Sonebi asserts the rheological characteristic, fluidity, and risk of cracking due to hydration heat of SCC may be enhanced by the incorporation of mineral admixture such as pulverized fuel ash (PFA), ground granulated blast furnace slag (GGBS), or limestone powder (LSP) [160, 162].

The second type of concrete used in this research is porous/pervious concrete. Strictly speaking, porous concrete has large volumetric void ratio in the concrete matrix. This might be obtained from infusing additives to form foam or gas bubbles into the fresh concrete or incorporating ultra-porous natural or synthetic aggregates. In this case the final product is concrete which has *large amount of relatively non-communicating voids*. This porous concrete exhibits properties of low to medium strength (± 15 to 50 N/mm²). Compared to normal concrete it demonstrates higher porosity (up to $\pm 30\%$) and higher thermal insulation values. Structural lightweight structures and walls with better thermal insulation are among the applications of this category of concrete [163].

The other type of porous concrete, also known as *no-fines, gap-graded, enhanced porosity concrete*, or *pervious concrete*, has millimetre-size air voids resulting from *coarse aggregate particles surrounded by thin layer of binder paste and abridged only in their point of contact* [163-166]. This deliberate mix design of uniform-sized aggregate and cement paste results into concrete which has high percentages of interconnected voids that allow fluid to permeate through the space between the particles. This special type of concrete possesses low to medium compressive strength (± 15 to 50 N/mm^2) and low tensile and bond strength as well. It exhibits higher porosity as well as higher permeability.

The recent interest on this materials of which its large implementation has been started in the first decade of twenty-first century is mostly due to environmental benefit in pervious concrete pavement [167]. Its water permeating and water draining properties outperform conventional concrete in; (1) controlling storm water runoff, therefore reduce flooding, (2) enhance ground water supplies, (3) controlling pollution, and (4) reduce aquaplaning therefore improve skid resistance in the pavement and runways during rainfall. Its sound absorbance property shows exceptional benefit in reducing traffic noise. Parking lots, sidewalks, driveways, vegetation bedding, embankment covers, beach structures and seawalls, and many architectural applications take benefits from this concrete. Recently a number of studies present the potential of porous concrete as energy absorbing material which may be used in low-cost blast protection structures [168-171].

Figure 2.2 reveals the internal structures of porous concrete. A thin layer of cement paste covers the aggregate and 'glues' aggregates together creating meandering and complex continuous pores in the order of millimetre. Observing this internal structure, it is obvious the load applied on the concrete is transferred through thin cement paste between aggregates. Moreover, as cement paste in the point of contacts is relatively weaker than the strength of aggregate and internal stresses are more concentrated in this link, this binder tends to act as point of failure in porous concrete. Consequently, porous concrete is more fragile than normal dense concrete. On the other hand, pore structures guide the ability of porous concrete to transport fluid from point to point.

Several fundamental studies have been carried out to examine factors influencing *rheological, mechanical* as well as *transport properties* of porous concrete [167, 172-180]. Characteristics and amount of *binder paste* which is affected by water to cement (w/c) or water to binder (w/b) ratio, composition of binder, amount of admixtures, viscosity and flow value determines not only workability/rheology but also strength of the final product and void structures [165, 166]. *Aggregate packing (aggregate interlocking)* which involves selection of proper size, shape, roughness and grading proportions of particles controls not only final strength but also pore size distribution, void ratio and total density [165, 178, 181, 182]. In addition, *Interfacial Transition Zone (ITZ)* in porous concrete affects overall strength and is dependent on the roughness and mineralogy of aggregate [165]. Contribution of densification/compaction is also significant to the strength and macroscopic pore structure [183-185].

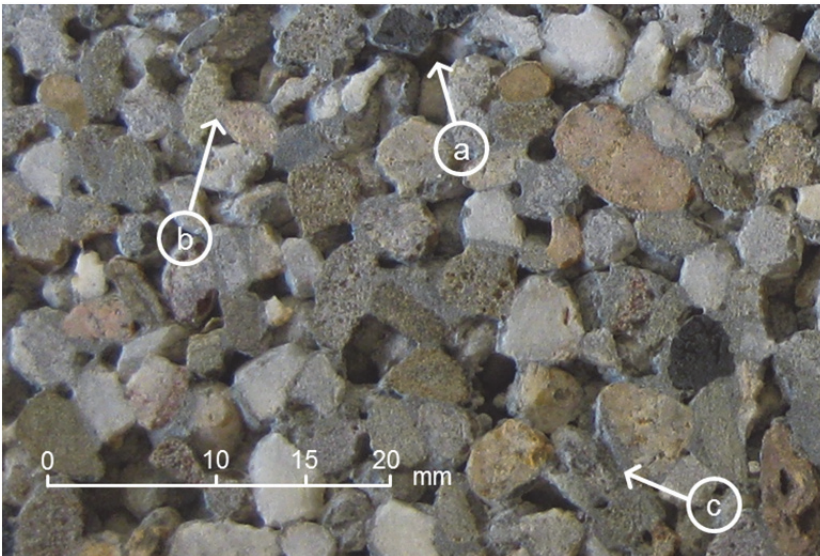


Figure 2.2. Cross section of porous concrete with uniform size gravel of 2-4 mm show some attractive features; (a) intentional continuous voids or 'empty spaces' within the porous concrete allowing liquid to permeate, (b) thin layer of cement paste abridge two adjacent aggregates, (c) cement paste clogged among aggregates.

Despite many parameters involved in determining mechanical quality of porous concrete, this thesis focuses solely on transport properties of POC where permeability is the key parameter. Permeability which is closely related to *porosity* and *hydraulic conductivity* is affected by *aggregate packing (aggregate interlocking)* and *amount of binder paste*.

As internal pores in the PNC are intentionally applied by using porous concrete therefore porosity (in %) and intrinsic permeability (κ) is important parameter of the system [172, 177, 186, 187]. In relation to permeability, hydraulic conductivity (K) describes the ease of fluid to move throughout the interconnected pores. This parameter is a function of intrinsic permeability, degree of saturation, density and fluid viscosity [179, 180].

2.2.1. Mix design and characterization of self-compacting concrete

The preliminary mix of self-compacting concrete in this research was formulated based on specification and guidelines for SCC provided by ERFNAC [188] and the work of Su *et al.* [152], Sonebi [160], and Asthiani, *et al.* [189]. Considering the reduction of the total strength after porous core is incorporated into the PNC, the 28 days strength target² was set should be above 35 N/mm².

Rheological properties of SCC, e.g. yield stress and plastic viscosity, can be determined by rheometer which is not always available. Therefore fresh properties (*workability*) of the material may be determined by means of several established simpler testing method [153, 190]. In this work slump flow and T_{50} flow rate test was used due to its simple mode of operation and requires only simple equipment.

² This is equal to typical concrete strength properties in Eurocode 2 $f_{ck}/f_{ck,cube} \sim 35/45$ N/mm² which has mean value of concrete cylinder compressive strength f_{cm} 43 (N/mm²).

The slump flow test measures total spread diameter of unrestricted deformability of fresh SCC on top of levelled smooth impermeable surface after the slump (Abrams) cone were lifted up. After SCC stops flowing, the largest diameter of the spread and the one perpendicular to that are measured. The value of the mean diameter is then calculated. Using this test, value of workable SCC should fall between 600 – 800 mm [189].

T₅₀ flow rate test was carried out simultaneously with slump flow measuring the time elapsed from the time the cone was lifted up to the time the SCC reaches 500 mm ring concentrically with the place of the mould. The time is measured with stopwatch having the accuracy of 0.1 second for recording the flow time T50. The acceptance value is 2 – 5 sec.

An alternative test is the spread flow test which may be used for SCC mortar. This test uses mini cone conforming to ASTM C 230/C 230 – 13. A truncated cone with Ø70 mm on top (henceforth all dimensions are in mm otherwise noted), Ø100 at bottom and 60 mm height is filled with non-compacted SCC mortar and placed in the centre of smooth surface. Concentric ring of Ø100, 250, 500 may be marked on top of the surface [190]. The value between 240 – 300 mm may be acceptable for SCC.

To allow a trade-off for low strength given by porous core in PNC two types of SCC mixtures were developed in this research; a normal strength concrete (NSC) and high strength concrete (HSC). For NSC the binder used consists of standard CEM I 42.5 and Fly Ash (class C as designated in ASTM C 618) meanwhile for HSC Silica Fumes were added to the binder mixed with tap water with ratio of water to binder (w/b) 0.40 for NSC and 0.30 for HSC. A polycarboxylic ether polymer based superplasticizer (SP) was used in the mixture which has 30% solid content and a specific gravity of 1.05.

Pertaining to the size of the PNC specimen, in all specimens, gravel aggregate with the largest value of 8 mm and specific gravity 2.67 (g/cm³) was employed. Quartz sand with specific gravity 2.61 (g/cm³) was used. The physical properties of concrete ingredients is shown in table 2.2

Table 2.2. Physical properties of cement and fly ash.

Physical properties	Cement	Fly ash	Silica fume	Gravel	River sand
Specific gravity (g/cm ³)	3.11	2.55	2.20	2.67	2.61
Bulk density (kg/m ³)	1506	1610	560	1530	1550
Void ratio	-	-	-	0.72	0.54
Mean diameter (µm)	45.0	20.5	0.65	-	-
Specific surface area (m ² /kg)	367	270	25000	-	-
Water absorption (%)	-	-	-	0.8	0.8

A finalized mixture was obtained after several trials which lead into composition as tabulated on table 2.3.

The mixing procedure (see figure 2.3), which applies for all concrete batches in this research, is as follows. At first, ingredients were dry-mixed for about 30 seconds at low speed and followed by 30 seconds at medium speed. The water and SP was

premixed and subsequently 2/3 was poured gradually into the mixing batch and an additional 1 min of mixing followed. The remaining 1/3 premixed solution was introduced for another minute while mixing. Afterwards for about a minute concrete is left at rest in the bucket after being scrapped from the bucket wall. At final stage the mixture is mixed for another minute.

Table 2.3. Composition of concrete mixture

Materials	Normal Strength NSC (kg/m ³)	High Strength HSC (kg/m ³)
Cement CEM I 42.5	425	435
Fly Ash C class	25	67.5
Silica Fume	-	45
Water	186	145
Aggregate 2-4 mm	328	318
Aggregate 1-2 mm	321	351
Aggregate 0.5-1 mm	345	345
Aggregate 0.25-0.5 mm	175	195
Aggregate 0.125-0.25 mm	-	100

The mixtures were poured into 40 × 40 × 40 mm³ cubes for determining strength development of 3, 7, 14 and 28 days. Mixtures were also poured into 150 × 150 × 150 mm³ cubes and Ø56 – 120 mm PVC cylinders for determining target strength of 28 days. After casting samples were then stored within wrapped plastic at 20 ± 3 °C for 24 hours prior to demoulding. Following that specimens were stored in the fog room with temperature about 20 ± 3 °C and RH 95 ± 5 % up to the day of compression testing.

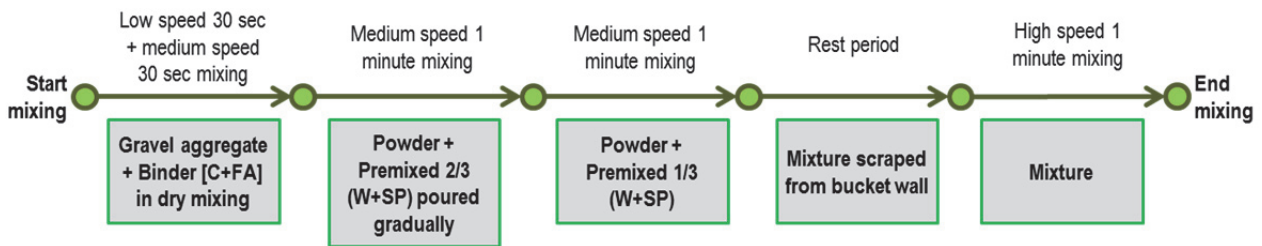


Figure 2.3. Diagram of mixing steps used in producing concrete batches

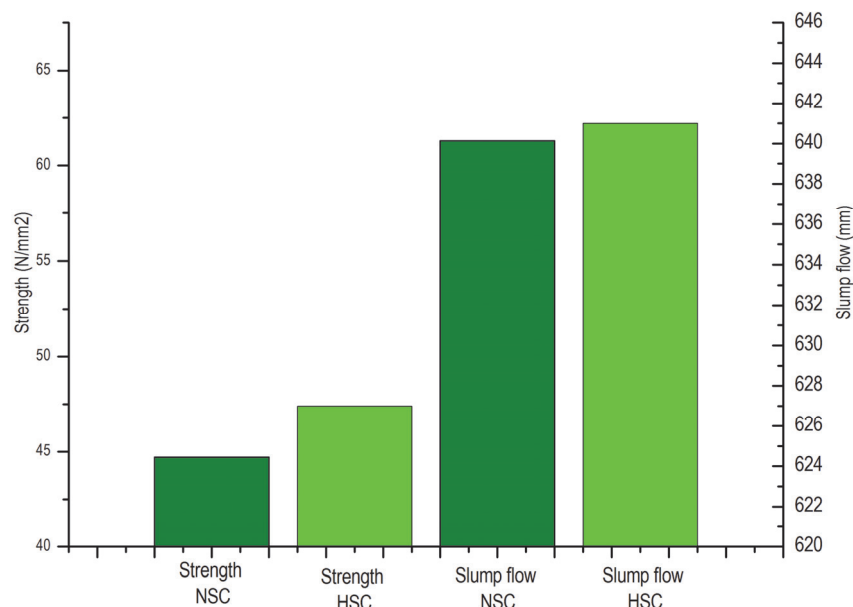


Figure 2.4. Strength (N/mm²) and slump flow (mm) of self-compacting concrete designed for main body of Porous Network Concrete

Figure 2.4 shows the results for NSC. The static strength obtained which is 44.7 N/mm² with standard deviation about 2.73 N/mm² and slump flow about 627 mm with standard deviation about 4.78 mm. For HSC the static strength obtained is 61.3 N/mm² with standard deviation about 3.11 N/mm² and slump flow about 641 mm with standard deviation about 3.12 mm.

2.2.2. Mix design of porous concrete

Production of a porous concrete having meso-size interconnected pores was accomplished by using single narrow graded coarse aggregate and eliminating fine aggregate in the mixture design. Recent studies [174, 176, 183-185] have provided insights of how mixture composition and compaction affect pore volume and structures in producing moderate to high compressive strength (10–40 N/mm²) pervious concretes. Random porous media such as porous/pervious concrete may exhibit different pore structures for a given porosity and vice versa. This in turn will affect the balance between functional requirements (e.g. permeability) with mechanical performance (e.g. strength) for desired levels of porosity.

The trial mix design of porous concrete in this research was formulated based on previous studies [191, 192]. The composition was 1513 kg/m³ gravel, 355 kg/m³ ordinary Portland cement CEM I 42.5, 22 kg/m³ Fly Ash (FA) and 1.0 l/m³ superplasticizer with 0.28 water/cement ratio. Three different single graded aggregates such as 1-2 mm, 2-4 mm and 5-8 mm were employed³.

The mixture was poured into the 40 × 40 × 160 mm steel mould and compacted by vibrating table for 30 sec. Afterward a plastic sheet was placed on top of the specimens which were then kept in the room at 20 ± 3 °C for 24 hours. After

³ Such aggregate size follows ASTM sieve number (i) #18 or 1.00 (passing 2.00 mm sieve, retained on 1.00 mm sieve), (ii) #10 or 2.00 mm (passing 4.00 mm sieve, retained on 2.00 mm sieve), (iii) #5 or 4.00 mm (passing 9.5 mm sieve, retained on 4.00 mm sieve).

demoulding the specimens were cured in the fog room for 7 days. The end product can be seen in figure 2.5.



Figure 2.5. Three porous concrete prisms 40 × 40 × 160 mm were made with different aggregate size, from left to right; 4-8 mm, 2-4 mm, and 1-2 mm.

It was observed that during production, the mix of fresh porous concrete has a low workability and is rather dry. In order to enhance the aggregate packing and interlock a proper compaction method and timing should be used. Extended compaction time will result in loss of moisture from the already dry mixture due to exposed particles to atmosphere. On the other hand it may improve specimen strength. In addition, vibration compaction promotes paste segregation. The paste flows and accumulates in the bottom side of the specimen creating uneven vertical porosity [180].

Table 2.4. Design experiment for porous concrete (A/B refers to aggregate to binder ratio).

A/B weight ratio	Aggregate size		
	1-2 (mm)	2-4 (mm)	4-8 (mm)
7.6 [1]	P12-1	P24-1	P48-1
5.0 [2]	P12-2	P24-2	P48-2
3.8 [3]	P12-3	P24-3	P48-3

Table 2.5. Composition of porous concrete mixture (A/B refers to aggregate to binder ratio).

Material (kg/m ³)	A/B ratio = 7.6			A/B ratio = 5.0			A/B ratio = 3.8		
	P12-1	P24-1	P48-1	P12-2	P24-2	P48-2	P12-3	P24-3	P48-3
Cement CEM I 42.5	183.5	183.5	183.5	275	275	275	367	367	367
Fly Ash C class	16.5	16.5	16.5	25	25	25	33	33	33
Water (w/b 0.33)	65	65	65	98	98	98	130	130	130
Agg. 2-4 mm	-	-	1513	-	-	1513	-	-	1513
Agg. 1-2 mm	-	1513	-	-	1513	-	-	1513	-
Agg. 0.5-1 mm	1513	-	-	1513	-	-	1513	-	-
SP (% vol to binder)	1%	1%	1%	1%	1%	1%	1%	1%	1%

Consistency of binder paste which is a function of type of binder, water-to binder (w/c or w/b) ratio, and the admixtures added is influential in achieving uniform distribution of binder paste phase throughout the porous concrete. Therefore, the admixtures (e.g. superplasticizer or set retarder) and water-to-cement ratio used in the mixture should be adjusted accordingly to obtain a workable and consistent mixture. While static compression and/or top impact compaction is preferable to consolidate porous concrete, in case set retarder is used, longer time for compaction will enhance strength and decrease porosity [183, 184].

This work requires porous concrete which has porosity and permeability (hydraulic conductivity) as large as possible while having moderate strength. These properties are required since the porous concrete will serve as channel in the core of PNC and is not required as load bearing component.

In order to satisfy the requirement a design experiment was set as depicted in the table 2.4. Gap-graded small particle size; 1-2 mm, 2-4 mm, and 4-8 mm aggregates were used. Aggregate weight was 1513 kg/m^3 with specific gravity of 2.67 g/cm^3 . Binder (*cement CEM I 42.5 and fly ash C class*) content was varied by weight ratio to aggregate with physical properties as in table 2.2. Water binder (w/b) ratio of 0.33 was kept at the same value for all mixture with polycarboxylic ether type SP (Glenium 51 which has 30% solid content) was set to have volume of 1% to binder. The design experiment is summarized in the table 2.4. P12 stands for porous concrete with aggregate size 1-2 mm and -1 refers to aggregate-to-binder ratio accordingly. Table 2.5 summarizes the composition of the porous concrete mixture.

To prevent agglomeration and ensure consistent mixture of paste, the binder was dry mixed for about 1 minute in epicyclical rotary mixer followed by another minute at medium speed prior to mixing with water. Following this dry mixing, a premixed water and superplasticizer was introduced gradually for about 1 minute mixing followed by another minute of paste phase mixing. Finally the aggregate was poured and mixed into binder paste for one minute in medium speed mixing. Mixing process was concluded by 1 minute mixing at high speed. Approximately 15 liter mixture was mixed per batch.

The compaction method used was hand compaction using a steel cylinder mounted on a long steel rod. This poker was then top-impacted by hammer which its end is covered with hard rubber. This will allow the particles in the porous concrete to interlock properly while the thin layer of paste binder is distributed evenly and will not flow and accumulate in a certain position, i.e. in the bottom side of specimen.

After mixing, the mixture was placed into PVC cylinder with inner diameter of 56 mm and height of 120 mm in three layers. Every layer was compacted by steel cylinder $\text{Ø}55\text{-}50$ mm mounted on 250 mm long steel. Acting as poker this compacter was hammered 10 time every layer. Prior to addition of the next layer, top surface of the last layer was roughened by steel rod allowing better particle interlocking with its subsequent layer. This type of specimen will then serve as porous concrete mechanical testing specimen and for transport properties characterization.

Specimens along with its mould were then wrapped with plastic and stored in the room with temperature of $20 \pm 3 \text{ }^\circ\text{C}$. Cylinder $\text{Ø}56 - 120$ mm specimens were

demoulded 24 hours after casting. Following demoulding, all specimens were cured in the fog room with temperature about 20 ± 3 °C and RH 95 ± 5 % for 28 days.

2.2.3. Characterization of porous concrete

a. General approach and mechanical test

In general mechanical properties of porous concrete can be satisfactorily described by its strength and stiffness. More detailed quantity may be derived from those two parameters or tested with specialized setup depending on the objectives of the experiment or the goal of porous concrete application [165].

The compression test is one of the common methods to determine static strength and stiffness, while direct tension, bending/flexural, splitting test which are common for concrete may also be employed for porous concrete. Impact test by means of dropped weight or field blast test have been applied to determine dynamic response and dynamic strength of moderate to high strength porous concrete [170, 193]. A computational procedure developed by National Institute of Standards and Technology (NIST) was employed by Sumanasooriya *et.al* to examine elastic properties of porous concrete on 3D reconstructed specimen [194]. Image processing and analysis supports the process in producing $100 \times 100 \times 100$ pixel representative volume element (RVE) [195].

Besides mechanical properties, functional properties of porous/pervious concrete are also of interest. These properties reflect not only the *transport properties (hydraulic performance)* – how easy fluid flows through its pores [172, 177, 179], e.g. porosity, permeability, of porous concrete but also *durability*, e.g. freeze-thaw resistance, abrasion resistance, sulphate resistance, clogging, [196, 197] and *sound absorbance* [186]. Among those properties, porosity and permeability is the most significant parameter studied in this work.

It is very intuitive to relate porous concrete performance with its porosity since this parameter is simple to measure and visually observable. Further, by the same intuition, one may relate that increasing porosity will, in general, increase permeability. However, while porosity arguably is one of the most important features, other pore parameters such as pore size and connectivity may also influence the hydraulic performance of porous concrete [172].

Experimental as well as computational studies may be implemented to characterize porous concrete pore structure and transport properties. Bentz reports an attempt to develop ‘Virtual Pervious Concrete’ at NIST [167], a computational program to create 3D microstructure to investigate percolation, conductivity, and permeability. Sumanasooriya *et al.* [195], implement automatic image analysis on 2-dimensional porous concrete sections which then is used to extract pore structures features. Following that, stereological algorithm is used to transform the image and determine 3-D pore structures characteristics. They develop a computational procedure to predict the permeability of 12 different 3D porous concrete mixtures based on planar images [173].

In this work three parameters are investigated namely static compressive strength, porosity and permeability (hydraulic conductivity). Triplicate measurements were conducted for each type of porous concrete and each test to calculate the mean value. Compressive strength was determined as per ASTM C39 where cylinders Ø56 – 120 were capped using polymer based on Poly-methyl methacrylate (PMMA) composed of a powder monomer PLEX® 7724-F containing initiator and a liquid monomer PLEXIMON® 801, at 28 days. Table 2.6 summarizes the strength of porous concrete individual specimens tested with uniaxial monotonic compression test.

b. Determination of porosity of porous concrete

Porosity is one important feature in transporting fluid through porous media although not all pores, i.e. isolated pores, contribute and take part in this transport process. This suggests that effective porosity which is the fraction of pores able to transfer fluid plays greater role. However, it is observed from many studies that for porous concrete most of the pore voids are sufficiently large enough to transfer water compared to other material with similar porosity [179]. Therefore porosity in this study may be thought as total porosity which value is almost equal to the effective porosity. One technique to ‘see’ effective porosity is by impregnating the porous core with epoxy resin contain fluorescent dye which differentiates pore phase from solid phase under UV light.

Porosity in this work was determined by two generally accepted methods; water saturation which takes the ratio between void occupied by water and the solid phase and image analysis which uses a digital image to extract information needed.

By means of water saturation, in this work, porosity was measured with two procedures. First procedure is as follows. Three porous concrete cylinders Ø56 – 120 for each type as indicated at table 2.4 were submerged in water for 24 h to saturate the pores in the paste matrix. After removing from water and achieving saturated surface dry (SSD) conditions, the specimens were tightly covered with two layers plastic wrap which was then enveloped with transparent adhesive tape. The specimens were placed on aluminium plates and the bottom of the cylinder was sealed with silicone sealant ensuring water stays in the porous concrete voids as depicted at frame 1 figure 2.6. The weight of these specimens, denoted as W_1 , was measured. Subsequently water was poured to saturate all interconnected pores in the porous concrete. The weight of the specimens with water added, denoted as W_2 , were then measured, see frame 2 figure 2.6. The weight difference, $\Delta W = W_2 - W_1$, was the weight of water in the voids. This weight was then converted into volumetric porosity (ϕ_v) as percentage of the total volume of porous concrete specimens [177, 186]. Table 2.6 shows the porosities of various specimen tested using the procedure abovementioned.

The second procedure is based on the void ratio. Porosity may be expressed as total void ratio (V_v) which was obtained by dividing the difference between the weight (W_2) of the cylinder specimen under water and that (W_1) measured at SSD condition, achieved by oven drying at 35°C, RH 50% for 24 hours. The equation used to obtain this value is as follows [51]:

$$V_t = 1 - \left(\frac{W_2 - W_1}{\rho_w V_{sp}} \right) \times 100\% \quad (2.1)$$

Where: V_t = Total void ratio of the porous concrete, (%); W_1 = weight of cylinder specimen in SSD, (kg); W_2 = weight of cylinder specimen under water, (kg); V_{sp} = Specimen volume, (mm^3); ρ_w = density of water, (kg/mm^3).



Figure 2.6. (i) Three porous concrete cylinders $\text{Ø}56 - 120$ were enveloped with plastic membrane for measuring volumetric porosity, (ii) specimen was weighed on a scale.

In addition to previous methods, porosity was also determined using planar image analysis procedure and automatic 3D reconstruction (tomographic image) obtained from micro CT scan. To obtain 2D digital image, porous concrete cylinders $\text{Ø}56 - 120$ mm specimens were impregnated with a premixed low viscosity epoxy with fluorescent powder dye (Epodye). The specimen was then sawn into three sections. A photograph of the surface was taken by a digital camera under ultraviolet light distinguishing pore phase (bright yellow) from the solid phase (dark). Following image acquisition, a well-established image analysis procedure was implemented using Image-J, an open (free) image processing software. The images were cropped and converted into grayscale and subsequently binary image. Afterwards the image was segmented by determining a threshold value from histogram, see figure 2.7. This process differentiates the pore and the solid spaces. Eventually, the area fraction of pore was obtained from ratio of pore area to total area of image. The result of the porosities of all specimens given in table 2.4 is summarized at table 2.6.

X-ray micro computed tomography (micro CT) is a recent effective technique to non-destructively characterize material. The procedure is even more compelling because it can ‘see’ the interior micro structure of the material under investigation. When an X-ray radiates onto a specimen a variation of absorption intensity is detected and recorded by a detector which then composes a 2D radiograph image. Combining information from a series of 2D X-ray images, a 3D digital image is reconstructed by means of tomographic algorithm by which each voxel (volumetric pixel) represent X-ray absorption of the point. In general working principle of this

powerful techniques can be seen in figure 2.8 [198]. Additionally, minimal specimen preparation is necessary for this procedure.

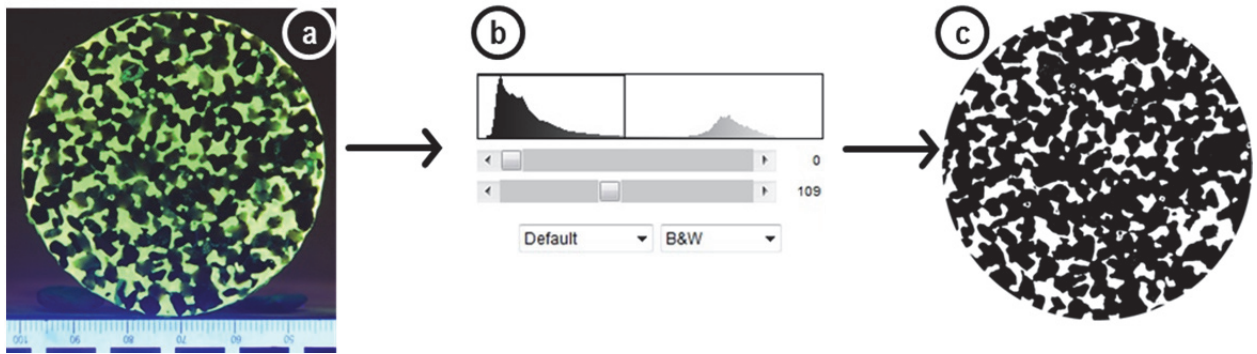


Figure 2.7. (a) An cross sectional image of epoxy impregnated porous concrete cylinders $\text{\O}56 - 120$ mm specimens was acquired by digital camera under UV light. The image was then cropped to obtain 600 pixel diameter and converted into binary image. (b) Image segmentation was carried out by defining a threshold value to discriminate pore phase from solid phase. (c) Binary image on which the pore fraction was calculated. The black area represents solid phase of porous concrete.

To construct 3D tomographic image, porous concrete cylinders $\text{\O}26 - 120$ mm specimens were cut to acquire specimens with length about 50 mm. The specimen was then placed on the object stage positioned in the chamber between X-ray source and detector. The object stage was rotated progressively at approximately 0.25° to acquire 1440 projections. As the specimen was maintained in the radiation field of view throughout the entire 360° rotation, ensuring complete full display of the sample, 2.3 magnification was obtained for $\text{\O}26$ mm specimen.

VGStudio MAX 2.0 software was used to automatically reconstruct the accumulated voxel intensity data. The remarkably valuable information retrieved from this volumetric reconstruction is voxel intensity histogram, see figure 2.8b. This 3D image can later be segmented by defining a threshold value separating pore phase and solid phase. Porosity then was determined of the ratio of pore volume to the total volume of the image. The result of the porosities of all various specimens is summarized at table 2.6.

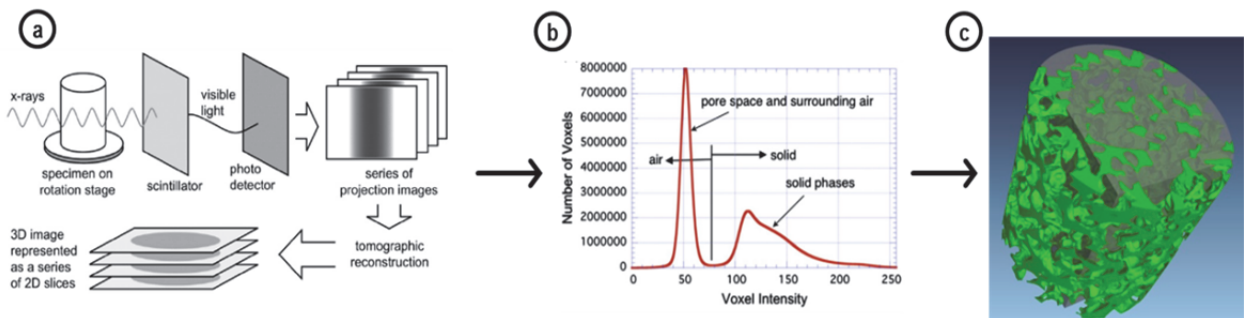


Figure 2.8. (a) Working principle of X-ray micro computed tomographic (CT) scan where series of planar (2D) radiographs recorded by photo-detector is reconstructed mathematically into 3D digital image. (b) Image segmentation process defines a threshold value on histogram of voxel intensity to separate pore phase and solid phase. (c) 3D reconstruction image is colour-coded on which void fraction may be distinguished and calculated. Frames (a) and (b) are taken from Landis and Keane [52].

In addition to the process aforementioned, for every specimen type one planar image taken from this micro CT is arranged according to aggregate size used and aggregate-to-binder (A/B) ratio and presented in the figure 2.9. These images visualize the internal pore structure of the porous concrete. It may be observed from the figure that from left-to-right the void fractions seemingly becoming higher as the bigger diameter aggregate was utilized. This trend is also recognized from bottom-to-top frames from figure 2.9 as the less binder content was used, the higher porosity obtained.

c. Characterizing hydraulic conductivity

As the design intention is that porous concrete should be easy for fluid to flow, porosity alone would not be sufficient as design parameter. Several condition such as; disconnected (dead-end) pores, stagnant pockets, capillary pores, small enough pores which reduce fluid flow due to surface tension, may lead into reduction of total (useful) porosity. Therefore drainable interconnected pore is the important descriptor for porous concrete in which hydraulic conductivity is a valuable parameter.

Hydraulic conductivity may be seen as a quantitative measure describing the ease of fluid, e.g. water, move through pore spaces. This parameter is derived from Darcy's Law of flow through porous media (Hillel, 1980; Bear, 1988). Several fundamental studies have been conducted to develop hydraulic conductivity (permeability) of pervious concrete test setup based on constant head or falling head principles. These setups are different from standardized method to measure permeability of porous media, e.g soil, due to large interconnected pore network in pervious concrete. Montes and Haselbach and Narayanan, *et al.*, developed a specialized U-shaped falling head permeameter for this purpose.

Adopting their approaches, in this work hydraulic conductivity setup is designed as computerized U-shape permeameter based on falling head principle depicted in figure 2.10.1. A 220 mm transparent PVC cylindrical tube with inner diameter of 50 mm was lathed to have inner diameter of 56 mm for 120 mm long in which specimen can be placed. A graduated cylinder having inner diameter 50 mm and length of 250 mm was placed tightly on top of it by means of threaded PVC connector. O-ring rubber was used inside of this connector to prevent water leakage. Through this transparent cylinder the water level could be monitored. A valve was connected at 10 mm from the bottom of the tube column allowing water flow to be controlled manually. A bucket to hold outflow water was put on top of a load cell next to the drain pipe allowing the flow rate to be recorded simultaneously over time. The scheme of water flow and the height of the tube water column can be seen in figure 2.10.3.

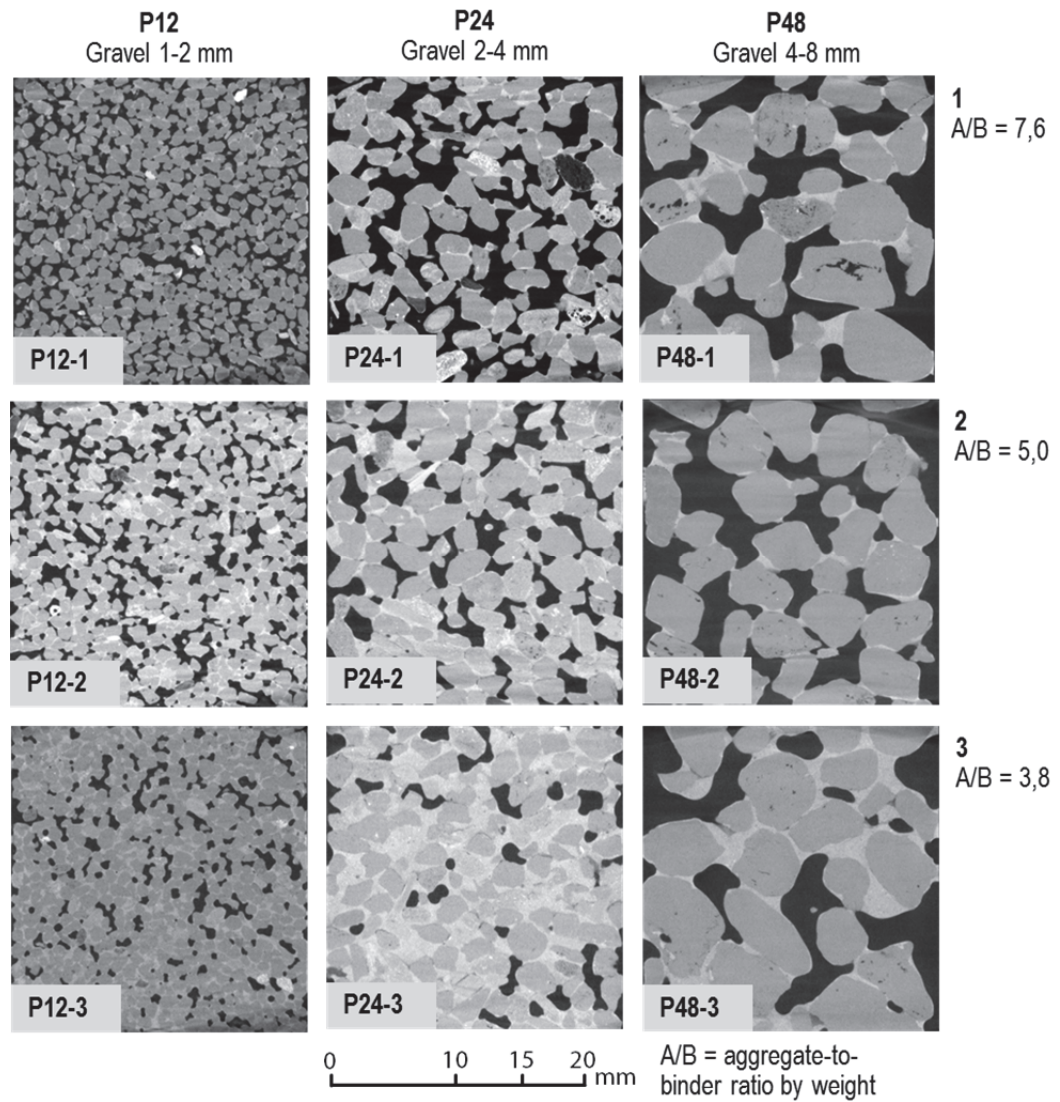


Figure 2.9. Series of images of individual porous concrete pore structure taken with micro CT-scan.



Figure 2.10. Setup of falling head permeability (hydraulic conductivity) test where (1) the permeameter is connected to PC for recording the time and weight increment of outflow water. (2) Specimen is inserted into permeameter setup and O-ring rubber is mounted to seal the setup from leakage. Frame (3) shows the scheme of water flow and dimension of the test cell.

The hydraulic conductivity test was started by inserting porous concrete $\varnothing 56 - 120$ mm specimen into the water column and an O-ring was placed on top of it as illustrated in figure 2.10.2. Subsequently the graduated cylinder was connected on top this water column tube. Water was poured into the graduated cylinder, flowing through the specimen compartment, and flowing out through draining tube. This was done in order to dispose of air entrapped in the system, to saturate the specimen completely, and to achieve same water level at drain pipe and graduate cylinder prior to the testing. Afterwards the valve was closed and water was filled into the graduate cylinder. The measurement started with the opening of the valve at time, t_1 , when the water head reached 260 mm to the final head 10 mm at, t_2 , was recorded. Triplicate measurement was taken and the mean value of time elapsed is used.

Following Montes and Haselbach [179], Narayanan, et.al [186], Bear [150], Hillel [199], and ASTM D 5084-03 (*Standard Test Methods for Measurement of Hydraulic Conductivity of Saturated Porous Materials Using a Flexible Wall Permeameter*), data obtained from the test was used to calculate hydraulic conductivity based on the equation as follow:

$$K_s = \frac{aL}{A\Delta t} \ln \frac{b_1}{b_2} \quad (2.2)$$

where K_s represent the saturated hydraulic conductivity, a is the cross-sectional area of graduated cylinder, A is the cross-sectional area of specimen, L is the length of the concrete sample, Δt is the time elapsed from which the water head reached the b_1 mark at 200 mm until the water head reached 1 mm at the b_2 . The result of the porosities of all various specimens is summarized at table 2.6.

Table 2.6 shows the results from characterization test sufficient for the purpose of the design of PNC materials. Compressive strength represents the mechanical property, *how strong is the material when load is applied*, and porosity and hydraulic conductivity represent transport properties, *how easy the fluid (e.g. healing agent from point to point can flow in the porous core flow) in the PNC*.

From table 2.6 it can be observed that the range of strength of the mixture falls between 12 – 22 N/mm² which may be thought is quite low to moderate compared to higher strength up to > 40 N/mm² developed by other researchers [18, 19, 44]. As the strength is considered secondary feature of the porous concrete used in the PNC, the results obtained from the mixtures are acceptable. Further, it is better to choose the mixture which would result in strength higher than 15 N/mm² as porous core specimen which may substantially contribute to the overall strength of PNC. Mixtures with darker code in the table fall in these criteria.

From the same table, the range of porosity of the mixtures is in between 11 to 27.5 %. P48-1 exhibit the highest porosity since it used higher aggregate size (4-8 mm) and used less binder, meanwhile P12-3 used the highest amount of binder and the smallest aggregate size (1-2 mm) and has the lowest porosity. It can also be seen that all mixture using aggregate size 1-2 mm have porosity values less than 20%. Mixtures with higher binder content or with aggregate-to-binder ratio 3.8 also show less than 20% porosity. Mixtures with a lighter grey mark in the table fall in this criterion.

Table 2.6. Mechanical and transport properties of porous (pervious) concrete; compressive strength (N/mm²), porosity (%) measured by water displacement and image analysis, and hydraulic conductivity (cm/sec).

Porous Concrete		Compressive strength (N/mm ²)	Volumetric porosity, ϕ_v (%)	Total void ratio, V_t (%)	Porosity based on 2D image (%)	Porosity based on 3D image (%)	Hydraulic conductivity (cm/sec)
A/B ratio	Code						
7.6 [1]	P12-1	12.3	18.7	17.8	19.9	19.9	0.97
	P24-1	14.7	26.3	25.4	23.2	21.6	1.39
	P48-1	14.5	26.9	27.3	24.7	24.2	1.82
5.0 [2]	P12-2	14.9	16.9	17.4	16.9	17.3	0.91
	P24-2	19.1	24.2	25.5	23.8	25.3	0.96
	P48-2	20.9	20.2	19.7	20.9	19.7	1.01
3.8 [3]	P12-3	17.5	13.6	14.9	11.6	15.5	0.52
	P24-3	19.7	19.5	18.5	17.7	19.1	0.76
	P48-3	21.4	16.6	15.1	14.6	17.6	1.01

All values of the hydraulic conductivity of the porous concrete mixtures produced in this work lay in between 0.5 to 1.9. Mixture P48-1 which had the least binder content and highest aggregate size (4-8 mm) produced the largest void (porosity) and the largest hydraulic conductivity (permeability) which makes this the most pervious specimen. P12-3 produced the lowest value of hydraulic conductivity since aggregate used is small and they are bound with higher amount of binder resulting in low pore diameter and interconnectivity. Based on the category set in the table 2.1 all mixtures may be seen as pervious concrete which may be used as porous core of PNC.

According to the design criteria set in the subchapter 2.1; P24-1, P24-2, P48-1, and P48-2 are the mixtures which have porosity > 20% and exhibit hydraulic conductivity in the *pervious regime*. Therefore these mixtures satisfy the requirement and may be used as porous core. By using this mixture in PNC, it is believed the porous core will be penetrable by liquid healing agent, effectively, depends on viscosity of healing agents. As four different mixtures were obtained another constraint has been set namely mixture which has strength > 15 N/mm². By applying this simple optimization procedure two porous concrete mixtures pass the evaluation and may be used for the porous core; P24-2 and P48-2. However, eventually, mixture P24-2 was chosen to be the core for the PNC cylinder and prisms tested for autonomous healing.

2.3. Porous Network Concrete

2.3.1. Mix design and production of Porous Network Concrete

a. Specimen design

In realizing the proposed self-healing concept production of Porous Network Concrete was accomplished by combining two components, self-compacting concrete (SCC) and porous concrete (POC). Two specimens have been designed; the *cylindrical specimen* mainly used at preliminary stage, i.e. material properties testing, and *prism (beam) specimen* which will be utilized fully in autonomous healing test.

The cylinder has dimension diameter $\varnothing 56$ – height 120 mm with a $\varnothing 26$ – 120 mm porous core in the centre. The cylindrical specimens serve as specimen for fluid transport test; e.g. measuring volumetric porosity, hydraulic conductivity and

permeability. The specimens also serve as samples for uniaxial monotonic compression for determining static compressive ‘strength capacity’ and tension test for crack formation to be sealed by healing materials manual injection. To provide stress concentration in the tension test specimen, a 4 mm wide and 4 mm deep circumferential notch was introduced in the mid height of the specimens. Figure 2.11 shows the schematic design of the material.



Figure 2.11. Artist render of Porous Network Concrete specimen. The cylinder specimen was designed to accommodate trial experiment proving the healing mechanism proposed.

The prism specimens have a dimension of $55 \times 55 \times 295$ mm and a $25 \times 25 \times 295$ mm porous core in the centre, illustrated in figure 2.12. The specimen is used for flexural three-point bending tests for crack formation and manual/automatic healing injection tests. A $\varnothing 2$ mm threaded steel reinforcement bar is placed underneath the porous core to ensure non-brittle failure of the prism when bending stress is applied.

b. Prefabrication and preparation of porous core

The first step to produce Porous Network Concrete is to produce its porous core. The mixing procedure followed the production of the porous concrete above mentioned. Two different moulds were used depending on the type of specimen. First mould was a PVC cylinder with inner dimension of $\varnothing 26 - 120$ mm which was then used for porous core for PNC. Similar procedure is used for mixture placement into the mould. For compaction a steel cylinder $\varnothing 25-50$ mounted to a long steel rod is used as compacter hammer 10 times for each layer. The top surface of the last layer was roughened by steel rod ensuring particle interlocking when the subsequent layer was added.

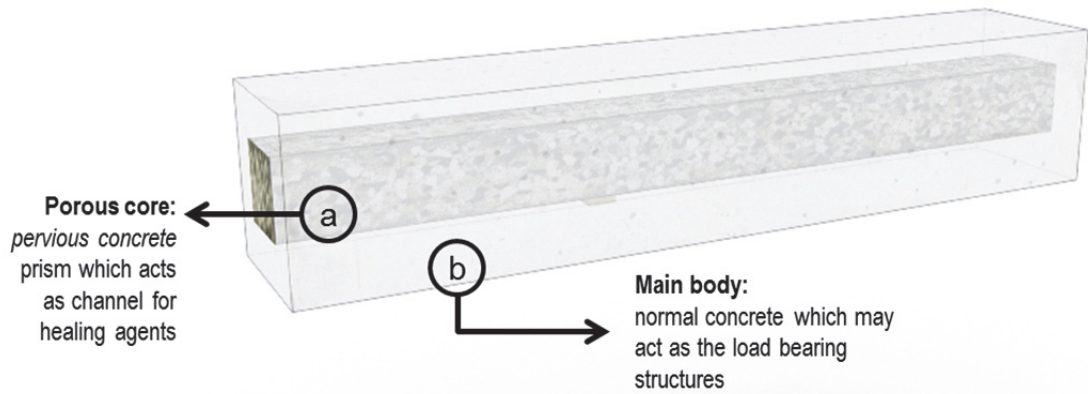


Figure 2.12. Porous Network Concrete prism specimen with prism porous core in the centre utilized for 3-point bending test.

The second wooden mould has a dimension of $25 \times 25 \times 295$ mm which was used to produce the porous core for the prism/beam specimen. The mixture was poured in two layers into the mould and was compacted by hand compaction. A steel strip was placed on top of the mixture and impacted by a hammer 10 times for each layer. A roughened surface with a fork was achieved prior to adding the next layer of porous concrete mixture.

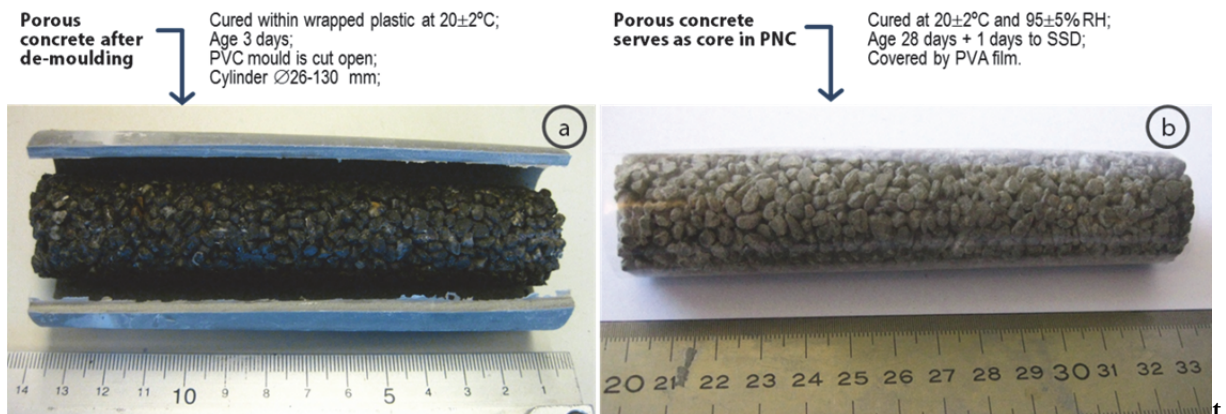


Figure 2.13. Figure (a) shows the porous core cylinder after the PVC mould was cut open longitudinally at 3 days and figure (b) exhibits the PVA film covered porous core ready to be placed in the mould for PNC production.

Specimens along with its mould were then wrapped with plastic and stored at room temperature of 20 ± 3 °C prior to demoulding. Prisms specimens were demoulded 24 hours after casting. Meanwhile cylinders $\text{Ø}26 - 120$ mm were demoulded 3 days after casting to achieve sufficient strength. It is observed that the vibration energy, when PVC mould was cut open longitudinally by electric hand saw, will break the specimen when demoulding was done earlier. Following demoulding, all specimens were cured in the fog room with temperature about 20 ± 3 °C and RH 95 ± 5 % for 28 days.

After 28 days, the specimens were taken out from the fog room and allowed to get SSD condition for 24 hours. Figure 2.13.b. shows the cylinder $\text{Ø}26 - 120$ porous

core that was prepared for casting of PNC. Two different treatments were adopted; in the first group of specimens the porous cores were covered with water soluble PVA film and the other group of specimens were not. The idea of covering the porous core came out of the fact that this film is used to package household laundry detergents. This film is able to isolate its content from the moment of packaging to the time when the dissolution is required. It is also used in handling toxic/contaminated disposal at hospitals.

c. Production of PNC cylinder

In the case of PNC production, covering porous core with this film until the moment (excess) water from fresh SCC poured dissolves the film will protect the core from being intruded by concrete matrix. In other words, the porous core stays porous as it is intended. In addition, this will also provide a chance to observe the effect of the PVA film in protecting the core and in the healing performance in general. For this PNC production, only one layer of PVA film is used that is glued at its edge by commercially available water soluble glue.

The film supplied by HARKE GmbH was SOLUBLON which is polyvinyl alcohol (PVA), grade KA with thickness of 40 μm having ability to completely dissolve at cold-to-hot water temperature. This KA 40 grade film is dissolved in 38 ~ 55 seconds at 10 °C and approximately 29 ~ 40 seconds at 20 °C.

The porous core was then placed in the center of a PVC cylinder mould having inner diameter of 56 mm. A PVC ring with thickness of 4 mm was used to hold the core. Two types of porous core; without and with PVA film cover were used in the production. Figure 2.14.a illustrate the PVC mould and PVC ring with two different porous cores and figure 2.14.b. shows the core in the centre of the mould.

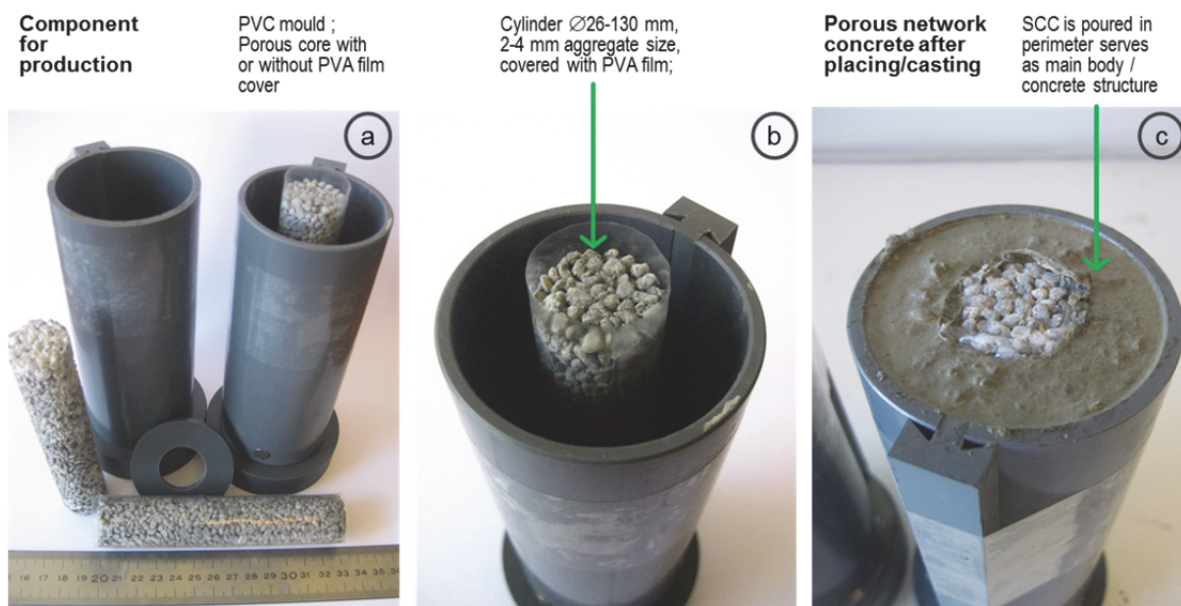


Figure 2.14. Production and preparation of the Porous Network Concrete cylinder. Figure (a) exposes the mould, the PVC ring, and the core either covered with PVA or not. Figure (b) shows how the porous core covered with PVA film is placed in the centre of the mould. Figure (c) displays the end-phase of casting.

Following the preparation of prefabricated porous core in the mould, the self compaction concrete (SCC) mixture was prepared according to the procedure explained in the subchapter 2.3.1. After mixing, this normal strength and high strength SCC was poured into the mould surrounding the porous core as shown in figure 2.13.c. The design experiment for this production is shown in the table 2.7, with ‘A’ in PNC code designation means without PVA film cover and ‘B’ stands for with PVA covering porous core.

After casting all the specimens were covered with plastic and stored in the laboratory casting room for 24 hours at ambient temperature (20 ± 3 °C). Following the procedure, specimens were demoulded and cured in the fog room at temperature 20 ± 3 °C and RH $95 \pm 5\%$. Specimens were cured for 28 days for porosity testing, compression, and tension-to-healing testing.

Table 2.7. Design experiment for Porous Network Concrete (PNC)

A/B weight ratio of porous core	Porous core			Main body			P24-1-(A/B) + High strength concrete
	aggregate size (mm)			Normal Strength Concrete			
	1-2	2-4	4-8	NSC	NSC	NSC	
7.6 [1]	P12-1	P24-1	P48-1	P12-1-A	P24-1-A	P48-1-A	P24-1-A-HSC
				P12-1-B	P24-1-B	P48-1-B	P24-1-B-HSC
5.0 [2]	P12-2	P24-2	P48-2	P12-2-A	P24-2-A	P48-2-A	P24-2-A-HSC
				P12-2-B	P24-2-B	P48-2-B	P24-2-B-HSC
3.8 [3]	P12-3	P24-3	P48-3	P12-3-A	P24-3-A	P48-3-A	P24-3-A-HSC
				P12-3-B	P24-3-B	P48-3-B	P24-3-B-HSC

Figure 2.15 exhibits the cross sectional visualization of PNC cylinder with interconnected pores in its interior. Figure 2.15.a is PNC which has PVA film covered core indicating a rather clear boundary between solid concrete and porous core. It is also observed visually that partial dissolution of the PVA film happens in the mixing process. It is hard to quantify the extent of the dissolution of the film. However this, as also will be proven in the Chapter 3, will not affect the healing agent from flowing out from the core to the crack opening. Figure b shows the PNC that has a porous core without PVA cover. No clear boundary between the two phase material is observed indicating that some concrete matrix, most probably cement or mortar paste, entered the surface of the porous core. One immediate thought is that porosity of the porous core would be reduced due to this infiltration. However, in the porosity testing and through micro CT scan (Chapter 3), this reduction will not affect significantly the capacity of the core to transport healing agent.

d. Production of PNC prisms

Prefabricated $25 \times 25 \times 295$ porous core prisms (beam) was allowed to achieve SSD condition after taken out from the curing room. This process was carried out by putting the specimen at ambient environment for 24 hour. Afterward one type of specimen was covered with PVA film and the other was not.

Wooden moulds of $55 \times 55 \times 295$ mm were used to cast the PNC prisms. U-shape wooden hooks were used to support the prefabricated porous core. To ensure non-brittle failure of the PNC prisms under three-point bending, a $\varnothing 2$ mm threaded steel

was put underneath the porous core. Figure 2.16. shows the specimen preparation steps. Following the preparation of the core, SCC mixture was prepared and mixed based on the procedure described in subchapter 2.3.1. The SCC mixture was then poured into the mould as demonstrated in figure 2.16.b.

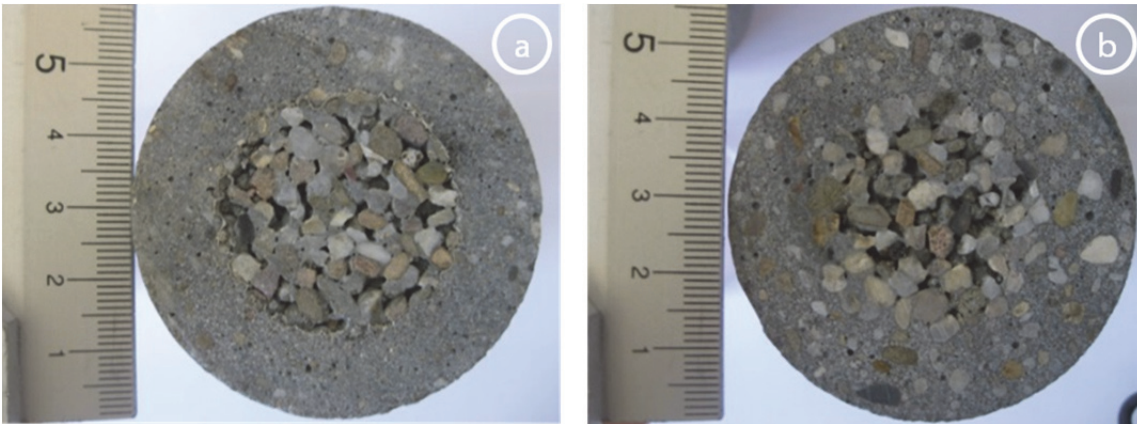


Figure 2.15. Cross section of the PNC specimen; figure (a) shows PNC with PVA film covering its porous core and clear indication of boundary between two phase of the material, figure (b) shows PNC without PVA film covering the core showing more a irregular transition between main body and the core.



Figure 2.16. Production of PNC prism; Figure (a) shows the mould with $\varnothing 2$ mm steel rebar that was put underneath the porous core prism which is supported by a wooden hook. Figure (b) demonstrates how the 'dense-normal' concrete is cast around the core.

The same curing process as in the production of the PNC cylinders was followed. The result is a Porous Network Concrete beam as shown in the figure 2.17, with the square side of the prism protruded out as the result of the wooden hook used for the casting. These bulges were sawn off to obtain $55 \times 55 \times 285$ mm PNC specimens ready for bending-to-healing testing. The longitudinal sectional of the prisms is

visualized in figure 2.17.b showing the porous core in the mid of the specimen height and rebar under the core.

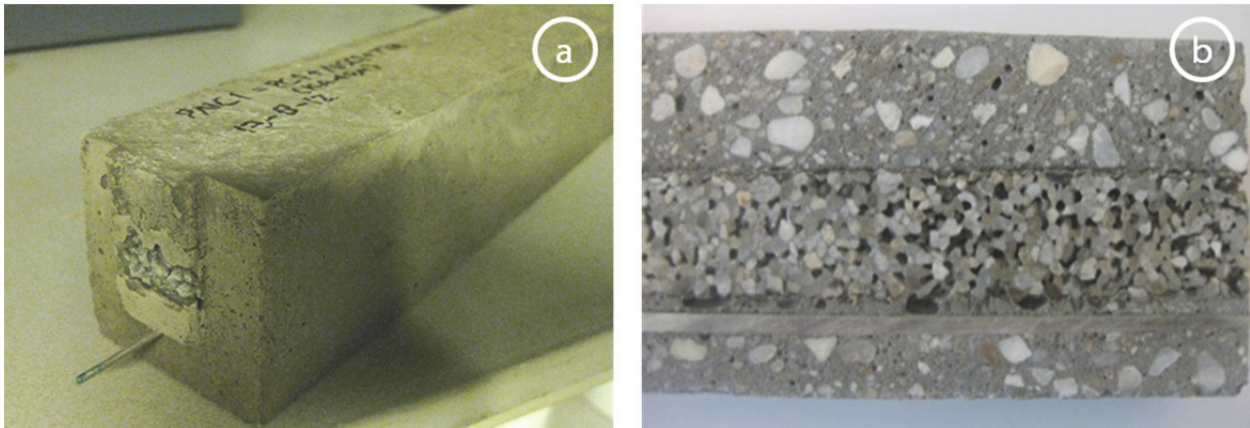


Figure 2.17. PNC prisms specimen; Figure (a) shows specimen before protruded section is sawn. Figure (b) portrays the section of PNC prism.

2.3.2. Characterization of Porous Network Concrete

Prior to characterize and study PNC mechanical properties, concepts and terms related to strength need to be clarified. Term ‘*strength*’ refers to a broader category of strength of material and structure and may not be applicable for the specimen studied in this work. Considering a PNC cylinder, different dimension of the porous part and main body will certainly result in different strength. Thus term ‘*strength*’ will be ambiguous. Henceforth, in this work the term ‘*strength capacity*’ is used. It refers to the strength (N/mm^2) of the PNC specimen with shape and dimension specified in this work.

It is worth noting that the strength of Porous Network Concrete depends not only on the strength of each its constituent material; porous concrete and normal dense concrete, but also on the geometry and configuration of the concrete structure element and reinforcement bar. However, during design phase, trade-off may be implemented with several approaches; e.g. compensating low strength of porous concrete core with high strength (dense) concrete main body.

In order to illustrate the trade off and to determine the *strength capacity* of Porous Network Concrete cylinder specimen, a compression test complying with ASTM C39 was employed. Specimen cylinders $\text{Ø}56 - 120$ mm were capped at 28 days and tested under uniaxial monotonic compression loading. It was assumed that the total area of cylinder would be the input for calculating stress and strength. Figure 2.18 shows the typical failure mode of the Porous Network Concrete specimen. It is beyond the scope of this thesis to explain the fracture mechanics of the failure mode. However, it might be seen that as the strength of the porous core is much less, the outer cylinder carry most of the stresses and fail as if it is a hollow cylinder. Table 2.8 recapitulates the results of the compression strength of PNC.

The micro CT scan technique was used for characterizing porosity and pore connectivity of the PNC considering its ability to discover the interior of the specimen non-destructively. The PNC $\text{Ø}56 - 120$ mm cylinders were used as

specimens in the test. Since it was difficult to produce PNC specimen with smaller diameter without losing its general characteristics; a trade-off was made by obtaining slightly lower image resolution. The specimen was scanned using the same equipment, Phoenix Nanotom 180 kV/15W resulting in ± 1100 images with resolution around ± 100 microns.

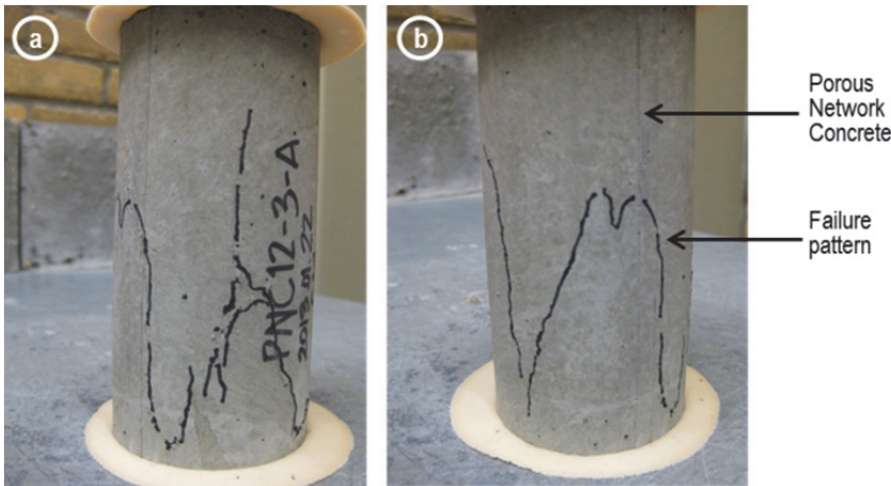


Figure 2.18. PNC cylinder specimen failure mode under compression; Figure (a) shows specimen from front side. Figure (b) shows the back side of the same PNC specimen.

Figure 2.19.a. illustrates the 3D image reconstructed, using VGStudio max 2.2, from radiographs. The image was then studied by assigning colour codes to different segmented material phases, as depicted in figure 2.19.b. By employing this procedure, it was possible to observe the interconnectivity of the porous core visually and also calculate other pore features quantitatively; e.g. porosity.

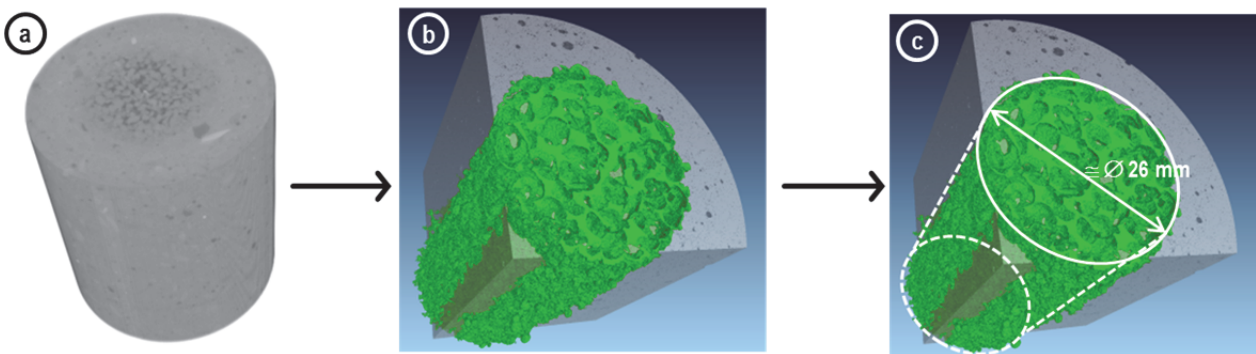


Figure 2.19. (a) 3D image reconstruction of PNC was obtained from radiographs of micro CT Scan which then was colour-coded in order to analyse the different phases in figure (b). Figure (c) shows the representative volume

A series of 2D radiographs taken from micro CT scan is arranged as shown in figure 2.19. to describe the interior of the PNC specimen. It can be seen from the pictures that PNC, with its porous core covered by PVA film, exhibit clear demarcation between two phases; porous core and main body. This implies that when SCC was

poured into the mould, the concrete matrix did not intrude into the voids of the core and the porous core stays porous. Therefore it may be concluded that there is (almost) no porosity and hydraulic conductivity reduction in the core of PNC compared to porous concrete.

On the other hand, PNC cylinder without PVA in the left side of the figure 2.20 shows no clear boundary indicating that the SCC matrix infiltrated the porous core. This is more pronounced in the P48-2-A which has bigger pore size due to the bigger aggregate size used. The implication from this phenomenon is that the core porosity and hydraulic conductivity may be reduced, although the extent of the reduction is more limited in the core with smaller aggregate size.

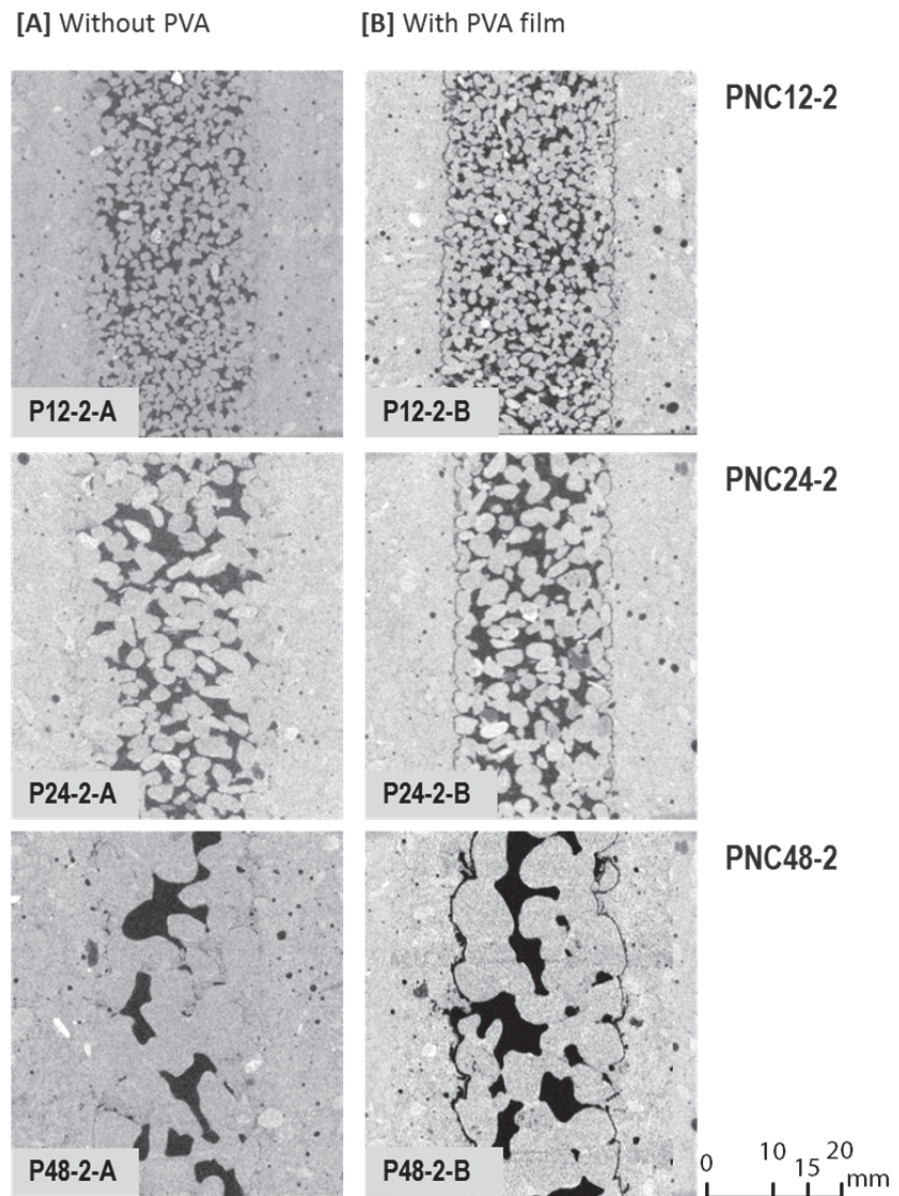


Figure 2.20. Series of images showing the centre of PNC using different aggregate size for porous core. Two type of specimen differ from another by the use of PVA film to cover the porous core during the placement of SCC main body.

For PNC, the porosity and hydraulic conductivity value was determined solely for the representative volume of core. This means that after setting the measurement scale, a representative volume (cylinder with diameter of 26 mm) was set in the specimen from the centre point. Hydraulic conductivity was measured on this volume according to the procedure developed for porous concrete in subchapter 2.2.3.c.

The recapitulation of the characterization results is presented in the table 2.8.a and table 2.8.b for PNC with normal strength concrete (NSC), meanwhile table 2.9 summarizes the properties of PNC with high strength concrete (HSC). In general specimens of PNC produced with normal strength concrete-SCC show compressive *strength capacity* at 28 days between 37 to 42 N/mm². PNCs which has aggregate size 1-2 mm show porosity less than 20% while PNC with high amount of binder (designated with -3-) also exhibit porosity > 20%. Additionally, it is observed that there is an average reduction approximately 4.78 % of the porosity value in PNC without PVA film covering its core compared to PNC without PVA film.

Hydraulic conductivity values of all PNC produced show no significant difference with the results of the porous core only. There is a slightly insignificant reduction in the average value of hydraulic conductivity of PNC with porous core covered with PVA compared to the one without except for the PNC with 4-8 mm aggregate. For this PNC, the reduction of hydraulic conductivity is significant if the porous core is not covered with PVA film.

Tabel 2.8.a. Mechanical and transport properties of Porous Network Concrete without PVA film; compressive *strength capacity* (N/mm²), porosity (%) measured by 3D image analysis, and hydraulic conductivity (cm/sec).

Porous Network Concrete		Compressive <i>strength capacity</i> (N/mm ²)	Porosity based on 3D image (%)	Hydraulic conductivity (cm/sec)
Aggregate size	Code			
1-2 mm	PNC12-1-A	37.9	17.7	0.86
	PNC12-2-A	40.4	16.3	0.89
	PNC12-3-A	41.1	14.6	0.49
2-4 mm	PNC24-1-A	38.6	23.6	1.22
	PNC24-2-A	41.5	22.3	0.96
	PNC24-3-A	42.3	16.1	0.71
4-8 mm	PNC48-1-A	36.6	22.2	0.52
	PNC48-2-A	40.2	20.7	0.51
	PNC48-3-A	41.8	18.6	0.67

Tabel 2.8.b. Mechanical and transport properties of Porous Network Concrete with PVA film covering the porous core.

Porous Network Concrete		Compressive <i>strength capacity</i> (N/mm ²)	Porosity based on 3D image (%)	Hydraulic conductivity (cm/sec)
Aggregate size	Code			
1-2 mm	PNC12-1-B	37.7	18.7	0.91
	PNC12-2-B	40.3	17.9	0.89
	PNC12-3-B	41.3	15.8	0.57
2-4 mm	PNC24-1-B	39.2	25.9	1.39
	PNC24-2-B	42.2	23.5	1.14
	PNC24-3-B	42.5	18.4	0.86
4-8 mm	PNC48-1-B	35.5	25.6	1.77
	PNC48-2-B	39.7	22.7	0.97
	PNC48-3-B	40.8	19.8	1.01

In table 2.9., it can be seen that PNC with main body made of high strength concrete the overall higher maximum load capacity is found while still maintaining its transport properties in *pervious regime*.

Tabel 2.9. Mechanical and transport properties of Porous Network Concrete porous core having 2-4 mm aggregate and high strength concrete (HSC) main body.

Porous Network Concrete		Compressive strength capacity (N/mm ²)	Porosity based on 3D image (%)	Hydraulic conductivity (cm/sec)
PVA film	Code			
no film	PNC24-1-A-HSC	55.4	23.2	1.12
	PNC24-2-A-HSC	56.7	21.9	0.91
	PNC24-3-A-HSC	58.9	17.2	0.81
PVA film	PNC24-1-B-HSC	55.9	23.2	1.26
	PNC24-2-B-HSC	58.1	23.5	1.18
	PNC24-3-B-HSC	58.2	17.9	0.91

2.4. Findings: PNC

Porous Network Concrete (PNC) designed in this chapter shows promising features for being used in self-healing concrete. The production process – *the making of the PNC* – has been shown and comprises of two parts, *the prefabricated porous core* and *the main body*. Seemingly there is no something extraordinary or sophisticated in the process.

The PNC main body which provides strength and stiffness for structural applications can be designed based on the current concrete making technologies. It is observed there is strength capacity reduction due the reduction of the area which carries the compressive stress; less cross sectional area, less strength. This is applies only to the specimen investigated in this work, as in the real structure the volume of porous core might be quite insignificant to reduce the structural strength. Further, it has been shown that the overall structural strength can be increased simply by using higher material strength of the concrete main body. Depending on the application the geometry and material quality can be fine-tuned to obtain the required level of strength.

The use of PVA film for covering the porous core during concrete casting ensures the core to stay porous and can be used for infusing fluid through its interconnected pores. However without PVA film, the porous core still functions as it is intended. The condition is the pore diameter should be kept small enough, thus, fresh concrete matrix does not to penetrate and clog in into the voids during casting. Except form PNC with aggregate of 4-8 mm, slight reduction of porous core effective porosities are observed and all specimens has porous core in the *pervious regime* as intended.

This page is intentionally left blank.

3.

Development of automatic healing system and test method

‘...Healing takes courage, and we all have courage, even if we have to dig a little to find it.’

- Tori Amos

The previous chapters have explained the process from conceptualization to realization of the Porous Network Concrete (PNC). It has been shown that the porous core in the PNC serves as medium for transporting healing agent. In order to materialize the healing process with minimum human intervention (that is why the term ‘self’ in self-healing concrete is manifested) an autonomous control system is designed in this chapter. Central to the designed system is a feedback mechanism. This mechanism comprises of a sensor which detects concrete displacement and sends a signal to an actuator which pumps the liquid healing agent according to a certain rule prescribed in the controller. The intention of the design is to be a proof-of-concept – thus not an early version of a product design (prototype) – which demonstrates that the concept has the potential of being used in the ‘real’ application. The proposed working principle is verified by mechanical and leakage (permeability, infiltration) testing.

Feedback mechanisms lay hidden, therefore many people are often *unaware* about it, in both the natural and the engineered world. Yet, its presence plays a pivotal role and can be ‘seen’ everywhere in our daily life. Feedback governs a *thermostat* that regulates room temperature using heating/cooling unit, or an *auto pilot* that flies an aircraft from one point to another. In living organism, *homeostasis* where many vital parameters, e.g. body temperature, sugar, and pH level in blood etc., are kept at a certain level is governed by feedback mechanism. In these mechanisms, the systems receives information (*input*) that is *fed back* to achieve the desired behaviour (*output*) of the systems.

During its life time living bone demonstrates an adaptation and remodelling making use of feedback mechanism. It performs a crucial role in fracture healing and recovery. In this chapter the mechanism is emulated to develop *automatic (autonomous)* healing for porous network concrete. The system differs from commonly manual repair of concrete in which autonomous healing takes place with minimum (*may be without*) human intervention.

3.1. Manual repairing vs. Engineered healing

Damage and deterioration in concrete or reinforced concrete structures is mostly manifested in scaling, spalling, curling and cracking [200]. The latest is the focus of this study. In principle *cracking* is material separation because local tensile strength is surpassed by tensile stress. By its cause cracks may be recognised as *shrinkage* cracking, *plastic* cracking, *thermally induced* cracking, *settlement* cracking, *structural* cracking, *tension* cracking, or *rust* cracking.

Often cracks are seen as symptoms of damage. Beyond certain level, however, the presence of cracks may signal more serious problems, e.g. structural problem, settlement, overload, etc. To some extent cracks only impair the concrete surface. Cracks may be dormant and isolated with indication that the causes may no longer exist. Such cracks might be acceptable for certain type of the structure, e.g. non-residential building. Yet, this condition might not be allowed for another type of structures depending on the function. Certain type of building or structure with critical function such as liquid-retaining structures or hazmat concrete container cracks might be intolerable. Storage tank, however, might tolerate crack developed to some crack width.

On the other hand, one that seemingly ‘not-so-serious’ cracks can also be active. These active cracks can grow very slowly or quite rapid depending on many variables. In spatial term crack may propagate in various direction, e.g. longitudinal, transversal, or random. It also has various geometries. Its width can be, for instance, fine/hairline to over 2 mm. Crack only affects concrete cover after initiated or it can propagate through the whole cross section of the structure.

Albeit its state and dormancy, if left unrepaired, cracks in concrete may provide easy means of entry for deleterious substances penetrate into the concrete and make contact with rebar. This may start a more substantial component damage, e.g. corrosion, or eventual failure of the structure. A successful crack repair should take into account the knowledge of crack causes and proper selection of repair procedure accordingly.

Several methods for concrete crack sealing and repairing have been developed such as polymer-based waterproofing, coatings, patching, concrete stitching, and crack injecting. Crack injection is the most common technique with the spectrum from simple injection for do-it-yourself level problems up to industrial scale with heavy duty devices for large scale repair. The underlying principle is to fill in a liquid material, e.g. chemical based or cementitious grout material, directly into the void left by the crack. Industrial standard of practice suggests that several holes might be drilled at 45 degree angle from the surface down to intersect the fault, see figure 3.1. After debris is removed, the holes may be used as the channel for infusing the grout or repair materials. Later when the material is hardened, the integrity and serviceability of the structure is restored.

Among the wide variety of injection materials (silicate, silicon-organic, acrylic, phenol formaldehyde, etc.), polyurethane based mixtures are the materials of choice due to their relatively simple preparation and pumping technologies.

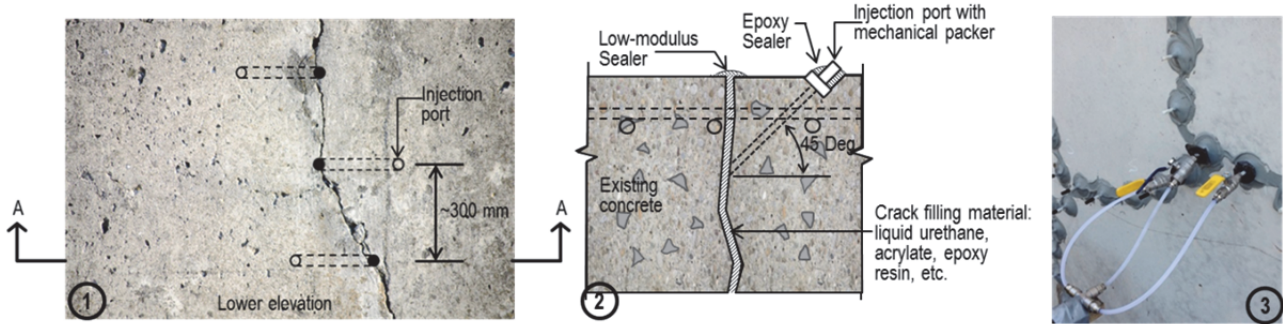


Figure 3.1. Method of injecting materials to repair cracks in concrete. Image (1) and (2) were adapted from FHWA report [201].

The standard practice of crack repair by injecting repair materials has been quite successful though it takes substantial amount of time for preparation and special labour qualification for its implementation. In the case where the timing of repair is critical, rapid and automated repair may be needed. The self-healing by means of Porous Network Concrete with autonomous injection trigger could provide an alternative solution.

3.2. Automatic repair system

The autonomous healing mechanism in the PNC is designed by incorporating the feedback mechanism; once a certain crack width is sensed, an action to heal takes place. As a proof-of-concept, in this work, a simple and intuitive approach to design a feedback system for Porous Network Concrete self-healing mechanism has been carried out.

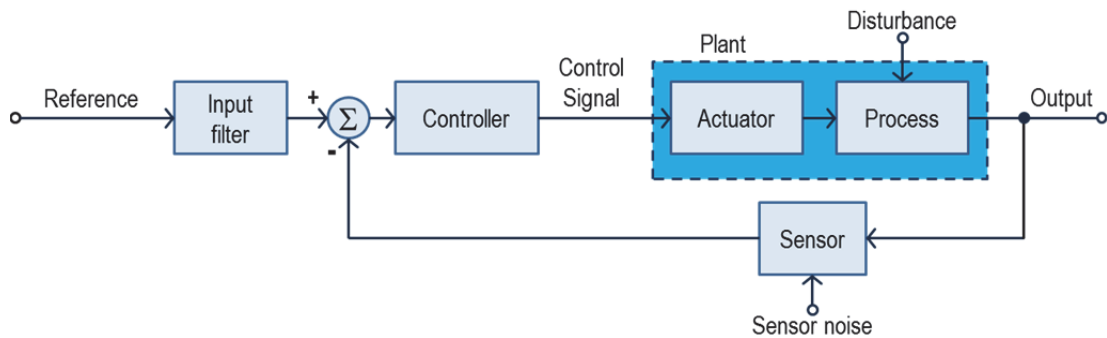


Figure 3.2. Block diagram showing a rudimentary feedback with its elemental components. Central in this diagram is the process for controlling the output. The graph is taken from Franklin, et al [202].

Franklin *et al.* elaborate the feedback mechanism in their book [202]. The principle of feedback mechanism is illustrated in general by the block diagram in Figure 3.2. Such a picture identifies the major parts of the system and shows the directions of information flow from one component to another. The mechanism can then be easily analysed qualitatively by following the arrows showing the flow of signal in the system.

The major part in the mechanism is the *process* which due to the disturbance e.g. *flows of energy*; produces output that out of the range from the reference, therefore needs to

be controlled. The actuator – a device that might have several components in itself – function is to influence the controlled variables. Together, process and actuator are called plant. The output signals from the process are measured by the sensors whose output itself will be used by comparator to compute the difference between the reference signals and the sensors output. The input filter converts the reference signals into electrical signals which later on will be used by controller to compute desired control signals. Based on this understanding, the feedback mechanisms to be used in the Porous Network Concrete autonomous healing was developed and depicted in the figure 3.3.

In general the flow of information within the system, see figure 3.3, is as follows. When the PNC structure, *the prism* (1), receives loads, e.g. from three-point bending, and builds up internal bending stress, it deflects and deforms. This deformation is detected by the displacement sensors, LVDT – *a transducer that converts movement into electric signal (voltage)*. This signal is read by ‘*the box*’ (2) which comprises of two components; a data acquisition card (I/O card) and a motor controller. This signal is recorded in the *channel table* in the computer (3) where a *script* (computer program) is run to monitor the deformation *records* in term of crack opening. Once the crack mouth opening reaches certain threshold value the event-driven digital signal is sent by the script to the motor controller to switch on the injector (4).

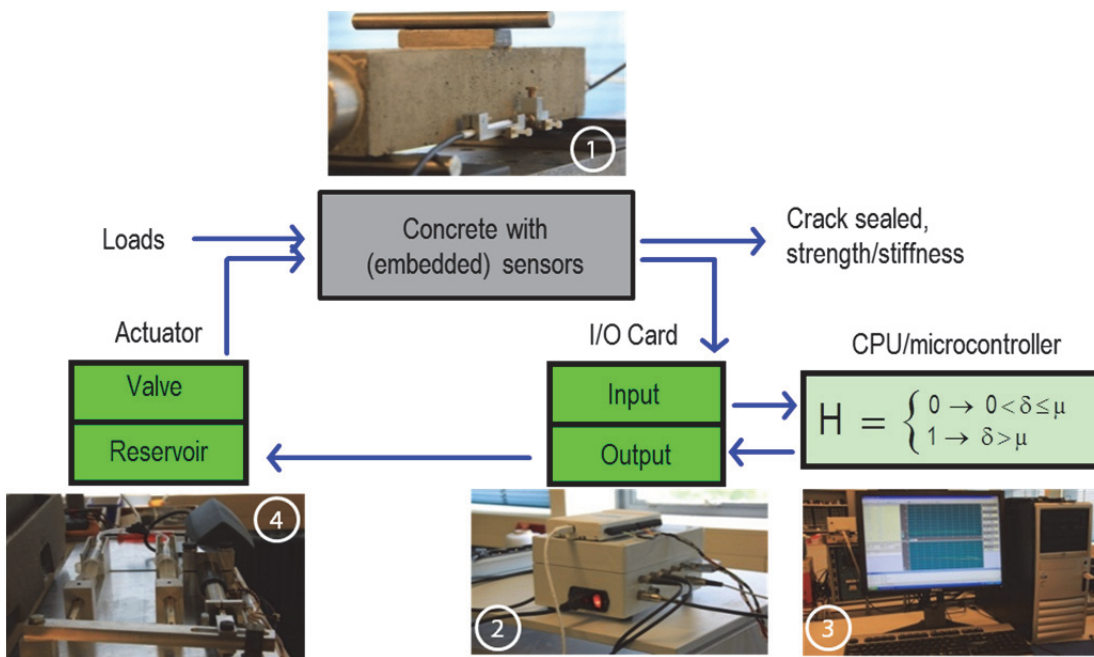


Figure 3.3. Conceptual block diagram of feedback mechanism implemented in the self-healing of Porous Network Concrete. (1) Load exerted in concrete creates deformation which is detected by (embedded) sensors. These sensors send signal into the ‘box’ (2) comprises of data acquisition card and motor controller. The signal is then manipulated with a script written in Lua in the computer (3) which then sends triggering signal to motor and run the injector (4).

When it is switched on, the mechanical injector starts to pump the liquid healing agent into the porous core. The pressure built up in the core is monitored by a pressure transducer. Later when the healing agents, e.g. epoxy resin, polyurethane, reaches the crack zone, hardens and seals the crack, the whole process of healing is completed. In this case crack is sealed and strength and stiffness may be recovered.

This process is autonomous and automatic while minimizing human intervention from monitoring crack and releasing healing agent. The system may also be considered *static* because there is no time-varying state exists.

The details of the design and prototyping, including mechanical injector, ‘the box’; motor controller and data acquisition system, the software and embedded script, and the control rule, are provided in the appendix 1.

3.3. Mechanical test

In order to test the autonomous healing-mechanism proposed, a crack formation and mechanical properties recovery evaluation in the specimen was carried out through mechanical tests; Monotonically Uniaxial Tension Test (MUTT) – *henceforth tension test* – and Three-Point Bending Test (TPBT) – *henceforth bending test*. A cylinder Specimen of $\text{Ø}56$ -120 mm was used for MUTT and a prisms (beam) of $55 \times 55 \times 285$ mm was used in TPBT.

3.3.1. Tension test for cylinder specimen

The Porous Network Concrete cylinder specimens were prepared according to the procedure described in the sub chapter 2.3. A circumferential notch was introduced in the specimen. Steel caps with M8 thread on top were used to hold specimen in the testing machine. The steel caps were glued to the PNC main body with polymer based on Poly-methyl metaacrylate (PMMA) composed of a powder monomer PLEX® 7724-F containing initiator and a liquid monomer PLEXIMON® 801. The composition of this two component adhesives is 1 part PLEXIMON® 801 with 2 parts PLEX® 7724-F and the curing time is in 4 – 7 minutes. C-clamps were also glued on the specimen side as illustrated in the figure 3.4 to hold LVDT's. Care was taken to ensure the glue only in contact with the main body and not with the porous part in order not to block the channel.

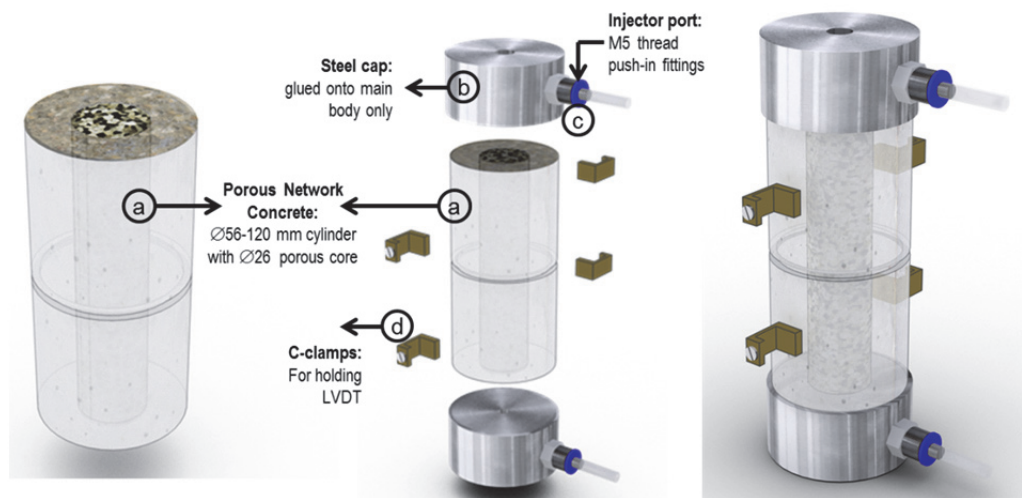


Figure 3.4. The rendering of the Porous Network Concrete cylinder $\text{Ø}56$ -120 mm specimen used for tension test

A hole was drilled to channel the liquid agent and connected with M5 FESTO push-in fittings on the side on the steel cap, see figure 3.4. The fittings were connected with plastic tube to the syringe. The top fitting would be used as injection port of the healing agents, while the bottom fitting serve as outflow port in case there was an excess healing agent in the specimen.

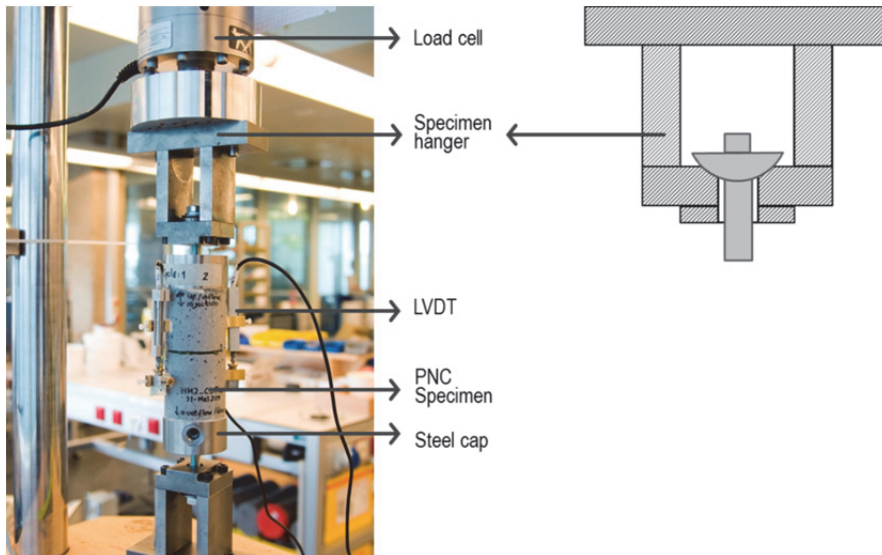


Figure 3.5. The tension test setup for cylinder PNC specimen with the hanger

The tension test was performed using a closed-loop displacement controlled system to be able to maintain uniform loading rate. The INSTRON® 8872 Servohydraulic Testing System with Dynacell™ load cell was used. The machine has a high stiffness reaction frame. To supply displacement data and measure crack width, two LVDTs were used. These Solartron AX/1/S LVDTs have measurement range of ± 1 mm with accuracy of $1 \mu\text{m}$ and each was held on the C-clamp. These C-clamps were attached to the side of the specimen in the arrangement as seen in the figure 3.10, in the mid height of the sample crossing the notch in which the crack is expected to grow. The cylinder specimen was put in the testing apparatus by means of a specimen hanger, see figure 3.5. The hangers which are connected onto the specimen top and bottom steel cap has special bowl-shape with concave hole. The bolts with convex head are mounted to the holes and are free to rotate. Thus, the moments in the connections are not restrained in this tension test setup.

3.3.2. Three-point bending test for prism specimen

The prism specimens for the bending test were prepared following the procedure explained in the subchapter 2.3. Cylindrical aluminium caps with $\text{Ø}55 - 20$ mm were made with M5 thread halfway through its height and $\text{Ø}7$ mm hole as a healing agent channel. M5 FESTO push-in fittings were connected to the cap as port of injection and port of outflow. These caps were glued with PMMA based adhesives to the PNC prisms. Similar to the cylinder specimen, the glue was smeared in the perimeter of the cap to make sure it has contact only with concrete main body and leave the

channel free. Figure 3.6 shows the rendering of the PNC prism specimen and its components for healing test.

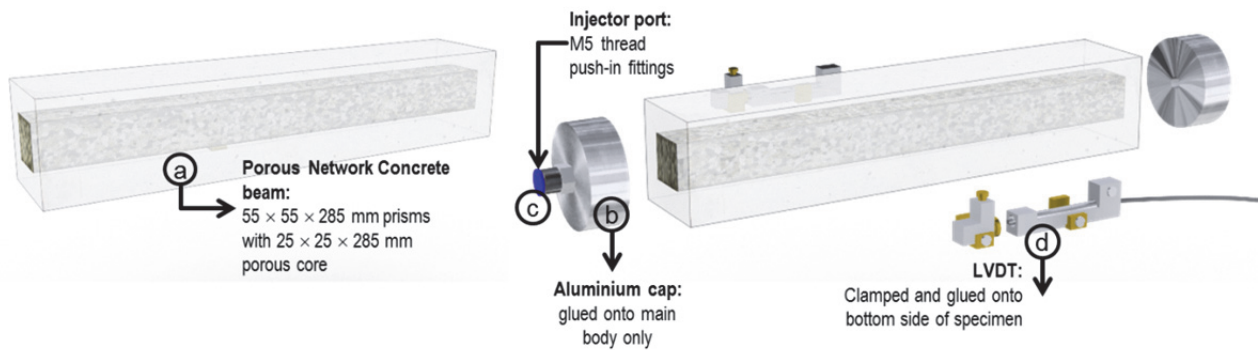


Figure 3.6. The rendering of the Porous Network Concrete prisms $55 \times 55 \times 285$ mm specimen (a) used for three-point bending test. The PNC specimen is equipped with port of injection (PI) and port of outflow (PO) made of aluminium cylinder (b) and M5 push-in fitting (FESTO) (c). Two LVDTs are attached to the side of the specimen.

To create a prescribed crack width in the mid of the beam/prism specimen, the three-point bending test was employed. Figure 3.7 illustrates the rendering of the TPBT setup. The load provided by INSTRON® 8872 was exerted in the mid-span of the beam sample which was propped horizontally onto two roller supports. The axis-to-axis distance of these supports was 250 mm. The Solartron AX/1/S LVDTs having measurement range of ± 1 mm and accuracy of $1 \mu\text{m}$ were clamped into the C-hooks. These C-hooks were glued onto bottom edge both side of the specimen surface by means of polymer based PMMA 25 mm to the right and left of the mid-span of the specimen.

These LVDTs supplied displacement data to the servo-hydraulic machine to be used for closed-loop strain controlled test. The signals from these LVDTs – representing crack opening width – were also sent to the data acquisition system (NI 6211 DAQ card). The average value of the signals was used for feedback mechanism for the injection of the healing agent.

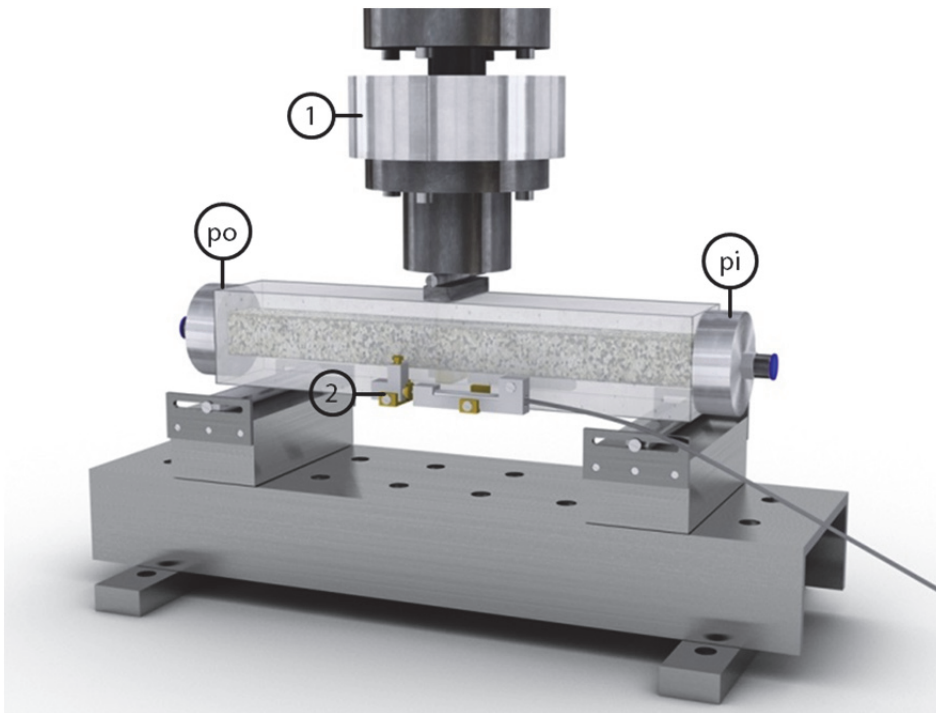


Figure 3.7. Rendering of the basic setup of three-point bending tests (TPBT) where a Porous Network Concrete (PNC) is loaded in the mid-span (1). Strain controlled tests are employed where crack mouth opening is monitored by two LVDTs (2) in the bottom side of specimen. PNC is equipped with port of injection (pi) and port of outflow (po) made of aluminium cylinder and M5 push-in fitting (FESTO).

3.4. Evaluation of the feedback mechanism efficiency

After several dry-run tests, the proposed autonomous-healing mechanism by means of on-off control was deployed. This section is devoted to evaluate the operation of the mechanism using a PNC cylinder diameter 56 mm -120 mm under tension loading.

As the specimen was prepared following the setup illustrated in the figure 3.8, several parameters such as threshold value of the crack opening, the pressure level, and the motor speed were set in the PC which runs the script. The prescribed threshold value for the crack opening displacement was set at 75 μm while for the pressure was set at 0.7 bar. The value for pressure level was set based on trial since there was no adequate model to calculate the pressure build up in the newly developed Porous Network Concrete.

It was estimated based on the porosity observed in the test (subchapter 2.3.3.b) that the average volume interconnected void contained in the PNC cylindrical specimen was in between 25 – 35 ml. Therefore, a premixed two-component epoxy resin and hardener was used and prepared into the 30 ml syringes. These syringes were put in the holder in the injector machine with the piston ready to push the plungers.

The operation of the simple on-off control appeared to function adequate on which all the components in the feedback mechanism worked as it was intended. Figure 3.8 demonstrates the condition after injection when the value of the crack opening was greater than the trigger level 75 μm .

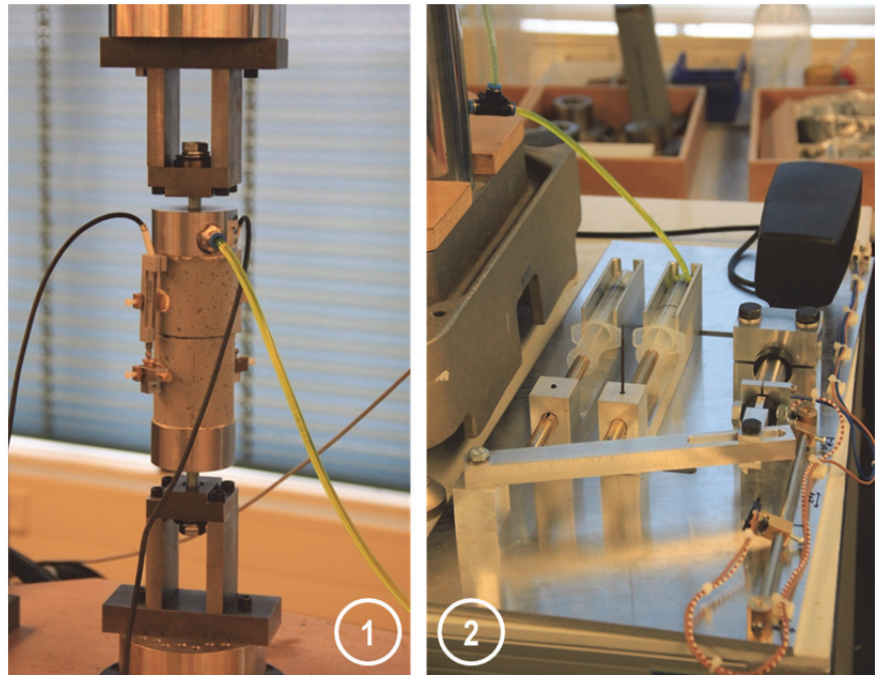


Figure 3.8. The tension test with the autonomous healing mechanism by means of on-off control. Figure shows the specimen (1) and the injector (2) after healing agent was fully infused into the porous core once the crack opening reached 75 μm .

Figure 3.9 exhibit the composite graph of the load-displacement and all the signals associated with the healing system. As the load increases up to 6.5 kN while the displacement of the specimen reaches 5.5 μm , concrete behaves essentially in linear elastic manner. However, a small number of stable microcracks may be developed. This is then followed by the softening curve of the sample when the displacement value increases while the load decreases exponentially. This implies that beyond its peak tensile strength the concrete loses its load capacity. It was observed visually that accumulated crack developed in the notch.

At this phase, certain features of the signals were observed in the PC monitor. The signals of the switcher, motor current (Amp) and pressure (bar) remain zero with some noise observed in the motor and pressure signal. In this case the switcher was off and the system remains at the state 1⁴. In the background, however, the LVDT's signal were passed into the script continuously.

At the specimen displacement value of 75 μm , the condition was met for the injector to turn on and the system move into state 2, the injection state. In the figure 3.9 the switcher signal is suddenly rise to 1 while motor current is raised to -0.1 Ampere which implies the voltage signal was sent to the motor and turn it on. As the motor starts running and push the piston and push the syringe, a pressure is built up in the porous core. This phenomenon is detected by the pressure transducer which then passed it through the DAQ and was read by the embedded script.

It was observed that the pressure built up in the core measured by the sensor was less than the prescribed pressure threshold value (0.7 bar). Therefore the criterion in

⁴ Explanation of the state may be found in the Appendix 1. The idea behind state is the condition represents the logic to generate event-driven action.

the state 3 (shut down the system if the pressure is too high) was not met. Thereafter the injector reached the lower-bound-relay and the whole process was stopped.

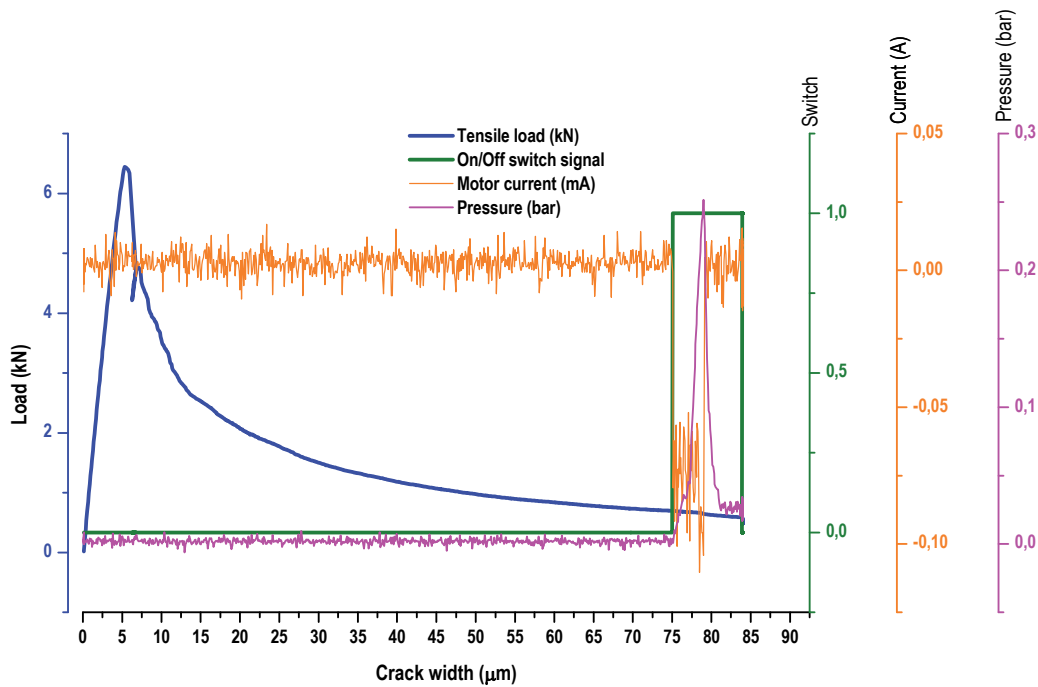


Figure 3.9. Graph of the load versus crack width of the tension test of cylinder specimen and the signals of automatic healing system. At crack opening of 75 mm the mechanical injector is turned on indicated by digital signal switched from 0 to 1.

Afterwards, as the script returns the control to the MP3, the servohydraulic loading machine (INSTRON® 8872) was automatically set on hold. This was done at the specimen crack opening of approximately $\pm 84 \mu\text{m}$. Then, visual observation was conducted and digital images of the specimen were acquired.

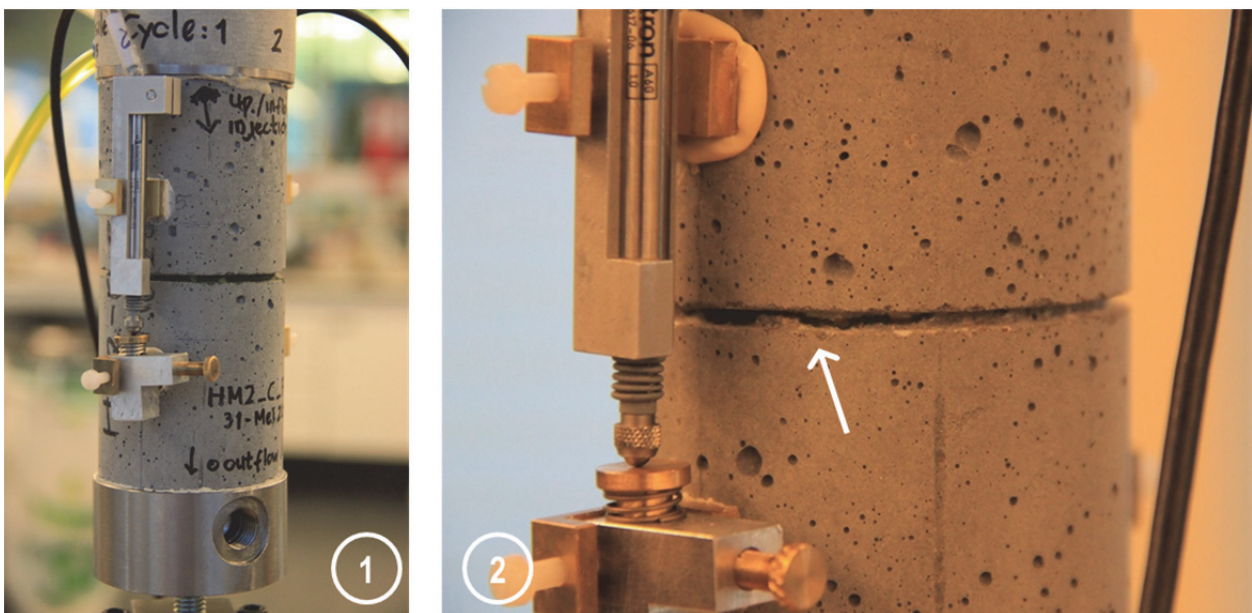


Figure 3.10. The close up cylindrical PNC specimen reveals the healing agent flow from inside-out through the crack opening.

Figure 3.10 demonstrates the result of the healing mechanism for the PNC. It can be seen crack opening occurs in the notch and it is infiltrated by the healing agent. The dark wetting area pointed by the arrow in the frame 2 of figure 3.16 indicates the epoxy flows out through the crack.

The process above mentioned strongly indicates the on-off control designed works well in injecting healing agent into the core. All-in-all, the feedback mechanism fully operates in making the Porous Network Concrete self-healing.

3.5. Evaluation of healing efficiency

This section is dedicated to discuss the evaluation methods used in this work to assess healing efficiency. Several standard evaluation techniques to investigate materials properties and characteristics – destructive test as well as non-destructive test (NDT) – have been employed to assess the effectiveness and efficiency of the self-healing mechanism [89]. Some of these have been modified to effectively verify the crack healing or crack sealing.

RILEM TC-221 SHC identifies several experimental techniques in their State of the Art Report [89]. In the report the technical committee categorizes these techniques based on the purpose; (1) to investigate crack healing, (2) to validate crack sealing intended for recovery against environmental action – *to what extent the crack is sealed which is related more to durability or leakage*, and (3) to justify mechanical recovery – *how well the healing recovers concrete mechanical properties; e.g. strength, stiffness*.

In the report, microscopy techniques, x-ray diffraction and Raman spectroscopy has been used to study crack healing with several goals [203]; e.g. (1) to check the quality and efficiency of the material designed for self-healing concrete, (2) to characterize the extent of damage, and (3) to determine the healing level. The permeability test using predefined crack in concrete disc modified from Wang [204] and Aldea [205] is mainly used by many researchers to study crack sealing with the goal to study durability performance of the healed concrete [203]. Mechanical test to create cracks in concrete and mechanical reloading after healing is the main destructive technique employed in assessing strength and stiffness regain in self-healing concrete.

Several other techniques; e.g. capillary water absorption; measurement based on properties of wave propagation in materials, i.e. ultrasonic (acoustic emission) and resonant frequency measurement; Computed Tomography [86] and Fourier-Transform Infrared Spectroscopy (FTIR) [114] have been conducted with more specialized target and requirement.

In this report, mechanical recovery after healing was evaluated by comparing strength and stiffness at crack formation and after healing. A special leakage (permeability) test by flowing water through porous core of the PNC has been designed and implemented to study the degree of sealing of the crack in PNC main body. Microscopy and image analysis techniques have been used intensively to observe healing development in PNC. X-ray computed tomography (CT) scanning and Environmental Scanning Electron Microscopy (ESEM) methods have been applied to investigate and characterize the healing process.

3.5.1. Mechanical properties regain by reloading

The crack formation was introduced to the specimen by the tension and the bending test. Mechanical reloading with the same test to the healed specimen may reveal the mechanical efficiency of the healing mechanism as well as healing agent performance. Comparing different mechanical features from the virgin (pre-healing) to the healed (post-healing) specimen is the central idea of the evaluation method; i.e. comparing peak strength of the specimen before and after healing [86].

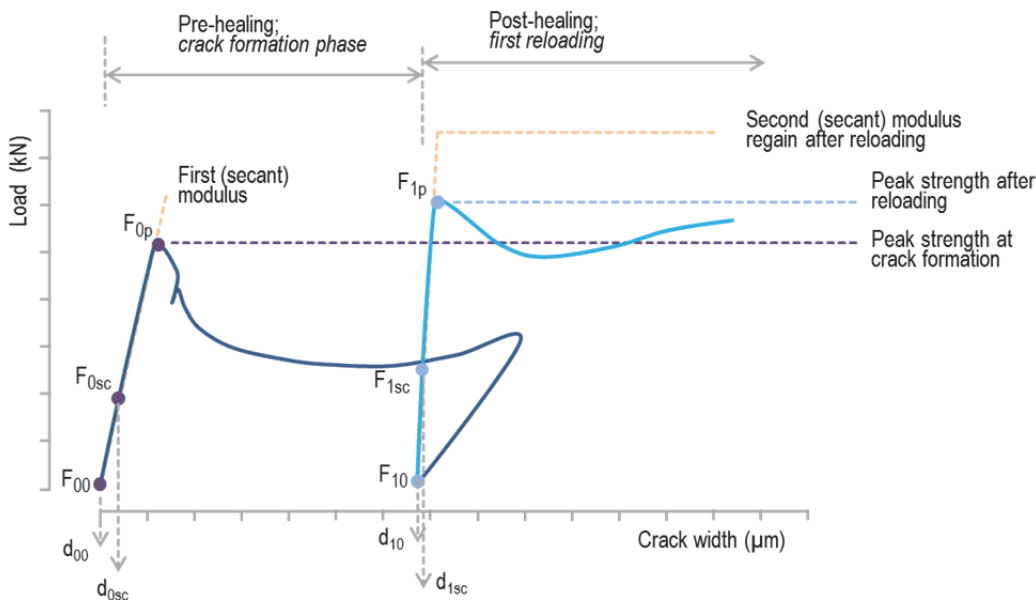


Figure 3.11. The expected load versus crack width graph of virgin and healed specimen and determination of strength and stiffness for self-healing efficiency. The graph is adapted from Van Tittelboom [86].

Based on the work of Van Tittelboom [86], the strength regain (recovery) is determined by calculating the ratio of the peak strength, F_{2p} , obtained from reloading of post-healing specimen to the peak strength of pre-healing specimen, F_{1p} . The stiffness regain (recovery) is determined by the ratio of the modulus of post-healing to the pre-healing specimens by means of static modulus of elasticity for cylindrical specimen under MUTT (*monotonic uniaxial tension test*) and secant modulus of specimen under TPBT (*three point bending test*).

Static modulus of elasticity is defined as the slope of the load-displacement / stress-strain curve for concrete under uniaxial tension loading. Meanwhile *the secant line* is defined as the slope of a line drawn from the origin to the point on the load-displacement (stress-strain) curve corresponding to 40% of the failure stress (peak strength, F_{0p} and F_{1p}) based on NEN-EN-1992-1-1 [206]. Chord modulus which is defined as the slope of a line drawn between origin points and peak strength point on the stress-strain curve may also be used in order to have more alternatives.

Using the definition above, the strength regain may be expressed as the equation 3.1

$$SH_{strength} = \frac{F_{1p}}{F_{0p}} \quad (3.1)$$

whereas $SH_{strength}$ denotes healing efficiency in term of strength regain (recovery) expressed in percentage (%), F_{1p} is the peak load of the reloading curve and F_{0p} is the peak load of the virgin specimen curve.

Secant modulus, E_{sc} , of the virgin specimen and of healed specimen are presented in the equation 3.2 as follows

$$E_{sc0} = \frac{F_{0sc} - F_{00}}{d_{0sc} - d_{00}} \quad (3.2)$$

$$E_{sc1} = \frac{F_{1sc} - F_{10}}{d_{1sc} - d_{10}}$$

where E_{sc0} and E_{sc1} are the secant modulus of the pre-healing concrete specimen and the post-healing concrete after reloading, respectively. F_{0sc} and F_{1sc} is the load corresponding to the 40% of the specimen peak load value before and after healing, while F_{00} and F_{10} are the zero loads of specimen before and after healing. In the denominator, d denotes the displacement or crack width pre- and post-healing associated with load displacement curve depicted in the figure 3.11.

The healing efficiency, therefore, is determined by the ratio as expressed in the equation 3.3

$$SH_{stiffness} = \frac{E_{sc1}}{E_{sc0}} \quad (3.3)$$

3.5.2. Permeability or leakage test

In this work, the leakage (permeability) test has been designed and developed taking into account the nature of the PNC. The idea is rather simple and can be described as follows. If water flows through the interconnected porous core from port of injection, it will end up flowing out from the other end (port of outflow) provided there is no leakage in the main body of the PNC. If cracks occur in the main body, water will leak out from the core. The sealed crack will certainly make the water remains in the core.

Figure 3.12 exhibits the rendering of the leakage test setup designed to evaluate the healing efficiency. The porous core in the figure can be seen through transparent main body. The setup was designed by implementing falling head permeability test.

The PNC prism (4) is propped horizontally on top of wooden support which has a rectangular hole 100×55 mm in the centre. Through the port of injection (pi), the flexible plastic tube is mounted into the fitting and channels the water from the bucket (1) with a valve (2) to open or close the flow. The bucket is claw-clamped and held to the static post (3). The head of 25 mm is maintained and measured from the

central axis of the specimen to the centre point of the valve. The initial volume of the water in the bucket before the valve is opened is 750 ml.

A container (6) is placed underneath the specimen to collect the water drained out through the crack opening. The digital scale (7) KERN 440-47 with maximum capacity of 2000 gr and resolution of 0.1 gr is used to measure the weight over time of the water outflow from the crack. The signal is read by the *measurement system application* (MP3) installed in the computer. A DAQ (*digital acquisition*) card is embedded in the computer.

In case there is no crack in the main body or the cracks is healed already, the water will flow out from port of output (po) provided it is open. When a stopper is plugged in into this port, there will be no flow at all.

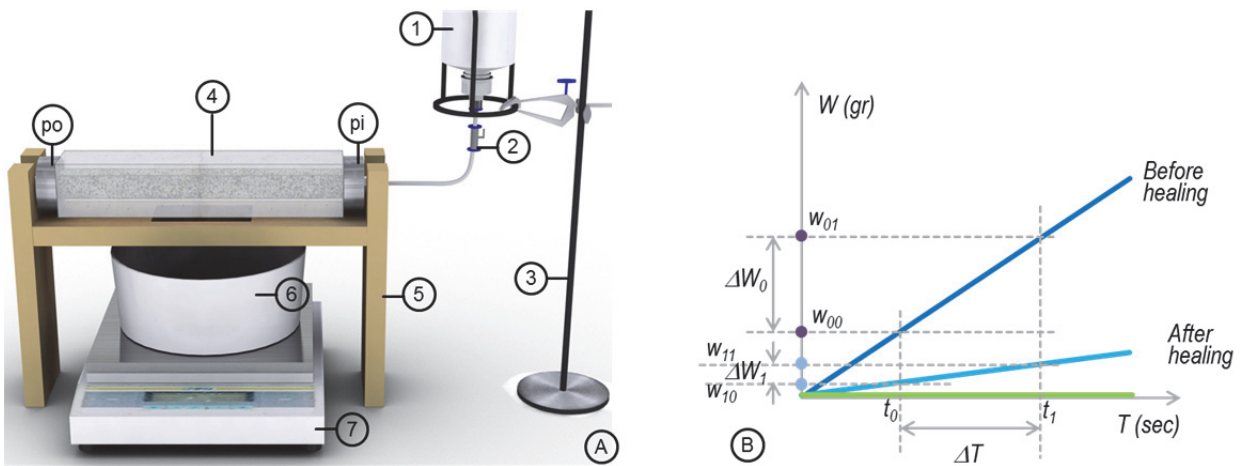


Figure 3.12. Basic setup of leakage (permeability/infiltration) test (a) and the expected (linearized) graph resulted from the test.

Figure 3.12.b. is the expected results from the test. A (linearized) graph of weight as function of time may be obtained from the weight of the water in the container. The ratio of the slope of the leakage curve before and after healing takes place may indicate the efficiency of the healing mechanism.

Using the definition above the leakage is determined by the equation 3.4 as follows.

$$LK_0 = \frac{w_{01} - w_{00}}{t_1 - t_0} \tag{3.4}$$

$$LK_1 = \frac{w_{11} - w_{10}}{t_1 - t_0}$$

where LK_0 and LK_1 are the amount of leakage after crack formation (pre-healing) and after crack is healed (post-healing), respectively. Meanwhile w denotes the weight of water dripped of from the crack opening over time t . The indices correspond to the points in the leakage curve before and after healing, see figure 3.12. Healing efficiency from leakage test, $SH_{leakage}$, is determined by the ratio as in the equation 3.5

$$SH_{leakage} = \frac{LK_1}{LK_0} \quad (3.5)$$

3.5.3. Visual confirmation; light and electron microscopy

Visual confirmation may be carried out to study whether the healing process occurs. The techniques may be started from a simple naked eye observation to digital image acquisition with camera under UV light. Digital image taken may serve as the source of the evidence and may also be used for an advance image analysis. These techniques will be used in the chapter 4 to support the investigation upon healing process.

As the eyes of the observer noticeably have limitation, microscope extends this visual observation capability. The concrete light microscopy techniques assist researchers in studying concrete microstructure. Sisomphon et.al implemented this technique to study the self-healing potential of mortar specimen incorporating calcium sulfoaluminate based expansive additive and crystalline additive [112]. Wiktor and Jonkers used optical microscope to analysis surface crack closure development mediated by bacteria and quantify healing efficiency in the concrete specimen [114]. The method developed by Wiktor and Jonkers will be used to evaluate healing efficiency in PNC injected by bacteria based solution in chapter 5.

An ESEM (*environmental scanning electron microscope*) makes use of electrons beam which are focused by electromagnetic lenses and directed onto the specimen surface. This extremely small probe may scan concrete surface area and generate signal captured by the detector. The acquired image reveals many interesting features of concrete microstructure. This technique will be employed to study the healing of the PNC injected by bacteria solution in chapter 5. Along with computed tomographic images of the porous concrete and the PNC obtained from the micro CT scan these various methods provide valuable information of the PNC material properties and it self-healing mechanism.

3.6. Concluding remarks

The aims of crack repair are to prevent deleterious substance to enter the concrete structure and therefore maintaining its total integrity. There are several currently available techniques. Crack grouting is the most common and preferred method. In this chapter, this outside-in injection method was inverted by injecting healing agent inside-out autonomously in the *Porous Network Concrete*. The keyword '*autonomous*' has been realized by designing feedback mechanism by means of simple '*on-off control*'. This *self-healing concrete* proof-of-concept has been proven to operate well.

This page is intentionally left blank

4.

Crack healing by means of chemical and cementitious grouting

‘...There is a crack in everything, that's how the light gets in.’

- Leonard Cohen

Biomimetic design process explained in the chapter 1 took inspiration from the bone, one of among abundant inspirational source in nature. Its morphology was mimicked combining porous and ‘normal’ concrete in chapter 2. Its internal feedback system was emulated in a simple on-off autonomous healing agent injection mechanism developed in chapter 3. The first development phase of this project has successfully designed the self-healing concrete by means of Porous Network Concrete (PNC).

The second phase is to test the system with different type of healing agent, a liquid that turns into hard substance and fills up the crack in the PNC main body. There are many researches develop healing agents and improve its performances in the healing process. There is no intention in pursuing healing agent development in this study, rather demonstrating several class of the liquid agent which may be used effectively in the PNC. This chapter describes the Porous Network Concrete which is cracked, injected and healed autonomously with ‘commercial-off-the-shelf’ healing agent; e.g. epoxy resin and cement grout material.

When one cuts one’s skin, a few drops of blood flow out and soon – almost instantly – coagulated, turning liquid phase into gel. This *hemostasis* – the natural body response to stop bleeding and keep the blood inside the damaged vessel – is the important aspect and the first step in wound healing. Subsequently, pairs of protein-clotting factors work together where one acts as substrate and the other acts as enzyme catalyst. In a cascading process, these factors are converted into another active enzyme successively. Eventually they produces fibrin transformed from fibrinogen allowing the wound to be ‘rebuilt’ later on [204, 207]. Blood is essential to the wound healing process. However, the coagulation cascade which clots the blood into a cross linked fibrin is imperative without which the bleeding may continue and fatal blood loss may be encountered.

Healing agent is ‘the blood’ in the self-healing concrete (SHC) process and system. When the inevitable fissures in the early age concrete or fractures due to excess loading occur, healing agent is transported into it and hardened in autogenic or autonomic manner [89]. The agent helps to seal concrete cracks and strength may be regained when it is cured properly.

The solidification process of self-healing agent is important and even critical for the success of the healing strategy and mechanism designed. In the SHC state-of-the-arts, several studies have been devoted in investigation, development or adoption of healing agents. The agent might be chemical-based or microbe-mediated-based.

Instead of developing new healing agent and investigating its behaviour, however, this present study aims to examine the effectiveness and efficiency of the healing process in the PNC with different classes of agents. This chapter starts with the discussion about the criteria developed by several researchers in determining the ‘best’ healing agent. Subsequently, three groups of healing agents are studied and its healing efficiency is tested by leakage and mechanical testing.

4.1. Introduction; the choice of healing agents

At the laboratory level, researchers have been investigating numerous types of healing agent and studying its fundamental behaviour in the healing process of concrete. At the beginning, cost of implementation is not considered and questions upon applicability mostly are kept under the idea of scientific advancement.

Concrete infrastructure construction and practice, however, is very mature and saturated with conventional-but-efficient techniques. Many of these construction practices are proven to be cost-effective. This makes construction industry uneasy to change or adopt new technologies. To be able to ‘create’ market in such a landscape [20], the self-healing concrete mechanism designed and its healing agents should be cheap enough to compete.

Particularly, it is imperative for concrete self-healing agent to exhibit some of the character such as [86, 113]:

1. *Ability to seal the crack*; the agents should be able to fill the additional void due to the crack formation but not to outstrip concrete tensile strength and create more microcracks. Therefore, reduction of permeability on the concrete is ensured. As the result, it satisfies the main purpose of self-healing to make cracked structure, i.e. concrete wall or floor, liquid-tight. Agents which are able to change its volume by expanding upon polymerization, i.e. polyurethane used by Van Tittelboom [86], and upon contact with moisture and concrete, i.e. sulfoaluminate based expansive additives adopted by Sisomphon *et al.* [112] are among the successful examples.
2. *Ability to flow into the crack zone*; the agent should possess appropriate viscosity to be able to flow to and remain in the crack zone until it hardens. Low viscosity agent will flow out from the crack and leave the crack open. Depending on the crack geometry, Dry suggested the viscosity of healing agent should be around 0.1 – 0.5 Pa-s (Pascal second) / 100 – 500 cP (centipoise) [86]. In the case of healing agent injected into the PNC, viscosity – *rheological properties* in general – plays important role. In steady flow, the liquid materials for injection may demonstrate different rheological properties; e.g. Newtonian, Bingham, shear thinning or shear thickening behaviour. For the injection into porous media, Bras *et al.* [208] argue the agent should possess self-levelling features with low yield stress.

3. *Ability to cure right on time and place* (curing condition and time); agent should be properly initiated and cured in the contact with concrete matrix and air in the crack surface either in dry or moist condition. Two compound agent may be adopted although is not preferable due to the fact that it depends on the proper proportion which hardly achieved in real system. A well-timed curing is also important. A quick setting agent, i.e. cyanoacrylate (CA) cured in less than 1 minute, might be beneficial in situation where rapid repair is the prime objective. Some other agents take more time to cure.
4. *Ability to be stable and durable over time*; the agent incorporated in the concrete should be compatible with the matrix and not in conflict with the concrete substrates. It has to be demonstrated to have the ability to stay active in the long-term period of concrete's service life where crack may occur due to many causes. Joseph [120] suggest continuous supply by employing 3D interconnected hollow tube network in the concrete structure with external reservoir having ability to pump the agent. To achieve multiple healing activity, Jonkers [113] recommend that healing agent may operate as catalyst instead of being consumed in the healing process.
5. *Ability to regain mechanical properties*; this may be attributed as less important feature due to the fact that overall strength of cracked concrete may be preserved. However agent able to provide stronger adhesive bond in the crack will prevent crack reopening when there is no more healing agent to refill.
6. *Ability to keep the price low and reasonable*; the total cost of healing agent and the healing mechanism design must be competitive compared to the conventional techniques.

4.2. Materials

Autonomous self-healing mechanism by means of Porous Network Concrete involves injection of liquid materials similar to the relatively mature technology of grouting. Pressure grouting comprises of injecting grout or other liquid materials to fill voids in concrete such as prestressed tendons, masonry grout, fissures in rock formation, soil grout for stabilization or cracks in concrete. Warner identifies several categories of materials may be used for injection namely: *cementitious* (slurries, suspensions), *chemical* (sodium silicate base, acrylates/acrylamide, urethanes), *resinous* (epoxies, polyesters, resinous foams) and *miscellaneous* (hot asphalt/bitumen, clay, high-calcium lime) [149].

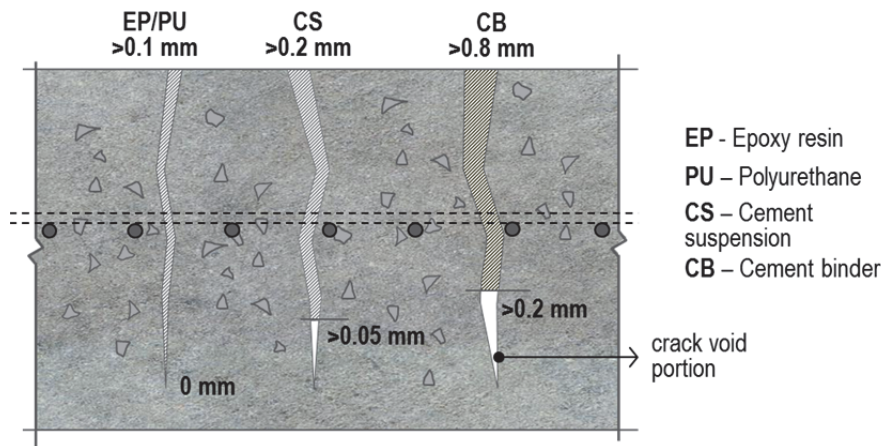


Figure 4.1. Crack opening width matched with the injection materials classes correspond to the void portion unable to fill. The image is adapted from Panasyuk et al [209].

With regards to the common repair materials – liquid or paste-like – able to be infused into the concrete crack or void, Panasyuk, V. V. *et al.* [11] specifies three classes; (i) cement mineral, (ii) cement and polymer components, and (iii) polymers such as polyurethanes which prevent leakage and epoxy which provide structural crack seal. Moreover, as depicted in the figure 4.1 Panasyuk, V. V. *et al.* asserts; (i) cement binder or mortar [**CB**] is applicable to the crack opening wider than 0.8 mm but left crack tip of 0.2 mm unfilled, (ii) cement suspension filler [**CS**] is appropriate for the crack opening wider than 0.2 mm however crack tip of 0.05 mm remain unfilled, and (iii) fluid polyurethane [**PU**] or epoxy resin-based fillers [**EP**] is relevant for crack opening wider than 0.1 mm and fills the remaining crack tip completely [209].

Three category of healing agent are used in technical testing phase in this work; chemical-based, cementitious grout, and uniquely developed bio-based solution [147]. The first two are employed in this chapter considering its potential to seal the crack structurally while the bio-based agents will be investigated in the chapter 5.

4.2.1. Three types of healing agents

The *first* type of the agent is single- and double-component chemical based which mostly works through poly-condensation or cross-link polymerization upon contact with the atmosphere, with the concrete matrix or within the reactants [86, 209]. In this work, epoxy resin was chosen. Epoxy injection is common practice in the concrete crack repair practice to glue crack faces together and provide structural integrity recovery [144, 209]. Epoxy may be cured by homo-polymerisation (one compound self-reaction) or by co-polymerisation (resin in reaction with poly-functional catalyst; i.e. hardener) in ambient temperature or with a heat input. A large variety of epoxy resin is manufactured by industry making it possible to have broad options.

In this study, two compound Bhisphenol epoxy resin and catalyst is used as it is easy to prepare and readily available. It is generally used to stabilize specimen for polished section investigation. Epoxy resin is Conpox Harpiks BY 158 mixed with catalyst

HärderHY 2996, both from Condor Kemi A/S. The composition from the supplier is 1800 kg BY 158 mixed with 0.540 kg HY2996. 1% of fluorescent powder dye (Epodye) was introduced into the mixture to enhance crack pattern under ultra violet (UV) light. The mixture possess low dynamic viscosity approximately 5-15 cP which is sufficient for injection with a syringe. Upon mixing the monomer resin reacts with the catalyst exothermically to form spatial (3D) cross-linked thermoset structures. The shelf-life after mixing is about an hour in ambient temperature. It is thought that these two components may be stored in the different syringe (container) and mix with static mixing nozzle upon injection.

The *second* healing agent used is grout material made of cementitious powder mix. Cementitious grout material can be thought as healing agent for concrete structures since it functions as crack sealant and void filler with the objective to restore structural integrity. In principle this grout material is prepared by mixing cement and water. Polymer modifiers or admixtures may be added to obtain certain properties; e.g. increasing the ability to inject by lowering viscosity, or if needed, delaying the setting time, provided the compatibility with the concrete substrate is assured. Bras *et al.* [208] identify the factors affecting the flow-ability of the grout materials such as binder type and composition, water-to-binder ratio (w/b) and admixture content type and dosage. Environmental factors, for instance moisture and temperature and mixing procedure also affects the quality of the grout.

Despite the commercially available grout materials, in this study, the grout was prepared by mixing CEM I 42.5 with tap water. The water-to cement ratio was 0.4 and 0.5% high range water reducer (HRWR/superplastizicer) was added to the mix. Prior to the water addition the cement powder was hand mixed by trowel to prevent granulation. Then the powder was poured into the Hobart bucket for automatic mixing. The water and SP was premixed and subsequently 2/3 was added first to the cement and mixed at medium speed for 2 minutes. Then the other 2/3 was added and again mixed for 2 minutes. Afterwards the mixture was mixed for one minute at maximum speed. Then the mixture was put into the syringe for injection in the PNC.

The *third* agent is bacteria-based repair solution. It contains (1) alkaliphilic bacteria able to facilitate bio-mineralization, (2) nutrients, and (3) transport solution. This unique solution was initially developed with the main target to repair aged cracked concrete. Chapter 5 is devoted to test its potentials and performances as agent injected into PNC.

4.2.2. Specimen type

For the rest of the technical testing phase the choice has been made to employ Porous Network Concrete with mixture P24-2-B for the porous core, see table 2.5. It has a composition of Cement CEM I 42.5 275 kg/m³, Fly Ash C class 25 kg/m³, gravel aggregate of 1513 kg/m³ with water-to-binder ration 0.33 and superplasticizer SP (Glenium 51 30% solid content) 1% to binder volume. A water soluble PVA film supplied by HARKE GmbH with grade KA 40 µm was used to cover the core prior to the casting of the concrete main body. Normal strength concrete was utilized for the main body of the PNC24-2-B which has a composition described in table 2.3.

Two types of specimens were used; (1) cylinder for tension test was prepared based on the procedure described in subchapter 3.3.1 and (2) prism for bending test was produced based on the procedure detailed in subchapter 3.3.2.

4.3. Test 1; Porous Network Concrete cylinder with epoxy resin

4.3.1. Manual healing of the PNC cylinder

Epoxy resin healing efficiency of the PNC was evaluated on cylinder specimens with manual and automatic injection. Three cylinder specimens were tested. Each had dimension diameter $\varnothing 56$ – height 120 mm with a porous core diameter $\varnothing 23$ mm in the centre longitudinally. The introduction of a crack in the notched zone was done by means of displacement controlled monotonic uniaxial tension test. The strain rate was $0.5 \mu\text{m}/\text{sec}$. An almost linear increment of load was observed in the elastic phase reaching a peak strength of about 2.1 kN followed by a softening curve where the increase of displacement corresponds to a decrease in load, see figure 4.3.

After the crack opening reached $200 \mu\text{m}$, the specimen was removed from the loading frame and the crack was stabilized by two layers of adhesive tape as depicted in figure 4.2. Then, the 30 mL premixed epoxy resin and catalyst was injected manually by means of syringe. The epoxy in the specimen was allowed to cure for 24 hour in the ambient temperature.

The second tension test was performed subsequently for two specimens. For this, the post-healing specimen was mounted back in the loading frame, see figure 4.2(2). The third specimen was cut open longitudinally to observe its interior. It was also observed that the epoxy resin in the syringe and connecting tube was also hardened making it unable to be removed.

The reloading of the healed specimen was performed with the same setup and strain rate until sudden brittle failure of the specimen. The average load-displacement response of the cylinders tested is presented in figure 4.3. Some tendencies have been recognized although there is certainly some variability in the results obtained from the experiments due to the heterogeneous nature of the system investigated.

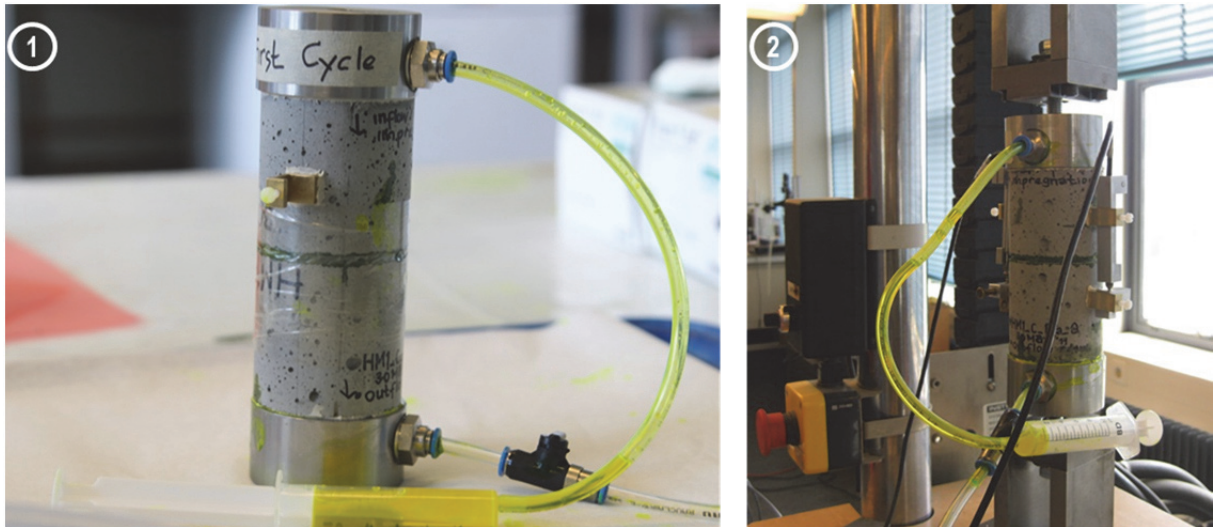


Figure 4.2. The cylinder PNC after crack formation; (1) crack is stabilized with adhesive tape and injected with epoxy resin, (2) second loading cycle after 24 hours curing.

It may be seen that for virgin (pre-healing) specimen there is a peak value of tensile load of 2.23 kN. It is noticed that the peak tensile load value occurs when the crack mouth opening displacement (CMOD) reaches 15 μm . It is then followed by non-linear softening behaviour until CMOD reached 200 μm when the test was stopped. Figure 4.4(1) visually confirms crack formation in the notch area of the cylinder.

The second loading cycle results in a similar load-CMOD response. It is obvious, however, that the peak load of the healed specimen is higher. The higher peak value, approximately 5.2 kN, is more than twice the peak load value of the pre-healing specimen. For the stiffness measured by secant line, it may be noted that no significant difference in material stiffness was observed in the linear elastic phase between virgin and injected specimen. Then it is followed by softening curve as can be seen in the figure 4.3.

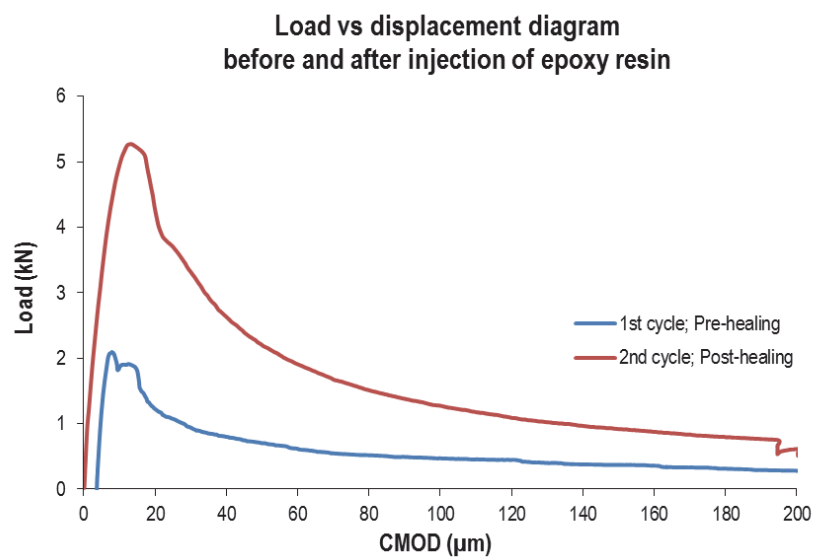


Figure 4.3. The load versus displacement of Cylinder specimen injected manually with epoxy resin.

The efficiency of the manually assisted healing action of porous network concrete may be examined by comparing the mechanical response of the healed cylinder to the initial response of the virgin cylinder. Noticeably, the manual healing of the PNC cylinder with epoxy regains the tensile strength. This apparent ‘enhancement’ of response in term of higher value of peak tensile load occurs due to the following reasons: The low viscosity epoxy flowed and filled up all void spaces in the porous concrete core including crack in the fracture process zone (FPZ). When it hardened it created a polymer-cementitious composite action which enhanced the tensile properties in the cylinder. The tensile force was distributed into the whole cross section in the denser cylinder. Therefore the tensile stress in the healed cylinder specimen is higher. The polymerisation of the resin, *the liquid monomer turns into 3D solid networks of polymer chains*, may be thought as reinforcement in composite action with the concrete main body.

Visual confirmation of healed response is provided by a new crack surface formation which occurred in the cylinder. Figure 4.4 shows the original and final crack patterns on the side face of the cylinder. As the epoxy filled the notch and hardened this region became stronger. The new fracture surface shifted a few millimetres away from the notched area where the previous crack was formed, see figure 4.4(2). This is because this area became weaker than healed crack zone. The crack at this location was not observed to occur in the first cycle. This provides a clear indication of the effectiveness of the healing capabilities using epoxy resin for Porous Network Concrete.



Figure 4.4. (1) The crack formation in the notch, (2) the new crack formation after the first was healed, and (3) the new crack face

Further qualitative evidence of the effectiveness of the autonomic healing process is given by visual confirmation of the longitudinal section of the sample which was portrayed under UV light as depicted by figure 4.4. The figure shows the different material phases in the hierarchical porous network concrete material. The bright green epoxy polymer can be seen filling up all voids including crack path in the middle of the specimen. It is also evident because the crack is sealed the liquid tightness through the main body is ensured. Since there is no empty void the permeability of the concrete is reduced and the overall strength increases. The tensile force which was distributed only to the concrete is now distributed to the whole cross section. The healed PNC now has higher internal stress capacity.

The boundary line between the main body and the porous concrete core is visible and filled with epoxy. This implies that the PVA film was dissolved during or after casting self-compacting concrete while protecting the core from cement paste intrusion into the voids in the interface. The further implication is that the level of designed porosity in the interior of the PNC can be achieved satisfactorily.

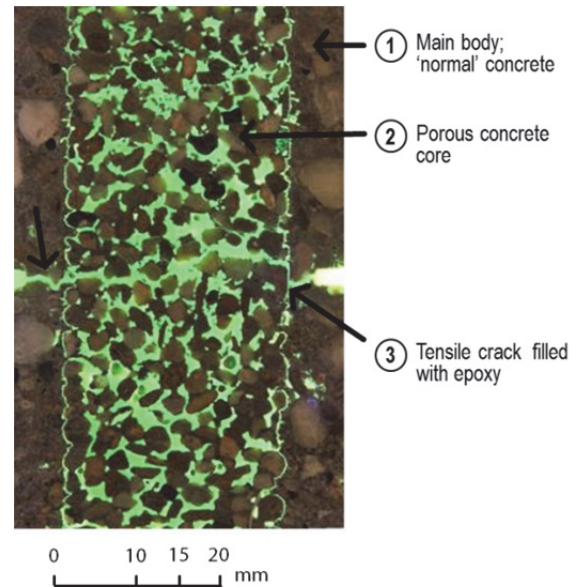


Figure 4.5. Longitudinal section of the cylinder portrayed under UV light showing the crack path filled with epoxy

4.3.2. Autonomous healing of the PNC cylinder

To make the healing mechanism 'truly' self-healing, a feedback system was designed and proved to be effective in the subchapter 3.4. In this section the same setup is employed to evaluate the healing efficiency with the epoxy resin as healing agent. Figure 4.6(1) demonstrates the displacement controlled tension test setup for cylinder specimen. Figure 4.6(2) shows the last stage of the automatic injector. The injector was switched off after pumping the premixed epoxy resin and catalyst completely through the porous core.

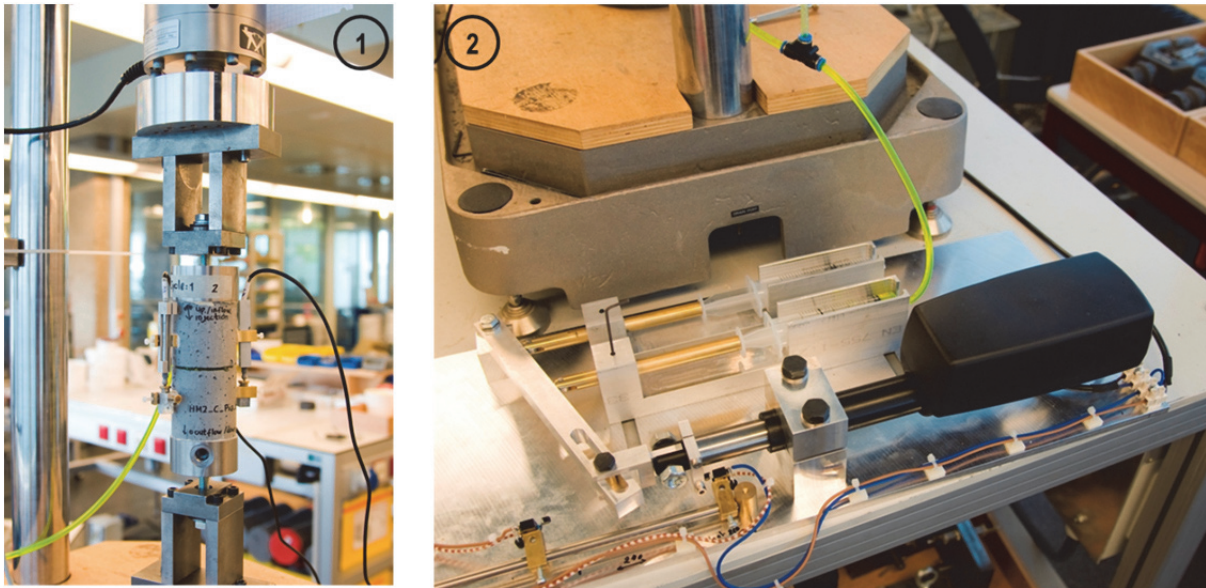


Figure 4.6. Setup of autonomous healing of the PNC. (1) Specimen PNC cylinder under uniaxial direct tension. (2) Injector in the last stage.

The test program involved a PNC cylinder (with duplicates) with a circumferential notch in its mid-height that was mounted in the loading frame, see figure 4.6(1). The load was exerted with the strain rate of $0.5 \mu\text{m/s}$. The loading curve is presented in figure 4.7 where the linear elastic part is observed up to the peak tensile load 6.56 kN. Then it is followed by the nonlinear softening curve when the crack widened in the specimen and the load gradually decreased. At the moment injector is in the 'off' state – *a stand-by mode* – as detected in the signal of the actuator, see the part (1) in the figure. As the crack mouth opening displacement (CMOD) of the specimen reached the pre-set threshold value, $75 \mu\text{m}$, the injector was switched on and started pumping the premixed epoxy resin and catalyst. After the injector fully infused the healing agent, the displacement of the specimen was set in the stationary point by close loop control mechanism in the INSTRON® 8872 for 24 hour, see the part (2) in figure 4.7. During this time, the healing agent polymerized.

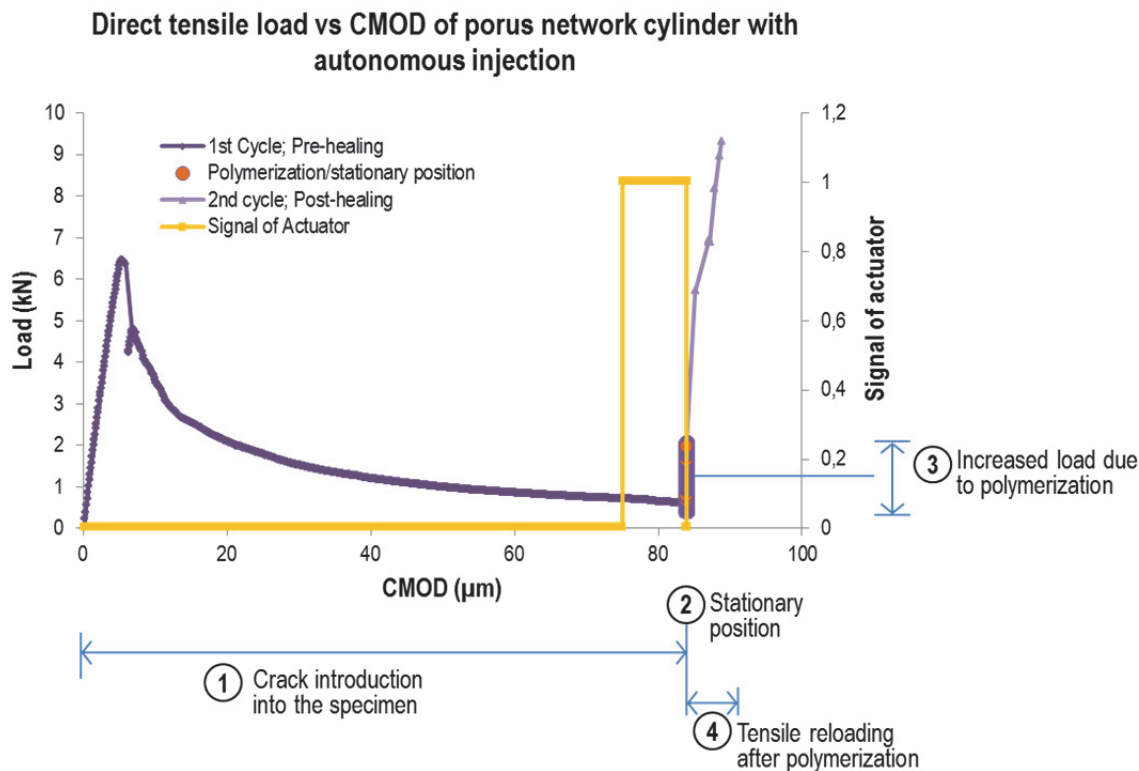


Figure 4.7. The composites graphs of load versus CMOD and signal of actuator of specimen injected automatically with epoxy resin.

Interestingly, a load increment was recorded by the DAQ system during the 24 hour polymerization indicated by part (3) in the figure 4.7. This can be attributed to the shrinkage of the epoxy resin during the process of solidification. As the agent shrank more load had to be exerted by the INSTRON® 8872 pneumatic system in order to keep the displacement at the stationary point.

The test was continued with the second loading cycle from the stationary point. The post healing curve in the figure 4.7 indicates the tendency of the specimen able to provide higher strength and stiffness compared to the virgin specimen. The specimen experienced sudden breakage at the peak load at about 9.68 kN. This peak load is higher than the peak load of pre-healing specimen by factor of 1.47.

Figure 4.8 (1) shows the wetted area in the notch suggesting that the healing agent flew inside out filling the void left by the crack and the void within the notch itself. Under UV light as depicted in the figure 4.8 (2) the agent completely occupies the porous core in the centre of the PNC.

In the pre-healed PNC cylinder under tension, the strength was determined by the stress concentrated in the notched cross section. After injection, the porous core and notch was filled with healing agent. When this agent hardened, the tension force was distributed within the whole cross section. This made the stiffness and strength of the post-healed specimen increased. The failure was a sudden breakage, a fully brittle failure, in the region very close to the glued interface between specimen and the steel cap, see figure 4.8 (3). The newly fractured zone was the weakest region as only the main body of the PNC carried the tensile stress.

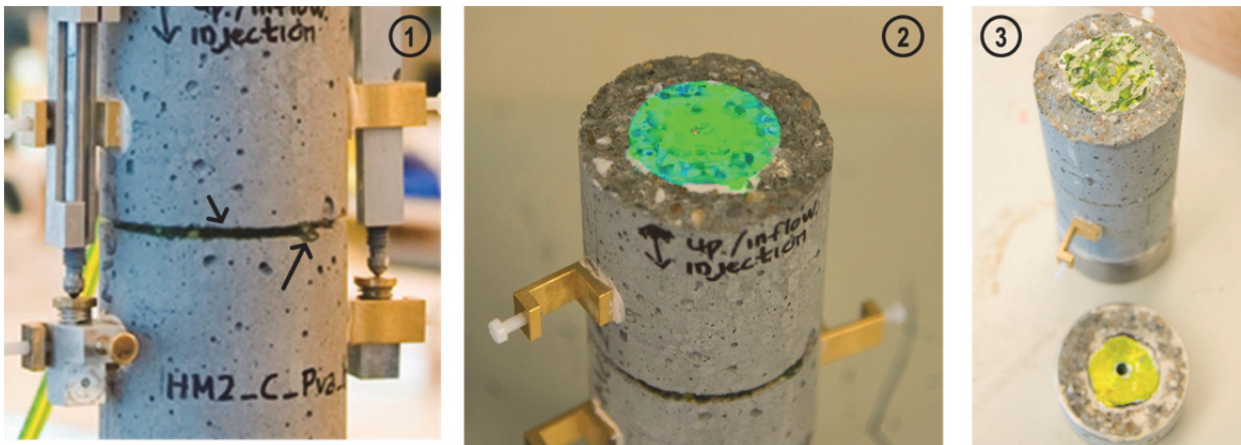


Figure 4.8. The PNC cylinder healed autonomously with epoxy resin. (1) Epoxy resin flow from porous core into the crack face. (2) Epoxy resin creates dense layer in the interior of PNC. (3) Failure zone after second loading.

4.4. Test 2; Prism with epoxy resin injection

Three types of prism specimen were used in this experiment; plain concrete prism, reinforced concrete prism, and porous network concrete prism. The PNC prisms were intended for self-healing mechanism testing either manual or autonomous. Both plain concrete and reinforced concrete prisms were meant as reference.

All specimens with duplicates has dimension of $55 \times 55 \times 285$ mm. Plain concrete (without rebar) and reinforced concrete specimen have normal strength concrete (NSC) design mixtures as in the table 2.3. The reinforced concrete specimen had a diameter $\varnothing 2$ mm threaded steel which was put 15 mm from the bottom side of specimen in the longitudinal axis.

To create the Porous Network Concrete, a porous concrete core of $25 \times 25 \times 295$ mm was made, covered with soluble PVA film $40 \mu\text{m}$ and placed in the centre interior of a concrete main body prism. A diameter 2 mm threaded steel was put underneath the porous core. The production process followed the procedure explained in the subchapter 2.3.1.

A simple water leakage test was designed for testing the ability of the PNC to flow fluid through its porous core. Subchapter 3.4.2 elaborates in greater detail on the working principles and how healing efficiency can be determined using this straightforward test as depicted in figure 4.9. The initial permeability test is intended to confirm the flow-ability of the core and carried out prior to the crack formation. The next step is blowing 0.7 bar pressurized air to flow through the porous core about 20 minutes allowing porous core in the prism to achieve saturated surface dry (SSD) conditions. The pre-healing leakage test is carried out after crack formation and followed by the blowing air in the same aforementioned procedure. Post healing leakage test is conducted after the healing action is carried out.

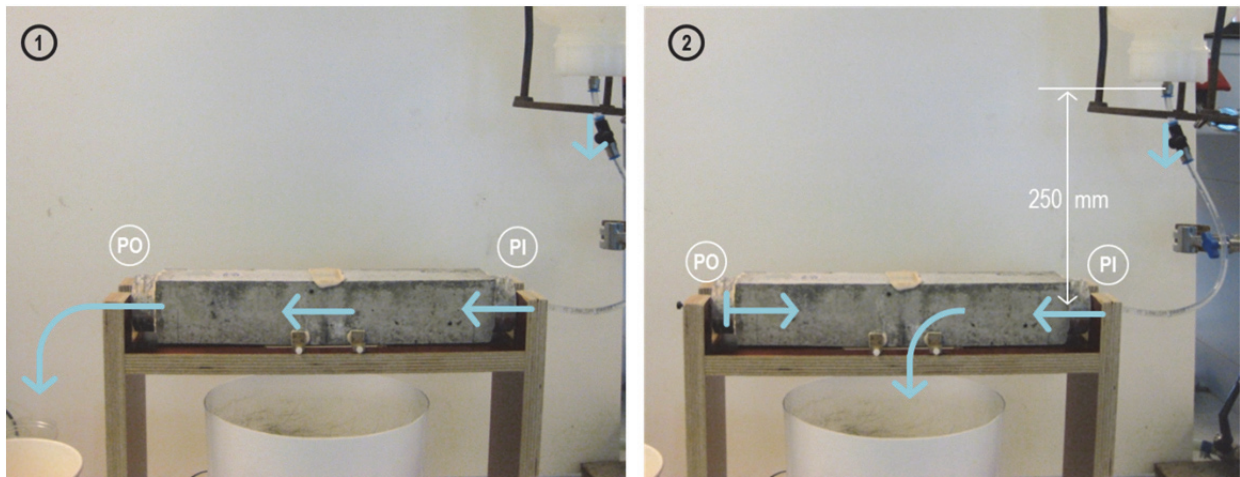


Figure 4.9. A water leakage (permeability) test for the PNC test. (1) Initial permeability where water flows from port of injection through the core and flow out. (2) The test where the port of outflow is plugged and water is forced to flow from (healed) crack opening.

The experimental program follows the design as depicted by the table 4.1 where it shows the different repair and healing mechanism.

Table 4.1. Experimental program for assessing healing efficiency of PNC prism. Note: n.a = not available, TPBT = three-point bending test, T = temperature; RH = relative humidity.

Procedure	Plain concrete	Epoxy Resin		
		RC	PNC	PNC
1. Initial leakage test	n.a	n.a	Yes	Yes
2. Crack creation	TPBT	TPBT	TPBT	TPBT
3. Pre-healing leakage test	n.a	n.a	Yes	Yes
4. Injection	n.a	Direct to crack zone	Manual	Autonomous feedback
5. Curing	n.a	T: 20±5°C RH: 35±5% 24 hour	T: 20±5°C RH: 35±5% 24 hour	T: 20±5°C RH: 35±5% 24 hours
6. Post-healing leakage test	n.a	n.a	Yes	Yes
7. Mechanical test	n.a	TPBT	TPBT	TPBT

4.4.1. Manual injection healing

a. Crack formation

Plain concrete, reinforced concrete, and porous network concrete prisms were loaded by three point bending test, as depicted in figure 4.10. The crack width was measured by means of a linear variable differential transformer (LVDT) with a measurement range of $\pm 500 \mu\text{m}$ and an accuracy of $1 \mu\text{m}$. Two LVDTs were placed at the bottom side of the specimen and the mean value was used to control the close-loop test.

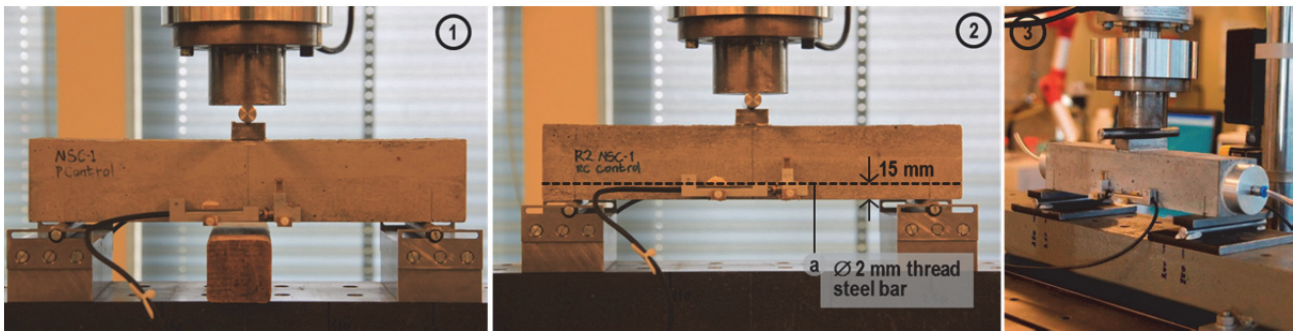


Figure 4.10. Three-point-bending test setup for (1) plain concrete, (2) reinforced concrete, and (3) Porous Network Concrete

For plain prism, the test was performed at strain rate of $0.5 \mu\text{m} / \text{sec}$ and was stopped at a crack opening of $100 \mu\text{m}$, yielding the softening curve as shown in the figure 4.11. For the other type of specimens, the deformation control test has been carried out at the rate of $1 \mu\text{m} / \text{sec}$ until a crack of $450 \mu\text{m}$ was reached. At that point, the load was removed causing the crack to close to the value approximately $250 \mu\text{m}$.

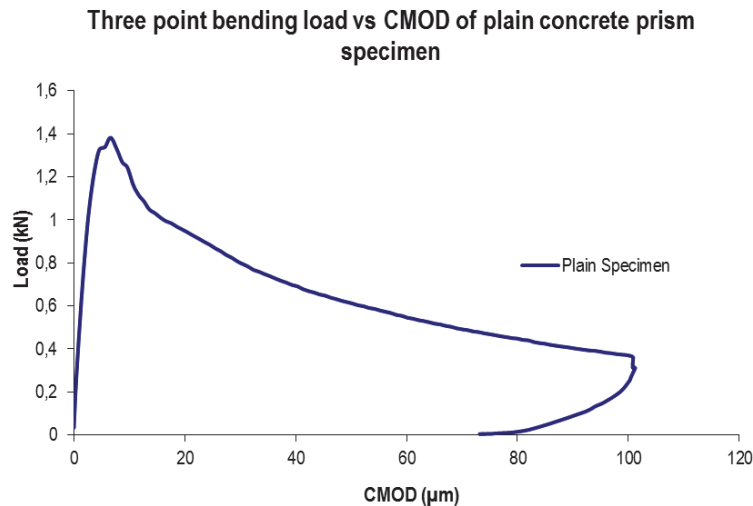


Figure 4.11. Load versus displacement curve of plain prism.

b. Epoxy injection

For the reinforced concrete prisms, after first loading cycle, the crack was directly injected with healing agent into the crack plane by means of syringe and needle. For the Porous Network Concrete, after the first crack had been created, the injection of healing agent was carried out through the porous core by means of syringe injection action. This is illustrated in the figure 4.12. To achieve complete polymerization of healing agents, the specimens were cured for 24 hours in the ambient temperature.

c. Tension test of the healed specimen and mechanical properties recovery

After healing, the reinforced concrete prisms and the Porous Network Concrete were mechanically tested again. The bending test setup and strain rate was kept the same as the previous test for pre healing (virgin) specimens.

For plain concrete during crack formation, it was seen that the load first increased without much deformations measured as crack mouth opening displacement (CMOD) in the concrete as depicted by figure 4.10. When the peak load was reached at approximately 1.4 kN the appearance of a crack could be observed. Afterwards the softening regime was observed in terms of increasing crack width with decreasing load.

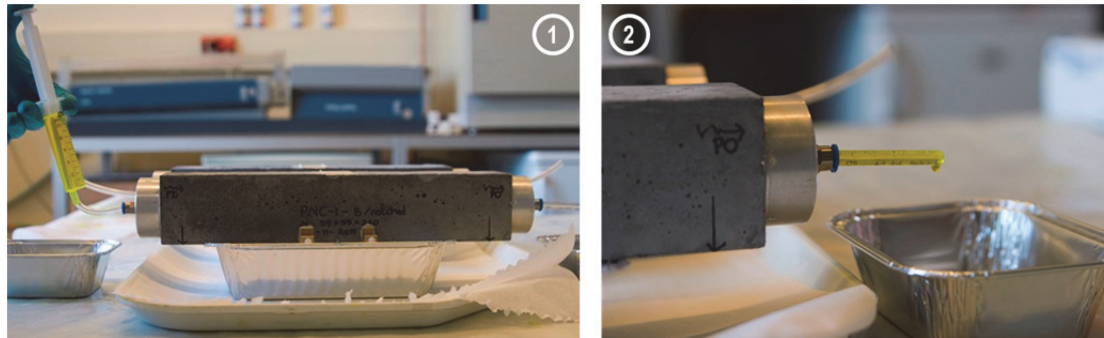


Figure 4.12. Injection of the epoxy resin into the porous concrete

When a crack width of $\pm 100 \mu\text{m}$ was reached in the reinforced concrete and Porous Network Concrete specimens, the load started to increase again. This hardening behaviour was caused by the fact that tensile stress was carried by rebar installed in the concrete prism specimens compensating the cracked concrete. When a crack width of $450 \mu\text{m}$ was reached, the specimens were unloaded with the same loading rate. It can be observed in the graph that the crack width decreased due to elastic unloading of the concrete and steel.

For the reinforced concrete (RC) specimens in which cracks were manually healed by direct injection (pressure grouting using the syringe), a second loading cycle was applied after hardening of the epoxy. The curves obtained during this reloading can also be seen in figure 4.13. It shows that there was a partial stiffness and strength regain. The stiffness is less than the first loading cycle stiffness curve or about 67.3 %. The peak load of the healed specimen is about 1.39 kN or 98.1% of the peak load obtained in first cycle (virgin specimen). This is due to the rebar which was able to carry the load and internal bending stress. It was also observed that the crack that was obtained in the first loading cycle just reopened after reloading. It can be concluded that crack sealing worked well while mechanical recovery in terms of strength and stiffness was provided by the rebar only.

For Porous Network Concrete (PNC), the first and second loading regime was applied in the same procedure as reinforced concrete (RC) specimen. In between loading cycle the porous core was injected manually with the procedure as explained above. In figure 4.14 the average load vs crack mouth opening displacement (CMOD) curve for the PNC is presented.

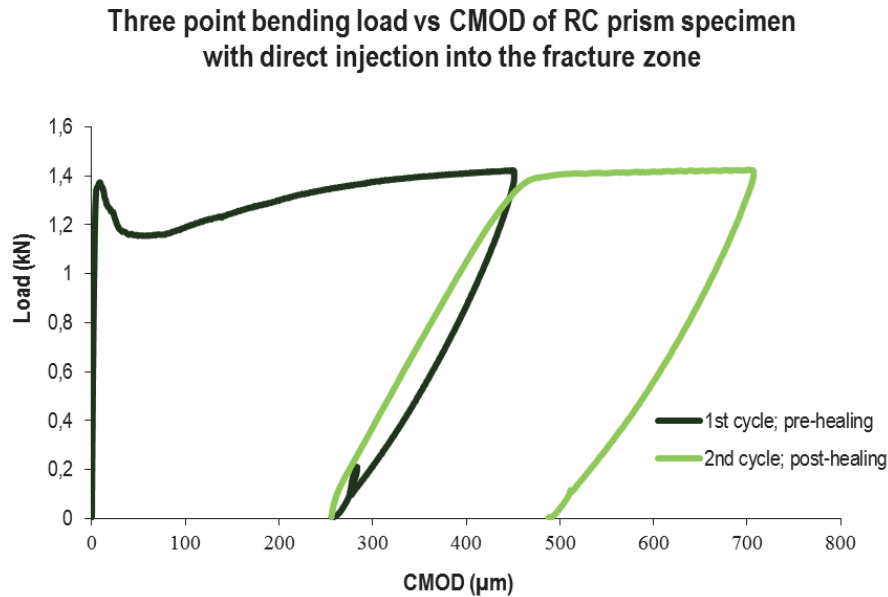


Figure 4.13. Load versus displacement curve of RC prism healed by direct injection into the crack face.

In the second loading stage, the ‘first’ cracking strength was achieved almost as the same as the original prism. Then it was followed by a strain hardening regime which shows increasing slope before the unloading stage was started. The changes in mechanical response is attributed to the fact that epoxy has filled up the porous core. This makes the whole cross section able to carry larger flexural stress. Furthermore the stiffness in the second loading stage was similar to the stiffness of the first loading stage. This also indicates that complete regain in strength and in stiffness was obtained due to crack healing action. It was also observed that new crack was formed upon reloading.

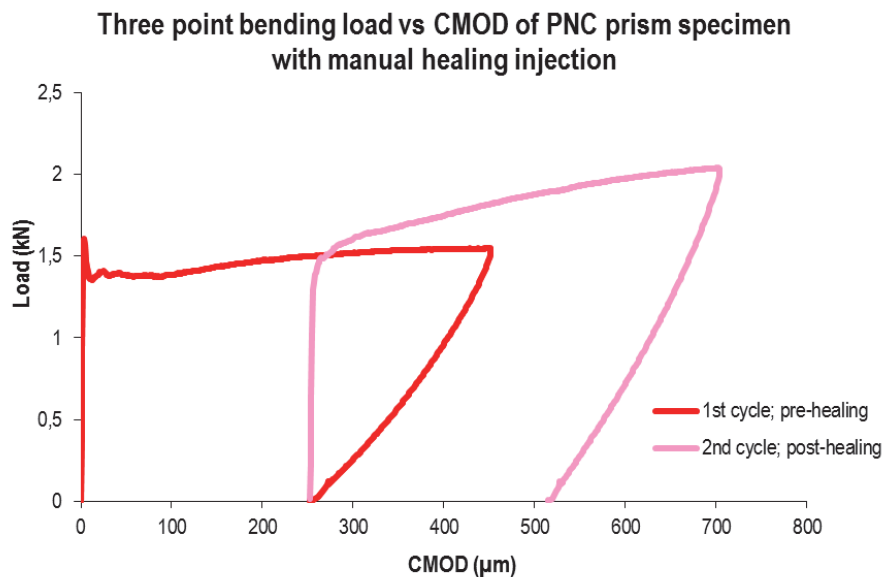


Figure 4.14. Load versus displacement curve of PNC prism healed by manual injection through porous core

d. Leakage (permeability) test

The result of initial, pre- and post-healing permeability test is presented in the figure 4.15 where weight of the water flow out increases over time. Initial permeability test of PNC prism was carried out before crack was formed in the first loading. The test confirmed that the interconnected pores allowed water to flow through the porous core the from port of injection to port of outflow. Pre-healing permeability test shows a less steep slope than initial test as the discharge opening (the crack) is not as large as the previous initial test. More water was retained in the porous core.

Interestingly, post-healing permeability test revealed a zero slope which can be interpreted there was no water flew out from the crack. Following the equation 3.7, the healing efficiency is determined by the ratio of slope of post- to pre-healing permeability curve. Therefore the healing efficiency is 100%. In other word, the crack was completely sealed.

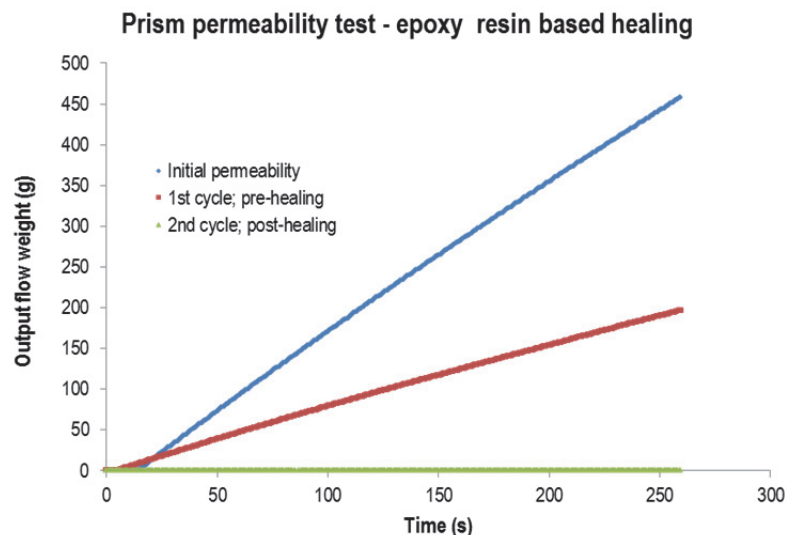


Figure 4.15. Permeability curve representing the weight of water discharged as function of time for initial condition, pre- and post-healing for the PNC with manual injection.

e. Visually qualitative evidence

For all test series, except for the plain concrete specimen, it was seen that the crack void was filled with epoxy. In case the cracks were directly injected, the healing agent was manually infused by a needle and syringe along the whole crack length. It could be seen that the healing agent was equally spread over the crack faces at the surface, covering almost half of the cross section.

For the manually injected healed PNC, the epoxy healing agent was injected into the porous core by syringe through the port of injection. All the interconnected pores (voids) in the porous network were filled as well as the crack zone, as shown by the cross section of the porous network concrete, see figure 4.16(1). Figure 4.16(2) shows the original flexural crack created by bending test in the mid span of the prism is filled with epoxy resin. Evidence of the healing efficiency is provided by a new crack formation which occurred in the prism. The final crack pattern which was not observed to occur in the first cycle is in different location from the crack in the first

loading. Further observation reveals that the liquid phase epoxy resin penetrate into the vicinity of the crack and when it is hardened (polymerization) it makes the fracture zone stronger and stiffer than the other part of the PNC. Upon reloading the failure of the PNC happened in the weaker part away of the healed fracture zone.

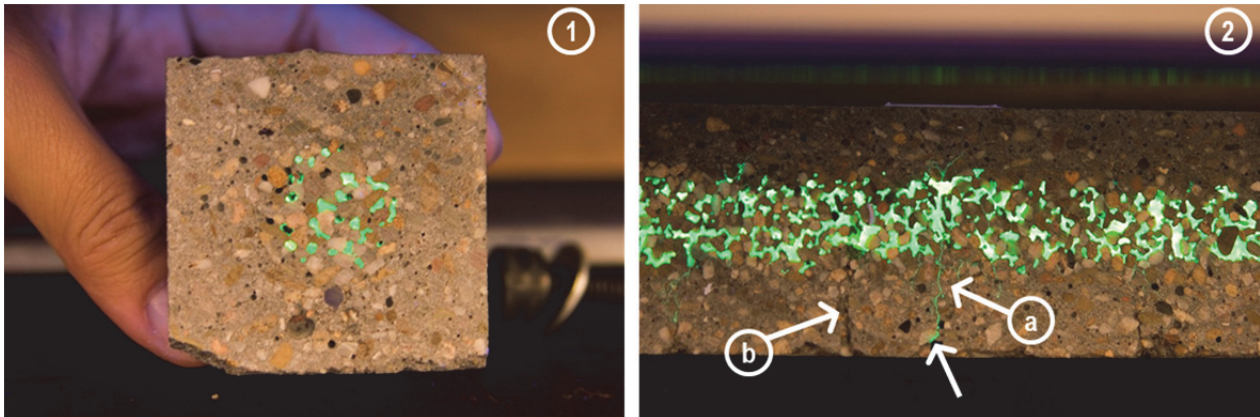


Figure 4.16. The cross and longitudinal section of the healed PNC specimen showing the filling of the porous core and the crack; (a) first crack and (b) second crack upon reloading.

Portrayed under UV light, bright green epoxy polymer can be seen filling up all space including the crack in the fracture process zone of the specimen, see figure 4.16. In this case it can be concluded that once the empty pores are filled up, permeability of the system is reduced and the intended liquid tightness is achieved. On the other hand, a subsequent similar healing process cannot be performed. For large infrastructures, however, it is possible to design a healing system with multiple injection points and or by embedding multiple porous cores.

4.4.2. Autonomous healing

a. Test setup and experimental program

The experimental program, see table 4.1, was designed to assess the healing efficiency of the PNC with premixed epoxy resin and catalyst injected autonomously. The focus of this section is to study the behaviour of the system, in particular, when the polymerization takes place in the porous core and the system.

Figure 4.17 exhibits the complete setup of the autonomous self-healing test of the PNC prism with four main components connected in the close-lope feedback system. The working principle was elaborated in great detail in the subchapter 3.2 with the proof of its efficiency in the subchapter 3.4.

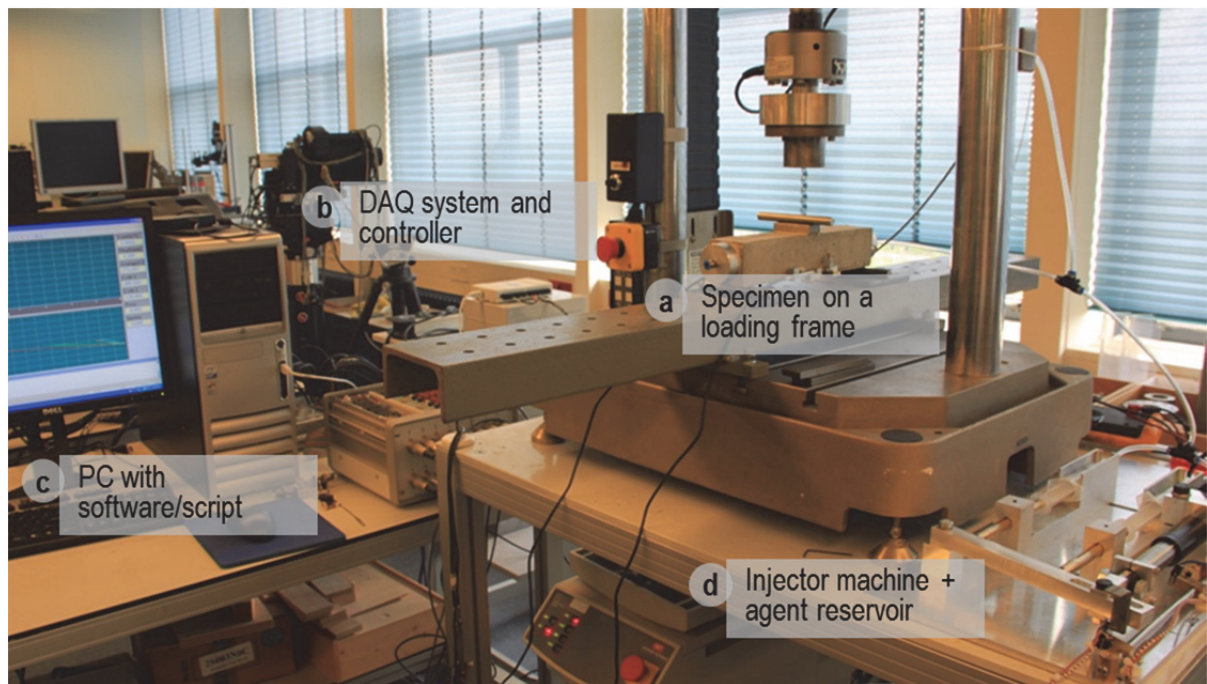


Figure 4.17. Test setup of the autonomous healing of PNC prism

The PNC prism is placed on the roller supports in the loading frame INSTRON® 8872 for closed loop displacement controlled three point bending test with strain rate of $1 \mu\text{m/s}$. When the crack mouth opening reached $250 \mu\text{m}$, detected by the sensor, a triggering signal was sent to switch on the actuator for supplying the premixed epoxy resin into the PNC. Later, as the pneumatic system of INSTRON® 8872 was maintained in stationary position for 24 hour, the healing agent in the PNC was allowed to harden. Eventually the prism was subjected to the second loading with the same loading rate.

b. Result and discussion

As the load exerted, the bending stress develops internally in the PNC prism where in the linear elastic phase the stress was distributed in the entire cross section of the prism. When the load reached its peak, a crack initiated and load decreased while the displacement continued to increase. The nonlinear relation between load (stress) and displacement (strain) was developed subsequently where the tensile stress mostly was carried by rebar installed.

This crack creation phase, where the actuator was in the 'off' state, remained up to the point where the sensor detected the crack opening of $250 \mu\text{m}$. In this phase, the pressure sensor detected an almost constant value of the porous core interior pressure. Subsequently, the pressure sensor sensed a built up pressure in the interior up to 0.3 bar which was still below the pre-set threshold value as epoxy was infused into the core. Later as the agent had been fully infused, the injector was switched off and the controller maintained the pneumatic system of INSTRON® 8872 in the last state for 24 hours. This allowed healing agent polymerization happened in the PNC at ambient temperature. Figure 4.18 presents the composite graph of load as function of displacement combined with the actuator signal and interior pressure of the PNC prism.

The second loading was started after 24 hours curing of the healing agent with the graph depicted in the figure 4.17. It is clear that the peak bending load, 2.49 kN, is almost as twice as the virgin (pre-healing) specimen. Meanwhile the stiffness regain of the healed specimen is up to 99.7% compared to the original stiffness. Similar to the phenomenon observed in the cylinder specimen, this may be attributed by the fact that the healed prism has denser cross section which may carry more bending stress. In this case the polymerized epoxy provides additional reinforcement that increases the strength as well as stiffness of the post-healing state.

As the peak load achieved by the healed specimen, the new formation of crack developed in the area weaker than the former healed crack. The load then decreased as the crack opening grew bigger up to the bending failure. During the process of the second crack opening, the tensile stress of in the lower part of the beam was carried solely by the reinforcement bar where it deformed plastically depicted in the softening curve

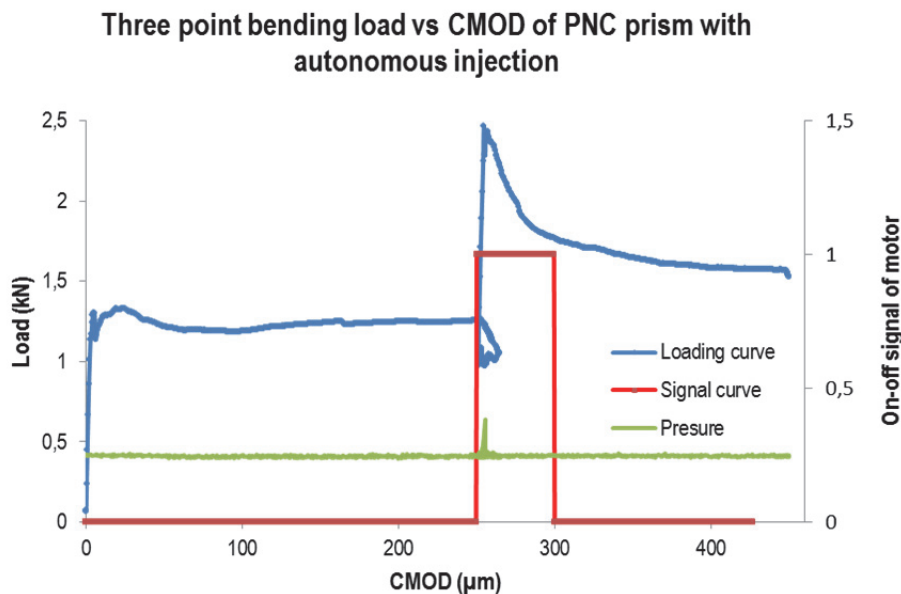


Figure 4.18. The load versus crack mouth opening displacement of PNC healed with epoxy resin autonomous injection

Figure 4.19 frame (1) displays the cracked specimen where the epoxy resin leaked out in the crack zone and few drops can be seen contained in the aluminium tray underneath the fracture zone. The specimen was kept immobile under the constant deformation state and the image of the crack was taken under UV light in the evening showing the fluorescent path of the crack, see figure 4.19 frame 2.

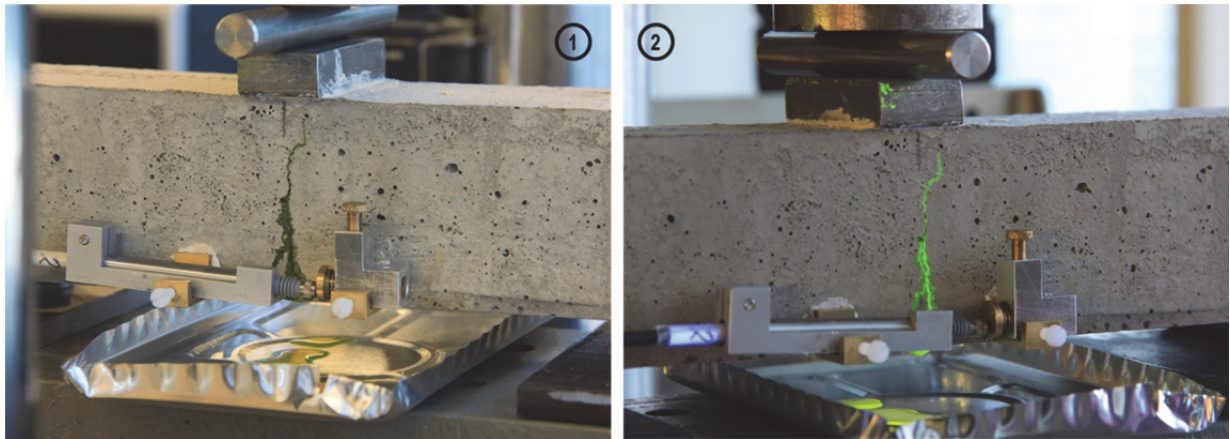


Figure 4.19. The Porous Network Concrete specimen; (1) right after injection where epoxy resin flew out and wetted the crack surface, and (2) after several hours of polymerization has formed portrayed under UV light

The images of the second crack formation are presented in the figure 4.20. Frame 1 depicts the specimen at the moment it failed due to the bending load. Meanwhile frame 2 is the image of the two pre- and post-healing bending crack formations. Even though in the experiment, the value for the crack threshold was pre-set at 250 mm, it is believed that larger crack opening can be healed with liquid low viscosity epoxy resin.

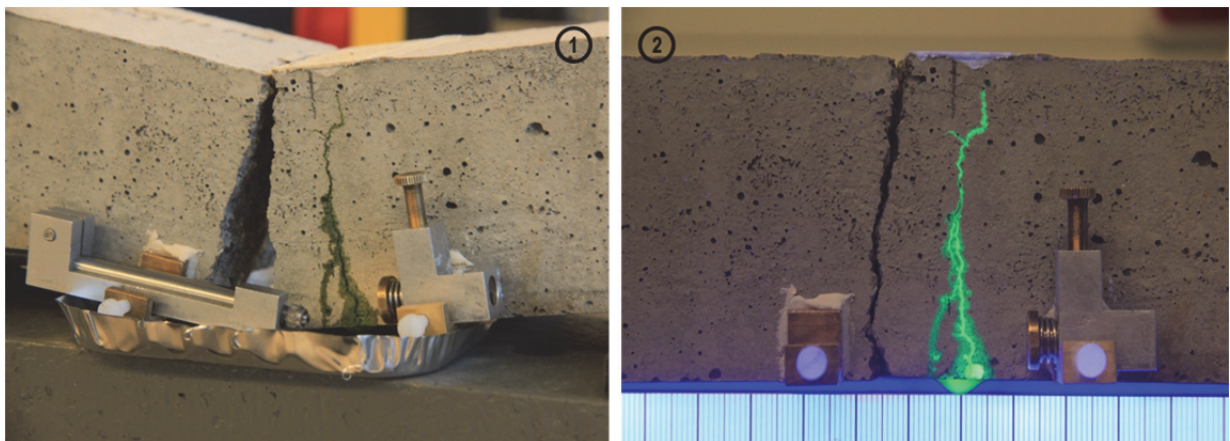


Figure 4.20. The Porous Network Concrete specimen; (1) right after failure where the second crack formed in the weaker plane, and (2) formation of the healed crack and the flexural failure portrayed under UV light

c. Leakage (permeability) test

Similar to the procedure of permeability test for the PNC with manual injection, the permeability test of PNC prism for autonomous injection was performed to obtain initial, pre- and post-healing permeability value. In general similar result was obtained and is presented in the figure 4.21. The permeability curve slope of post-healing specimen is zero as it was no water leaked out. Meanwhile the slope of pre-healing specimen is higher which indicate the water was leaked out from the crack mouth. Therefore the crack was completely sealed and the healing efficiency reaches 100%.

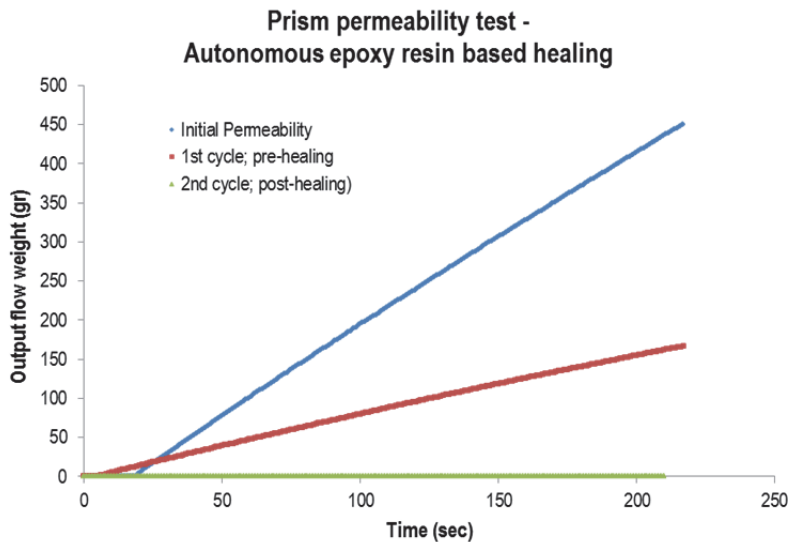


Figure 4.21. Permeability curve representing the weight of water discharged as function of time for initial condition, pre- and post-healing for the PNC with autonomous healing mechanism.

4.5. Test 3; PNC prism cementitious grout injection

a. Grout materials

Many commercially available grouts have been developed for different kind of purpose. There are general purpose cementitious grouts for general civil engineering works. Some other grouts are available for specific targets, i.e. masonry grout, non-shrink high strength grout for crack repair, or prestressed tendon cement grout.

Grout is slurry, thick emulsions, or paste-like, containing dispersed particles able to flow and fill voids. The particles create an internal network to bear yield stress. The grout behaves elastic to viscoelastic if the stress applied is lower than its yield point. However it will flow whenever it is subjected to shear stress higher than the yield limit. Several investigations have been carried out to reveal fundamental knowledge and understanding the grout material for better prediction of its impact in grouting soil, rock, and structures [149, 208, 210-214].

According to Bras *et al.* [208] cementitious grout are colloidal suspensions comprises of water and cement where admixtures may be added into the mix to gain certain properties. The particles in the controllable suspension – mostly exhibit non-Newtonian characteristic – operate in certain manner, create hardened microstructures, and provide strength to the substrate.

Several properties of grout materials have been identified as valuable for certain application. *Rheology*, (penetrability and flow-ability) is the most important. The self-levelling grout is able to flow and penetrate in small voids and ensure the complete filling of the tendon duct, the crack in the dam or for stabilization of sand column. *Stability* and volume change of grout is one of the important features. The value of volume change for many grouts should be maintain in a specified range about zero. The expansion or shrinkage of the grout may create more problems in crack filling.

Strength of the grout is considered to indicate grout quality regarding its bond and shear strength. *Durability* of the grout is deemed to demonstrate its ability to withstand environmental load; e.g. freeze-thaw, chloride attack, etc.

In this study, the grout was prepared according to the aforementioned procedure in subchapter 4.4.1.

b. Experimental program

Two Porous Network Concrete PNC24-2-B prisms having porous core with 2-4 mm aggregate were subjected to the initial water permeability test. They were subsequently loaded by three point bending test, as depicted in figure 4.9. The crack width was measured by means of a linear variable differential transformer (LVDT) with a measurement range of $\pm 500 \mu\text{m}$ and an accuracy of $1 \mu\text{m}$. Two LVDTs were placed at the bottom side of the specimen and the mean value was used to control the close-loop test.

The test was conducted in strain controlled mode with strain rate of $1 \mu\text{m/s}$ and CMOD about 550 -600 μm . As the load was released the final crack opening about 250 – 300 μm was obtained for each specimen. After crack formation the specimen was removed from the loading frame.

Manual injection of cement grout was executed by means of 30 ml syringe mounted into port of injection of the PNC. The specimen, then, was allowed to cure and sealed with plastic wrap in the ambient temperature for 7 days. Eventually the specimens were tested in the second post-healing test namely post-healing leakage (permeability) and bending (mechanical) test.

c. Result and proposed improvement

PNC24-2-B has a porous core with pore diameter approximately 0.5 – 1.5 mm formed by interconnected aggregate size of 2–4 mm. The porosity of the core is about 22.3% with hydraulic conductivity about 0.96 cm/s which means it has a pervious regime. However, the grout injected manually by means of syringe into the core through port of injection demonstrates insignificant penetration. Clogging of the grout in the midway between port of injection and the crack zone, about 6.5 cm from the port of injection, was observed as depicted in the figure 4.22. Even though constant manual pressure was implemented for several minutes, the injection process had come to a standstill without indication the grout penetrated further. There was no grout material leaked out form the crack mouth opening.

This phenomenon may be allocated to the fact that, despite the high porosity of the porous core, the tortuosity of the porous concrete is also quite high. This makes the flow path in the interconnected pore system being twisted or having many turns which may easily provide blockage to the non-Newtonian viscous grout.

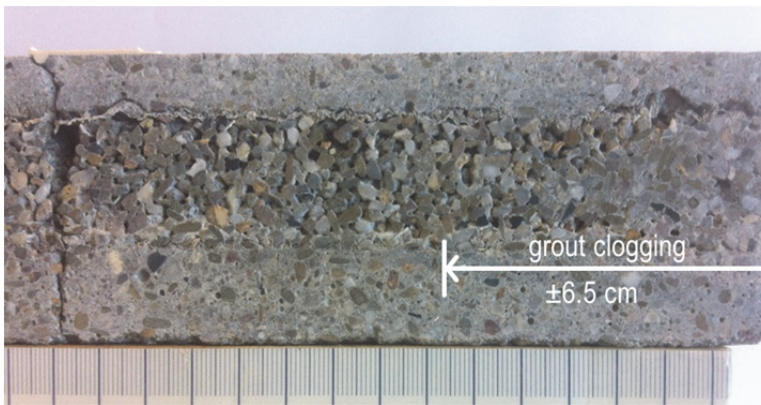


Figure 4.22. The clogging of the cement grout close to the port of injection

The second cycle mechanical test resulted on the failure of the specimen previous cracked zone while the post-healing permeability test shows meaningless insight. The result suggests two points. Firstly, reducing the tortuosity of the porous core and enlarging the pore average diameter may solve the problem of grout clogging. Secondly, grout rheological properties play important role in the PNC healing. The use of micro/ultrafine cement particle [213] and adjusting setting time [212] by incorporating retarding admixtures may be beneficial in this case.

An attempt to improve the healing of PNC using cementitious grout was carried out by changing the PNC mixture into PNC48-1-B. It has a porous core with aggregate size of 4-8 mm and less binder (binder-to-aggregate ratio of 3.4). This mixture has larger porosity and higher hydraulic conductivity but the strength is also less. Figure 4.23 exhibits the 4-8 mm aggregate size porous core replacing the core with smaller aggregate size (2-4 mm).

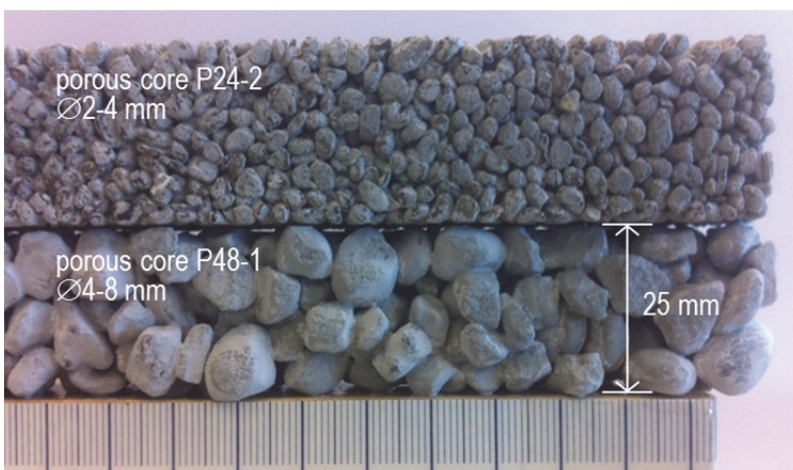


Figure 4.23. The 2-4 mm aggregate size porous core was replaced with the porous core that has aggregate size of 4-8 mm.

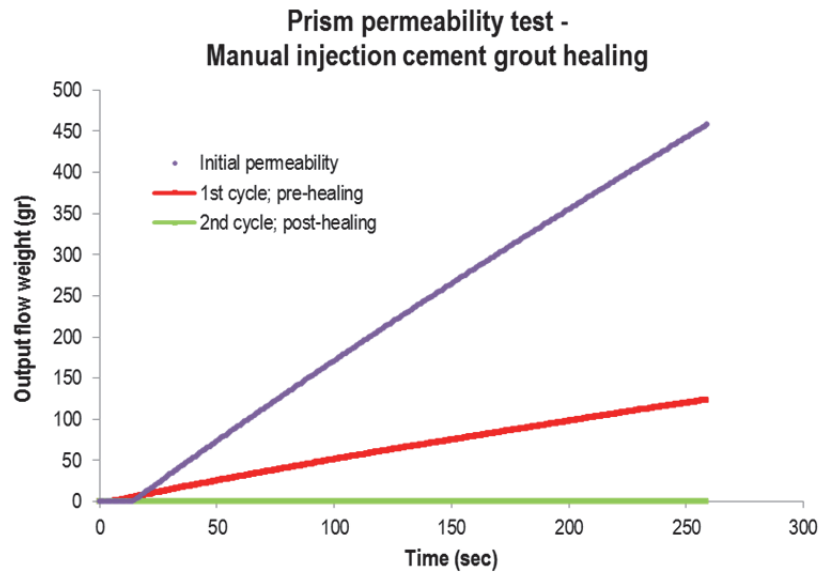


Figure 4.24. Permeability curve representing the weight of water discharged as function of time for initial condition, pre- and post-healing for the PNC with manual injection of cement grout.

The same cycle of experimental program was employed in the prism specimen, started with initial permeability, crack formation by bending test, followed by pre-healing permeability test. Then, the grout with 0.85% superplasticizer was injected into the cracked PNC. After 7 days of curing, the post-healing permeability tests were employed followed by bending test.

The result of permeability test is presented in the figure 4.24. The graphs resemble the similar characteristic with most of the other PNC specimens. On the other side, the result of bending test is presented in the figure 4.25. The healed specimen established a higher peak stress upon reloading. A new crack formation, however, was not formed and the previous crack was reopened. This indicated that the grout did not sufficiently enter the crack zone and glued the crack faces together. It may be associated with the size of the crack opening ($\pm 250\text{-}300\ \mu\text{m}$) being too small to be filled with cement binder. The grout only filled this crack partially and left still a weak spot for the bending stress to concentrate and reopen it.

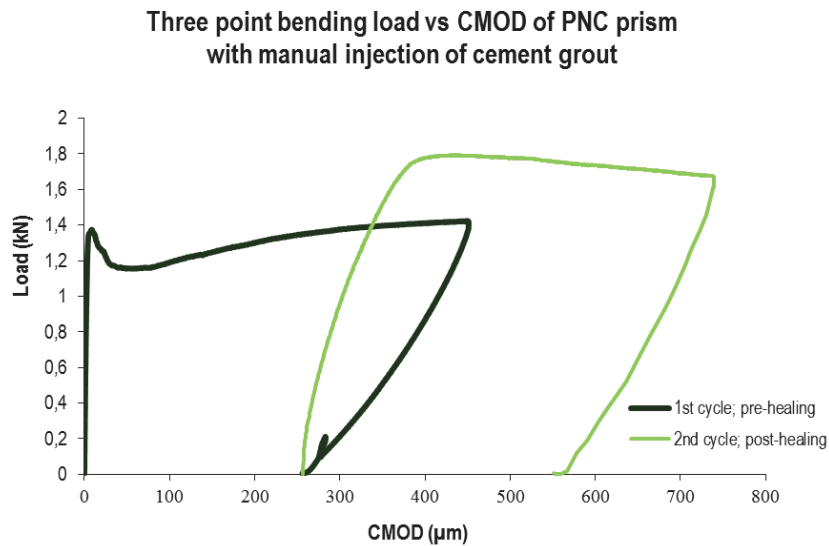


Figure 4.25. Load versus displacement curve of PNC prism healed by manual injection of cement grout

Figure 4.26 shows the longitudinal section of the prisms PNC48-1-B where the grout materials penetrated throughout the interconnected pore. Unlike epoxy resin, the grout did not completely fill up all the space and left several air pockets.

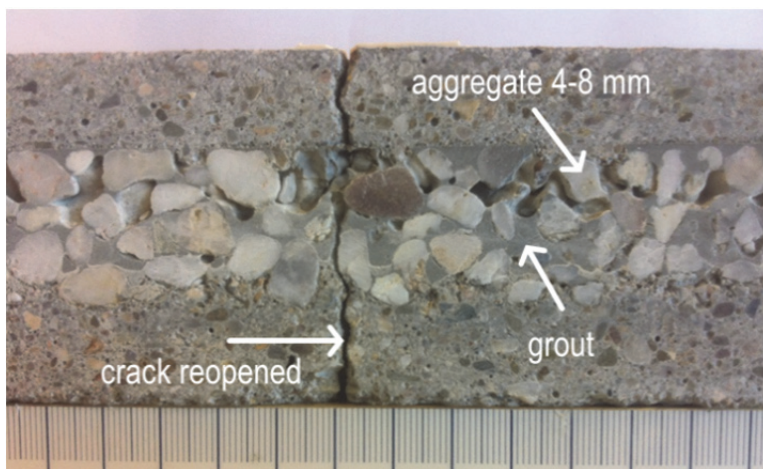


Figure 4.26. Longitudinal section of the PNC injected with cement grout

4.6. Evaluation of crack repair

The initial permeability tests of all specimens for injection (manually or automatically) epoxy and cement grout show roughly equal values of permeability line slope. Intrinsic permeability coefficients determined by Darcy law exhibit that the entire PNC specimen used possess porous core in the *pervious regime*. Therefore all PNC specimens satisfactorily fulfil the criteria of having a porous core as media to transfer healing agent into the place where the crack in the main body occurs. The pre-healing permeability slope also revealed that water can infiltrate through the crack opening in the main body. This condition implies that liquid tightness was disrupted.

The post-healing slopes of permeability line of every healed specimen with epoxy and cement grout were zero. Confirmed by visual observation of cut-open specimens, the healing events were successful in every specimen, either manually or automatically injected by epoxy, and specimen P48-1-B manually injected with cement grout. Table 4.2 recapitulates the result from the permeability test where $SH_{leakage}$ the value of sealing efficiency, reach 100% for all the specimen and healing agent. Based on this, the leakage is prevented completely and liquid tightness is ensured.

Table 4.2. Recapitulation of the healing efficiency of Porous Network Concrete beam

Specimen	Healing		Intrinsic Permeability (cm/s)		$SH_{leakage}$ (%)	$SH_{strength}$ (%)	$SH_{stiffness}$ (%)
	Agent	Mech.	Initial	regime			
RC	Epoxy	Direct inj.	n.a	n.a	n.a	98.1	67.3
PNC24-2-B	Epoxy	Manual	1.12	Pervious	100	131.3	99.2
PNC24-2-B	Epoxy	Auto.	1.07	Pervious	100	184.6	98.7
PNC24-2-B	Grout	Manual	1.08	Pervious	n.a	n.a	n.a
PNC48-2-B	Grout	Manual	1.65	Pervious	100	124.2	79.2

Regarding the permeability test setup developed in this work, however, a subtle ‘question’ may arise. Can the permeability test show the crack sealing efficiency if the porous core is blocked before the crack? If the porous core is blocked between the point of injection and the crack then it may appear that 100% sealing is obtained. Admittedly, this permeability test is ineffective if these regions are clogged by healing agent even though the crack is still unsealed.

Direct injection (outside-in) into the crack face, as what has been employed in existing conventional method, demonstrates a good repair action. The epoxy as adhesive repair agent fills in the crack void and binds the crack face. The polymerization of epoxy resin in the crack zone seals and glues the crack faces which shows a tendency to recover strength and stiffness of the healed specimen. This definitely prevents the crack from intrusion of water or any other substance. The adhesive force between concrete matrix and hardened epoxy provide strength and stiffness recovery for the concrete structure.

Table 4.2 summarizes the healing efficiency of the PNC specimen in term of strength capacity regain, $SH_{strength}$, and stiffness regain, $SH_{stiffness}$. The hardened epoxy in the porous core most likely also acts as ‘secondary’ reinforcement with benefit of not only recovering but also increasing specimen strength. As the healing agent solidified, the cross section of what was previously partially hollow became a denser section and able to provide larger moment of resistance against the external loading. In this view, the healing mechanism by means of PNC is achieved.

The term ‘self’, in what was claimed as self-healing by means of the Porous Network Concrete, is manifested in the feedback mechanism. This was proven to work effectively in the closed-loop on-off control.

This page is intentionally left blank

5.

Porous Network Concrete healing by means of bacteria based repair solution

'...We mostly don't get sick. Most often, bacteria are keeping us well.'

- Bonnie Bassler

Apart from diseases it may cause, recently bacteria community have been successfully exploited to seal and to heal fissure in concrete in the lab scale. At Microlab, Faculty of Civil Engineering and Geosciences, TU Delft, one among few research groups pioneering in bio-based self-healing concrete in the world, the success story has been enhanced by developing a bacteria-based repair system to repair existing damaged concrete⁵. The solution developed by Wiktor and Jonkers [145-147, 215] contains bacteria which promote calcite precipitation, nutrients, and buffer compound. A collaborative multidisciplinary experiment was setup to explore its potential as healing agent to be injected through the Porous Network Concrete (PNC) developed by Sangadji and Schlangen [62, 142, 148]. It is expected the solution reaches fracture zone in the concrete, precipitate Ca-carbonate, and seal the crack. This chapter starts with the explanation of working principles of bacteria-based self-healing concrete, and then describes how the solution works in precipitating Ca-carbonate in PNC. A preliminary test was carried out followed by an attempt to study and optimize the solution by testing its performance for the porous core. Eventually the healing efficiency test in the PNC prism is presented and the result is discussed.

Bacteria are ubiquitous. These micrometre size organisms live in different habitat, from city to deep sea, from forest to desert, from tropic to Antarctic. They are present in enormous diversity and abundance. Just like any other living organism, they live and multiply. This reproduction will continue as long as the conditions allows, with the ability to adapt to local environment to some type and less adaptive to some other type of bacteria [216].

What do the word bacteria bring to mind? For many laypeople, bacteria mean disease producing agent – *pathogen* – and indeed there are several deadly bacteria. The vast

⁵ Patent pending No.P100120PC00.

majority of these bacterial communities, however, have no connection with human. In addition to that negative or neutral relation to human, studies also reveal bacteria inhabit healthy human skin, mouth, genital areas and intestine. These commensalism or mutualism symbiotic host-microbe are complex ecosystem, coined by Nobel laureates Joshua Lederberg as *human microbiome*, play vital roles in helping human maintain basic physiological processes [217-220]. Surprisingly the number of microbial cell hosted is estimated larger than human somatic and germ cell by factor of ten [221, 222]. The gene distributions of these beneficial bacteria are far exceeding the number of genes human inherited. Moreover, each individual carries specific microbiome and their gene, even twin has different microbiome composition [223].

Many bacterial communities have direct positive impacts in human life, such as helping human digestion or indirectly such as fermenting human food and fixating atmospheric nitrogen into usable one in soils. Recent biotechnology purposefully makes use of bacteria for serving human needs and enhancing life quality. Bacterial communities were applied – to name the *few* applications – for CO₂ sequestration [224], bioremediation of waste water or contaminated soils [225, 226], and soil consolidation and remediation [135, 136].

Specific to concrete technology, the potential benefit of bacteria has been investigated. Ghosh *et al.*, reported improvement of cement mortar strength by incorporation of thermophilic⁶ anaerobic bacteria [227]. De Graef *et al.*, used bacteria of the genus *Thiobacillus* to clean weathered concrete surface from lichens [228]. Dick and co-worker at Ghent University attempted to restore degraded limestone with bacterially mediated protective calcite layer by means of *Bacillus* strains [137]. Concrete fracture healing/sealing as well as pore filling have been investigated by Stocks-Fischer *et al.* [229], Bang *et al.* [139], Ramakrishnan [230], De Muynck *et al.* [231], Jonkers *et al.* [232, 233], and Wiktor and Jonkers [114].

The first section of this chapter (section 5.1) is a literature review. It is devoted to discuss the working principles of the bacteria based self-healing concrete. The section also studies the development of bacteria-based repair solution as its spin off. This liquid-based system, developed by Wiktor and Jonkers [147], shows the potential as healing agent to be injected through the core of the PNC and seal cracks in the main body.

Subsequently the chapter is dedicated to optimize this solution and investigate its efficiency in the porous concrete. The solution is injected into porous concrete cylinder Ø 25 mm and followed by observation of its bio-mineral product over time. A simple permeability pre- and post-injection test is carried out to assess how effective bio-mineral product seals the interconnected pores. Then the precipitates is identified and evaluated by several complementary techniques.

The last part of this chapter studies the healing efficiency of the PNC prism by injection of bacteria-based solution. The crack is introduced into the prisms by

⁶ Extremophile is an organism that vigorously grow and develop in extreme conditions while polyextremophiles thrive in more than one 'extreme'. These physically (i.e. temperature, radiation, or pressure) or geochemically (i.e. desiccation, salinity, pH, oxygen species or redox potential) extreme conditions may be damaging to common life on Earth. Macelroy first coined this term combining 'extremus' (latin) and 'philos' (greek). Most extremophiles are classified based on the environmental niche; e.g. **thermophilic** grow optimally at 45 – 80°C, while **hyperthermophilic** grow at temperature greater than 80°C, e.g. *Pyrolubus fumarii*, 113°C. **Alkaliphilic** reproduce and thrive at pH 9 – 11.

bending test followed by solution injection through the porous core and flow out from the crack opening. The permeability test is carried out prior and after healing as the crack is filled by the bio-mineral products to examine the healing efficiency.

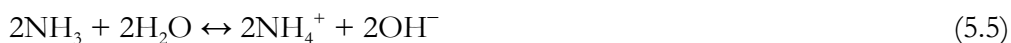
5.1. Introduction; working principle of bacteria based self-healing concrete and the success story

In nature bio-geochemical-mineralization⁷ processes – *microbiologically induced calcium carbonate precipitation* – precipitate calcium carbonate in three different polymorphs, *calcite*, *aragonite*, and *vaterite*. Calcite is the thermodynamically most stable and vaterite is the least. The ionic reaction $[Ca^{2+}] + [CO_3^{2-}] \rightarrow CaCO_3$ can be mediated by bacteria through several pathways – e.g. *urea hydrolysis*, *metabolic conversion of salt and carbon*, *denitrification*. Increasingly important research of bacterially mediated self-healing concrete make use of calcite precipitating bacteria for enhancing durability of concrete [113, 137-140, 230, 231].

5.1.1. Urea hydrolysis

In number of published studies, scientists investigated the potentials of bacteria to facilitate calcium carbonate precipitation by means of degrading urea to ammonia and carbon dioxide. Bang *et al.* in 2000 published a study where *Bacillus pasteurii* immobilised in the Polyurethane was employed to precipitate calcite. Ramachandran *et al.* also used *B. pasteurii* and filled it in simulated cracks in mortar, meanwhile Bachmeier *et al.* investigated *Escheria coli* and found the bacteria produced significant level of precipitation although less than *B. pasteurii*.

Researchers from Ghent University, Belgium, developed the system in which precipitation of calcite is based on major mechanism of *enzymatic hydrolysis of urea*. The bacteria used – *Bacillus sphaericus* – produce *enzyme urease (urea amidohydrolase, E.C. 3.5.1.5)* which catalyses the hydrolysis of urea into ammonium (NH_4^+) and carbonate ions CO_3^{2-} [115, 116, 231]. Van Tittelboom [86] elaborates the chemical reaction as follows; urea is internally hydrolysed by the bacteria producing carbamate acid and ammonia in equation 5.1. Carbamate is then hydrolysed into ammonia and carbonic acid at equation 5.2 which in turn develops new dissolved inorganic carbon balance (5.5) and increases pH of the concrete matrix.



⁷ Dhami *et al* define **biomineralization** as 'biologically induced process in which organism creates a local micro-environment with conditions that allow optimal extracellular chemical precipitation of mineral phases'. Two different categories are: (i) biologically controlled mineralization (BCM) where, in most cases, 'mineral are synthesized at specific location within (intracellular) or on the cell' and (ii) biologically induced mineralization (BIM) where due to metabolic activity and its by-products the chemical environment nearby the cells is altered making minerals grow extracellular.



These carbonate anions, $[\text{CO}_3^{2-}]$, in turn react with calcium cations, $[\text{Ca}^{2+}]$, present in the concrete matrix which are attracted into negatively charged bacteria cell wall in equation (5.7) and precipitate Ca-carbonates as expressed in equation (5.8) that fill the fissure in concrete structure [230].



Decreasing water permeability and crack sealing was observed in the specimen with *B. sphaericus* immobilized in silica gel or polyurethane by means of ultrasonic transmission measurement. Visual examination confirmed the sealing takes place in the crack surface [115, 116]. Despite the ease to control, the chemical reaction mechanism, however, may lead into problematic side effect for the environment due to two ammonium ions for each carbonate ion produced [86, 113]. Additionally, as Dhami *et al.* suggested, risks of concrete salt damage may arise from the production of ammonium molecules in hydrolysis of urea or where this ammonia is converted into nitric acid by nitrifying bacteria [234].

5.1.2. Metabolic conversion of nutrient

A different approach has been carried out by Jonkers and Schlangen [232], Jonkers *et al.* [113, 233, 235], and Wiktor and Jonkers [114] where they employed a different route to obtain bacteria mediated calcite precipitation. The bacteria metabolically convert nutrients-salt and change the micro chemical environment in their vicinity to be able to precipitate calcite. The requirements for the bacteria are that they should be alkaline resistant and oxygen tolerant. The reason is that they must survive in the highly alkaline concrete (fresh) matrix which is typically characterized by pH values between 11 and 13. They must also be viable for a prolonged period started from the mixing time. They should therefore also be able to form spores. The bacteria can be receptive to oxygen diffused in the concrete matrix. On the other hand the presence of oxygen is unnecessary if nitrate reduction is employed.

Figure 5.1 demonstrates the working principle of a two-component bacteria based self-healing concrete developed at Microlab, Faculty of Civil Engineering and Geosciences, TU Delft. The system comprises of bacteria spores and organic compound as nutrient, e.g. Ca-lactate. The *spores* after germination due to the present water and oxygen in the cracked concrete *metabolically* convert the nutrient and produce CO_2 which in turn chemically converted into carbonate ions $[\text{CO}_3^{2-}]$. These ions then react with calcium ions $[\text{Ca}^{2+}]$ to precipitate Calcium Carbonate, CaCO_3 . The growth of this mineral will seal cracks and reduce concrete porosity.

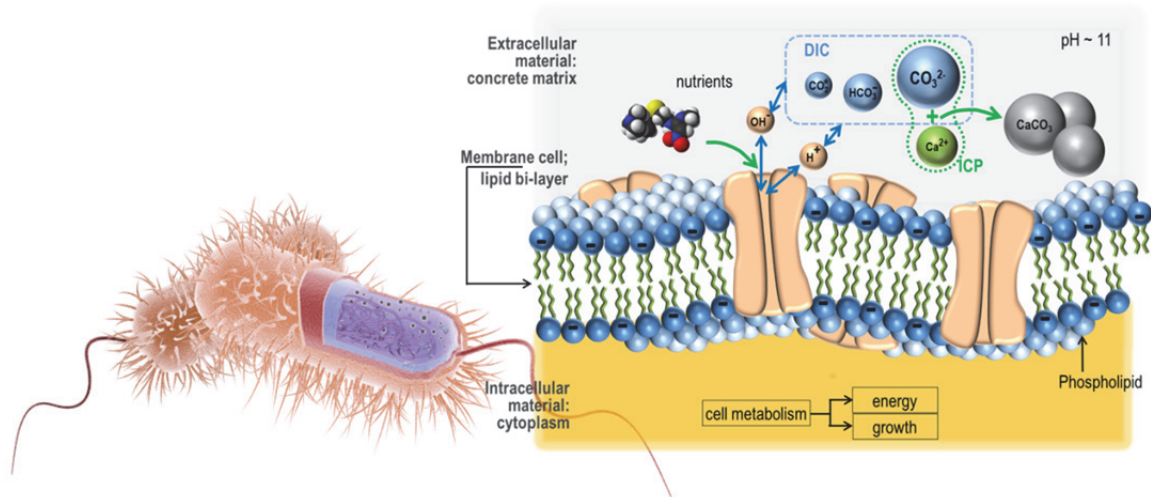
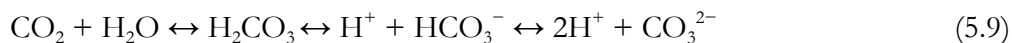


Figure 5.1. Working mechanism of bio-based concrete healing developed at Microlab, Faculty of Civil Engineering and Geosciences. While metabolizing nutrients and producing carbon dioxide bacteria change extracellular microenvironments leading to the bio-mineralization of Ca-Carbonate.

While the presence of bacteria may be thought as the nucleation point for bio-mineralization of *calcium carbonates* (CaCO_3), several factors influence the emergence of bacterially mediated CaCO_3 precipitation. These factors are: (1) the *pH* of the solution, (2) the presence of *calcium ion* [Ca^{2+}], and (3) the *carbonate equilibrium* in the solution. The latter is determined by concentration of *dissolved inorganic carbon*, (DIC) in the solution – which includes chemical species of carbon dioxide [CO_2], carbonic acid [H_2CO_3], bicarbonate anion [HCO_3^-], and carbonate anion [CO_3^{2-}], see DIC pool in the figure 5.1.

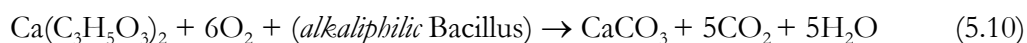
In the solution, the relative concentration of each chemical species in DIC is a function of *pH* and expressed by the following chemical equilibrium (5.9):



Based on Bjerrum plot [236], in acidic conditions ($\text{pH} < \sim 6.4$), the dominant form is carbon dioxide CO_2 or carbonic acid H_2CO_3 . In alkaline (basic) solution ($\text{pH} > \sim 10.3$), e.g. concrete matrix, the dominant form is carbonate anion [CO_3^{2-}]; and in between, the bicarbonate anion [HCO_3^-] is the dominant form, see equation (5.9).

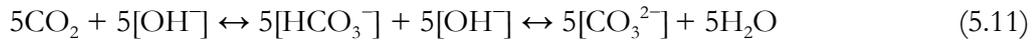
As concrete matrix has approximately *pH* 11–12 (*alkaline*), the dissolved inorganic carbons take the form of *carbonate ions* [CO_3^{2-}]. In the figure 5.1 the DIC pool is dominated (not to scale) by carbonate ions.

The system working principles may be expressed as straightforward equilibrium as suggested by Jonkers *et al* [235]. Bacteria metabolically convert 1 mole of calcium lactate, $\text{Ca}(\text{C}_3\text{H}_5\text{O}_3)_2$, into 1 mole of Ca-carbonate as in equation (5.10).



Therefore, taking into account the calcium hydroxide (*portlandite*) – which is essential hydration product of cement particles – and the *carbonate equilibrium* in the alkaline

concrete, the chemical equilibrium influenced by bacterial communities is as follows; 5 moles CO₂ is the respiration product of *alkaliphilic Bacillus* (5.11) which later on is reacted with 5 moles Calcium-hydroxide, Ca(OH)₂ (5.12).



The cations of calcium, [Ca²⁺], present in the concrete are then attracted into negatively charged bacteria cell wall and reacted with carbonate anions, [CO₃²⁻], to create 5 moles of Calcium-carbonate according to equation (5.13) [230].



From this process, however, bacteria cannot be seen to directly precipitate Ca-carbonate. By altering the chemistry of extracellular micro-environments in their vicinity due to the metabolism (or hydrolysis), the precipitates are able to form.

The reaction resulting in Ca-carbonate to seal (heal) cracks takes place outside of cell membrane as depicted at figure 5.1. The equations suggest theoretically that the system produce more CaCO₃ molecule for each molecule Ca-Lactate metabolized by bacteria.

Jonkers *et al.*, [38] have made use of several aerobic alkaliphilic endospore forming bacteria from genus *Bacillus*⁸. To induce massive formation of spore the bacteria strains were cultivated in an alkaline – pH was close to 10 – liquid media as energy and carbon source for growth [114, 235]. Aerobic incubations of the cultures were carried out in Erlenmeyer flasks on a shaker table at 150rpm meanwhile a routine microscopic observation analyzes the growth and sporulation yield of bacteria. Vegetative cells were harvested from senescent cultures containing high number of spores. Repeated centrifugation and re-suspension of the cell pellet in sterile tap water were conducted to separate them for the cultures residue. Inactivation of the obtained suspensions was then carried out by preserving at 4°C up to the preparation for further use. The most probable number cultivation–dilution technique was employed to quantify the number of viable spores in suspensions.

For the production of concrete specimens, two different techniques have been utilized: (1) direct incorporation both bacteria, i.e. *B. cohnii*, and nutrients, i.e. *Ca-lactate*, in which both were mixed with the fresh cement paste/mortar, and (2) immobilization and protection of both bacteria and nutrients in porous expanded clay particles [114, 235]. The first technique revealed no significant compressive strength reduction even though bio-mineralization capacity was limited from 7 days up to few months old concrete specimens. It was thought that the spores were mechanically damaged, cells were disintegrated due to hydration causing pore matrix less than 1 µm, and or inactivated due to high alkalinity [86, 113, 114].

⁸ They were obtained from the German Collection of Microorganisms and Cell Cultures (DSMZ), Braunschweig, Germany (strain *Bacillus pseudofirmus* DSM 8715 and *Bacillus cohnii* DSM 6307 originally isolated from alkaline soil) and by isolating it (strain C2-C2-1 A) from a natural soda lake sediment (Wadi Natrun, Egypt). A 98.7% homology to *Bacillus alkalinitrilicus* – an alkali-resistant soil species – was acknowledged from the 16S rRNA gene sequence analysis of the latter bacterium.

Jonkers [113] and Wiktor and Jonkers [114], subsequently, developed the second alternative method. Bacteria as well as the nutrients-salt were impregnated inside of porous expanded clay particles (Liapor R 1–4 mm, Liapor GmbH Germany), therefore protected from direct contact with concrete matrix. These impregnated particles have threefold functions; (1) constituents of concrete materials and structures, (2) internal reservoir supplying bacteria food, and (3) protective shell for the bacteria ready to function on time.

The preparation process is as follows; the nutrient was a calcium lactate- (80 g/l) and yeast extracts (1 g/l) solution which was impregnated in two times into the particles using vacuum. Afterwards, the bacteria spores suspension was impregnated with the same vacuum process followed by drying in the oven at 37°C for 5×24 hours. The final composition is 6% by weight (grams) calcium lactate and 1.7×10^5 bacterial spores per gram particles ready to be incorporated into concrete matrix.

Jonkers reported that immobilized bacteria promote bio-mineralization (precipitate Ca-based mineral) and, moreover, no negative effect on concrete mechanical properties, i.e. strength reduction, was observed in the specimen with bacteria and certain classes of food [113, 233]. Wiktor and Jonkers have proven that bacteria were metabolically active converting the food by measuring the oxygen consumed in the system. In the specimens with bacteria based expanded clay particle, the oxygen concentration was decreasing over time and depth. This two-component biochemical healing agent immobilized in expanded clay particles has also been proven to be effective in sealing cracks up to 500 μm [114].

In general, as Ca-carbonate is deposited on the cell wall layer by layer as long as the micro chemical environment suits. The bacteria eventually will be entombed by the precipitate. On the other hand the bulk mineral will be used as it is particularly designed; in soils, it will help consolidation; in limestone monument surface, it will treat the damage; in the concrete fissure, it will deposit and seal the opening.

5.1.3. Bacteria based repair solution

The demand to repair existing damaged concrete using environmentally friendly repair materials has motivated the development of a bacteria-based repair system (Wiktor and Jonkers [145]). This bio-based system is a liquid system containing alkaliphilic calcite precipitating bacteria, nutrients and transport solution leading to porosity reduction of concrete matrix. This system has been applied by spraying the solution onto the surface of a cracked concrete structure, where it yields to crack closure.

The bacteria-based repair system is designed to have three components as depicted in the figure 5.2; *transport solution*, *alkaliphilic bacteria*, and *nutrient*. Each of these components has its function and criteria however they all must interact.

a. Transport solution

The transport solution is to ensure that the bacteria and nutrients are transported efficiently into the cracks or the concrete interconnected pores. This solution is required to have pH sufficient for the bacteria to grow as well as preventing nutrients

precipitation prematurely. Wiktor and Jonkers [147] have selected a silicate-based, i.e. Sodium silicate (Na_2SiO_3), solution as transport solution ensuring the liquid bio-based repair system to have alkaline pH. Furthermore, alkali silicate solutions are known to react with *portlandite* ($\text{Ca}(\text{OH})_2$) in the hydrated cement paste to form insoluble calcium silicate gels, which results as well in the decrease of the concrete porosity.

b. Bacteria

Bacteria in the system metabolize dissolved nutrients precursor compound which are converted into Ca-based mineral. The same alkaliphilic spore-forming bacteria from genus *Bacillus* may be utilized as the previous section shows a promising result [114, 235].

c. Nutrients

Nutrients provide energy, carbon, essential elements and calcium sources for the bacteria to grow and metabolically convert the food, therefore changing its micro environment fits for the calcite to precipitate. Thus, nutrients are essential. However, if the nutrient source contains calcium, it might generate premature precipitation in reaction with silicate-based transport solutions. Ca-source may therefore come from the concrete itself; e.g. cement paste hydration product or from another solution.

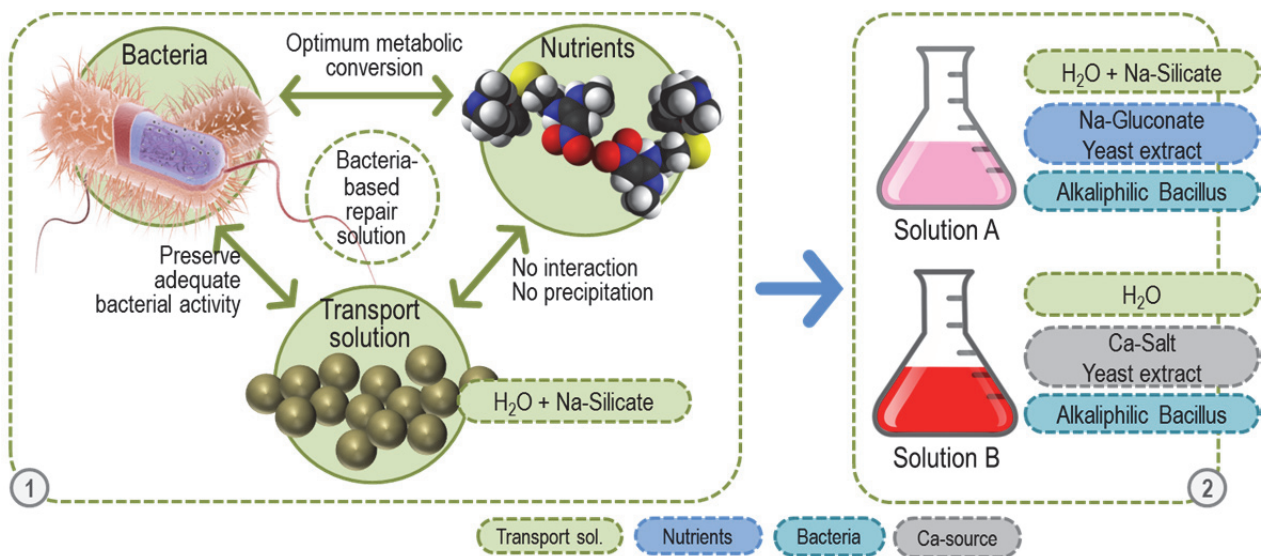


Figure 5.2. The principle and components of the bacteria-based repair system where the three components in the frame (1) are incorporated into two different solutions, solution A and solution B, in the frame (2). The figure is adapted from Wiktor and Jonkers [145].

During developmental phase of their system, Wiktor and Jonkers investigated several candidates for the transport solution and their pH effect to the bacterial activity and nutrients. Glucose (D+ Glucose monohydrate, Boom, the Netherlands) [215] and Sodium-gluconate (sodium D-gluconate 97% Sigma-Aldrich) [147] is selected as the carbon source. Wiktor and Jonkers have investigated the effect of the pH of the solution on the bacterial activity where carbon source nutrients solutions were prepared either in demineralized water (neutral pH) or in Sodium silicate (*water-glass*, Na_2SiO_3) providing alkaline pH, both with or without bacteria.

Vaterite formation, the least stable polymorph of carbonate, was formed in the mortar specimen treated with glucose repair solution with or without bacteria, with limited bacterial activity observed. On the other hand, combination of Na-gluconate and bacteria dissolved in the water glass [147] solution promoted denser cement paste matrix microstructure and demonstrated bacterial activity as the imprint was observed under ESEM, see figure 5.3. The latter composition is defined as *solution A* as depicted in the figure 5.2. frame 2.

It is expected that substantial amount of calcite would be precipitated. As 2 moles of sodium gluconate in solution A (if totally converted) may generate 1 mole of carbonate ions and 11 moles of CO₂ according to equation 5.15.



As the pH of the matrix is alkaline, the dissolved inorganic carbon pool in the vicinity of bacteria is then changed and the carbon dioxide present turned into carbonate anions, [CO₃²⁻], which in turn reacts with Ca cations, [Ca²⁺], present in the matrix, i.e. from Ca(OH)₂.

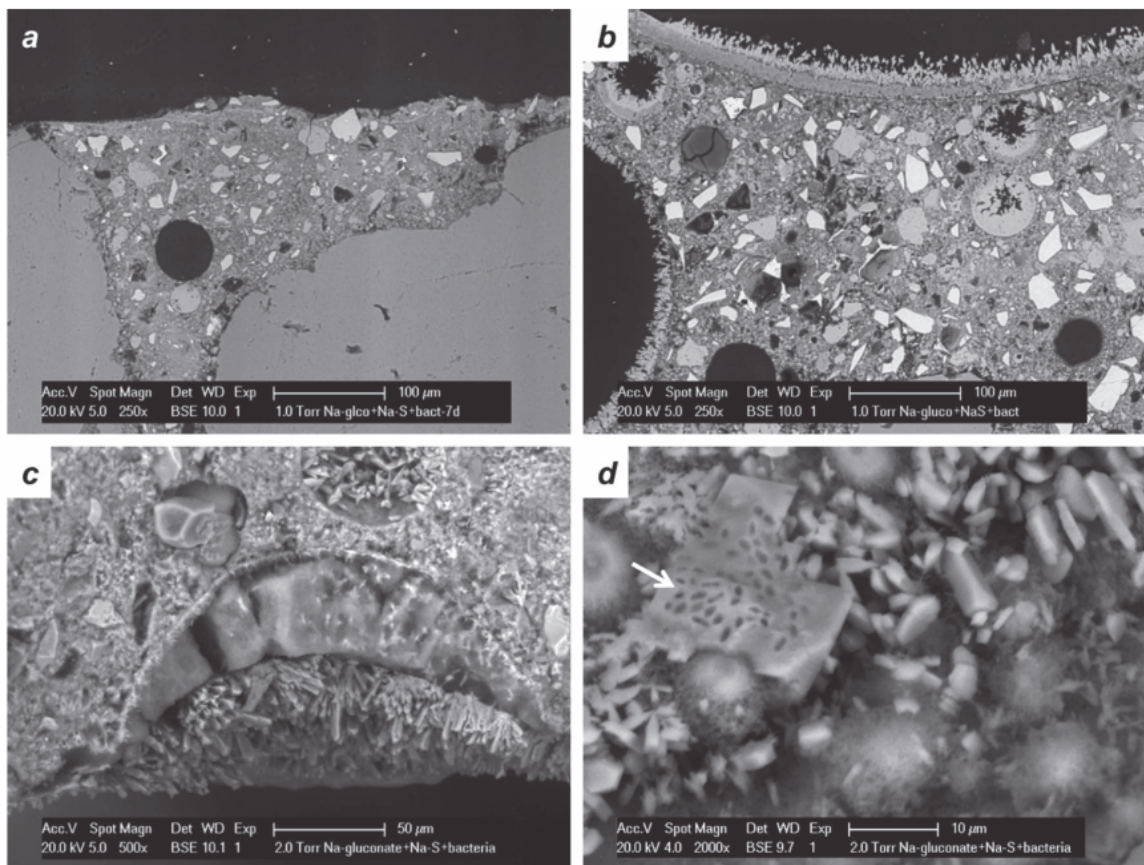
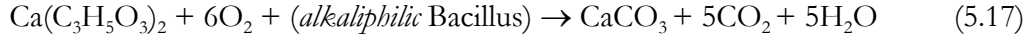
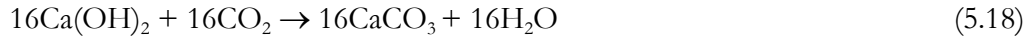


Figure 5.3. Observation under ESEM of specimens treated with Na-gluconate NaS + bacteria. Figure (a) and (b) are polished sections. Figure (a) shows specimen at 7 days and figure (b) is specimen at 28 days. Figure (c) exhibits pore structures at the surface of the specimen a calcium-based layer on top of a gluconate-based layer. Figure (d) shows the crystal of Ca-carbonate and bacteria imprints (arrow). The figure is of courtesy of Wiktor and Jonkers [147].

Meanwhile, in order to promote more ca-based mineral precipitation, Ca-salt based nutrient solution, i.e. Ca-lactate ($\text{Ca}(\text{C}_3\text{H}_5\text{O}_3)_2$) and or Ca-nitrate ($\text{Ca}(\text{NO}_3)_2$), may be used in separate solution from solution A. This is called *solution B*. Ca-lactate is metabolized by bacteria producing ca-carbonate as in equation 5.17.



Theoretically, a considerable number of ca-carbonate molecules are produced when solution A and solution B are combined as depicted by chemical reaction 5.18.



It seem that large carbonation may occur due to reaction of portlandite, $\text{Ca}(\text{OH})_2$, with carbon dioxide, CO_2 . However, this happens only if the Na-Gluconate, $\text{Na}(\text{C}_6\text{H}_{11}\text{O}_7)$, and Ca-lactate ($\text{Ca}(\text{C}_3\text{H}_5\text{O}_3)_2$) are fully converted, which may not always be the case. Moreover this carbonation process may occur locally in the crack region where bacteria are active.

Ca-nitrate, $\text{Ca}(\text{NO}_3)_2$, which has higher solubility than Ca-lactate, may also be used for solution B to provide more ca-source available to precipitate calcite mineral. In this case chemical equilibrium for the solution A remained as equation 5.14. Dissolution of Ca-nitrate in solution B is depicted in equation 5.19 provides Calcium ions, $[\text{Ca}^{2+}]$, which then react with Carbonate ions, $[\text{CO}_3^{2-}]$ to precipitate CaCO_3 in the vicinity of the bacterium as in the equation 5.8.



Where oxygen is depleted in the local environment around bacteria, nitrate reduction process may continue as shown in the equations 5.20



Again this would alter the pool of dissolved inorganic compound in the vicinity of bacterium allowing the precipitation of calcium carbonate, CaCO_3 .



Having knowledge of how bacteria based repair solution may help to promote self-healing concrete, a test campaign was implemented and described in the rest of the chapter. The roadmap of these tests is presented in the figure 5.4. The first test was performed to address the feasibility of the bacteria based repair solution as healing agent. The second test was devoted to optimize the performance of the bacteria based repair solution. The third test focused on the assessment of healing efficiency of solution in the Porous Network Concrete prisms.

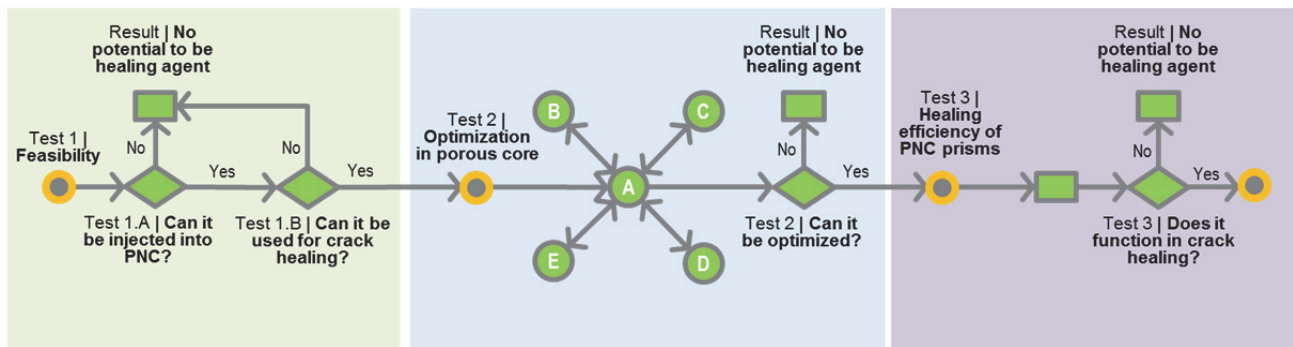


Figure 5.4. Roadmap of the test campaign implementing bacteria based repair system as self-healing agent in the Porous Network Concrete.

5.2. Test 1: Feasibility of the bacteria-based repair solution for the PNC

The primary intention in designing the bacteria-based repair solution is to apply it for repairing cracked or porous concrete. The solution is sprayed onto concrete surface and the bacteria facilitate calcium carbonate precipitation as the solution penetrates into the crack opening. In the lab scale the system has been tested and effective mineral precipitation was observed.[147, 215].

The solution developed is a very low viscosity liquid. It can be effortlessly injected through the porous core of the PNC and reaches the fracture zone in the main body. The question is whether it is feasible to inject that same solution through the Porous Concrete network (PNC) to make the crack healing (sealing) takes place from the inside of the structure outwards.

This section investigates the prospect by a rapid preliminary test. The solution is injected through the porous network until it reaches and flows out through the crack opening in the concrete specimen. The bacteria should then precipitate calcium carbonate sealing the crack. The healing efficiency is measured by two methods. The first method is by comparing water permeability (or leakage) before and after healing. The second method consists of assessing mechanical properties pre and post-healing.

5.2.1. Materials; the PNC and solution preparation

The concept of healing the Porous Network Concrete was tested by injecting the bacteria-based repair solution through the PNC prisms with dimension of 55×55×285 mm. The specimen had a 23×23×285 mm porous concrete core in the longitudinal center interior. The core consisted of porous concrete with mixture P24-2 based on the table 2.5 (aggregate size 2-4 mm with aggregate to binder ratio of 5.0). A 285 mm long Ø2 mm threaded steel rebar was installed below the core. The PNC production was conducted according to the procedure explained in the subchapter 2.3.1., section d. Subsequently the specimen was prepared for the test as discussed in the subchapter 3.3.2.

Based on the concept discussed at section 5.1.3, in this study the bacteria-based repair solution (or system) were designed to have two forms; solution A and solution B, as depicted in figure 5.2. The healing liquid used was based on the concept discussed above. Two solutions A and B as depicted in figure 5.2 were subsequently injected.

Table 5.1. The composition of solution A where Na-silicate solution provides the alkaline environment (pH 10.5 after mixing with solution B) fit for the bacteria to grow.

Category	Ingredients	Concentration (g/L)	Weight (g) per 250 mL
Transport solution	Na-silicate 37-40%	48.5	12.125
Nutrients	Na-Gluconate	125	31.25
	Yeast Extract	1	0.25
Alkaliphilic bacteria	Zeolite powder 8×10^8 spores/g powder 1.6×10^8 spores/L	0.2	0.05

Table 5.2. The composition of solution B where Ca-lactate is provided to feed bacteria and bring a calcium source to the system. The pH of this solution is neutral.

Category	Ingredients	Concentration (g/L)	Weight (g) per 250 mL
Transport solution	H ₂ O		
Nutrients	Ca-Lactate	80	20
	Yeast Extract	1	0.25
Alkaliphilic bacteria	Zeolite powder 8×10^8 spores/g powder 1.6×10^8 spores/L	0.2	0.05

Solution A, see table 5.1., was composed of (i) sodium silicate (*water glass*) solution (37-40% Brenntag Ned. BV), (ii) Na-gluconate (sodium D-gluconate 97% Sigma-Aldrich, E 576) which have concentration of 125 g/l, (iii) yeast extract 1 (g/l), and (iv) Zeolite powder having 8×10^8 spores/g powder. The sodium silicate ensures alkaline pH for the bacterial growth in the system, the Na-gluconate and yeast extract provide respectively the organic carbon and essential elements necessary for bacterial growth. The zeolite powder is the carrier of bacterial spores.

Solution B consisted of (i) calcium lactate with concentration of 80 g/l as organic carbon source, (ii) yeast extract 1 (g/l), and (iii) Zeolite powder having 8×10^8 spores/g powder. This solution which exhibited neutral pH, provided the Ca-source needed for massive calcite precipitation. After mixing with solution A, the final pH of the system is 10.5. Table 5.2. summarizes the composition of solution B.

5.2.2. Testing cycle

Bending test and leakage test setup described in the chapter 3 were used in this test to introduce crack, observe mechanical regain and to assess healing in the specimen respectively. As a rapid preliminary check the solution was injected manually by a syringe into the PNC.

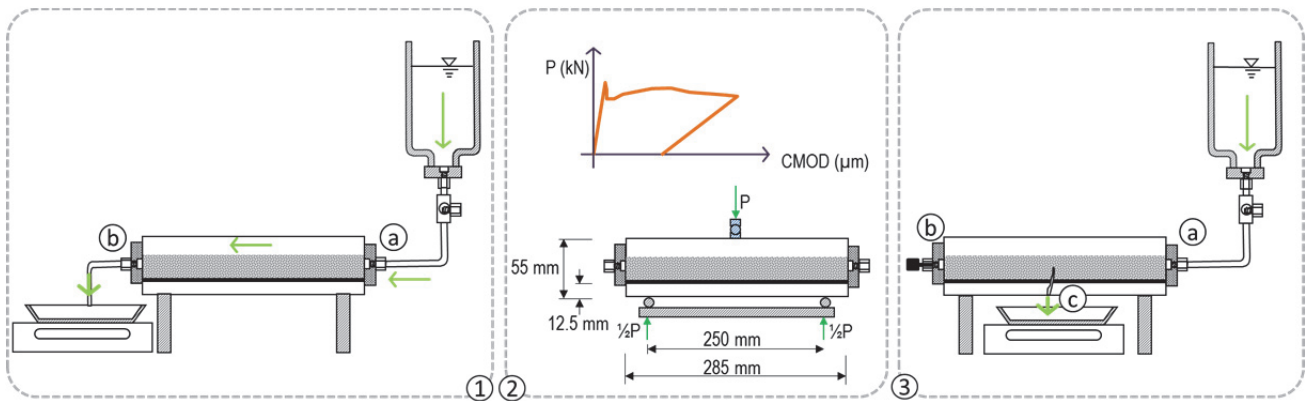


Figure 5.5. Testing procedure where frame (1) shows the initial leakage (permeability) test, frame (b) shows three-point-bending test to introduce crack into the specimen, and frame (c) exhibits pre-healing leakage test to determine the permeability of the system before bacteria-based repair solution is injected and Ca-based mineral precipitate.

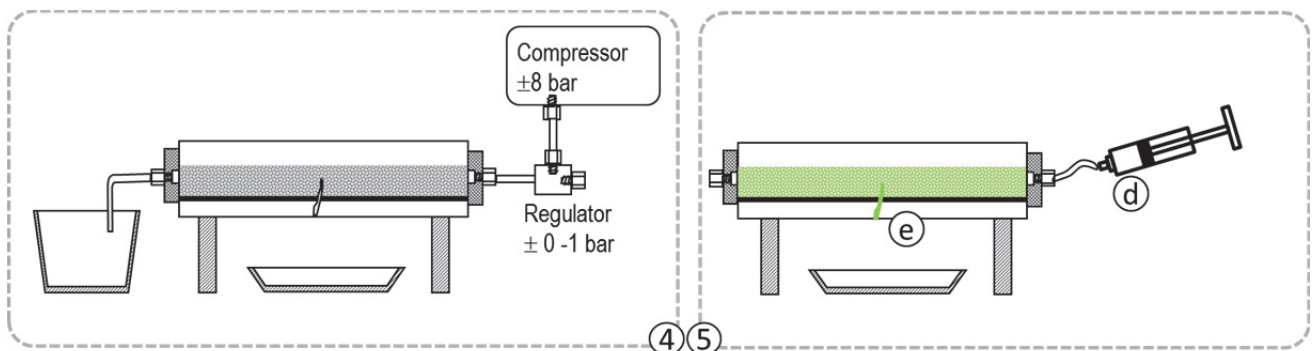


Figure 5.6. Testing procedure where frame (4) indicates steps to drain out water inside the porous core and crack zone, and figure (5) shows the manual injection of the solution.

Initial falling head water permeability test, see fig 5.5 frame (1), was performed according to the setup explained on the subchapter 3.4.2 figure 3.18. The specimen was placed on top of wooden support and water was flown from the port of injection, point (a), to the opposite port of outflow, point (b), prior to crack formation in the PNC prism. This test is carried out to check the porosity and permeability of the PNC prism.

Using closed loop strain controlled three-point loading (bending) test, a crack up to 600 μm was formed in the PNC. After the loading was released approximately 300 - 350 μm wide crack opening in main body remains. The strain rate of the test was 0.5 $\mu\text{m}/\text{sec}$. Figure 5.5. frame 2 sketches this step.

Then post-crack leakage (permeability) test as can be seen in figure 5.5 frame (3), was carried out by blocking the end connector, point (b), with a plug-in water stop allowing water to flow out into container, point (c). The excess water from the leakage test was drained out from the porous core by blowing ± 0.5 bar pressurized air for about ± 20 minutes as illustrated in the figure 5.6. frame 4.

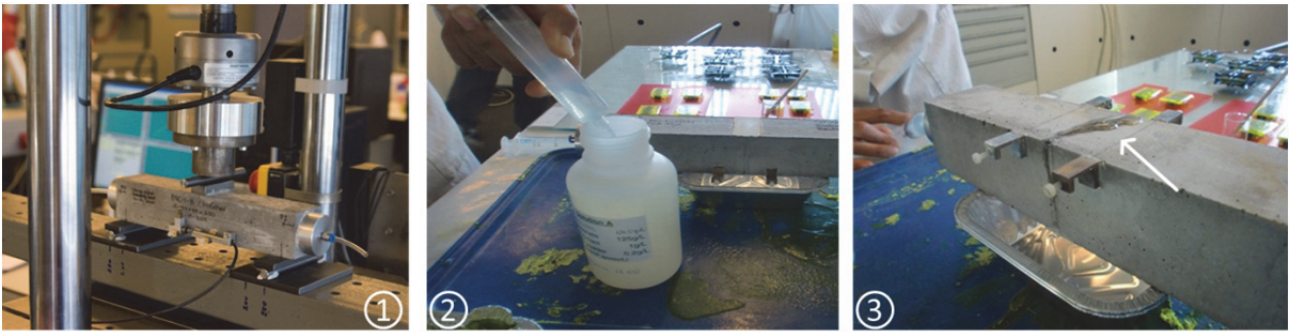


Figure 5.7. Three-point bending test was performed to introduce the crack into the PNC specimen, frame (1). It was followed by manual injection of solution, frame (2). The specimen was turned upside down by which the wetted area where the solution leak out can be seen, (arrow) frame (3).

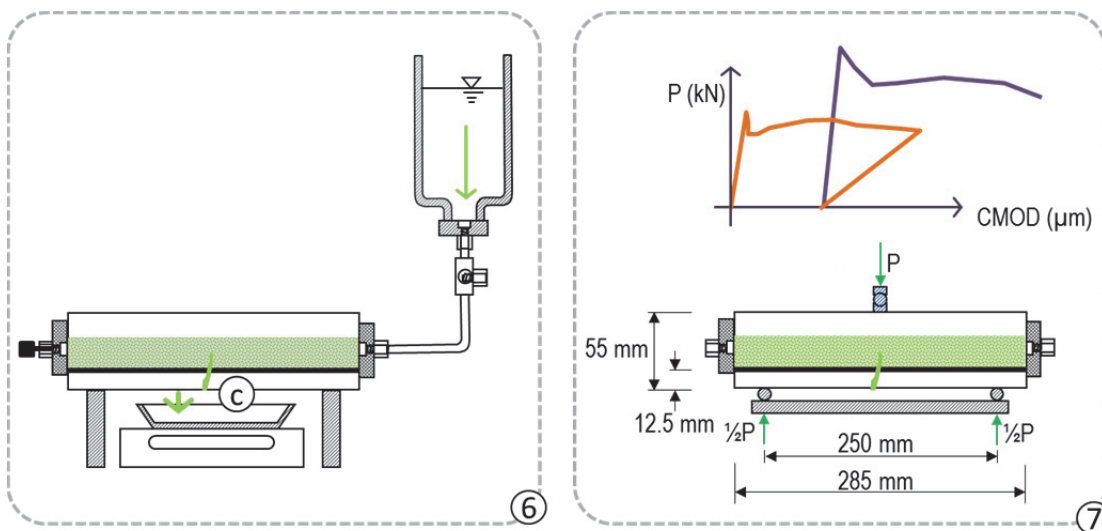


Figure 5.8. Testing procedure where frame (6) sketches the post-healing leakage (permeability) test. Point C in the frame indicates the crack opening is expected to be sealed by Ca-carbonate mediated by bacteria. Frame (7) describes the reloading of the healed specimen to assess the mechanical properties regain.

The bacteria-based repair solution was injected through one port illustrated in the frame 5 of figure 5.6 and figure 5.7 frame 2 by means of syringe (d) which then flew out through the crack, point (e). In this preliminary experiment, the injection sequence was carried on a trial basis, solution A followed by solution B. The first injection comprised of 90 mL solution A and 60 mL solution B in the sequence of 30 mL A + 30 mL B + 30 mL A + 30 mL B + 30 mL A. The second injection was conducted two hours after the first one by injecting 15 mL solution A and 20 mL solution B with the sequence of 10 mL A + 10 mL B + 5 mL A + 10 mL B. In the figure 5.6 frame 3, it can be seen that the solution reaches the fracture zone indicated by a wetted area in the bottom face and the side face of the specimen. The solutions A and B are injected in layers in order to ensure the gel formation and a good distribution of the bacteria, nutrients and calcium within the crack volume.

Afterwards the specimen was sealed with plastic for 24 hour to keep the specimen from evaporation. Subsequently, the specimen was cured under lab condition with RH $35 \pm 5\%$ and temperature $20 \pm 3 \text{ }^\circ\text{C}$ for 10 days.

Post-healing permeability test and second mechanical three-point bending test was carried out with the similar aforementioned procedure. They are depicted in the figure 5.8 frame 6 for leakage test and frame 7 for the bending test.

The efficiency of the healing is determined by ratio of the slope of the leakage curve before and after healing and ratio of strength and stiffness pre- and post-healing. The procedure for determining the healing efficiency was explained in the chapter 3.

5.2.3. Results of injection bacteria-based solution to the PNC

The assessment post-healing leakage (permeability) test was carried out 11 days after the injection of the bacteria-based solution. Figure 5.9. is a graph showing the weight of the water outflow as function of time elapsed from the start of the permeability test. The cracked specimen prior to healing has steep permeability slope, about 2.2 gr/sec, while the slope of healed specimen is much lower, about 0.8 gr/sec. However, even though not much, there is clear difference between the slope of permeability curve of healed specimen at 11 and 19 days⁹.

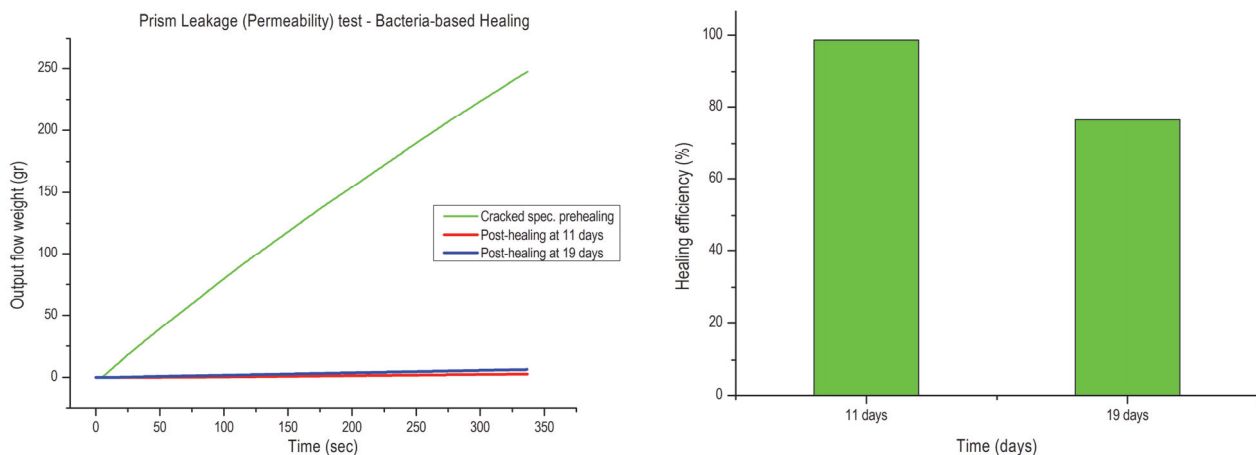


Figure 5.9. Graph of leakage (permeability) test of the prism over time and the histogram representing the healing efficiency.

This test shows a very promising preliminary result. More than 90% (96.7) permeability reduction has been achieved at 11 days which appears to be temporary since after 19 days permeability reduction drop to 70% (76.7), as illustrated in the histogram, figure 5.9. This could be attributed to the flushing of the bacteria based solution after 11 days. In other words the permeability test after 11 days disrupts the bio-mineralization process as the process was probably not yet complete. Another reason might be that there was no good adhesion of the repair product with the crack wall resulting in temporary repair.

Further the load versus crack opening graph obtained from bending test is shown in the figure 5.10 where the first loading curve is subsequently followed by second loading curve. It is obvious that the strength post-healing mediated by bacteria is lower than the peak strength of the original state of the specimen. The stiffness of the healed sample has also shown a lower value as the slope of the curve is less steep

⁹ The age (days) were chosen on trial basis (arbitrary); 11 days is in between one and two week and 19 days is in between two and three week.

than the virgin specimen. This may be attributed to the fact that the precipitate in the crack zone did not act as a 'glue' binding the crack faces therefore showing no contribution to the fracture toughness of the specimen. On the other hand, the precipitated mineral may be thought as necessary barrier to protect the crack opening from other deleterious substance.

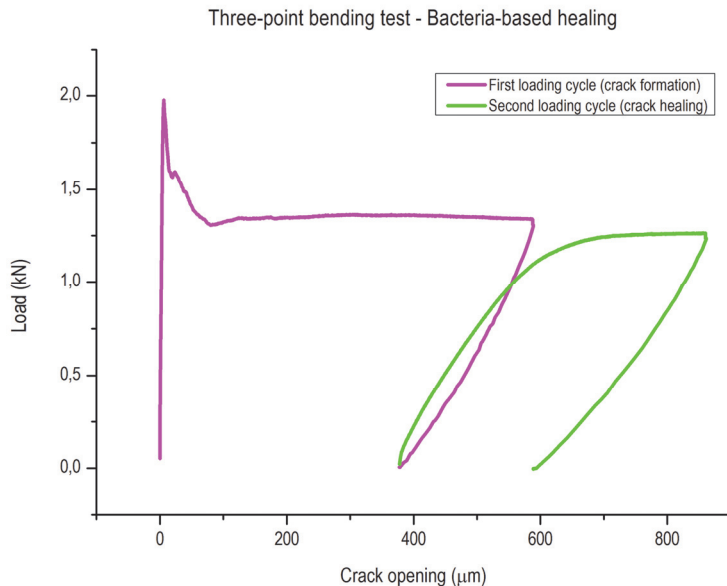


Figure 5.10. Load versus crack opening displacement graph of three-point bending test of the prisms injected by bacteria-based solution.

5.3. Test 2: Optimization of the solution by injecting it into porous core

As temporary healing was observed in the PNC specimen, an investigation to assess the capacity of the bacteria-based solution as healing agent was conducted. The necessity to further investigate its healing capacity was driven by the fact that the trial test provides minimum insight whether the bacteria were truly active in the concrete matrix and to what extent the bio-mineralization took place.

Prior to optimization of the bacteria-based repair solution as healing agent, several questions arose;

1. How much time was needed for the bacteria based repair system to achieve good quality?
2. After how long the bacteria based solution could develop sufficient mineral in the system and the healing should be tested?
3. Were several injections needed?
4. What was the optimum mix composition, what was the optimum ratio sol A/sol B?
5. What was the 'right procedure' to inject the solutions?
6. How to quantify the effectiveness of the bacteria-based repair solution to heal the PNC?

Several parameters were also required to test. The first factor to consider was the kinetics of the Ca-carbonate formation in time taking into account an assumption of healing time less than 28 days. The second was the procedure of injection based on the composition of the solution used in the trial test. For instance, layering solution

A followed by solution B repeatedly, premixed solution AB or layering solution A and then solution B injected several time with periodic time interval.

5.3.1. Rationalization and approach to experiment

An approach has been set to investigate in greater detail the healing capacity of the bacteria-based repair solution in the PNC. Figure 5.11 summarizes the plan and concept where several series of the experiment around the central series ‘A’ has been set. The tests were performed at 3, 7, 14, 21 and 28 days after injection and 2 replicates were used per time. This will allow assessing the kinetics of the biomineralization over time.

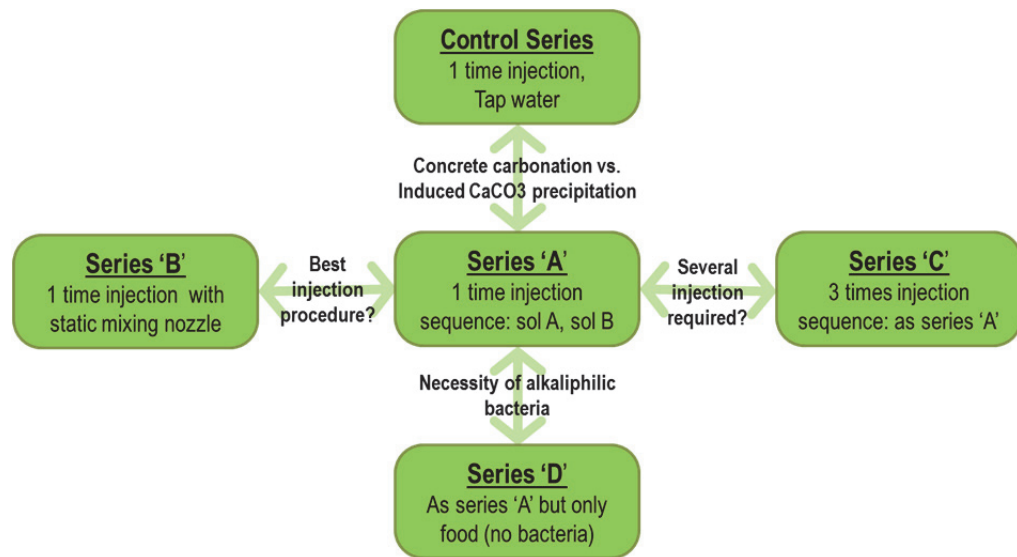


Figure 5.11. Experimental approach in optimizing the healing capacity of the bacteria-based solution

Table 5.3. Experimental matrix for assessing and optimizing the bacteria-based repair solution

Series	Impregnation condition	Time (days)					
		0	3	7	14	21	28
A	Sol A + Sol B	-	A3-1	A7-1	A14-1	A21-1	A28-1
	1 time impregnation	-	A3-2	A7-2	A14-2	A21-2	A28-2
B	Sol AB - mixing nozzles	-	B3-1	B7-1	B14-1	B21-1	B28-1
		-	B3-2	B7-2	B14-2	B21-2	B28-2
C	Sol A + Sol B	-	C3-1	C7-1	C14-1	C21-1	C28-1
	3 times impregnation.; d0, d1, d2	-	C3-2	C7-2	C14-2	C21-2	C28-2
D	Sol A + Sol B	-	-	-	-	-	D28-1
	without bacteria	-	-	-	-	-	D28-2
Control	Tap water	Ctrl0	Ctrl3-1 Ctrl3-2	Ctrl7-1 Ctrl7-2	Ctrl14-1 Ctrl14-2	Ctrl21-1 Ctrl21-2	Ctrl28-1 Ctrl28-2

The specimens in series ‘A’ were treated by manually injecting solution A followed by solution B for one time injection with syringes for each solutions. Series ‘B’ referred to the specimens having one-time-injection, solution AB is premixed by static mixing nozzle right after the open end tube of each syringe. This was intended to compare

and identify the effect of the injection procedure between layering (solution A then B) and premixing (solution AB).

Specimens in the series ‘C’ were treated as series A, with the injection of solution A followed by solution B, three times with 24 hours interval. Consequently, the total volume of the bacteria-based repair solution injected in the specimens was larger for series C than for the series A, B, and D. This was motivated by the need to study the effect of several injections on the development of bio-mineral deposition in the PNC. Further, series ‘D’ was designed to inject only nutrients compound into the concrete to reveal whether alkaliphilic bacteria were needed in the system or the sole food conversion into Ca-based mineral was adequate. Apart from the other series, in series D specimens were tested only at 28 days.

The control series specimens were treated solely with tap water injection to investigate whether the process was ‘truly’ microbial induced Ca-carbonate precipitation or common concrete carbonation. The experimental design is summarized in the table 5.3 showing the 5 different series, impregnation conditions and the day the specimens were tested.

5.3.2. Material and specimen preparation

Due to the high number of specimens required, the experiment was performed using porous core apart from the PNC main body. Design mixture of the porous concrete was prepared as described in the subchapter 2.3.2. The mixture was P24-2 which has aggregate size of 2-4 mm with aggregate-to-binder ratio of 5.0. The composition as described in the table 2.5 was; 275 kg/m³ CEM I 42.5, 25 kg/m³ fly ash class C, and 1513 kg/m³ gravel aggregate. Water-to-binder ratio was kept at 0.33 with *superplastizicer* equal to 1% of binder.

The porous concrete cores were mixed, casted and cured following procedure described in the subchapter 2.3.1. point b. The porous cores were cylinders (with a length of 30 mm) which were cut in smaller specimen of 3 cm high. Subsequently specimens were covered with two layers plastic wrap and tightened with transparent adhesive tape. Figure 5.12 illustrates the specimen preparation.

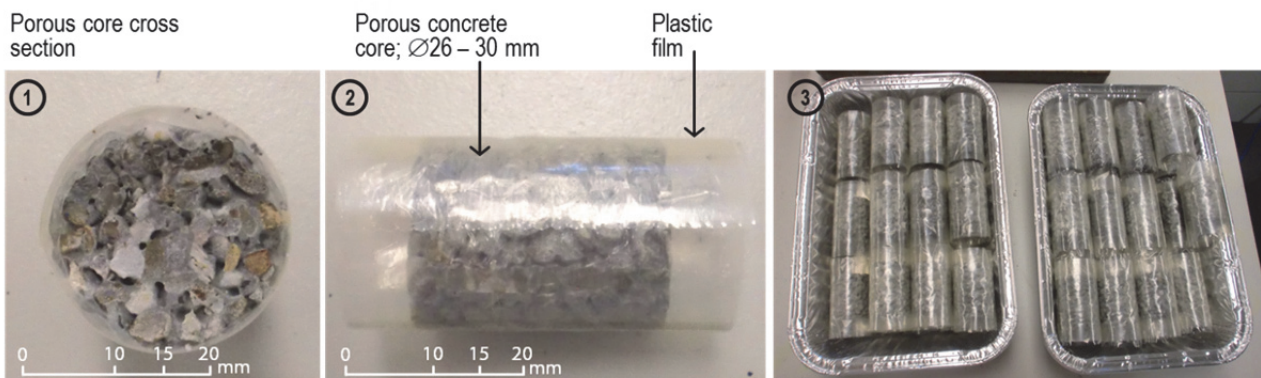


Figure 5.12. Specimen prepared by covering porous concrete core with plastic film and adhesive tape shown in frame 1 and 2. Frame 3 shows a collection of ready-to-test specimens.

The two solutions, A and B, have the same composition as described in the subchapter 5.2.1 table 5.1 and 5.2 respectively. The solutions were prepared immediately prior to the test and pH was checked using pH indicator strip.

5.3.3. Methods and evaluation techniques

a. Testing cycle

Figure 5.13 illustrates the general cycle of experimental test. It is started by tightly covering specimens with plastic film and adhesive transparent tape for specimen preparation (figure 5.13, step 0). Initial permeability (step 1) was performed subsequently followed by preparing specimens for injection of bacteria based repair solution (step 4). This was carried out by covering the bottom side of specimens with plastic film and adhesive tape ensuring the solution stayed in the porous core (step 3). Series 'B' underwent pre and post solution impregnation (step 3 and 5). Second permeability (step 6) test was conducted to assess the extent of biomineralization.

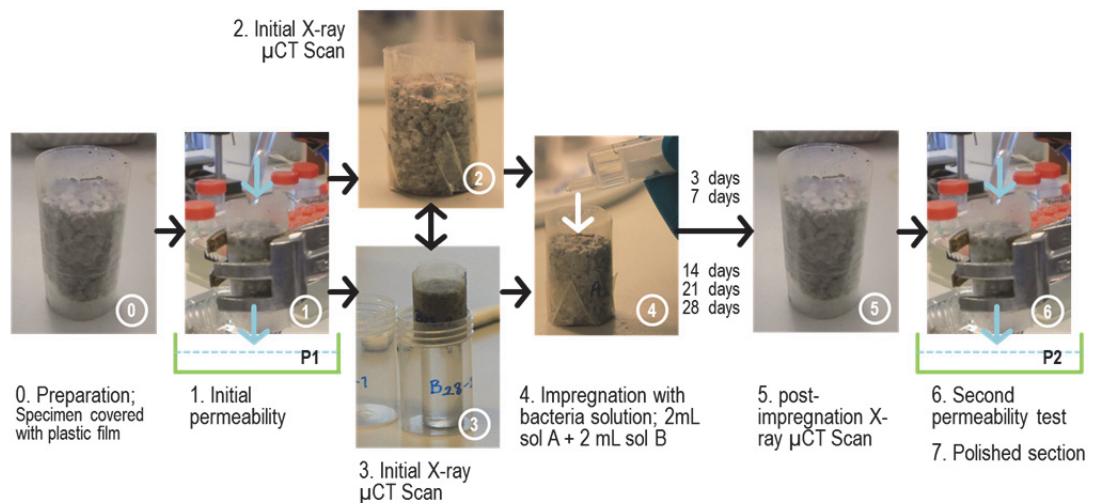


Figure 5.13. Experimental test cycle showing six steps from preparation of specimen up to the eventual polished section for ESEM observation.

Solution (A or B) was impregnated into the porous core as depicted in figure 5.13 step 4. The total 4 mL was injected by means of syringe each for different solution consisted of 2 mL solution A and 2 mL solution B. One control (tap water injection) and four different series (bacteria-based repair solution injection) with two replicates were carried out according to the experimental matrix, see table 5.1.

b. Evaluation techniques 1; Permeability test

Water permeability test was conducted before (step 1) and after (step 6) the injection of the bacteria-based repair solution at regular time interval to determine the sealing efficiency of the system. Figure 5.14. illustrates the setup of injection and permeability test. The test was performed while the specimen was gripped with a clamp and flowing 15 ml water with syringe in 10 sec. A manual stopwatch was used to monitor this time interval. A bucket was put underneath the specimen to contain

output flow weight over time. The ratio of slope of the permeability curve as function of time between initial and healed specimens was used to determine the healing capacity.

c. Evaluation techniques 2; Micro CT-scan

Bio-mineral precipitation was monitored at 3, 7, 14, 21, and 28 days using several techniques. One compelling method for healing capacity assessment of the bacteria-based repair solution is by monitoring the production of bio-minerals over time non-destructively and non-invasively. X-ray micro CT scan was used to observe the specimens porosity before and after the injection in order to monitor in time the deposition of the bio-mineral. Only specimen in the series B would undergo CT scan starting 3 days after solution injection. As the specimen was held in the object stage between x-ray source and the detector which then rotated progressively, a stack of images was obtained. The rotation of the object stage was set progressively at approximately 0.25° to acquire about 1440 projections with resolution of about $6\ \mu\text{m}$.

The tomographic 3D volumetric model of the porous cores was reconstructed automatically using VGStudio MAX 2.0 software. Comparison of porosity feature between pre-and post-healing specimen was carried out by analyzing the image at the same region of interest (ROI) dimension set for each 3D model.

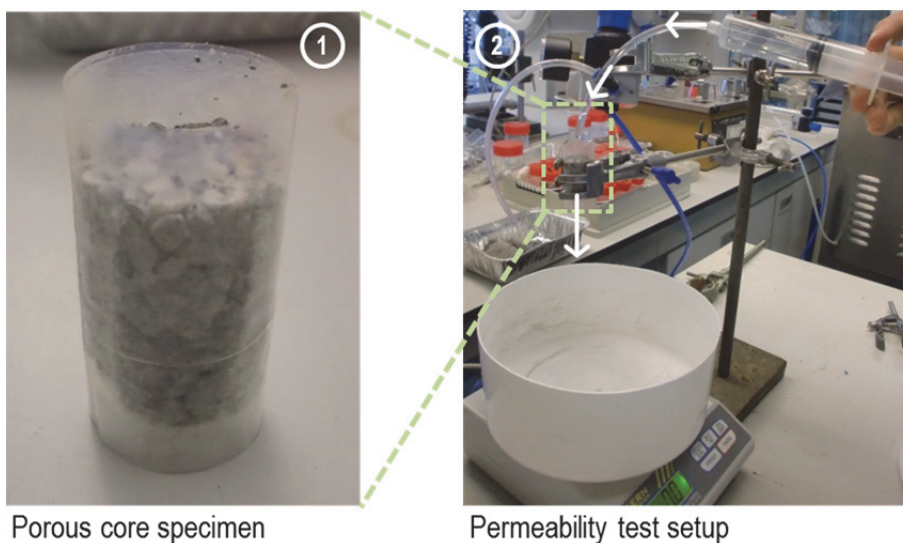


Figure 5.14. Setup of Injection test and permeability test where the porous core specimen in the frame 1 is held by a clamp shown in the frame 2

d. Evaluation techniques 3; Fourier Transformed Infra-Red

When possible, sampling of the minerals deposited in the specimen is performed with the aid of a pincer by gently scrapping the surface of the core. These precipitates are examined with Fourier-Transform Infrared (FT-IR) spectrometry for further analysis and identification.

Chemical composition of materials is defined by the bond energy between the atoms in the materials molecule. Taking into account this property, infrared spectroscopy method is based on the interaction between infrared waves with the bonds of the

atoms of molecules in the material. The energy activates molecular bonds, e.g. change in the dipole moment, to vibrate or rotate at specific frequency, which in turn may reduce the energy at distinct frequency partly or totally. This frequency will then be sensed and recorded by a detector. As a result, the infrared spectrum shows the molecular characteristic from reflected or absorbed light indicated by certain band or peaks in the spectra at a particular energy level.

In this study, the suspected Ca-based whitish minerals deposited between aggregates in porous core were found in a few specimens. After removal, the minerals were collected in the flask and used for FT-IR spectral analysis. The spectra were collected using universal Attenuated Total Reflection (ATR) unit on a Perkin–Elmer Spectrum 100 Series spectrometer. The benefit with this ATR unit is that it requires less than 5 mg sample without laborious preparation or specimen dilution. Background signal scanning calibration was required prior to the scanning. The spectral range was of 4000–600 cm^{-1} with 2 cm^{-1} resolution and 16 scans were collected each time.

e. Evaluation techniques 4; Microscopy

Eventually, at the end of the healing period, polished sections of injected specimens were prepared by impregnating the specimen with epoxy resin and then grinding (rough-to-fine polishing) its surface which was ended by solvent surface cleaning. The grinding process sequence and the grit size (average size of abrading particle) was as follow; 10 minutes P500 (30.2 μm), 10 minutes P800 (21.8 μm), 10 minutes P1200 (13.3 μm), and 15 minutes P4000 (5.2 μm). Manual hand pressure and water flow was exerted into the specimen while it was ground on top of rotating table with designated sand paper.

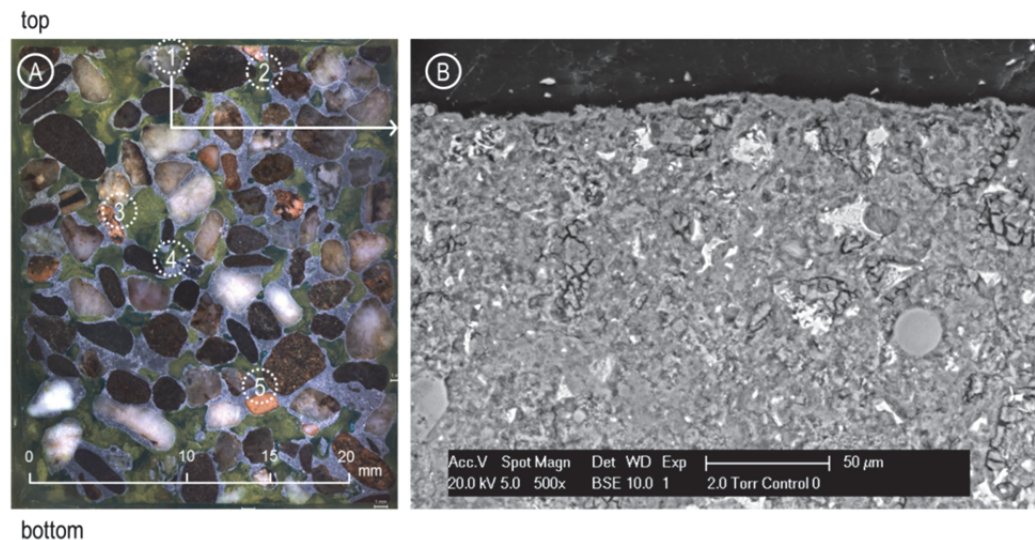


Figure 5.15. (A) Surface of polished section marked with points where in-depth ESEM observation will be spotted. (B) The image taken at the top surface of the specimen point 1.

The specimen was first observed under light microscope to analyze and locate the expected bio-minerals deposition. It was planned the observation would be carried out in five different points throughout the depth of the specimen as sketched in figure 5.15 frame A; in the top surface, slightly below the surface, two points in the mid-section, and in the bottom area. This was intended to obtain higher likelihood to collect evidence of bacterial activity and identify mineral characteristics.

An Environmental Scanning Electron Microscope (ESEM, Philips XL30 Series) equipped with an Energy Dispersive X-ray (EDS) element were employed to analyze in depth the surface feature of the polished section. Figure 5.15 frame B exhibits the ESEM image taken at point 1 from control specimen at t0 prior to tap water injection.

5.3.4. Results and discussion

a. Evaluation techniques 1: Permeability test

To assess the healing capacity of the solution, the slope value of the permeability curve pre-healing is compared to the slope value post-healing for each specimen tested. Figure 5.16 shows the histogram of the slope of permeability curve of post-healing specimens on top of the slope value of permeability curve of pre-healing specimens for each type of series over time (3, 7, 14, 21, and 28 days). The D series only has one permeability slope value at 28 days.

The results for water permeability test showed sparse data and no significant difference is observed between the series. It is also found there is no such specific trend inferred from the data. This might be explained from the fact that the specimens were very porous and had limited amount of cement paste matrix to supply Ca-hydroxide and not enough calcium ion from the Ca-lactate is available to produce sufficient Ca-carbonate.

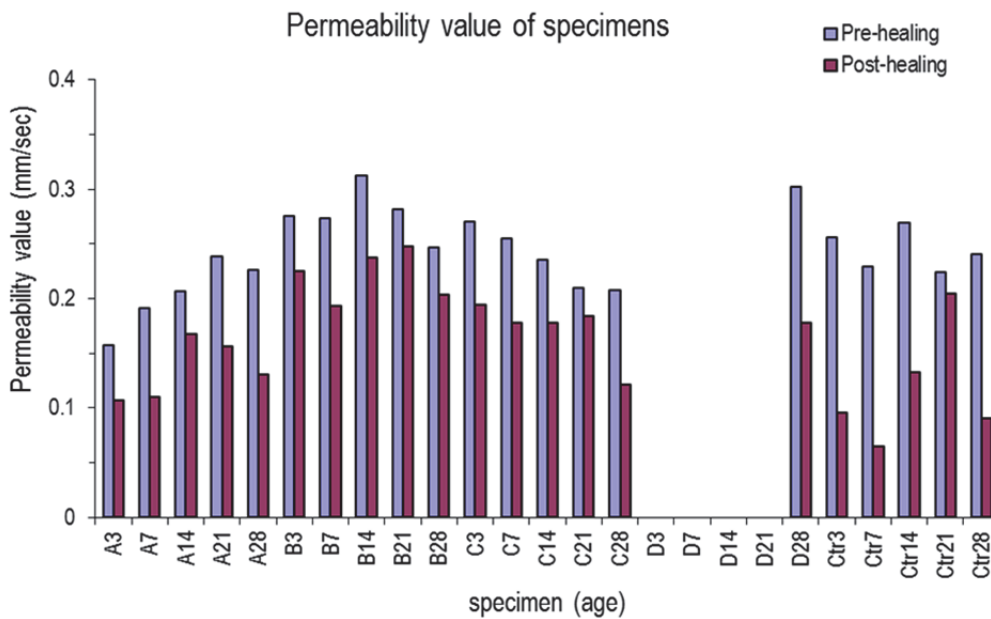
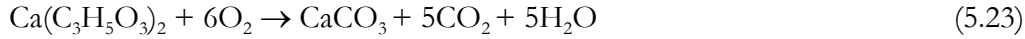


Figure 5.16. Histogram of permeability value in the porous cores before and after healing with bacteria-based solution

How much CaCO_3 can be formed in the bacteria-based concrete healing system depends on the amount of calcium ion, $[\text{Ca}^{2+}]$, present in the system. This is influenced by amount of portlandite, $\text{Ca}(\text{OH})_2$, in the concrete, and the amount of calcium ions supplied from nutrients, for the present case Ca-lactate. Theoretically, the calcium carbonate produced from Ca-lactate conversion – without taking into

account reaction with Ca-hydroxide from concrete – can be expressed as in the equation 5.23.



The mass of Ca-lactate, m_{Ca} (g), available in the solution is the product of the concentration of calcium in the solution, C_{Ca} (g/L), which has value of 80 g/L and volume of the solution injected in the system, V_{Ca} (L), which has value of 2 mL. This is expressed by the equation 5.24

$$C_{Ca} = \frac{m_{Ca}}{V_{Ca}} \quad (5.24)$$

$$m_{Ca} = C_{Ca} \times V_{Ca}$$

Thus the mass of the Ca-lactate in the 2 mL solution injected into the porous concrete was

$$m_{Ca} = 80 \text{ g/L} \times 0.002 \text{ L} = 0.16 \text{ g.}$$

The quantity of molecule Ca-lactate, n_{Ca} (mol), in the solution is then determined as the ratio of the mass of Ca-lactate, m_{Ca} (g), to the molar mass of Ca-lactate molecule, M_{Ca} (g/mol), as expressed in the equation 5.25.

$$n_{Ca} = \frac{m_{Ca}}{M_{Ca}} \quad (5.25)$$

$$n_{Ca} = \frac{0.16 \text{ g}}{308 \text{ g/mol}} = 5.2 \times 10^{-4} \text{ mol}$$

As 1 mole of Ca-lactate is converted into 1 mole of CaCO_3 , based on the equation 5.9, n_{Ca} (mol) equals to n_{CaCO_3} (mol). The latter refers to the number of mole (quantity of molecule) CaCO_3 . Thus, the mass of CaCO_3 , m_{CaCO_3} (g), produced is the product of the number of mol Ca-carbonate, n_{CaCO_3} (mol), and the molar mass of Ca-carbonate molecule, M_{CaCO_3} (g/mol) expressed in the

$$m_{CaCO_3} = n_{CaCO_3} \times M_{CaCO_3}$$

$$m_{CaCO_3} = (5.2 \times 10^{-4}) \times 100 = 0.052 \text{ g}$$

As the density of CaCO_3 , ρ_{CaCO_3} (kg/m^3), is known from literature ($2.71 \times 10^3 \text{ kg/m}^3$), the volume of CaCO_3 , V_{CaCO_3} (m^3), can be determined by the following equation:

$$\rho_{CaCO_3} = \frac{m_{CaCO_3}}{V_{CaCO_3}} \quad (5.26)$$

$$V_{CaCO_3} = \frac{m_{CaCO_3}}{\rho_{CaCO_3}} = \frac{(0.052 \times 10^{-3})}{(2.71 \times 10^3)} = 1.9 \times 10^{-8} \text{ m}^3 = 19 \text{ mm}^3$$

The porosity of the porous core is approximately 20% therefore the volume of void fraction of the core, V_{por} , is about $3 \times 10^3 \text{ mm}^3$. Comparing the V_{CaCO_3} (mm^3) to the

volume of porous core void, V_{por} it is known that V_{CaCO_3} occupied only 0.65% of total volume of the porosity which is very low to make substantial blockage or clog in the porous core. Based on theoretical calculations the maximum volume of $CaCO_3$ which can be formed in these conditions is less than 1% of the total porosity. This explains why the water permeability test results are not relevant in the present case.

b. Evaluation technique 2: micro-CT-scan

Figure 5.17 displays the two images from the same specimen 'B21-1' before (initial) and 21 days after injection bacteria-based repair solution. Formation of suspected newly Ca-based mineral is visually seen by comparing the images.

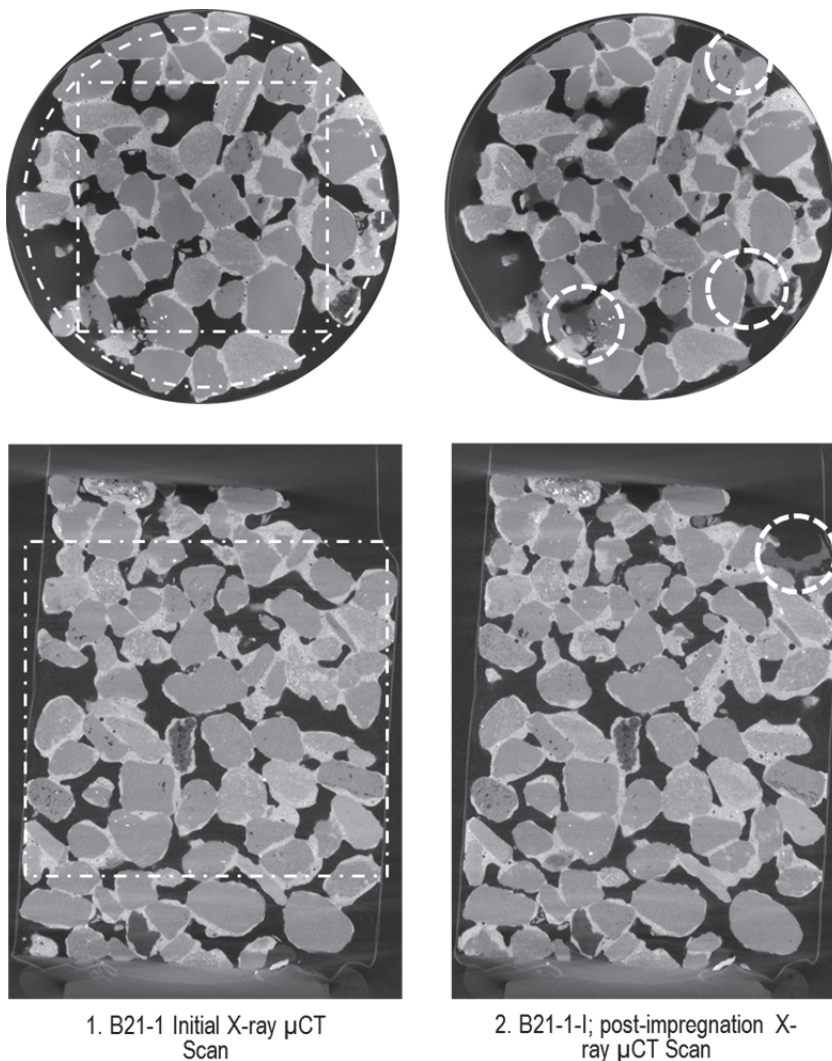


Figure 5.17. Images of pre- and post-injection specimen were taken by x-ray micro CT scan showing the newly formed materials suspected as Ca-based mineral.

Following the visual observation, the image analysis was carried out for the CT scan images of the sample at 3, 7, 14, 21, and 28 days. Image segmentation was performed by setting a region of interest (ROI). A threshold value was set from the voxel

intensity histogram using VGStudio Max 2.0. The number of voxel obtained was then converted into volume. Volume of newly material formed, M (%), is expressed in the following equation (eq. 5.27);

$$M = \frac{(V_{mat(P1)} - V_{mat(P0)})}{V_{mat(P0)}} \quad (5.27)$$

Where, $V_{mat(P1)}$, is the volume of material after treatment (bacteria-based repair solution is injected) and $V_{mat(P0)}$, is volume of material before treatment.

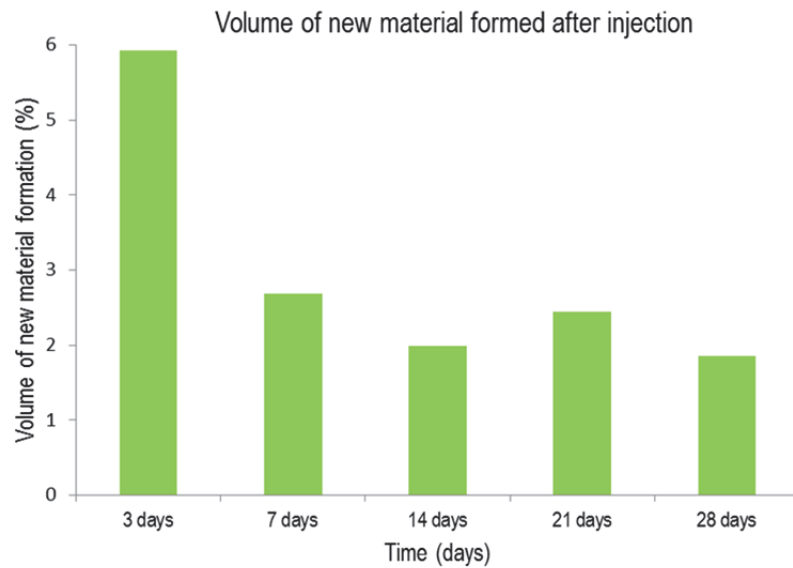


Figure 5.18. histogram of volume of new material in the porous core after injection of bacteria-based solution as calculated from x-ray micro CT scan 3D tomographic model.

Processing of CT-scan data showed that 3 days after injection ~6% of the material volume corresponds to new material. This percentage decreases to ~2% after 7 days and approximately stays constant until 28 days as can be seen in the histogram figure 5.18. Even though bacteria start to grow within the first 24h, they cannot yet produce that high volume of CaCO_3 . This means that after 3 days mainly the solution that has been injected into the porous core is detected with this technique. With time the solution dries out so that its volume decreases. As a conclusion, it is very hard to distinguish between food (organic precipitates) and converted food (bio-minerals) with CT-scan analysis in these experimental conditions.

c. Evaluation technique 3: ESEM

Figure 5.19 presents the images of ESEM observation of ‘Control’ series polished specimen under ESEM. The image was taken from top surface of the specimen and interface of pore and concrete matrix. Observation revealed Ca-based surface layer which may be attributed due to carbonation. Thicker layers on top of porous concrete matrix have been found in the specimen of 14 and 28 days indicating the progress of carbonation over time.

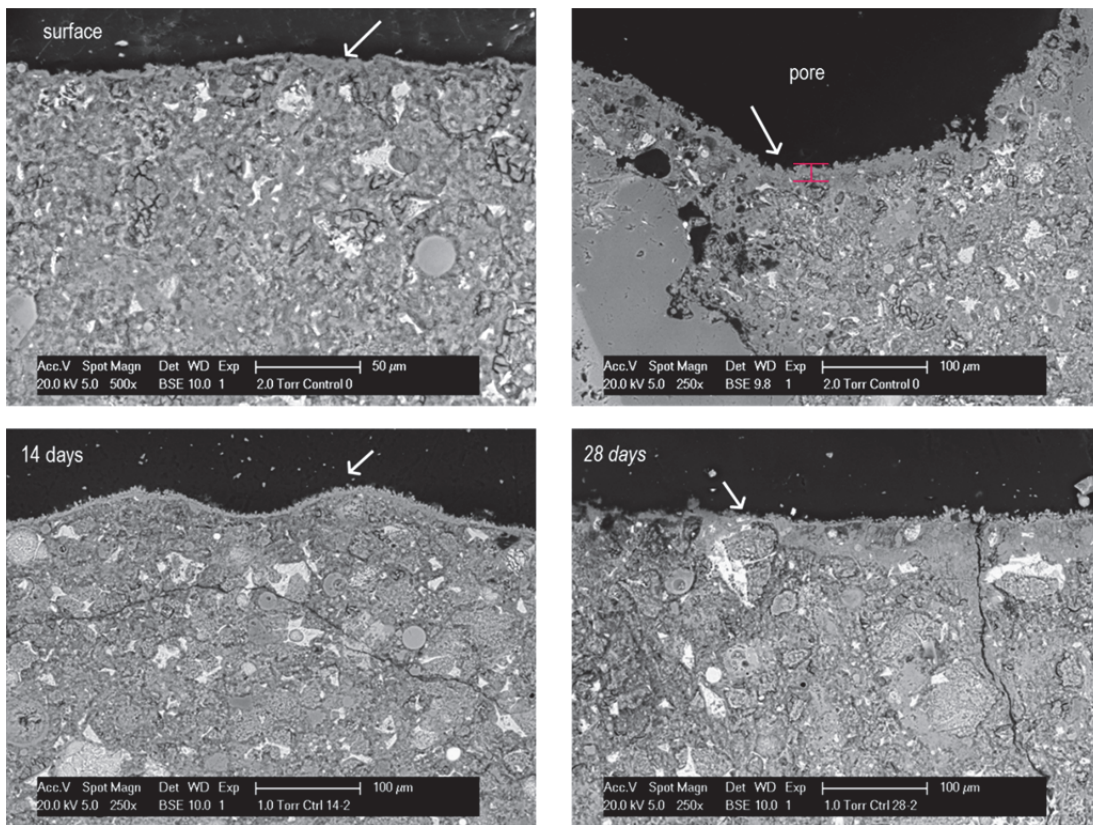


Figure 5.19. ESEM pictures of polished sections of Control series at top surface of the specimen, at surface of the aggregate and pore, 14, and 28 days. Layer of Ca-based mineral due to carbonation is observed in this series.

Observations of polished sections under stereomicroscope and ESEM exhibited some cavities between porous concrete matrix and epoxy resin in the series comprising nutrients (series A, B, C and D). It seemed that the bonding between the epoxy and the specimen is 'bad', see figure 5.20. However further analysis attributed this to the food dissolution during the grinding process with water. Taking into account that during the preparation of the polished sections each specimen has been in contact with the grinding paper for about 45 minutes while water was continuously flown, it can be concluded that the food dissolved resulting in holes what then appears as bad bonding between epoxy and the matrix. However, further higher magnification observation into this cavity appears to be a good indicator for the location of bacteria-based solution (nutrients) and therefore to the possible presence of calcium carbonate, CaCO_3 , precipitates due to bacterial activity.

Figure 5.20 displays ESEM pictures of polished section of series A at 7, 14, 21, and 28 days. Epoxy-concrete matrix can be seen quite obvious leading to in depth observation of chemical element analysis for that particular spot. For series 'A', limited Ca-based mineral is noticed in the specimen at 7 and 14 days. Small Ca-based crystals are observed 21 days after injection. After 28 days less de-bonding and more Ca-based crystals are noticed suggesting that their formation could be due to bacterial activity. Further reflection leads into the hypothesis that CaCO_3 formation due to bacterial activity may be materialized between 14 to 21 days.

Element maps have been acquired from polished section by means of Energy-Dispersive X-Ray Spectroscopy (EDS) showing the spatial distribution and compositional zonation of elements in a specimen series A. Comparing the elemental maps in figure 5.20, the Ca-based mineral right on top of cement matrix might have been resulted from the carbonation process as it mainly composed of calcium (Ca) and no silicon (Si) was observed. Meanwhile the compound based on silicon might be resulted from repair product; e.g. composed of Ca-silicate hydrate gel, Ca-based biomineral, and unconverted food.

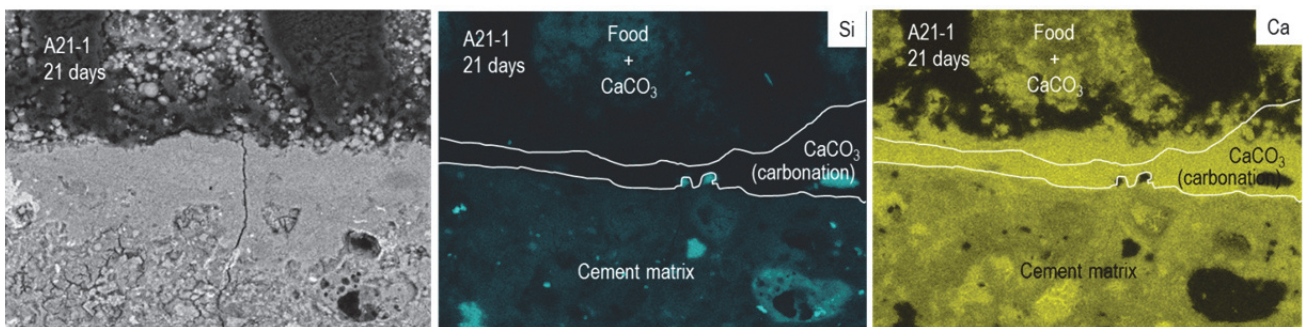
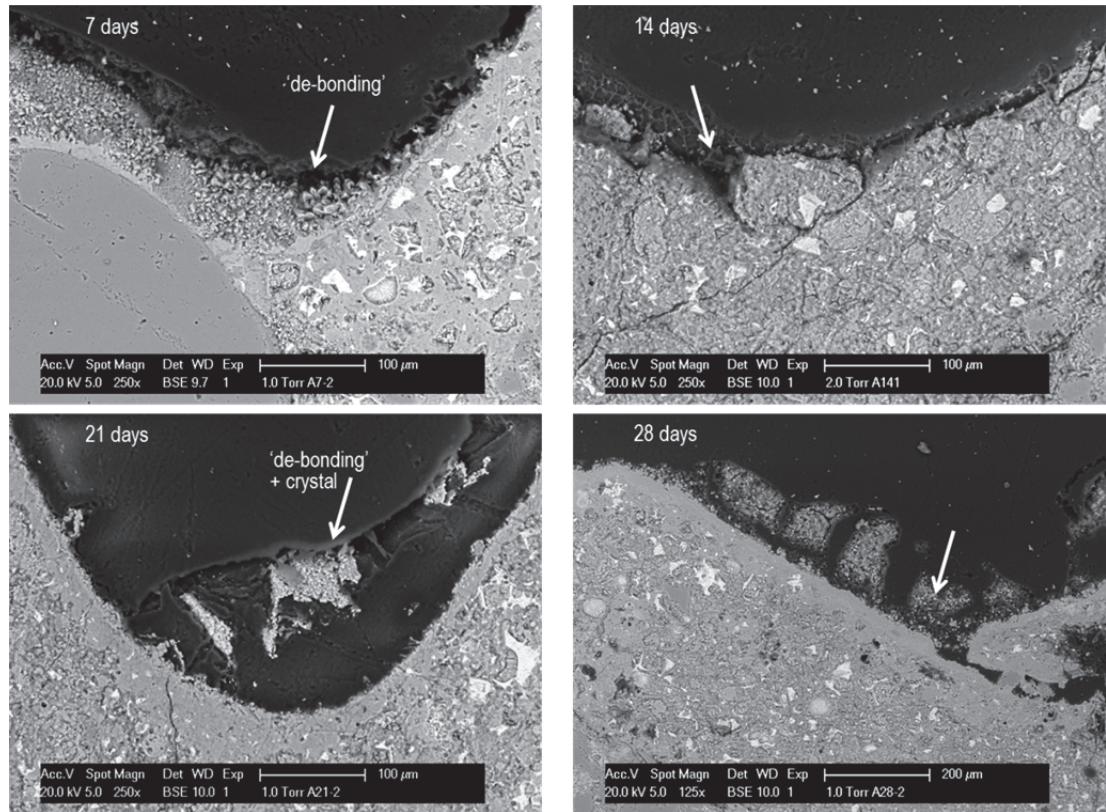


Figure 5.20. ESEM pictures of polished sections of series A at 7, 14, 21, and 28 days. De-bonding of epoxy-matrix is obviously seen and small crystals is observed in the specimen at 21 days where elemental mapping confirms the Ca-based mineral.

Similar observations are made for series 'B' (specimen injected using mixing nozzle). However it seems that less crystals are formed in series 'B' compared to series 'A'. Interestingly, large globular Ca-based minerals were observed under ESEM. Larger magnification revealed these globular adjacent into the 'de-bonding' area where the nutrients were largely found, as depicted in the figure 5.21. Energy Dispersive X-ray (EDS) analysis confirm the chemical element of calcium, carbon and oxygen in the

crystal which is essentially associated with Ca-carbonate precipitates mediated by bacteria.

Figure 5.22 is the spectra of FTIR analysis on precipitate scrapped from the edge of the specimen (B21-2) at 21 days. This spectrum shows that the precipitate is composed in majority of Ca-lactate, and to a lower extent of Calcium carbonate, CaCO_3 . These results combined with the ESEM observation strongly indicate that bacteria were active at 21 days.

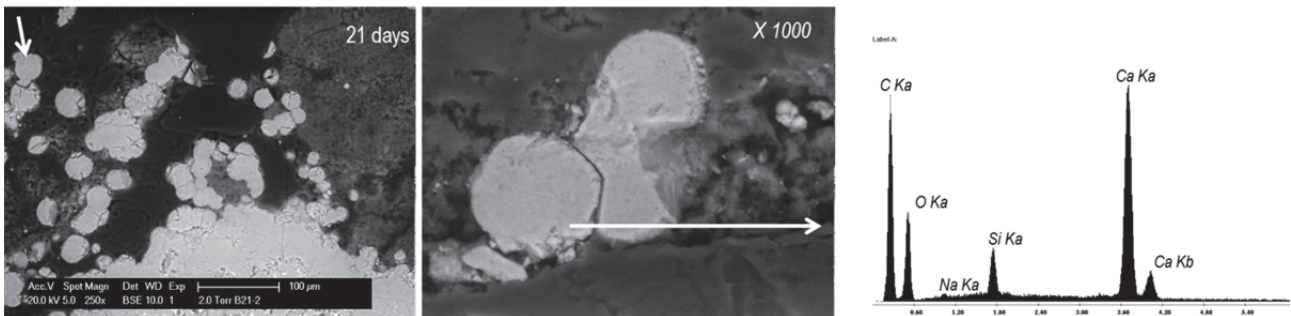


Figure 5.21. ESEM pictures of polished sections of series B showing globular Ca-based mineral.

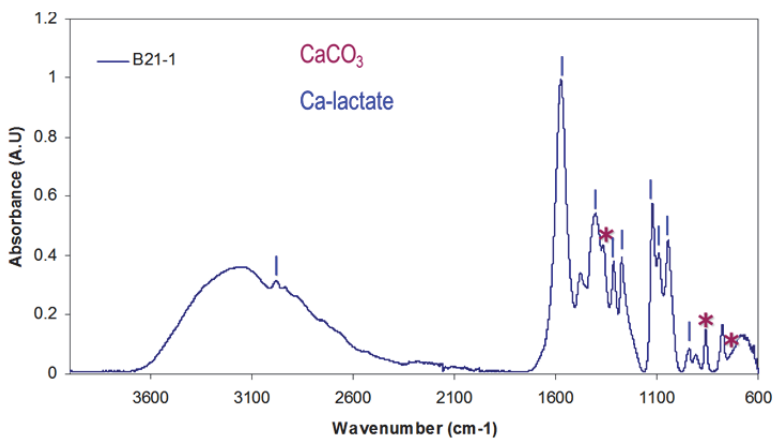


Figure 5.22. FT-IR spectra of the precipitates showing indication of Ca-carbonate peaks among Ca-lactate.

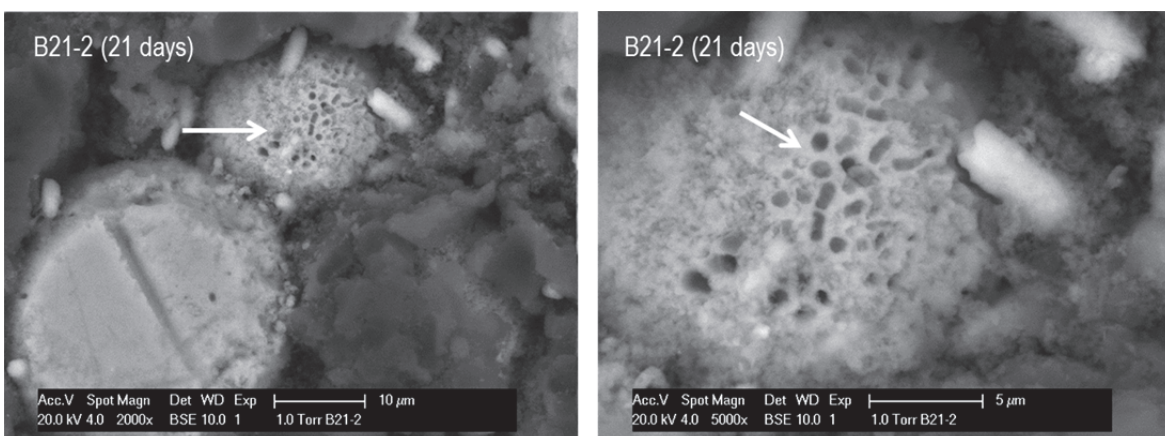


Figure 5.23. Bacteria imprints in the globule Ca-based mineral of series B indicating that bacteria were active, metabolically converted nutrients, produced layers of mineral and entombed it selves.

Larger magnification into the globules revealed significant bacteria imprints. In the figure 5.23 the imprints show random orientation of rod-like shape which may be attributed to the shape of alkaliphilic *Bacillus* used in the solution.

Bacteria reproduce asexually by binary fission. One cell is divided into two genetically identical daughters' cell assuming there is no mutation all the way. It can grow rapidly in the order of hours. The double number leads bacteria to grow exponentially provided enough growth condition and resources, for instance food. Alkaliphilic bacteria in the porous concrete core are metabolically active by consuming energy form the food. Meanwhile their respirations change the chemical micro-environment in their vicinity. This new chemical balance leads into Ca-carbonate precipitations that 'bury' the bacteria and make them die. This result in bacterial 'signature' – rod-like bacillus imprint – found in the specimen injected by the solution.

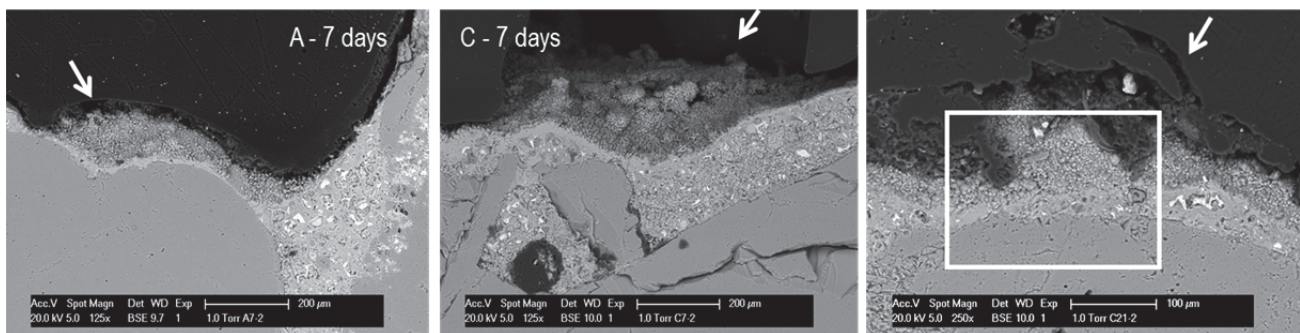


Figure 5.24. ESEM pictures of polished sections of series A in comparisons to series C where more obvious cavity appear in the specimen series 'C'.

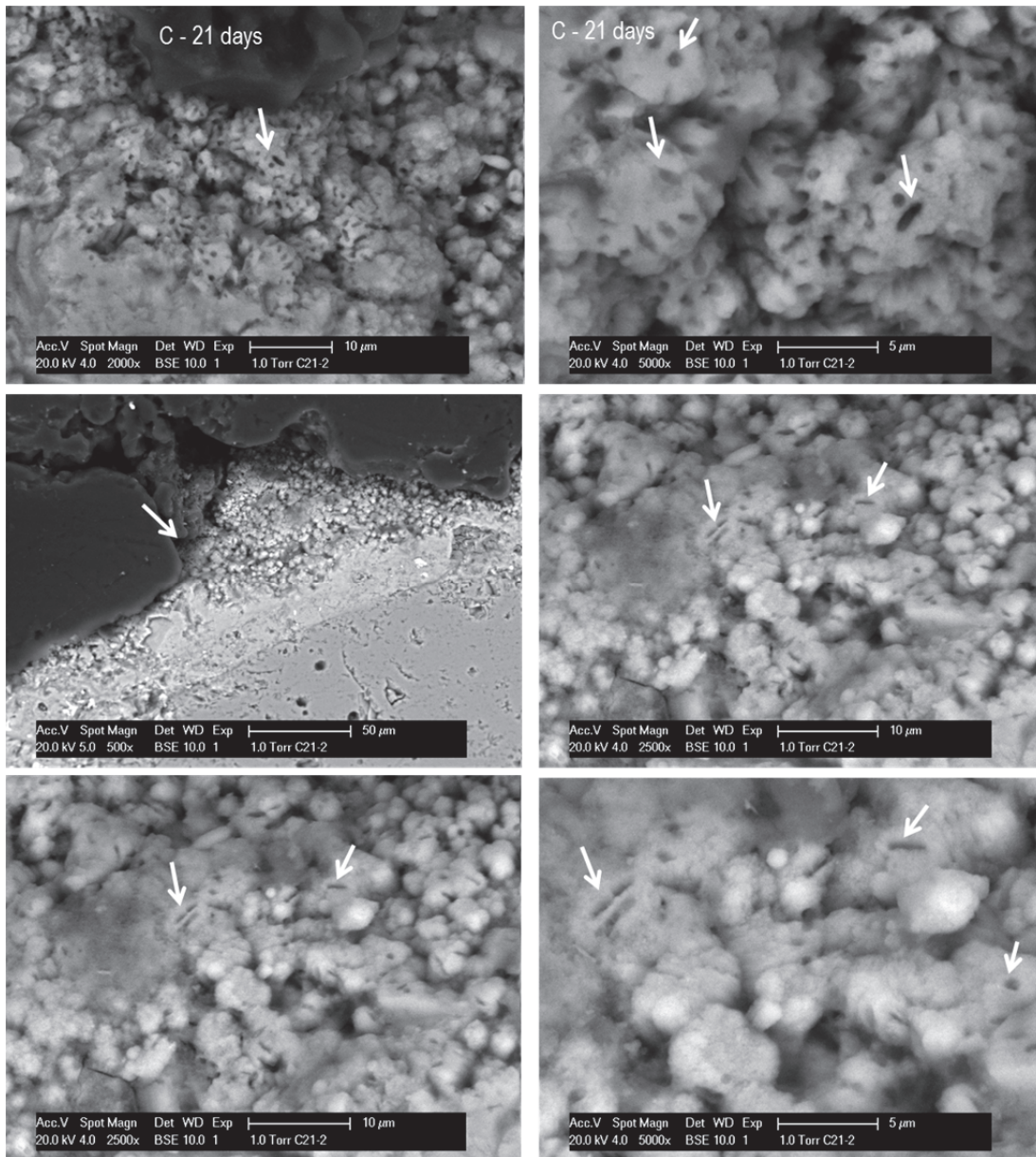


Figure 5.25. Massive bacteria imprints have been found in different spot in the series C indicating high activity due to the layering of solution in the system.

Observations for series ‘C’ showed similar results as in series ‘A’ but with a more pronounced cavity, ‘de-bonding’ between epoxy and mineral matrix. It can be seen in the figure 5.24, the cavity in the ‘C’ series, i.e. C-7 days, is substantially larger compared to the cavity in the specimen series A at the same age. This is explained by the fact that 3 injections have been made for series ‘C’ compared to 1 for series ‘A’ resulting in more food.

Moreover, bacteria imprints on Ca-based mineral were observed in different spots at 21 and 28 days specimen C21-1 and C28-1. Figure 5.25 depicts several ESEM images of the imprints which clearly show the random bacillus-shape bacteria entombed in the mineral grown extracellular. This constitutes the evidence of the involvement of the bacteria in the formation of CaCO_3 at 21 days. This result leads to the implication that bacteria-based repair solution can successfully be injected into porous network concrete as crack-healing agent.

Observing ESEM images of series 'D' and the control series, it is found a similarity where a layer of crystal deposited in the internal surface of the porous concrete cement matrix. This can be seen quite clear in the figure 5.26. In this figure frame 1 and 2 exhibit series 'D' while frame 3 illustrates the control series. The crystal minerals may be attributed as carbonation product in both series.

Further in series 'D' cavities, 'de-bonding' of epoxy resin and concrete matrix are found indicating the dissolution of nutrients which previously was present in the system but was not converted into Ca-based mineral. Combined with the fact that there was no bacterial activity in the control series, due to the pH being too high for tap water bacteria to grow in the system, it can be concluded that the alkaliphilic bacteria are the essential part of the bacteria-based healing system. for the porous network concrete

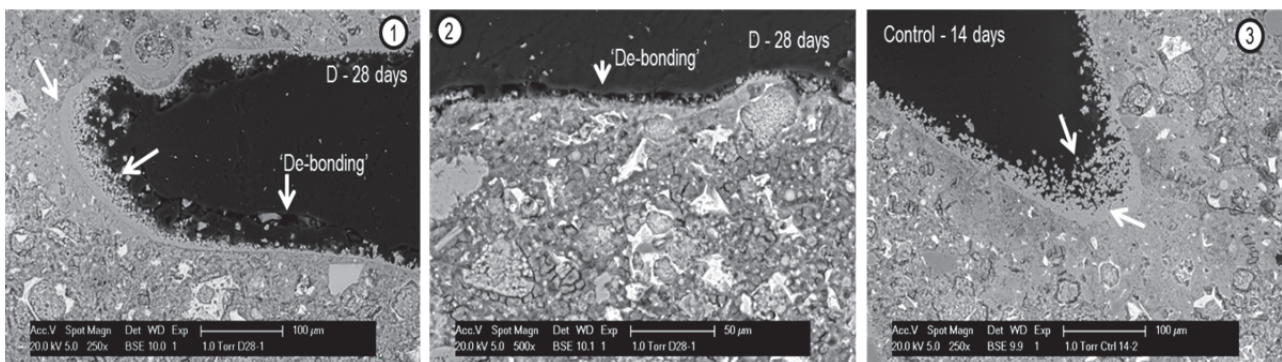


Figure 5.26. Layer of crystal observed in the surface of void of porous concrete core in series D as well as cavity due to nutrients dissolution, frame 1 and 2. Frame 3 exhibit layer of crystal which might attributed to the carbonation, however there were no cavities observed.

5.3.5. Findings

A large volume of solution is required to provide massive CaCO_3 precipitation for blocking the porous core with pore diameter approximately 0.3-1 mm and total volume of about 19 mm^3 . It was found that the amount of Ca-carbonate was too low compared to what was required.

However, bacteria imprints obtained from ESEM observations of polished section of $\text{Ø}26\text{-}30$ mm cylindrical porous core 21 days after injection with the solution provided *strong indication* of bacterial activity. This implies bacteria-based repair solution can successfully be used as healing agent into PNC providing that more Calcium is brought to the system.

Impregnation condition or injection sequence may also influence the precipitation of Ca-based mineral. There times injection sequence (layering) solution A followed by solution B with 24 hours intervals in series C precipitated massive mineral as the higher amount of nutrient have been provided for conversion by bacterial communities indicated by extensive bacteria imprint. One time impregnation of series B (premixed solution AB with mixing nozzle) also showed a precipitation product with lesser intensity. Meanwhile layering solution A followed by solution B in the series showed the least intensity of precipitation. It is admitted, however, that it is hard to draw conclusion which injection method (impregnation condition) will

end up showing better result between series A and B, as precipitation occurred very locally therefore it also hard to find and observe it under ESEM.

5.4. Test 3: Healing efficiency of the PNC prism

Test 2 demonstrates that the bacteria-based repair solution works in the porous core and may act as healing agent in the Porous Network Concrete structure. This section is devoted to investigate the healing efficiency when the optimized bacteria-based solution is injected into the PNC prisms.

5.4.1. Experimental program

A research program (see table 1) has been devised to implement injection of bacteria based solution into PNC specimen and heal the crack in its main body. Two type of treatment were implemented with 2 replicates. The ‘control’ series received injection of 30 ml tap water and ‘bacteria’ series received injection of bacteria-based solution. Two different curing were conducted in which ‘wet’ series were cured in $\pm 95\%$ RH and $\pm 20^\circ\text{C}$ curing chamber while ‘dry’ series were cured under lab condition abovementioned, in order to assess the effect of curing regime on the healing efficiency. Table 5.4 summarizes the experimental design to assess the healing efficiency of the PNC prisms by means of bacteria-based solution as healing agent.

Table 5.4. Matrix of experimental program of healing efficiency of the PNC prism

		Curing regime	
		Wet (Fog room) T: $20 \pm 2^\circ\text{C}$; RH: $95 \pm 5\%$	Dry (Lab room) T: $20 \pm 2^\circ\text{C}$; RH: $35 \pm 5\%$
Treatment	Control	CrtlW-1	CrtlD-1
		CrtlW-2	CrtlD-2
	Bacteria	BactW-1	BactD-1
		BactW-1	BactD-1

5.4.2. Materials

Specimens for the test are the Porous Network Concrete prisms with the dimension of $55 \times 55 \times 285$ mm. Each specimen center interior is $23 \times 23 \times 285$ mm porous concrete and $\text{Ø}2$ mm threaded steel rebar was installed under the core. The PNC mixture was P24-2-B based on the design mixture explained in subchapter 2.3. The porous core comprises of aggregate 2-4 mm bound by 275 kg/m^3 CEM I 42.5 and 25 kg/m^3 fly ash C class with water-to-binder ratio 0.33 and superplastizicer 1% of binder volume. The core was covered with water soluble PVA film prior to the casting of the main body. This main body comprises of normal strength concrete as described in table 2.3. The production and curing of the PNC followed the procedure explained in subchapter 2.3.1. point d.

Ports of injection and outflow were cylindrical aluminium caps with $\text{Ø}55 - 20$ mm connected with M5 FESTO push-in fittings. These ports were glued to the prism specimen with PMMA based adhesives as depicted in figure 3.9.

5.4.3. Optimum solution

The same solution A, designed in subchapter 5.2.1. table 5.1, was used as healing agent. Meanwhile as it was found that the precipitate volume was too low in porous core test, the Ca-lactate was replaced by Ca-nitrate, $\text{Ca}(\text{NO}_3)_2$, in the solution B (see table 5.2) to provide more Calcium for the calcium carbonate precipitation. Ca-nitrate may be converted into Ca-carbonate in the *alkaliphilic* Bacillus micro-environment in the concrete matrix as depicted by equation 5.18.

Ca-nitrate is 15 times more soluble than Ca-lactate. As a result, for a given volume of solution much more calcium can be brought to the system when Ca-nitrate is used instead of Ca-lactate. The concentration of Ca-nitrate used is 2.21 mol.L^{-1} , therefore in the 2 mL solution B, a volume of CaCO_3 , V_{CaCO_3} , about 156 mm^3 can theoretically be produced. As the crack opening in the prisms was targeted about $300 - 350 \mu\text{m}$ which has a crack volume¹⁰, V_{crack} , of approximately $330 - 385 \text{ mm}^3$, the volume of solution injected in the PNC should be roughly 24 mL of solution A and 4.7 mL of solution B. This specific ratio was intended to obtain maximum production rate of CaCO_3 . The ratio used in the solution was rounded up to 25 mL solution A and 5 mL solution B.

5.4.4. Testing methods

In general, similar test procedure as described in preliminary program was performed. Three point bending was used to introduce crack in the main body and test the mechanical regain after healing. Leakage (permeability) test is used to assess the healing (crack-sealing) efficiency. Eventually, visual confirmation of crack closure is carried out by observing the prisms surface under light microscope and compare crack opening before and after healing. The general testing cycle followed the procedure described in subchapter 5.2.2, figure 5.5, 5.6 and 5.8. Initial permeability, see figure 5.27 (1), was intended to check the porous core water flow-ability where Darcy law may be used to determine the permeability index. Initial crack width in the prisms bottom side was achieved around $\pm 350 \mu\text{m}$ by closed loop strain controlled three point bending test, see figure 5.27 (2). The value was achieved by exerting load until the specimen achieve crack mouth opening up to $\pm 600 \mu\text{m}$ before load is removed.

Pre-healing leakage (permeability) test was employed to obtain permeability curve – outflow discharge over time. Later, the excess water in the porous core was drained out by pressurized air, $\pm 0.5 \text{ bar}$ for about 20 minutes. Following that the injection of 30 mL water into ‘control series’ and the solution A and then solution B into ‘bacteria series’ cracked specimens was implemented, see figure 5.28. The volume of water injected was determined based on the sum of volume solution A and solution B.

¹⁰ Crack was assumed to have wedge-like shape with crack height up to 40 mm. The volume, then, was calculated as $V = \frac{1}{2} (\text{crack opening} \times \text{crack height} \times \text{specimen weight})$.

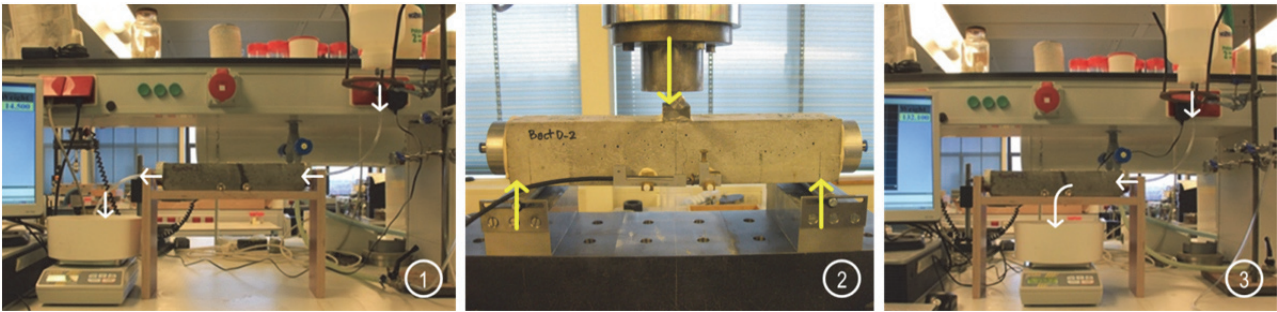


Figure 5.27. Testing procedure; [1] initial permeability test, [2] crack formation by three-point bending test, and [3] pre-healing permeability test of cracked specimen.

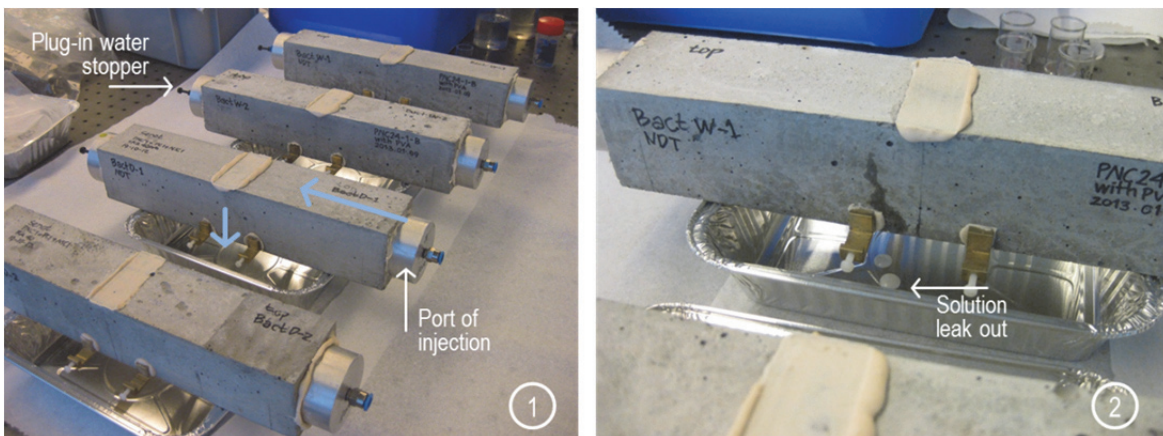


Figure 5.28. Injection of bacteria based repair solution; [1] specimens are prepared and [2] solution leaks out from crack opening.

Crack closure has been monitored before and 7, 14, 21, and 28 days after injection under stereomicroscope. 28 days post-healing permeability test, see figure 5.27 (3), was executed to measure permeability reduction. Eventually the specimens were tested mechanically using three-point bending setup to assess strength and stiffness regain.

5.4.5. Results and discussion

The leakage (permeability) test measures the weight of the water flowing out through the porous core or crack as a function of time. Figure 5.29 depicts the result of the leakage (permeability) test where the upper (linear) line is the initial permeability (Ctrl D-P0) and permeability of pre- (Ctrl D-P1) and post-healing (Ctrl D-P2) specimen, successively. It is obvious that the slope of the graphs become less steep from initial test to the specimen treated by tap water injection and curing. From these graphs it can be seen that the steeper the slope the more the water leaks out from the port of outflow (in initial permeability test) or through crack in PNC main body. Therefore comparing the slope of the graphs can provide insight in how efficient the PNC self-healing is.

The slope, following the general mathematical concept described in the figure 3.18, is determined by the procedure explained in the subchapter 3.4.2 equation 3.6. The

healing efficiency from leakage test, $SH_{leakage}$ is the ratio of slope of post-healing graph to the pre-healing as expressed in equation 3.7.

Crack sealing was observed due to the slope reduction of permeability curve of the post-healing specimen with tap water injection into the cracked specimen. This might be caused by several factors including the contraction and unloading of the rebar which may decrease crack opening and or autogeneous self-healing of the specimen, e.g. continued hydration, physical clogging. It can also be explained by swelling of the material at both sides of the crack wall due to water absorbed. However further investigation is required for in-depth analyses and assessment of the contribution of the aforementioned factors. It is also noticed that the complete healing was not achieved; i.e. no full crack-sealing was observed in the control specimen.

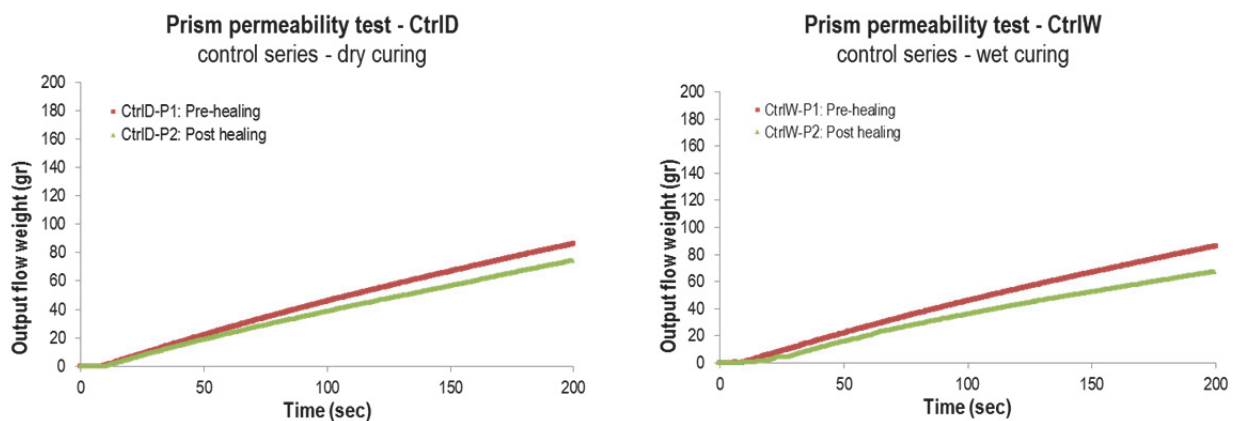


Figure 5.29. Graphic of output flow weight (water permeability) over time for control specimen

Very small cracks in the surface are found disappeared in the control series of the PNC specimen cured in the humid condition. This is visually confirmed in the figure 5.30 of the bottom surface of CtrlW specimen under direct observation with light microscope. Several tiny fissures branching out from the main flexural cracks detected under microscope in the first day after bending test were no longer exist. Continued hydration may be attributed as the most plausible cause as the PNC specimen is considered young concrete and the moisture from the ambient promote the on-going hydration process to occur. Meanwhile in the surface crack of CtrlD, specimen injected with tap water and dry cured, shown in the figure 5.30, the flexural crack pattern remained after 28 days from the bending test.

Figure 5.31 presents the graph of the leakage (permeability) test of the PNC specimen injected with bacteria-based repair solution with two different curing conditions; wet and dry curing. Similar to the previous graph (control specimen), the initial permeability graph exhibits the steepest slope followed by pre- and post-healing graph. The slope of the post-healing graph has value of zero (100 % permeability reduction) which indicates there was no water leakage from the porous core through the crack. This phenomenon has not been observed in the control specimen. This implies that the crack was sealed probably by mineral deposit mediated by bacteria. However, as it is with the control specimen, factors like rebar contraction and unloading and autogeneous healing may also contribute to the crack healing process.

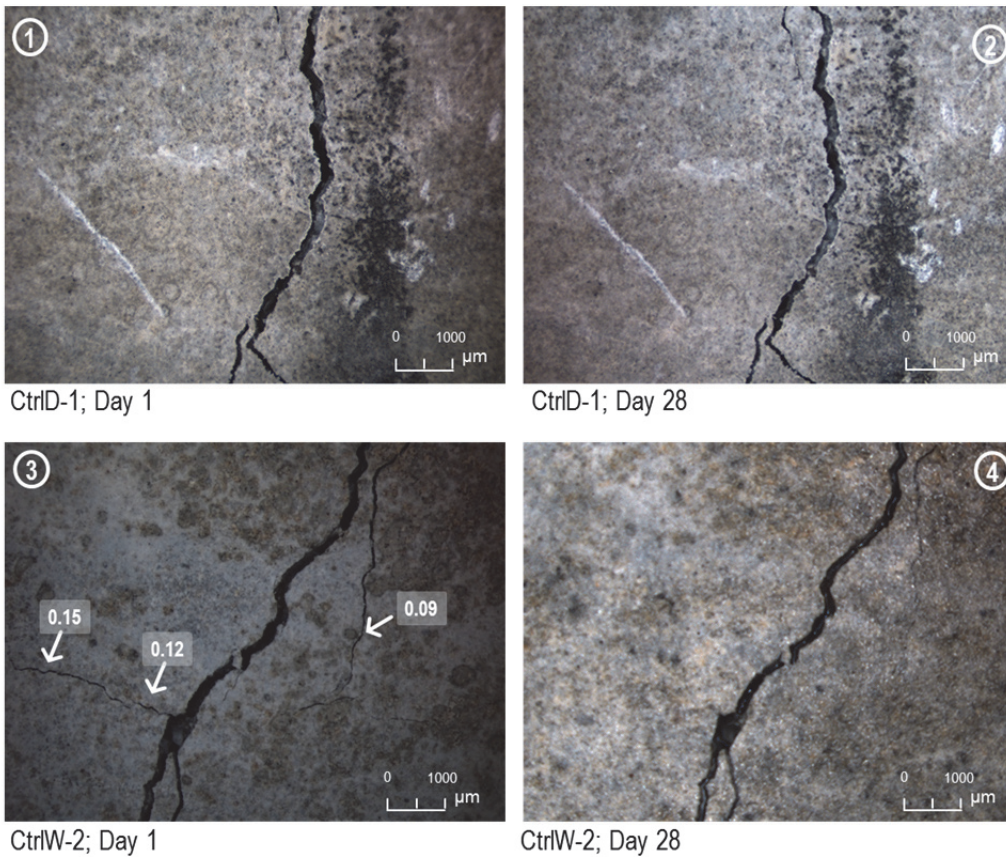


Figure 5.30. Bottom surface flexural crack of the control PNC specimen (1) injected with tap water at day 1 and (2) after dry cured for 28 days. (3) Small fissures (arrow) of control specimen at day 1 after bending test are undetected after 28 days curing the humid environment (4).

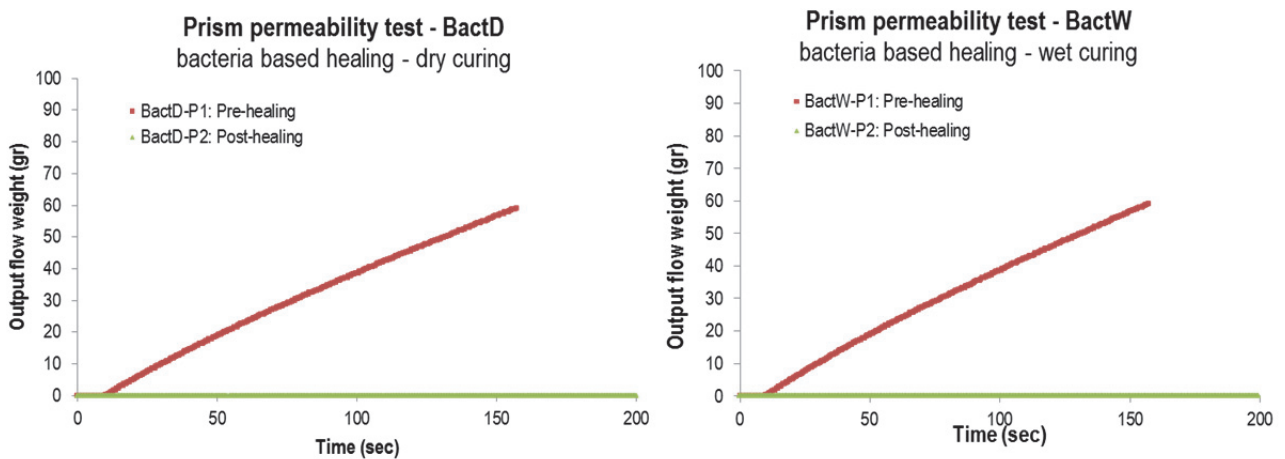


Figure 5.31. Graphic of output flow weight (water permeability) over time for specimen treated by bacteria-based solution injection

Direct observation of the flexural crack in the bottom surface of the PNC prisms under stereomicroscope reveals some interesting result, as can be seen in the figure 5.32. Specimen injected with bacteria-based repair solution and then dry-cured shows some whitish material deposited in the crack opening face. Figure 5.32 frame 1

shows the flexural crack at the first day after bending test and frame 2 depicts the crack in the specimen at 28 days at similar spot. The specimen in the frame 3 figure 5.32 shows significant larger crack opening next to the edge and cavity in the first day after bending test. After injection and wet curing for 28 days, however massive precipitation of mineral has clogged the location of crack. Supported by the previous test result it is most probably the mineral is Ca-based mineral formed due to metabolic activity of the bacteria.

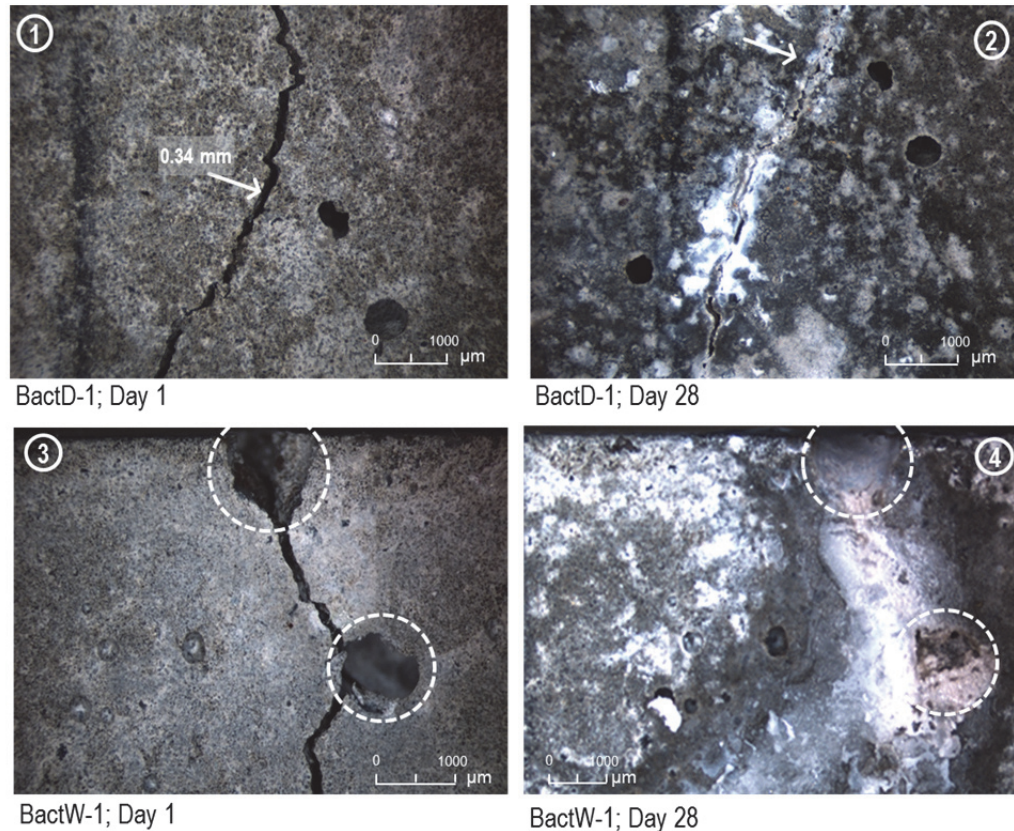


Figure 5.32. Bottom surface flexural crack of the PNC specimen injected with bacteria-based solution (1) at day 1 and (2) after dry cured for 28 days. (3) Significant void (dotted circle) of control specimen at day 1 after bending test were sealed after 28 days curing the humid environment (4).

The first strain controlled three-point bending test was employed for crack formation. The test followed the same setup and procedure explained in the subchapter 3.3.2 and described in the figure 3.13. However, the injection of the bacteria-based solution was carried out manually with syringe, see figure 5.28. The second loading with the similar strain rate carried out at 28 days after injection and curing has been utilized to assess how effective the healing is for regaining the PNC strength and stiffness.

Typical load (kN) versus crack mouth opening displacement (CMOD, µm) resulted from the test comprises of two loading-unloading cycle. Comparing the mechanical properties from the first and the second loading curve will reveal the efficiency of the healing process in term of strength and stiffness. In short, the efficiency is determined by the strength and stiffness ratio explained in the subchapter 3.4.1.

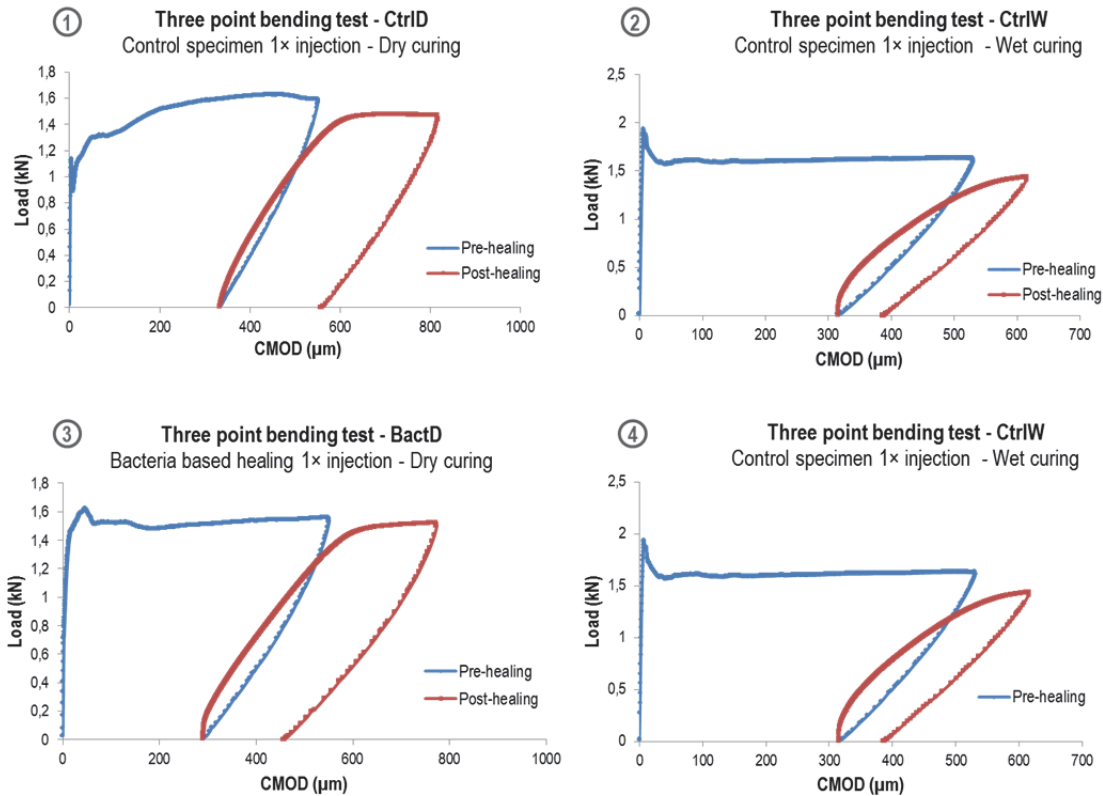


Figure 5.33. Graphic load versus crack mouth opening displacement (CMOD, μm) after three-point bending test

Figure 5.33 shows the load versus CMOD of the specimen treated with water and bacteria –based healing agent and curing regime. The graphs, however, reveal a similar behavior for all specimens. The first loading cycle exhibits the specimen peak load between 1.2 to 1.9 kN with high stiffness as the curve is almost vertical. The stiffness of healed state of all specimens show no significant regain indicated by the slope of the secant line of the reloading graphs which is lower than the virgin specimen. As it was observed during preliminary test, the mineral deposited in the fracture site provide no ‘binding’ action for the crack face therefore no additional strength and stiffness regained. Further investigation is required to study the adhesion of this bio-mineral with the concrete substrate.

Table 5.5. Recapitulation of the PNC prisms healing efficiency test result

Specimen code	Condition	Healing efficiency (%)		
		Permeability reduction	Strength recovery	Stiffness recovery
BactD	Dry; T $\pm 20^\circ\text{C}$; RH $\pm 30\%$	100	86.6	18.9
BactW	Wet; T $\pm 20^\circ\text{C}$; RH $\pm 95\%$	100	89.3	23.8
CtrlD	Dry; T $\pm 20^\circ\text{C}$; RH $\pm 30\%$	77.4	80.4	18.4
CtrlW	Wet; T $\pm 20^\circ\text{C}$; RH $\pm 95\%$	81.9	85.3	16.5

Table 5.5 summarizes the results of the test. The PNC injected by bacteria-based healing agent reduces completely its leakage due to flexural crack showing permeability reduction of 100%. Meanwhile only partial reductions have been observed in the specimen with tap water injection. On the other hand no complete

strength and stiffness recovery is monitored in the system. The strength and stiffness after second loading may be explained due to the rebar which carry the flexural stress since the crack is reopened.

On the other hand no complete strength and stiffness recovery is monitored in the system regardless of the healing agent type. It is clear that these mechanical properties recovery value do not reach the complete healing line in the histogram.

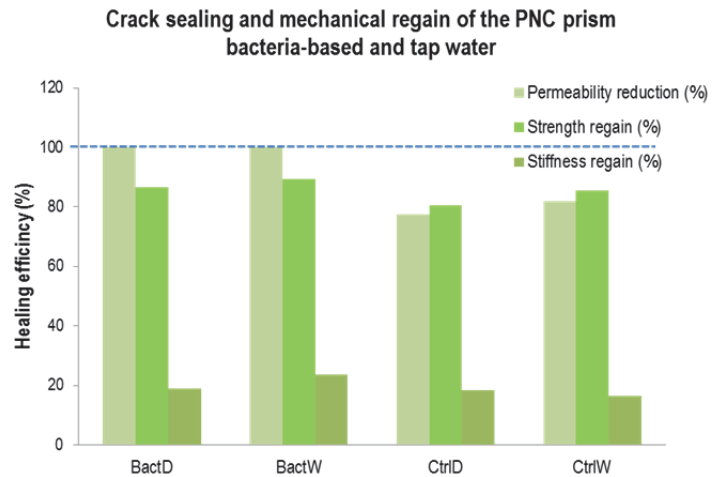


Figure 5.34. Histogram of the bacteria-based healing efficiency test in the PNC prism

Polished sections were prepared for the specimen with crack reopened at 28 days to observe the mineral deposited in the crack wall. Figure 5.35 shows the images taken by ESEM.

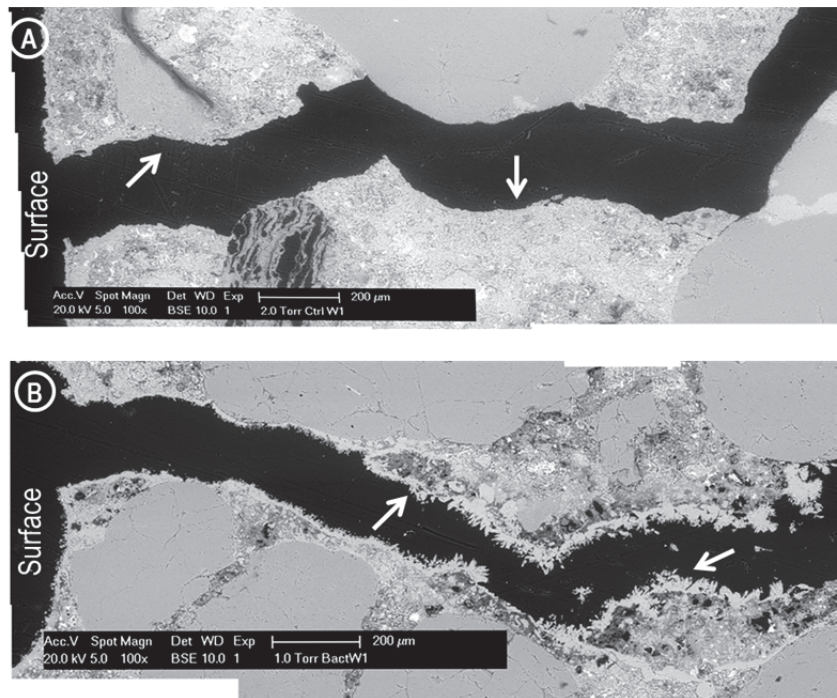


Figure 5.35. ESEM images of the crack reopened: (A) control series shows no mineral deposition in the crack wall while (B) Ca-based mineral, most probably due to bacteria metabolism, deposited on the crack wall.

The images of the crack reopening exhibit a clear difference between the crack wall of control specimen and bacteria-based specimen. For control specimen the crack walls shows no mineral deposition while in the bacteria based specimen substantial amount of bio-mineral deposited in the crack. As supported by the previous test (test 1 and 2), the mineral deposit was apparently caused by the metabolism of Alkaliphilic bacteria from bacteria based repair system injected into the porous core. This deposition sealed the crack and prevented the water leakage which in agreement with the result of permeability (leakage) test.

5.4.6. Findings

Based on the ESEM observations and results of test 2, the crack sealing of the PNC injected with the bacteria-based solution can be attributed to Ca-based mineral precipitation most probably mediated by bacteria activity. Even though mechanical regain in term of strength and stiffness of bacteria-based post-healing beam is quite limited or not present at all, crack sealing works effectively and liquid tightness may be assured.

5.5. Conclusion of healing efficiency of the PNC prims by means of bacteria

Healing process designed for crack in the concrete may yield in the total or partial recovery of the concrete properties. It may reduce leakage or permeability and/or recover mechanical strength and stiffness. The RILEM state-of-the-art Report on Self-Healing Phenomena in Cement-Based Materials (IC 221-SHC) categorizes this healing phenomena into two classes; recovery against environmental action and recovery against mechanical actions [89].

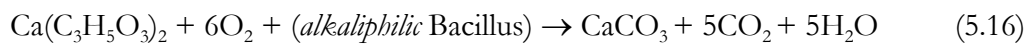
To recover its environmental resistance, many self-healing concrete methods are designed and developed with intention to 'seal the crack' therefore enhance concrete resistance to easy ingress of deleterious substance from its exterior environment. The results of the various tests in this study exhibit the bacteria-based healing is efficient to seal the crack even though quite unlikely to recover concrete mechanical properties.

Self-healing which recovers the earlier concrete performance disruption may be caused by autogeneous action where concrete inherent material perform the recovery or by autonomous action [89]. Autogeneous healing of concrete has been reported in the published studies caused by several mechanism; e.g. on-going hydration, swelling of hydration product, precipitation of calcium carbonate in the carbonation, and particle clogging in through-crack. In the PNC prism this autogenous self-healing capacity was observed when the small cracks up to 150 μm were closed and no longer detected in the surface of the control specimen cured in the humid condition. The relaxation of the rebar present in the concrete prism provides confinement to the matrix and retains the surface crack narrow. The presence of moisture in the environment promotes the further hydration of un-hydrated cement particles. This similar to the information found in the literature where autogeneous healing may be allocated to the continued hydration or carbonate precipitates in the main body [89, 97, 114, 237, 238].

Improved crack healing capacity may be obtained by autonomous healing strategy [86, 89]. Embedding bacteria able to induce mineral precipitation is one of the promising techniques. One important spin off is bacteria-based liquid repair system utilized in this study as healing agent. The injected three integrated component solution, consisting a viable alkaliphilic bacteria spore, nutrient and transport solution (Na-silicate based) into the porous core promotes massive precipitation of bio-minerals [147].

Studying the morphology of the precipitates from the test 2 with ESEM, it was found globular (figure 5.19 and 5.22) mineral layer deposited in the ‘cavity area’ between concrete matrix and the epoxy resin where the nutrient was present and dissolved, leaving a cavity. Different morphologies and Ca-carbonate polymorphs have been observed and are presented in published studies [114, 239-241]. Wiktor and Jonkers [114] reported 3D deformed rhombohedra of a mixture of Ca-carbonate polymorph mediated by bacteria immobilized in the expanded clay. This was similar to the morphology of calcite crystals formed facilitated by bacteria in soils reported by Lian et al [240] or vaterite in the porous ornamental limestone reported by Rodriguez-Navarro et al [239], the type of crystal shape and texture that is not found in this study.

A strong indication of the bacterially induced precipitation process has been found with the observation of *bacteria imprints*, the self-entombed bacteria within the layer of minerals, see figure 5.22 and 5.23. According to FT-IR and EDS analysis, the mineral deposited in the porous concrete core is calcium carbonate and most probably formed due to the active metabolism of the alkaliphilic bacteria based on the chemical equation 5.16.



As Ca-hydroxide may be present in the concrete matrix and carbonate ions, $[\text{CO}_3^{2-}]$, may be obtained from conversion of respiration product, CO_2 , in supersaturated solutions, the *carbonation* reaction may yield to even more Ca-carbonate molecules [235].

In this way bacteria intensify the precipitation of carbonate precipitation through [114, 235]; (i) metabolic conversion of nutrient promoting supersaturated solution where dissolved inorganic carbon pool provides more carbonate ions and (ii) serving itself as nucleation site where Ca-carbonate crystals grows, see figure 5.2 subchapter 5.2.2.

An issue, however, emerged that the bacteria functioned as intended the amount of the Ca-carbonate precipitated inadequate to provide complete porosity filling of the porous core. Therefore Ca-nitrate was utilized for Ca-source for the bacteria-based solution injected into PNC prism.

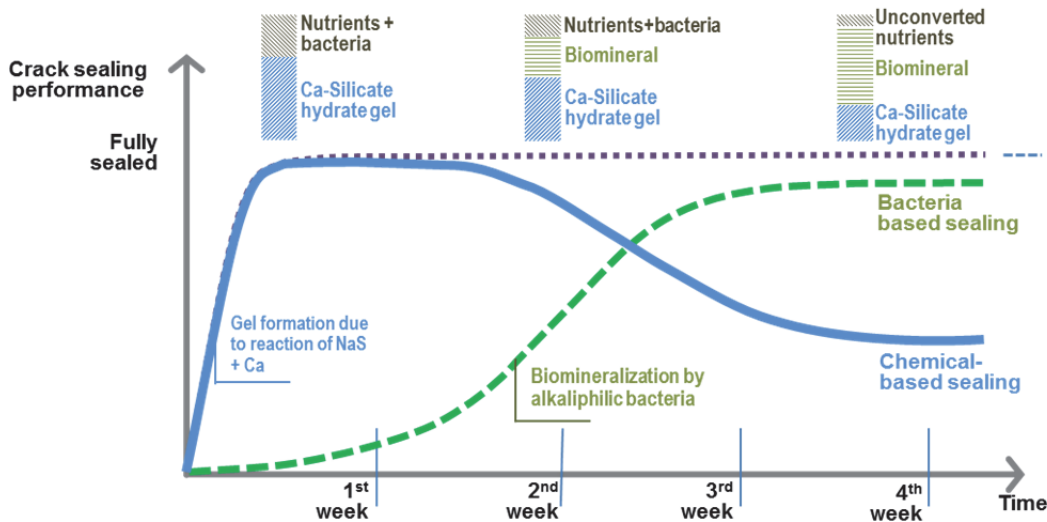


Figure 5.36. Diagram of the crack sealing performance over time by means of bacteria based repair solution into Porous Network Concrete.

It is hypothesized that the sealing performance over time may be caused by two mechanisms in the different time phase. Figure 5.36 provides a general insight on how chemical-based sealing and bio-based sealing mechanisms play their mutual role in the crack healing of Porous Network Concrete. After injection of bacteria based repair system gel formation – *Ca-Silicate hydrates* – due to reaction of Na-silicate and Calcium is immediately formed upon mixing solution A and solution B. This dominates the sealing mechanism in the early phase (hours). The substantial amount of gel formed might be beneficial in clogging the crack in concrete matrix and entrapping Ca-source while the bacteria becoming metabolically active. The slow biologically induced mineralization process is started when alkaliphilic *Bacillus* consume nutrients. The by-product of this metabolism is carbon dioxide and alteration of bacteria micro-environment accumulating Ca-based mineral precipitates.

Meanwhile, in second phase (week), the amount of the gel is decreasing due to the gel restructuring and drying shrinkage. On the other hand biomineral is accumulated as bacteria grow and consume more nutrients until no more food or no more space to grow. In this case bacteria entomb themselves under the CaCO_3 mineral and bacteria imprint is the legacy and have been captured under ESEM. At the final phase, it may be deduced from the test 2 results that the end product is Si-based compound, Ca-based mineral and unconverted food.

It is believed this diagram may also be generalized for bacteria based repair solution application in concrete.

A setup was designed making it possible to introduce crack and to test the permeability or water leakage in the Porous Network Concrete healed specimen. This facilitates a direct observation of permeability to healing capacity which indeed shows that specimen injected with bacteria-based solution demonstrates complete crack sealing. As supported by ESEM/EDS and FTIR proofing bacterial activity and combined with the visual crack filling by mineral deposition observation, it is conclusive that liquid tightness may be assured in the bacteria-based specimen.

The novel development of bacteria-based solution, indeed improved the autogeneous self-healing capacity which can seal cracks by filling it with Ca-based mineral layers. However, it was not found in the present study complete recovery of strength and stiffness.

This page is intentionally left blank

6.

Conclusion and outlook

We are at the very beginning of time for the human race. It is not unreasonable that we grapple with problems. But there are tens of thousands of years in the future. Our responsibility is to do what we can, learn what we can, improve the solutions, and pass them on'

- Richard Feynman

"I don't like the word 'futurist'. I think we should be now-ists. Focus on being connected, always learning, fully aware and super present."

- Joi Ito

The self-healing concrete by means of the Porous Network Concrete, taking inspiration from bone healing process, has been demonstrated to be effective in this thesis. It also has been construed from experiments that the different classes of healing agent are capable to seal and heal crack in the PNC main body; chemical based agents, cementitious grout and uniquely developed bacteria-based solution. This chapter remarks the work done in the previous chapters by providing the conclusion, discussing the speculation of the upscaling to application, and the improvement that may be taken.

6.1. Fundamental approach

One promising concept to design new concrete structures to achieve higher durability is incorporating self-healing mechanism found in nature into cement-based materials / concrete structural element. If unavoidable cracks due to inherent brittleness in concrete could be self- sealed/healed/repared, concrete will certainly serve longer, more durable and sustainable.

Klaas van Breugel posed a question, "Is there a *market* for self-healing cement based materials?" during the First International Conference on Self-Healing Materials held in the Netherlands, 2007. This question arguably is fundamental in assessing the likelihood of self-healing implementation in the near future. Up to the moment this thesis is conducted, the market, *construction industry*, has already recognized the self-healing concrete proof of concept at the laboratory scale and is waiting for the practical implementation in real situation. On the other hand, starting with *fundamental research* – the level this work was conducted – allows the exploration of different concepts, approaches, and possibilities of self-healing concrete. This in turn will provide sound basis to development and diffusion of this innovative technology to the industry and public.

Concrete possesses capacity to heal its own small fissures and cracks, *autogeneous healing*, which may consist of several mechanisms. Many studies have been conducted to improve this inherent beneficial feature. However, many cases concrete cracks might require a different approach of *autonomous healing*. Examples of such cases are (i) crack width larger than what is allowed, or (ii) the need of rapid large crack sealing in hazardous leakage. This thesis started with the problem of preventing leakage and securing liquid tightness therefore enhancing concrete durability. The self-healing has been designed to be autonomous by means of Porous Network Concrete with three type of feasible healing agent; e.g. *crack self-sealing making it impenetrable for fluid*.

6.2. Design and Performance of Porous Network Concrete

6.2.1. Porous Network Concrete

It has been demonstrated that the Porous Network Concrete proposed and designed in this work has a good prospect for making concrete structural elements self-healing. It is a hybrid system – comprising of two parts, *the prefabricated porous core* and *the main body* – in which highly permeable porous (*pervious*) concrete is embedded in the interior or exterior of normal dense concrete, taking inspiration of bone morphology. The porous network core provides easy means for transporting temporary or permanent materials to form a dense layer in the later stage and distributing healing agent from point of injection to cracks in the concrete main body. Furthermore the porous core can be placed in the region prone to cracking. The main body provides strength and stiffness for structural applications. This deliberate design and choice of material will *increase the survivability and compatibility of the core as transport medium* during concrete structure (in-situ or prefabricated) casting.

The production process – *the making of the PNC* – follows the current standard for both of the main and porous part. To some extent, the cross section of the porous core may not be large compared to the overall structural element size which in turn the overall element strength and stiffness properties will not be hampered. Depending on the application, the material quality and structural component geometry can be fine-tuned to obtain the required level of strength and stiffness. For instance, the overall structural strength can be increased simply by using higher material strength of the concrete main body.

The use of PVA film for covering the porous core during concrete casting ensures that the core stays porous and able to be used for infusing fluid through its interconnected pores. However without PVA film, the porous core still functions as it is intended provided the pore diameter used is small enough for fresh concrete matrix not to penetrate and clog into the voids during casting. Without PVA a slight reduction of porous core total porosity is observed which does not influence the intended goal.

Bearing in mind the initial aim of the Porous Network Concrete development, which is mainly to prevent leakage and enhance concrete durability, the initial and pre healing cracked specimen permeability (leakage) test was implemented. The initial permeability tests of all specimens show roughly equal values of permeability. Intrinsic permeability coefficients (following Darcy law) determined on the porous cores show that all mixtures used for the pores cores are in the *pervious regime*.

Therefore all PNC specimens satisfactorily fulfil the criteria having a porous core as media to transfer healing agent into the place where the crack in the main body occurs.

The pre-healing permeability slope of cracked specimen also revealed that water can flow through the crack in the main body (the concrete specimen). This condition implies that the crack is leaking and thus liquid tightness was no longer guaranteed.

The *autonomous* feature of the concept has been realized by designing a feedback mechanism employing simple closed-loop on-off control. The proof-of-concept has been designed by integrating several components; deformation in *concrete* specimen was detected by *sensors* (LVDT) which in turn send *signals* into a *controller* which then transfers a trigger signal to an *actuator* to pump in healing agent into the cracked region in the right time. It has been proven to operate well.

6.2.2. Healing efficiency upon different healing agent

Even though the influence of the viscosity of the healing agent has not been studied in this work, it is believed that Porous Network Concrete can be automatically injected with low viscosity liquid healing agent. Employing what is already available in the state-of-the-art healing agents, three groups of healing agents were studied; chemical-based, cementitious grout and bacteria-based. Two compound epoxy resin and cement grout (slurry) was used. The bacteria based method makes use of a – *bacteria-based repair solution* – that was uniquely developed in Microlab TU Delft with the intention to use it for repair of aged concrete.

a. Polymer and cement based healing agent

Due to its low viscosity, epoxy resin can flow and penetrate into the micro-voids in the PNC. The epoxy as adhesive repair agent – cured in ambient environment in the order of hours – fills in the crack void and binds the crack face. This low viscosity is beneficial in the healing and repair process since it leaves no empty space that may become a weaker spot and hamper post-healing durability and structural integrity.

It was observed that the cement grout cannot reach smaller voids. Clogging of cementitious grout was observed in the specimen with porous core made of aggregate with diameter of 2-4 mm. This might be attributed to the viscosity of the cement grout which was rather high. However, healing occurred in the specimen P48-1-B, which was manually injected with cement grout. The specimen has a porous core made of aggregate with diameter of 4-8 mm which results in a larger pore network diameter approximately 0.5 – 3 mm.

The post-healing slopes of permeability line of every healed specimen with epoxy and cement grout were zero. The value of *sealing* efficiency reaches 100% for all the specimen and healing agent. Based on this, the leakage is prevented completely and liquid tightness is ensured. Moreover the dense layer of epoxy and grout may also provide a barrier for the ingress of deleterious substance into the interior layer of concrete.

Confirmed by visual observation on a cut-open specimen, the healing events were successful in every specimen, either manually or automatically injected by epoxy, and specimen manually injected with cement grout.

The hardened epoxy resin and cement grout in the crack zone seal and glue the crack faces which show a tendency to recover strength and stiffness of the healed specimen. The hardened epoxy in the porous core most likely not only recover but also increase specimen strength. In the tests, however, the size of the core was rather big compared to the cross section of the specimen. In practical applications this will not be the case and the effect of this extra reinforcement might be neglectable. As the healing agent solidified, the cross section of what was previously partially hollow became a whole and able to provide larger moment of resistance against the external loading. In this view, the healing mechanism by means of PNC is achieved.

b. Bacteria based repair solution

The bacteria-based repair solution comprises of three integrated component solution; a viable alkaliphilic bacteria spore (e.g. genus *bacillus*), nutrient (e.g. Ca-salt, Na-gluconate) and transport solution (e.g. Na-silicate based). The impregnation test of the solution into porous core shows the mineral deposited is calcium carbonate and most probably formed due to the active metabolism of the alkaliphilic bacteria.

As free calcium ion may be present in the concrete matrix and carbonate ions may be obtained from conversion of respiration product in supersaturated solutions, the *carbonation* reaction may yield to even more Ca-carbonate molecules. In this way bacteria intensify the precipitation of carbonate precipitation through [114, 235]; (i) metabolic conversion of nutrient promoting supersaturated solution where dissolved inorganic carbon pool provides more carbonate ions and (ii) serving itself as nucleation site where Ca-carbonate crystals grows. A strong indication of the bacterially induced precipitation process has been found with the observation of *bacteria imprints*, the self-entombed bacteria within the layer of minerals.

An issue, however, emerged that even the bacteria functioned as intended, the amount of the Ca-carbonate precipitated is inadequate to provide complete porosity filling of the porous core. As Ca-nitrate is 15 times more soluble than Ca-lactate, therefore, for a given volume of solution much more calcium can be brought to the system when Ca-nitrate is used instead of Ca-lactate. This is the reason Ca-nitrate was utilized for Ca-source for the bacteria-based repair solution injected into PNC prism.

Two complimentary mechanisms in different time phase is believed to occur in the healing event based on bacteria based repair solution. Firstly, *Ca-Silicate hydrates* gel – product of Na-silicate and Calcium – is formed immediately after the solution A and solution B is mixed or layered in the porous core and crack face. The advantage is that the gel formation fills the void and entraps the Calcium source which will be used later by the bacterial community. The biologically induced mineralization process begins at the moment bacteria consume the nutrients. Their respiration product is carbon dioxide which in the supersaturated environment turns into carbonate anions. These ions then react with calcium cations present in the system, e.g. solution and concrete matrix accumulating Ca-based mineral precipitates.

Secondly, the gel formation is decreasing presumably during the second week. This process may be caused by the gel shrinkage and restructuration. As it is aforementioned, accumulation of biomineral rise when bacteria consume more food to grow up to the condition where there is no more space to grow or there is no more food. Kinetic of the process may be deduced from the observation that it may start at slow rate and then at higher rate until bacteria entombed in the CaCO_3 mineral. From this research it was found that bacteria imprints can be observed under ESEM. At the final phase, it may be deduced that the end product is Si-based compound, Ca-based mineral and unconverted food.

The permeability or water leakage in the Porous Network Concrete healed specimen with bacteria-based solution demonstrates complete crack sealing by mineral deposition.

The novel development of bacteria-based repair solution, indeed improved the autogeneous self-healing capacity which can seal cracks by filling it with Ca-based mineral layers. The presence of alkaliphilic bacteria is essential in the system converting food into Ca-based precipitates. A humid curing regime promotes the bacteria based self-healing.

However, it was not found in the present study that there is the complete strength and stiffness regain. Even though mechanical regain in term of strength and stiffness of bacteria-based post-healing beam is quite limited, crack sealing works effectively and liquid tightness may be assured.

6.3. What we need to improve: outlook

The Porous Network Concrete has been developed, tested in the lab scale and proven to be self-healing effectively. The PNC production method for lab scale specimen turned out not to be complicated and can be up-scaled. The liquid healing agent may be chosen from a wide variety of commonly available healing agents in the market. The benefit of PNC is that the concrete is compatible with the cement grout/slurry and that the injection takes place from the inside out.

A larger scale experimental campaign and specimen such as PNC wall with constant pressure of water may be used to test the performance of the system in the more real situation. Another experimental set may involve constant cyclic loading. Moisture friendly and fast rate polymerization resin may be utilized in this case. This will allow researcher to tackle problem of leakage in the (hazardous) liquid container or underground tunnel with combined environmental and mechanical loads. This testing situation may generate a lot of data, information and knowledge to improve the PNC performance.

Numerical modelling of the Porous Network Concrete – *fracture process coupled with healing agent flow and hardening simulation* from the point of injection through porous core into crack zone – is required to study the healing behaviour and optimize the system. This model will allow researchers to determine how parameters, e.g. liquid viscosity, pores network properties, and chemical species of the healing agent may interact, seal, and heal the crack.

One interesting aspect in the implementation self-healing concrete by means of the Porous Network Concrete is the detection and localization of the most likely random orientation and occurrence of crack in the large structural component, e.g. basement wall, bridge beam, etc. Several methods and algorithms have been devised that may be implemented to provide the feedback system with damage data. The data is then used to inform the controller to the healing action. The autonomous system may be implemented using embedded cheap open-hardware one card microcontroller with wireless data communication among devices. Embedded sensors, e.g. fibre optic, cement based piezoelectric strain sensor, may be exploited in the next development phase.

Appendix 1

Development of automatic on-off control system

'Appendix usually means "small outgrowth from large intestine," but in this case it means "additional information accompanying main text." Or are those really the same things? Think carefully before you insult this book.'

- Pseudonymous Bosch, The Name of This Book Is Secret

This appendix explains in detail the design and prototyping of the on-off control mechanism for autonomous injecting healing agent.

A.1. Automatic repair system; design and prototyping

a. Mechanical injector

Despite the commercially available industrial standard injection pump and dispensing machine, it was thought that simple automatic injector can be custom built. Medical syringes with plunger inside the cylindrical tube may be used as the pump. A static mixing nozzle may also be used to mix low viscosity two compound agents which pump out from two syringes. The injector can be seen in figure A.1.

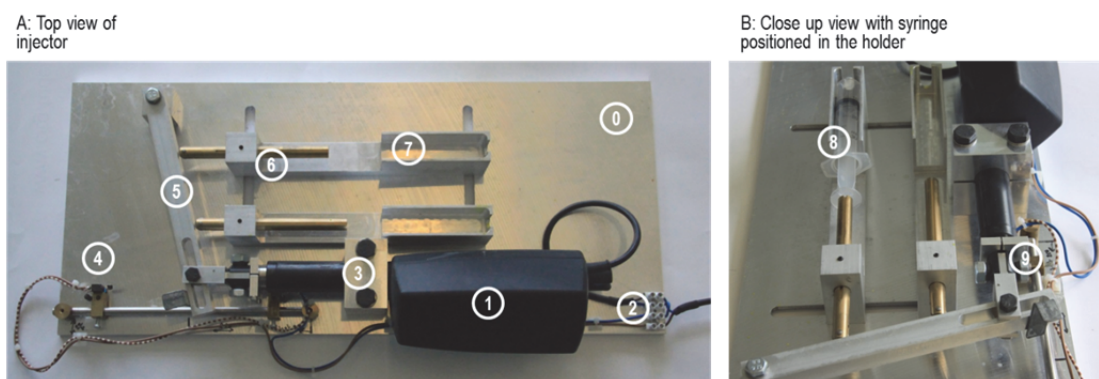


Figure A.1. Custom built on top of aluminium plate (0), the automatic injector is used to pump healing agent through porous core in the PNC. It comprises of linear actuator (1) which speed can be controlled by voltage (2). This motor is clamped onto the plate (3) with safety relay (4 & 9) and pull lever arm (5). In turn, this lever arm will push two piston (6) and syringe (7 & 8).

The basic working mechanism is to transfer motorized linear movement into two linear pistons. The components of injector are mounted on top an aluminium plate. A linear actuator, a device that converts the rotational motion of a low voltage DC motor into linear motion by means of a motor, a gear and a spindle, see figure 3.4.a (1). produces a linear movement (push and pull). The advantages of electric actuator over e.g. hydraulic / pneumatic systems are easy installation, pumps or hoses are unnecessary, therefore takes up much less space. A LINAK[®] electric linear actuator 24 V DC was used and clamped (element 3 in the figure 3.4.a.) onto the aluminium baseplate. Next to it a steel rod was installed as guard rail with a relay (4 & 9) which switches of the machine when the actuator touches it. These relays act as electric fuse and provide boundary and safety to the motor.

Linear motion provided by actuator is then transferred into two pistons (6) by means of lever arm (5). These two pistons push the plunger of the syringes (8) which are put in the holder (7).

The position of these parallel pistons on the base plate can be adjusted in order to obtain required proportion of the two compound (e.g. epoxy and hardener) healing agent.

b. 'The box'; motor controller and data acquisition system

The movement of the linear actuator is controlled by 'the box', illustrated in the figure A.2. This device, see figure 3.5.1., consist of; (i) a custom built electronic circuit for controlling motor and (ii) NI 6211 Data Acquisition (DAQ) card from National Instruments for 'reading' sensors input signal and 'producing' output analogue and digital signal. Technically the hardware processes the sampling signals (*kilo samples per second*) from the physical world; i.e. voltage, and converts it into digital numeric values that later can be manipulated in the computer. NI 6211 has aggregate sampling rate of 250 kS/s.

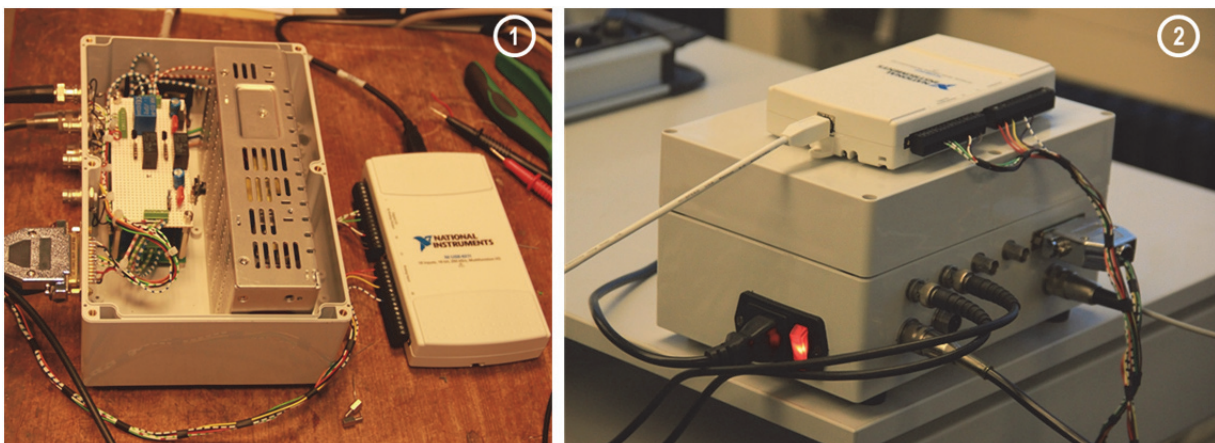


Figure A.2. 'The box' is used to regulate the actuator by sending voltage signal. Figure (1) shows the interior of the box comprising of powers supply system and electronic circuit which controls the motor speed. NI 6211 Data Acquisition is employed to acquire signal from sensors, communicate with PC, and send digital (0 or 1) output signal used to switch on or off the motor.

In general the working principle of ‘the box’ can be described briefly based on the diagram in figure A.3. In the electronic circuit, a power transformer transforms 230 V AC into 24 V DC which then supplied into motor controller coupled with directional controller – a device with on-off switches. The speed of the motor (M) is controlled by the voltage signal sent from one analogue output (AO) channel in the NI 6211 DAQ card. Meanwhile two digital output (DiO) channel form the DAQ card send digital signal; 0 means motor off (standing still) and 1 means motor on and run in one direction left (L) or right (R). This motor then produces linear motion required to push piston and pump the healing agent in the syringe.

On the other hand, LVDT (*linear variable displacement transducer/transformer*) transform linear motion of the needle-like armature inside the coil into a voltage signal. This voltage is then amplified and conditioned in the signal conditioner and send into analogue input (AI) of the card. Pressure sensor converts pressure into voltage connected to analogue input (AI) of the card. These signals are essential in determining the crack opening in the concrete and pressure built up in the core. Two LVDTs and one pressure sensor was used occupying three analogue input channel in the NI 6211 DAQ.

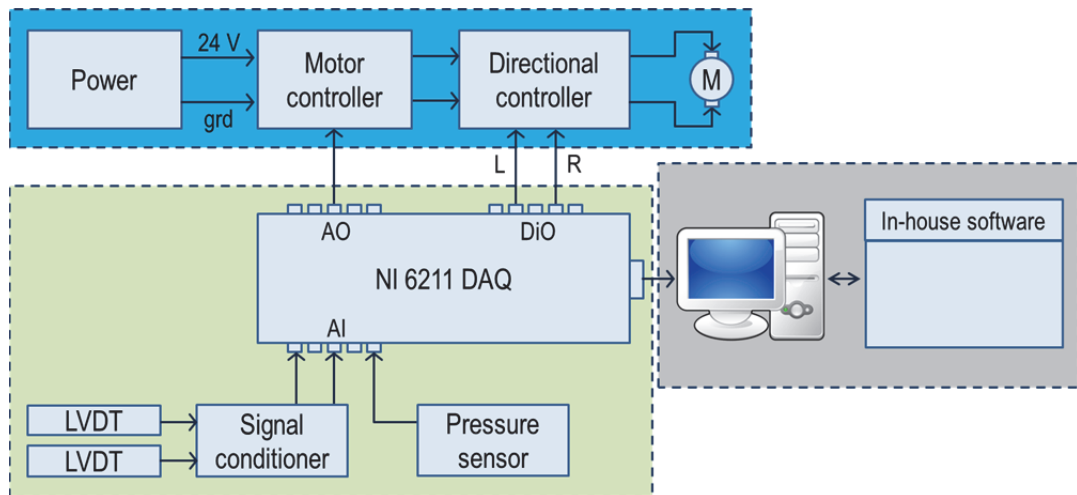


Figure A.3. Block diagram showing the flow of electronic signal in the system.

c. The software measurement system

In the signal processing block, NI 6211 DAQ is connected to the computer via *computer bus* – USB – with the NI device *driver* installed allowing the PC to access the hardware and enable these two devices to communicate with each other. In the PC, an in-house measurement system application (MP3) is installed having interface recognizing the card signal with the sampling rate specified at 1 kS/s in order to filter out noise; i.e. spike in the signal. The system is illustrated in the figure A.4.

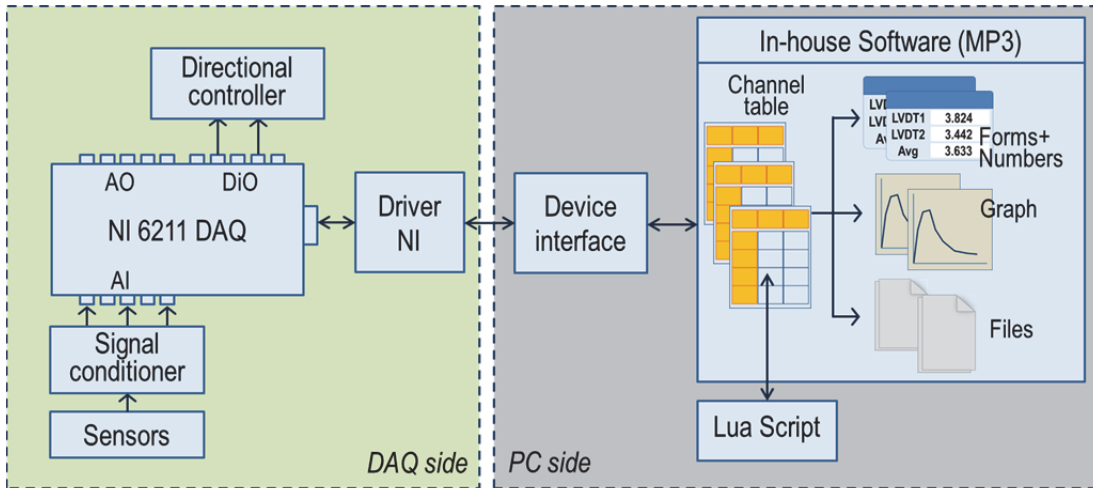


Figure A.4. Block diagram showing the communication between data acquisition (DAQ) system and measurement software where a Lua Script is implemented to ‘read’ signal and ‘decide’ the action according to the predetermined ‘rule’.

Central to the *measurement system application* (MP3) software is the channel table that records the signals from every device connected. These records then can be conveniently converted into forms and numbers, graphs, and spreadsheet files to be processed later on. In this application the user can define sampling data rate, usually at the lower rate, independent of the sampling rate from the device. A script, see figure 3.7., can be written and embedded in the software requesting it to do specific tasks and add some functionalities to the MP3 software; e.g. to access hardware, to generate signal function, etc.

d. The control rule and its implementation

In order to control the injector automatically, a simple (positive) feedback was implemented creating switching behaviour [242]. The concept is that the system output maintains its given state as far as input signal crosses a threshold value. Due to its simplicity, an on-off control was employed described in the equation A.1.

$$u = \begin{cases} u_{\max} & \rightarrow e > 0 \\ u_{\min} & \rightarrow e < 0 \end{cases} \quad (\text{A.1})$$

$$e = r - y$$

Where the e is the control error, r is the reference signal and y is the output of the system, meanwhile u is the command of actuation or action taken. The representation of an ideal on-off signal with its modification can be seen in the figure A.5.a-c.

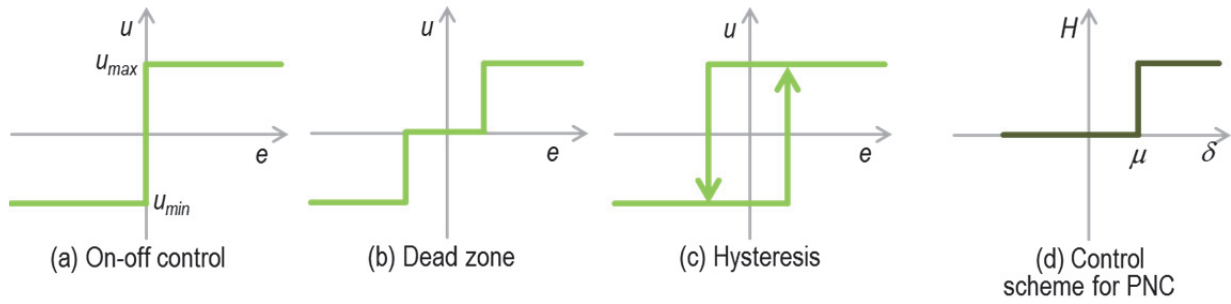


Figure A.5. Representation of on-off controller input-output feature. Figure (a) shows an ideal on-off controllers base on equation 3.1, while a modification of dead zone (b) or hysteresis (c) may also be implemented.

Implementing the switching behaviour, two events are defined for the control rule in this work, as expressed mathematically by equation A.2 and illustrated in the figure 3.8.d.

$$H = \begin{cases} 0 \rightarrow 0 < \delta \leq \mu \\ 1 \rightarrow \delta > \mu \end{cases} \quad (\text{A.2})$$

Where H is the state of action taken by injector; 0 means machine off and 1 means machine on into one direction, δ represent the crack opening of the concrete structure, and μ is the pre-set value (threshold). This expression may be thought as follows; while the displacement value recorded as crack opening (δ) in the channel table is above zero but less than or equal to certain predetermined value (μ), the script generate state 0. This is translated by DAQ card as 0 into the directional controller. Or else if the crack signal value in the channel table (δ) is larger than parameter value, μ , the state 1 is generated.

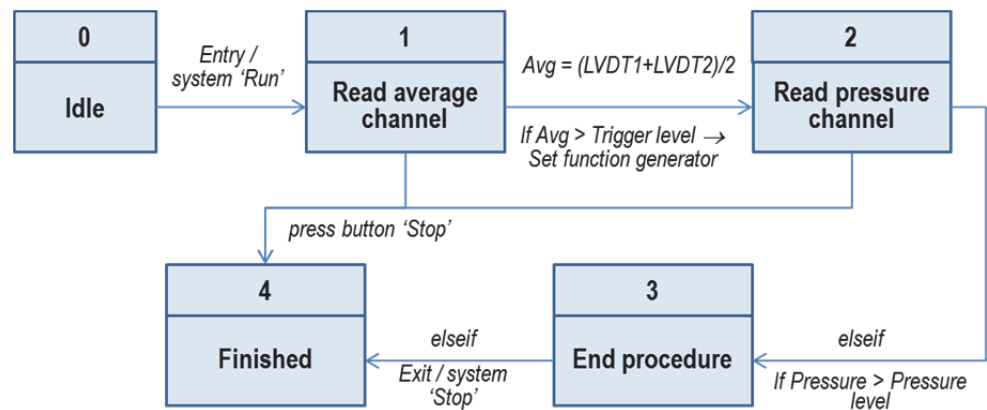


Figure A.6. State machine diagram represents the logic allowing the script to generate event-driven action. The boxes represent the states and state's number while the arrows represent the transition from one state to another.

This rule is then translated into embedded computer program. Lua, a scripting language, was chosen as it is lightweight, fast and embeddable by which it can register the C/C++ functions in the *measurement system application* (MP3), allowing the application to implement some of the switching functionality. The data in the

application channel table will be passed to the script. In the script, a *while-loop* run for every 50 millisecond monitors the records in the channel of LVDT average value. The script will parse it and do some event-driven specific logics implementing concept of state machine as depicted in the figure 3.9. Then script will return a state – a function generator – which trigger machine to pump healing agent.

Some parameters have been defined in the script; such as RunSpeed = the motor pulling speed (injection), ReturnSpeed = the motor pushing speed (back to initial position), TriggLevel1 = threshold value of crack opening, TriggLevel2 = threshold value for pressure build up in the porous core. The decision taken by the system is carried out in the *while-loop*. At state 0 the system does nothing at all (idle status). After the system has been started, the system is in the state 1 and reads the values of average LVDT signals. Then the system transitions into decision criterion if average value of LVDT's signal (represents crack opening) is larger than TriggLevel1, a switching function is generated, and system in the state 2. Physically, during the transition, actuator is in standby position ready to be switched on when the threshold value achieved.

In the state 2 system reads signal from pressure channel. If the system in transition detects criterion 2, pressure is larger than TriggLevel2, system enters into state 3 and exits into state 4 immediately, and the system is stopped. In physical world, the injector pumps the liquid agents in the syringe.

If criterion 2 is not met, the system runs until it exits in the state 4. In this case injector will receive voltage generated by function generator in the script until it reaches mechanical relay connected in the steel rod which acts as a fuse. When linear actuator reaches it, the machine is switched off. After the process the script then return the control back to the software (MP3) to be able to perform its regular function.

References

1. Bentur, A., *Cementitious Materials—Nine Millennia and A New Century: Past, Present, and Future*. Journal of Materials in Civil Engineering, 2002. **14**(1): p. 2-22.
2. Ronen, A., A. Bentur, and I. Soroka, *A Plastered Floor from the Neolithic Village, Yiftabel (Israel)*. Paléorient, 1991: p. 149-155.
3. Garfinkel, Y., *Burnt Lime Products and Social Implications in the Pre-Pottery Neolithic B Villages of the Near East*. Paléorient, 1987: p. 69-76.
4. Mindess, S., *Advanced concrete for use in civil engineering*, in *Advanced civil infrastructure materials: Science, mechanics and applications*, H.C. Wu, Editor. 2006, Woodhead Publishing. p. 376.
5. Snell, L.M. and B.G.I. Snell, *The Early Roots of Cement*. Concrete International, 2000. **22**(2): p. 3.
6. Blezard, R.G., *The History of Calcareous Cements*, in *Lea's Chemistry of Cement and Concrete (Fourth Edition)*. 2003, Butterworth-Heinemann: Oxford. p. 1-23.
7. Malinowski, R., *Concretes and Mortars in Ancient Aque-Ducts*. Concrete International, 1979. **1**(01): p. 11.
8. Mehta, P.K. and P.J.M. Monteiro, *Concrete: Microstructure, Properties, and Materials*. 3rd ed.: McGraw-Hill.
9. Rubenstein, M. *Mitigating Emissions from Cement*. The GNCS Factsheets 1 June 2013; Available from: http://www.thegnscs.org/?id=mitigation_factsheets.
10. WBCSD, *Cement Technology Roadmap: Carbon emissions reductions up to 2050*. 2009, World Business Council for Sustainable Development.
11. Flatt, R.J., N. Roussel, and C.R. Cheeseman, *Concrete: An eco material that needs to be improved*. Journal of the European Ceramic Society, 2012. **32**(11): p. 2787-2798.
12. Jahren, P. and T. Sui, *Concrete and Sustainability*. 2013: CRC Press, Taylor & Francis. 462.
13. Saeed, K. and H. Xu, *Infrastructure Development as a Policy Lever for Sustainable Development*, in *Handbook of sustainable development planning: Studies in modeling and decision support*, M.A. Quaddus and M.A.B. Siddique, Editors. 2004, Edward Elgar Publishin: Cheltenham.
14. van Oss, H.G. and A.C. Padovani, *Cement Manufacture and the Environment Part II: Environmental Challenges and Opportunities*. Journal of Industrial Ecology, 2003. **7**(1): p. 93-126.
15. van Oss, H.G. and A.C. Padovani, *Cement Manufacture and the Environment: Part I: Chemistry and Technology*. Journal of Industrial Ecology, 2002. **6**(1): p. 89-105.
16. IPCC, *Climate Change 2007: Mitigation of Climate Change* B. Metz, et al., Editors. 2007, Intergovernmental Panel on Climate Change (IPCC): Cambridge, United Kingdom.
17. Mahasenan, N., S. Smith, and K. Humphreys, *The Cement Industry and Global Climate Change: Current and Potential Future Cement Industry CO₂ Emissions*, in *Greenhouse Gas Control Technologies - 6th International Conference*, J. Gale and Y. Kaya, Editors. 2003, Pergamon: Oxford. p. 995-1000.
18. Akashi, O., et al., *A projection for global CO₂ emissions from the industrial sector through 2030 based on activity level and technology changes*. Energy, 2011. **36**(4): p. 1855-1867.
19. Hammond, G.P. and C.I. Jones, *Embodied energy and carbon in construction materials*. Proceedings of the ICE - Energy, 2008. **161**(2): p. 87 -98.
20. van Breugel, K. *Is There A Market for Self-Healing Cement-Based Materials?* in *the First International Conference on Self Healing Materials*. 2007. Noordwijk aan Zee, The Netherlands: Springer.
21. Emmons, P.H. and D.J. Sordyl, *The State of the Concrete Repair Industry, and a Vision for its Future*. Concrete Repair Bulletin, 2006. **July/August**: p. 8.
22. Yunovich, M. and N.G. Thompson, *Corrosion of Highway Bridges: Economic Impact and Control Methodologies*, in *Concrete International*. 2003.
23. Siddique, R. and M.I. Khan, *Supplementary Cementing Materials*. 2011: Springer.

24. Lothenbach, B., K. Scrivener, and R.D. Hooton, *Supplementary cementitious materials*. Cement and Concrete Research, 2011. **41**(12): p. 1244-1256.
25. van der Zwaag, S., *An Introduction to Material Design Principles: Damage Prevention versus Damage Management*, in *Self Healing Materials: An Alternative Approach to 20 Centuries of Materials Science*, S. van der Zwaag, Editor. 2008, Springer: Dordrecht, The Netherlands. p. 1-18.
26. van Breugel, K. *Self-Healing Materials Concepts as Solution for Aging Infrastructure*. in *37th Conference on Our World in Concrete and Structures*. 2012. Singapore: CI-Premier PTE Ltd.
27. Vogel, S., *Rhino horns and paper cups: Deceptive similarities between natural and human designs* Journal of Biosciences, 2000. **25**(2): p. 191-195.
28. van der Zwaag, S., et al., *Self-healing behaviour in man-made engineering materials: bioinspired but taking into account their intrinsic character*. Philosophical Transactions of the Royal Society A: Mathematical, Physical and Engineering Sciences, 2009. **367**(1894): p. 1689-1704.
29. Trask, R.S. and et al., *Self-healing polymer composites: mimicking nature to enhance performance*. Bioinspiration & Biomimetics, 2007. **2**(1): p. P1.
30. Benyus, J.M., *Biomimicry; Innovation inspired by nature*. . 2002: Harper Perennial. 320.
31. Milwich, M., et al., *Biomimetics and technical textiles: solving engineering problems with the help of nature's wisdom*. American Journal of Botany, 2006. **93**(10): p. 1455-1465.
32. Bar-Cohen, Y., *Biomimetics—using nature to inspire human innovation*. Bioinspiration & Biomimetics, 2006. **1**(1): p. P1.
33. Barnes, C., et al., *Biomimetics: strategies for product design inspired by nature – a mission to the Netherlands and Germany*. 2007, DTI Global Mission Watch. p. 64.
34. Bhushan, B., *Biomimetics: lessons from nature-an overview*. Philosophical Transactions of the Royal Society A: Mathematical, Physical and Engineering Sciences, 2009. **367**(1893): p. 1445-1486.
35. Bhushan, B., *Biomimetics; Bioinspired Hierarchical-Structured Surfaces for Green Science and Technology*. Biological and Medical Physics, Biomedical Engineering. 2012: Springer Berlin Heidelberg.
36. -, *Inspired by Biology: From Molecules to Materials to Machines*. 2008: The National Academies Press.
37. Vogel, S., *Nature's Swell, But Is It Worth Copying?* MRS Bulletin, 2003. **28**(06): p. 404-408.
38. Reed, E.J., et al., *Biomimicry as a route to new materials: what kinds of lessons are useful?* Philosophical Transactions of the Royal Society A: Mathematical, Physical and Engineering Sciences, 2009. **367**(1893): p. 1571-1585.
39. Vincent, J.F.V., *Applications — Influence of Biology on Engineering*. Journal of Bionic Engineering, 2006. **3**(3): p. 161-177.
40. Ball, P., *Life's lessons in design*. Nature, 2001. **409**(6818): p. 413-416.
41. Yoo, S.-H., *Sustainable Design by Systematic Innovation Tools (TRIZ, CAI, SI, and Biomimetics)*, in *Handbook of Sustainable Engineering*, J. Kauffman and K.-M. Lee, Editors. 2013, Springer Netherlands. p. 451-470.
42. Cowin, S.C., *The False Premise in Wolff's Law*, in *Bone Mechanics Handbook, Second Edition*. 2001, CRC Press. p. 30-1-30-15.
43. Blossey, R., *Self-cleaning surfaces - virtual realities*. Nat Mater, 2003. **2**(5): p. 301-306.
44. Bard, A.J. and M.A. Fox, *Artificial Photosynthesis: Solar Splitting of Water to Hydrogen and Oxygen*. Accounts of Chemical Research, 1995. **28**(3): p. 141-145.
45. Knippers, J. and T. Speck, *Design and construction principles in nature and architecture*. Bioinspiration & Biomimetics, 2012. **7**(1): p. 015002.
46. Lienhard, J., et al., *Flectofin: a hingeless flapping mechanism inspired by nature*. Bioinspiration & Biomimetics, 2011. **6**(4): p. 045001.
47. Walters, P., et al., *Artificial heartbeat: design and fabrication of a biologically inspired pump*. Bioinspiration & Biomimetics, 2013. **8**(4): p. 046012.
48. Vincent, J.F.V., et al., *Biomimetics: its practice and theory*. Journal of The Royal Society Interface, 2006. **3**(9): p. 471-482.
49. Vincent, J.F.V. and D.L. Mann, *Systematic technology transfer from biology to engineering*. Philosophical Transactions of the Royal Society of London. Series A: Mathematical, Physical and Engineering Sciences, 2002. **360**(1791): p. 159-173.

50. Lepora, N.F., P. Verschure, and T.J. Prescott, *The state of the art in biomimetics*. Bioinspiration & Biomimetics, 2013. **8**(1): p. 013001.
51. Badarnah Kadri, L., *Towards the Living Envelope, Biomimetic for building envelope adaptation*, in *Architecture*. 2012, TU Delft: Delft.
52. Jenkins, C.H., *Bio-Inspired Engineering*. 2012, New York: Momentum Press.
53. Speck, T. and O. Speck, *Process sequences in biomimetic research*. WIT Transactions on Ecology and the Environment, Design and Nature IV, 2008. **114**: p. 9.
54. Vattam, S., M.E. Helms, and A.K. Goel, *Biologically-Inspired Innovation in Engineering Design: a Cognitive Study*. 2007, Georgia Institute of Technology.
55. -. *Biomimicry Design Lens, A Visual Guide*. 2013 g1.0 03.01.2013 12 June 2013]; Available from: <http://biomimicry.net/about/biomimicry/biomimicry-designlens/biomimicry-thinking/>.
56. Gebeshuber, I.C. and M. Drack, *An attempt to reveal synergies between biology and mechanical engineering*. Proceedings of the Institution of Mechanical Engineers, Part C: Journal of Mechanical Engineering Science, 2008. **222**(7): p. 1281-1287.
57. Singer, A.J. and R.A.F. Clark, *Cutaneous Wound Healing*. New England Journal of Medicine, 1999. **341**(10): p. 738-746.
58. Doblaré, M., J.M. García, and M.J. Gómez, *Modelling bone tissue fracture and healing: a review*. Engineering Fracture Mechanics, 2004. **71**(13-14): p. 1809-1840.
59. Fratzl, P. and R. Weinkamer, *Hierarchical Structure and Repair of Bone: Deformation, Remodelling, Healing*, in *Self Healing Materials*, S. Zwaag, Editor. 2008, Springer Netherlands. p. 323-335.
60. Kalfas, I.H., *Principles of bone healing*. NEUROSURGICAL FOCUS, 2001. **10**(4): p. 1-4.
61. McKibbin, B., *The biology of fracture healing in long bones*. Journal of Bone & Joint Surgery, British Volume, 1978. **60-B**(2): p. 150-162.
62. Sangadji, S. and E. Schlangen, *Mimicking Bone Healing Process to Self Repair Concrete Structure Novel Approach Using Porous Network Concrete*. Procedia Engineering, 2013. **54**(0): p. 315-326.
63. León, J., E. Rojo, and J.J. Sánchez-Serrano, *Wound signalling in plants*. Journal of Experimental Botany, 2001. **52**(354): p. 1-9.
64. Fratzl, P. and R. Weinkamer, *Nature's hierarchical materials*. Progress in Materials Science, 2007. **52**(8): p. 1263-1334.
65. Taylor, D., J.G. Hazenberg, and T.C. Lee, *Living with cracks: Damage and repair in human bone*. Nat Mater, 2007. **6**(4): p. 263-268.
66. Weinkamer, R. and P. Fratzl, *Mechanical adaptation of biological materials — The examples of bone and wood*. Materials Science and Engineering: C, 2011. **31**(6): p. 1164-1173.
67. Nair, A.K., et al., *Molecular mechanics of mineralized collagen fibrils in bone*. Nature Communications, 2013. **4**.
68. Launey, M.E., M.J. Buehler, and R.O. Ritchie, *On the Mechanistic Origins of Toughness in Bone*. Annual Review of Materials Research, 2010. **40**(1): p. 25-53.
69. Ritchie, R.O., *The conflicts between strength and toughness*. Nature Materials, 2011. **10**(11): p. 817-822.
70. Weiner, S. and H.D. Wagner, *The material bone: Structure mechanical function relations*. Annual Review of Materials Science, 1998. **28**: p. 271-298.
71. -, *New Insights in Bone Biology*. 2012.
72. Lemaire, T. and S. Naili, *Multiscale Approach to Understand the Multiphysics Phenomena in Bone Adaptation*, in *Multiscale Computer Modeling in Biomechanics and Biomedical Engineering*, A. Gefen, Editor. 2013, Springer Berlin Heidelberg. p. 31-72.
73. Seeman, E. and P.D. Delmas, *Bone Quality — The Material and Structural Basis of Bone Strength and Fragility*. New England Journal of Medicine, 2006. **354**(21): p. 2250-2261.
74. Gupta, H.S., et al., *Cooperative deformation of mineral and collagen in bone at the nanoscale*. Proceedings of the National Academy of Sciences, 2006. **103**(47): p. 17741-17746.
75. Klein-Nulend, J., R.G. Bacabac, and M.G. Mullender, *Mechanobiology of bone tissue*. Pathologie Biologie, 2005. **53**(10): p. 576-580.
76. Robling, A.G., A.B. Castillo, and C.H. Turner, *Biomechanical and Molecular Regulation of Bone Remodeling*. Annual Review of Biomedical Engineering, 2006. **8**(1): p. 455-498.

77. Raggatt, L.J. and N.C. Partridge, *Cellular and Molecular Mechanisms of Bone Remodeling*. Journal of Biological Chemistry, 2010. **285**(33): p. 25103-25108.
78. Liedert, A., et al., *Signal transduction pathways involved in mechanotransduction in bone cells*. Biochemical and Biophysical Research Communications, 2006. **349**(1): p. 1-5.
79. Rubin, J., C. Rubin, and C.R. Jacobs, *Molecular pathways mediating mechanical signaling in bone*. Gene, 2006. **367**(0): p. 1-16.
80. Shier, D., J. Butler, and R. Lewis, *Hole's human anatomy & physiology*. 12th ed. 2010: McGraw-Hill.
81. Blaiszik, B.J., et al., *Self-Healing Polymers and Composites*. Annual Review of Materials Research, Vol 40, 2010. **40**: p. 179-211.
82. Malinskii, Y.M., et al., *Investigation of self-healing of cracks in polymers*. Polymer Mechanics, 1970. **6**(2): p. 240-244.
83. Dry, C., *Procedures developed for self-repair of polymer matrix composite materials*. Composite Structures, 1996. **35**(3): p. 263-269.
84. Dry, C.M., *Passive Smart Materials for Sensing and Actuation*. Journal of Intelligent Material Systems and Structures, 1993. **4**(3): p. 420-425.
85. White, S.R., et al., *Autonomic healing of polymer composites*. Nature, 2001. **409**(6822): p. 794-797.
86. Van Tittelboom, K., *Self-Healing Concrete through Incorporation of Encapsulated Bacteria or Polymer-Based Healing Agents*, in *Faculty of Engineering and Architecture*. 2012, University of Gent: Gent, Belgium.
87. Van Tittelboom, K. and N. De Belie, *Self-Healing in Cementitious Materials—A Review*. Materials, 2013. **6**(6): p. 2182-2217.
88. Schlangen, E., *Other Materials, Applications and Future Developments*, in *Self-Healing Phenomena in Cement-Based Materials*, M. de Rooij, et al., Editors. 2013, Springer Netherlands. p. 241-256.
89. Mario de Rooij, K.V.T., Nele De Belie, Erik Schlangen, *Self-Healing Phenomena in Cement-Based Materials*, in *State-of-the-Art Report of RILEM Technical Committee 221-SHC: Self-Healing Phenomena in Cement-Based Materials*. 2013, Springer Netherlands.
90. Mihashi, H. and T. Nishiwaki, *Development of Engineered Self-Healing and Self-Repairing Concrete-State-of-the-Art Report* Journal of Advanced Concrete Technology, 2012. **10**(Special Issue Advances in Self-healing Cementitious Materials): p. pp.170-184.
91. Neville, A., *Autogenous Healing—A Concrete Miracle?* Concrete International, 2002. **24**(11): p. 76-82.
92. Hearn, N., *Self-sealing, autogenous healing and continued hydration: What is the difference?* Materials and Structures, 1998. **31**(8): p. 563-567.
93. Hearn, N. and C.T. Morley, *Self-sealing property of concrete—Experimental evidence*. Materials and Structures, 1997. **30**(7): p. 404-411.
94. Reinhardt, H.W., et al., *Recovery against Environmental Action*, in *Self-Healing Phenomena in Cement-Based Materials*, M. de Rooij, et al., Editors. 2013, Springer Netherlands. p. 65-117.
95. Reinhardt, H.-W. and M. Jooss, *Permeability and self-healing of cracked concrete as a function of temperature and crack width*. Cement and Concrete Research, 2003. **33**(7): p. 981-985.
96. Edvardsen, C., *Water Permeability and Autogenous Healing of Cracks in Concrete*. ACI Materials Journal, 1999. **96**(4): p. 448-454.
97. ter Heide, N., *Crack healing in hydrating concrete*, in *Faculty of Civil Engineering and Geosciences, Microlab*. 2005, Delft University of Technology: Delft.
98. Ter Heide, N., E. Schlangen, and K. van Breugel. *Experimental study of crack healing of early age cracks*. in *Knud Hojgaard conference on Advanced Cement-based Materials*. 2005. Lyngby, Denmark.
99. Schlangen, E., N.t. Heide, and K.v. Breugel, *Crack healing of early age cracks in concrete*, in *Measuring, Monitoring and Modeling Concrete Properties*, M. Konsta-Gdoutos, Editor. 2006, Springer Netherlands. p. 273-284.
100. Li, V.C., Y.M. Lim, and Y.-W. Chan, *Feasibility study of a passive smart self-healing cementitious composite*. Composites Part B: Engineering, 1998. **29**(6): p. 819-827.

101. Yang, Y., E.-H. Yang, and V.C. Li, *Autogenous healing of engineered cementitious composites at early age*. Cement and Concrete Research, 2011. **41**(2): p. 176-183.
102. Qian, S., et al., *Self-healing behavior of strain hardening cementitious composites incorporating local waste materials*. Cement and Concrete Composites, 2009. **31**(9): p. 613-621.
103. Homma, D., H. Mihashi, and T. Nishiwaki, *Self-Healing Capability of Fibre Reinforced Cementitious Composites*. Journal of Advanced Concrete Technology, 2009. **7**(2): p. 217-228.
104. Sakai, Y., et al. *Experimental study on enhancement of self-restoration of concrete beams using SMA wire*. 2003.
105. Yachuan, K. and O. Jinping, *Self-repairing performance of concrete beams strengthened using superelastic SMA wires in combination with adhesives released from hollow fibers*. Smart Materials and Structures, 2008. **17**(2): p. 025020.
106. Kuang, Y.-c. and J.-p. Ou, *Passive smart self-repairing concrete beams by using shape memory alloy wires and fibers containing adhesives*. Journal of Central South University of Technology, 2008. **15**(3): p. 411-417.
107. Isaacs, B., et al., *Crack healing of cementitious materials using shrinkable polymer tendons*. Structural Concrete, 2013. **14**(2): p. 138-147.
108. Jefferson, A., et al., *A new system for crack closure of cementitious materials using shrinkable polymers*. Cement and Concrete Research, 2010. **40**(5): p. 795-801.
109. Lee, H.X.D., H.S. Wong, and N.R. Buenfeld, *Potential of superabsorbent polymer for self-sealing cracks in concrete*. Advances in Applied Ceramics, 2010. **109**(5): p. 296-302.
110. Snoeck, D., et al., *Self-healing cementitious materials by the combination of microfibres and superabsorbent polymers*. Journal of Intelligent Material Systems and Structures, 2012.
111. Sisomphon, K., O. Çopuroğlu, and A.L.A. Fraaij, *Durability of blast-furnace slag mortars subjected to sodium monofluorophosphate application*. Construction and Building Materials, 2011. **25**(2): p. 823-828.
112. Sisomphon, K., O. Copuroglu, and E.A.B. Koenders, *Self-healing of surface cracks in mortars with expansive additive and crystalline additive*. Cement and Concrete Composites, 2012. **34**(4): p. 566-574.
113. Jonkers, H.M., *Self Healing Concrete: A Biological Approach*, in *Self Healing Materials*, S. Zwaag, Editor. 2008, Springer Netherlands. p. 195-204.
114. Wiktor, V. and H.M. Jonkers, *Quantification of crack-healing in novel bacteria-based self-healing concrete*. Cement and Concrete Composites, 2011. **33**(7): p. 763-770.
115. Van Tittelboom, K., et al., *Use of bacteria to repair cracks in concrete*. Cement and Concrete Research, 2010. **40**(1): p. 157-166.
116. Wang, J., et al., *Use of silica gel or polyurethane immobilized bacteria for self-healing concrete*. Construction and Building Materials, 2012. **26**(1): p. 532-540.
117. Yang, Z., et al., *A self-healing cementitious composite using oil core/silica gel shell microcapsules*. Cement and Concrete Composites, 2011. **33**(4): p. 506-512.
118. Van Tittelboom, K., et al., *Self-healing efficiency of cementitious materials containing tubular capsules filled with healing agent*. Cement and Concrete Composites, 2011. **33**(4): p. 497-505.
119. Joseph, C., et al., *Experimental investigation of adhesive-based self-healing of cementitious materials*. Magazine of Concrete Research, 2010. **62**(11): p. 13.
120. Joseph, C., *Experimental and numerical study of the fracture and self-healing of cementitious materials*. 2008, Cardiff University: Cardiff. p. 228.
121. Nishiwaki, T., et al., *Development of Self-Healing System for Concrete with Selective Heating around Crack*. Journal of Advanced Concrete Technology, 2006. **4**(2): p. 267-275.
122. Dry, C. and M. Corsaw, *A comparison of bending strength between adhesive and steel reinforced concrete with steel only reinforced concrete*. Cement and Concrete Research, 2003. **33**(11): p. 1723-1727.
123. Dry, C.M., *Smart multiphase composite materials that repair themselves by a release of liquids that become solids* Proceedings SPIE: Smart Structures and Materials: Smart Materials, 1994. **2189** p. 62-70.
124. Dry, C.M. *Design of self-growing, self-sensing, and self-repairing materials for engineering applications*. 2001.

125. Dry, C.M. *Self-forming polymer ceramic composite made by an in-situ process to yield superior microstructure while using materials and energy efficiently*. 2001.
126. Dry, C.M., *Three designs for the internal release of sealants, adhesives, and waterproofing chemicals into concrete to reduce permeability*. Cement and Concrete Research, 2000. **30**(12): p. 1969-1977.
127. Alex D. Rogers, et al., *The Discovery of New Deep-Sea Hydrothermal Vent Communities in the Southern Ocean and Implications for Biogeography*. PLOS Biology, 2012. **10**(1): p. 17.
128. Vrijenhoek, R.C., *On the instability and evolutionary age of deep-sea chemosynthetic communities*. Deep Sea Research Part II: Topical Studies in Oceanography, 2013. **92**(0): p. 189-200.
129. Anderson, R.E., et al., *Microbial community structure across fluid gradients in the Juan de Fuca Ridge hydrothermal system*. FEMS Microbiology Ecology, 2013. **83**(2): p. 324-339.
130. Jørgensen, B.B. and S. D'Hondt, *A Starving Majority Deep Beneath the Seafloor*. Science, 2006. **314**(5801): p. 932-934.
131. Dorn, R.I. and T.M. Oberlander, *Microbial Origin of Desert Varnish*. Science, 1981. **213**(4513): p. 1245-1247.
132. Fajardo-Cavazos, P. and W. Nicholson, *Bacillus Endospores Isolated from Granite: Close Molecular Relationships to Globally Distributed Bacillus spp. from Endolithic and Extreme Environments*. Applied and Environmental Microbiology, 2006. **72**(4): p. 2856-2863.
133. de la Torre, J.R., et al., *Microbial Diversity of Cryptoendolithic Communities from the McMurdo Dry Valleys, Antarctica*. Applied and Environmental Microbiology, 2003. **69**(7): p. 3858-3867.
134. Pedersen, K., et al., *Distribution, diversity and activity of microorganisms in the hyper-alkaline spring waters of Maqarin in Jordan*. Extremophiles, 2004. **8**(2): p. 151-164.
135. DeJong, J., M. Fritzges, and K. Nüsslein, *Microbially Induced Cementation to Control Sand Response to Undrained Shear*. Journal of Geotechnical and Geoenvironmental Engineering, 2006. **132**(11): p. 1381-1392.
136. DeJong, J.T., et al., *Bio-mediated soil improvement*. Ecological Engineering, 2010. **36**(2): p. 197-210.
137. Dick, J., et al., *Bio-deposition of a calcium carbonate layer on degraded limestone by Bacillus species*. Biodegradation, 2006. **17**(4): p. 357-367.
138. Bachmeier, K.L., et al., *Urease activity in microbiologically-induced calcite precipitation*. Journal of Biotechnology, 2002. **93**(2): p. 171-181.
139. Bang, S.S., J.K. Galinat, and V. Ramakrishnan, *Calcite precipitation induced by polyurethane-immobilized Bacillus pasteurii*. Enzyme and Microbial Technology, 2001. **28**(4-5): p. 404-409.
140. De Muijnck, W., N. De Belie, and W. Verstraete, *Microbial carbonate precipitation in construction materials: A review*. Ecological Engineering, 2010. **36**(2): p. 118-136.
141. Jonkers, H.M. and M.C.M. van Loosdrecht, *BioGeoCivil Engineering*. Ecological Engineering, 2010. **36**(2): p. 97-98.
142. Sangadji, S. and E. Schlangen, *Self-Healing of Concrete Structures - Novel Approach Using Porous Network Concrete*. Journal of Advanced Concrete Technology, 2012. **10**(Special Issue Advances in Self-healing Cementitious Materials): p. pp. 185-194.
143. Glisic, B. and D. Inaudi, *Fibre optic methods for structural health monitoring*. 2007: Wiley. 276.
144. Issa, C.A. and P. Debs, *Experimental study of epoxy repairing of cracks in concrete*. Construction and Building Materials, 2007. **21**(1): p. 157-163.
145. Wiktor, V. and H.M. Jonkers. *Application of bacteria-based repair system to damaged concrete structures. in the 2nd International Workshop on Structural Life Management of Underground Structures*. 2012. Daejon.
146. Wiktor, V., et al. *Potential of Bacteria-based Repair Solutions as Healing Agent for Porous Network Concrete. in Fourth International Conference on Self-Healing Materials*. 2013. Ghent, Belgium: Magnel Laboratory for Concrete Research.
147. Wiktor, V., A. Thijssen, and H.M. Jonkers. *Development of a liquid bio-based repair system for aged concrete structures. in 3rd International Conference on Concrete Repair, Rehabilitation and Retrofitting*. 2012. Cape Town, South Africa: CRC Press.

148. Sangadji, S., et al. *Injecting a Liquid Bacteria-based Repair System to Make Porous Network Concrete Healed*. in *Fourth International Conference on Self-Healing Materials*. 2013. Ghent, Belgium: Magnel Laboratory for Concrete Research.
149. Warner, J., *Practical handbook of grouting: soil, rock, and structures*. 2004: Wiley.
150. Bear, J., *Dynamics of Fluids in Porous Media*. 1988, New York: Dover Publications, Inc.
151. Okamura, H. and M. Ouchi, *Self-Compacting Concrete*. *Journal of Advanced Concrete Technology*, 2003. **1**(1): p. 5-15.
152. Su, N., K.-C. Hsu, and H.-W. Chai, *A simple mix design method for self-compacting concrete*. *Cement and Concrete Research*, 2001. **31**(12): p. 1799-1807.
153. Schutter, G.D., et al., *Self-Compacting Concrete* 2008: Whittles Publishing.
154. Daczko, J.A., *Self-Consolidating Concrete: Applying What We Know* 2012: Spon Press.
155. Khayat, K.H., *Viscosity-enhancing admixtures for cement-based materials — An overview*. *Cement and Concrete Composites*, 1998. **20**(2–3): p. 171-188.
156. Ferrara, L., Y.-D. Park, and S.P. Shah, *A method for mix-design of fiber-reinforced self-compacting concrete*. *Cement and Concrete Research*, 2007. **37**(6): p. 957-971.
157. Choi, Y.W., et al., *An experimental research on the fluidity and mechanical properties of high-strength lightweight self-compacting concrete*. *Cement and Concrete Research*, 2006. **36**(9): p. 1595-1602.
158. Akalin, O., K.U. Akay, and B. Sennaroglu, *Self-Consolidating High-Strength Concrete Optimization by Mixture Design Method*. *Materials Journal*, 2010. **107**(4): p. 357-364.
159. Mohammed, M.K., A.R. Dawson, and N.H. Thom, *Production, microstructure and hydration of sustainable self-compacting concrete with different types of filler*. *Construction and Building Materials*, 2013. **49**(0): p. 84-92.
160. Sonebi, M., *Medium strength self-compacting concrete containing fly ash: Modelling using factorial experimental plans*. *Cement and Concrete Research*, 2004. **34**(7): p. 1199-1208.
161. El-Dieb, A.S., *Mechanical, durability and microstructural characteristics of ultra-high-strength self-compacting concrete incorporating steel fibers*. *Materials & Design*, 2009. **30**(10): p. 4286-4292.
162. Sonebi, M. and P.J.M. Bartos, *Filling ability and plastic settlement of self-compacting concrete*. *Materials and Structures*, 2002. **35**(8): p. 462-469.
163. Ghafoori, N. and S. Dutta, *Building and Nonpavement Applications of No-Fines Concrete*. *Journal of Materials in Civil Engineering*, 1995. **7**(4): p. 286-289.
164. Huang, B., et al., *Laboratory evaluation of permeability and strength of polymer-modified pervious concrete*. *Construction and Building Materials*, 2010. **24**(5): p. 818-823.
165. Agar-Ozbek, A.S., et al., *Investigating porous concrete with improved strength: Testing at different scales*. *Construction and Building Materials*, 2013. **41**(0): p. 480-490.
166. Chindapasirt, P., et al., *Cement paste characteristics and porous concrete properties*. *Construction and Building Materials*, 2008. **22**(5): p. 894-901.
167. Bentz, D.P., *Virtual Pervious Concrete: Microstructure, Percolation, and Permeability*. *ACI Materials Journal*, 2008. **105**(3): p. 297-301.
168. Agar Ozbek, A., et al., *Drop Weight Impact Strength Measurement Method for Porous Concrete Using Laser Doppler Velocimetry*. *Journal of Materials in Civil Engineering*, 2012. **24**(10): p. 1328-1336.
169. O'Neil, E.F., et al., *Safety concrete—development of a frangible concrete to reduce blast-related casualties*. 2004, Infrastructure Technology Institute, Northwestern University: Evanston, IL.
170. O'Neil, E.F., et al., *Development of Frangible Concrete to Reduce Blast-Related Casualties*. *Materials Journal*, 2012. **109**(1): p. 31-40.
171. Alhadid, M.M.A., et al., *Critical overview of blast resistance of different concrete types*. *Magazine of Concrete Research*, 2014. **66**: p. 72-81.
172. Neithalath, N., D.P. Bentz, and M.S. Sumanasooriya, *Predicting the Permeability of Pervious Concrete; Advances in characterization of pore structure and transport properties*. *Concrete International*, 2010. **32**(02).
173. Sumanasooriya, M.S., D.P. Bentz, and N. Neithalath, *Planar Image-Based Reconstruction of Pervious Concrete Pore Structure and Permeability Prediction*. *ACI Materials Journal*, 2010. **107**(4): p. 413-421.

174. Deo, O. and N. Neithalath, *Compressive behavior of pervious concretes and a quantification of the influence of random pore structure features*. Materials Science and Engineering: A, 2010. **528**(1): p. 402-412.
175. Hatanaka, S., et al., *Fundamental Study on Properties of Small Particle Size Porous Concrete*. Journal of Advanced Concrete Technology, 2014. **12**(1): p. 24-33.
176. Deo, O. and N. Neithalath, *Compressive response of pervious concretes proportioned for desired porosities*. Construction and Building Materials, 2011. **25**(11): p. 4181-4189.
177. Neithalath, N., M.S. Sumanasooriya, and O. Deo, *Characterizing pore volume, sizes, and connectivity in pervious concretes for permeability prediction*. Materials Characterization, 2010. **61**(8): p. 802-813.
178. Sumanasooriya, M.S., O. Deo, and N. Neithalath, *Particle Packing-Based Material Design Methodology for Pervious Concretes*. Materials Journal, 2012. **109**(2): p. 205-214.
179. Montes, F. and L. Haselbach, *Measuring Hydraulic Conductivity in Pervious Concrete*. Environmental Engineering Science, 2006. **23**(6): p. 960-969.
180. Haselbach, L. and R. Freeman, *Vertical Porosity Distributions in Pervious Concrete Pavement*. ACI Materials Journal, 2006. **103**(6): p. 452-458.
181. McGeary, R.K., *Mechanical Packing of Spherical Particles*. Journal of the American Ceramic Society, 1961. **44**(10): p. 513-522.
182. Crouch, L.K., J. Pitt, and R. Hewitt, *Aggregate Effects on Pervious Portland Cement Concrete Static Modulus of Elasticity*. Journal of Materials in Civil Engineering, 2007. **19**(7): p. 561-568.
183. Kevern, J.T., V.R. Schaefer, and K. Wang, *Evaluation of Pervious Concrete Workability Using Gyrotory Compaction*. Journal of Materials in Civil Engineering, 2009. **21**(12): p. 764-770.
184. Suleiman, M., et al. *Effect of compaction energy on pervious concrete properties*. in *Submitted to Concrete Technology Forum-Focus on Pervious Concrete, National Ready Mix Concrete Association, Nashville, TN, May*. 2006.
185. Mahboub, K.C., et al., *Pervious Concrete: Compaction and Aggregate Gradation*. ACI Materials Journal, 2009. **106**(6): p. 523-528.
186. Neithalath, N., J. Weiss, and J. Olek, *Characterizing Enhanced Porosity Concrete using electrical impedance to predict acoustic and hydraulic performance*. Cement and Concrete Research, 2006. **36**(11): p. 2074-2085.
187. Sumanasooriya, M.S. and N. Neithalath, *Pore structure features of pervious concretes proportioned for desired porosities and their performance prediction*. Cement and Concrete Composites, 2011. **33**(8): p. 778-787.
188. EFNARC, *Specification and Guidelines for Self-Compacting Concrete*. 2002.
189. Ashtiani, M.S., A.N. Scott, and R.P. Dhakal, *Mechanical and fresh properties of high-strength self-compacting concrete containing class C fly ash*. Construction and Building Materials, 2013. **47**(0): p. 1217-1224.
190. Jin, J., *Properties of Mortar for Self-Compacting Concrete*, in *Department of Civil and Environmental Engineering*. 2002, University College London: London. p. 398.
191. Yang, J. and G. Jiang, *Experimental study on properties of pervious concrete pavement materials*. Cement and Concrete Research, 2003. **33**(3): p. 381-386.
192. Lian, C. and Y. Zhuge, *Optimum mix design of enhanced permeable concrete – An experimental investigation*. Construction and Building Materials, 2010. **24**(12): p. 2664-2671.
193. Agar Ozbek, A.S., et al., *Dynamic behavior of porous concretes under drop weight impact testing*. Cement and Concrete Composites, 2013. **39**(0): p. 1-11.
194. Sumanasooriya, M.S., O. Deo, and N. Neithalath. *Computational Prediction of Elastic Properties of EPC Using Reconstructed 3D material Structures*. in *The 9th Brittle Matrix Composites, Warsaw, Poland, October 2009*. 2009. Warsaw, Poland.
195. Sumanasooriya, M.S. and N. Neithalath, *Stereology- and Morphology-Based Pore Structure Descriptors of Enhanced Porosity (Pervious) Concretes*. ACI Materials Journal, 2009. **106**(5): p. 429-438.
196. Kevern, J.T., et al., *Pervious Concrete Mixture Proportions for Improved Freeze-Thaw Durability*. Journal of ASTM International, 2008. **5**(2): p. 12.
197. Muñoz, A.M., *Evaluation of Sustainability, Durability, and Effect of Specimen Type in Pervious Concrete Mixtures*. 2012, Texas State University-San Marcos.

198. Landis, E.N. and D.T. Keane, *X-ray microtomography*. Materials Characterization, 2010. **61**(12): p. 1305-1316.
199. Hillel, D., *Fundamentals of Soil Physics*. 1980: Academic Press.
200. Penttala, V., *1 - Causes and mechanisms of deterioration in reinforced concrete*, in *Failure, Distress and Repair of Concrete Structures*, N. Delatte, Editor. 2009, Woodhead Publishing. p. 3-31.
201. FHWA. *Technical Manual for Design and Construction of Road Tunnels - Civil Elements: Chapter 16 - Tunnel Rehabilitation*. 2013 [cited 2013 1 June 2013]; Available from: <http://www.fhwa.dot.gov/bridge/tunnel/pubs/nhi09010/16.cfm>.
202. Franklin, G.F., J.D. Powell, and A. Emami-Naeini, *Feedback Control of Dynamic Systems*. 6th ed. ed. 2010: Pearson.
203. Çopuroğlu, O., et al., *Experimental Techniques Used to Verify Healing*, in *Self-Healing Phenomena in Cement-Based Materials*, M. de Rooij, et al., Editors. 2013, Springer Netherlands. p. 19-63.
204. Furie, B. and B.C. Furie, *Thrombus formation in vivo*. The Journal of Clinical Investigation, 2005. **115**(12): p. 3355-3362.
205. Aldea, C.M., et al., *Extent of healing of cracked normal strength concrete*. Journal of Materials in Civil Engineering, 2000. **12**(1): p. 92-96.
206. NEN, *NEN-EN 1992-1-1 Eurocode 2: Design of concrete structures - Part 1-1: General rules and rules for buildings*. 2005.
207. Davie, E.W. and O.D. Ratnoff, *Waterfall Sequence for Intrinsic Blood Clotting*. Science, 1964. **145**(3638): p. 1310-1312.
208. Bras, A., et al., *Development of an injectable grout for concrete repair and strengthening*. Cement and Concrete Composites, 2013. **37**(0): p. 185-195.
209. Panasyuk, V.V., V.I. Marukha, and V.P. Sylovanyuk, *Injection Technologies for the Repair of Damaged Concrete Structures*. 2014, Dordrecht: Springer.
210. Eriksson, M., M. Friedrich, and C. Vorschulze, *Variations in the rheology and penetrability of cement-based grouts—an experimental study*. Cement and Concrete Research, 2004. **34**(7): p. 1111-1119.
211. Moosavi, M. and W.F. Bawden, *Shear strength of Portland cement grout*. Cement and Concrete Composites, 2003. **25**(7): p. 729-735.
212. Perret, S., D. Palardy, and G. Ballivy, *Rheological Behavior and Setting Time of Microfine Cement-Based Grouts*. Materials Journal, 2000. **97**(4): p. 472-478.
213. Pantazopoulos, I.A., et al., *Development of microfine cement grouts by pulverizing ordinary cements*. Cement and Concrete Composites, 2012. **34**(5): p. 593-603.
214. Björnström, J. and S. Chandra, *Effect of superplasticizers on the rheological properties of cements*. Materials and Structures, 2003. **36**(10): p. 685-692.
215. Wiktor, V. and H.M. Jonkers, *The potential of bacteria-based repair system to increase the durability of repaired concrete structures*, in *Second International Conference on Microstructural-related Durability of Cementitious Composites*. 2012: Amsterdam, The Netherlands.
216. Wassenaar, T.M., *Bacteria: The Benign, the Bad, and the Beautiful*. 2011, New Jersey: Wiley-Blackwell.
217. Bäckhed, F., et al., *Host-Bacterial Mutualism in the Human Intestine*. Science, 2005. **307**(5717): p. 1915-1920.
218. Consortium, T.H.M.P., *Structure, function and diversity of the healthy human microbiome*. Nature, 2012. **486**(7402): p. 207-214.
219. Turnbaugh, P.J., et al., *The Human Microbiome Project*. Nature, 2007. **449**(7164): p. 804-810.
220. Ley, R.E., D.A. Peterson, and J.I. Gordon, *Ecological and Evolutionary Forces Shaping Microbial Diversity in the Human Intestine*. Cell, 2006. **124**(4): p. 837-848.
221. Blaser, M.J., *Who are we? Indigenous microbes and the ecology of human diseases*. EMBO reports, 2006. **7**(10): p. 956-960.
222. Relman, D.A., *Microbiology: Learning about who we are*. Nature, 2012. **486**(7402): p. 194-195.
223. Dethlefsen, L., M. McFall-Ngai, and D.A. Relman, *An ecological and evolutionary perspective on human-microbe mutualism and disease*. Nature, 2007. **449**(7164): p. 811-818.
224. Salek, S.S., et al., *Mineral CO₂ sequestration by environmental biotechnological processes*. Trends in Biotechnology, 2013. **31**(3): p. 139-146.

225. Gross, A., D. Kaplan, and K. Baker, *Removal of chemical and microbiological contaminants from domestic greywater using a recycled vertical flow bioreactor (RVFB)*. Ecological Engineering, 2007. **31**(2): p. 107-114.
226. Bestawy, E., et al., *Bioremediation of heavy metal-contaminated effluent using optimized activated sludge bacteria*. Applied Water Science, 2013. **3**(1): p. 181-192.
227. Ghosh, P., et al., *Use of microorganism to improve the strength of cement mortar*. Cement and Concrete Research, 2005. **35**(10): p. 1980-1983.
228. Graef, B., et al., *Cleaning of concrete fouled by lichens with the aid of Thiobacilli*. Materials and Structures, 2005. **38**(10): p. 875-882.
229. Stocks-Fischer, S., J.K. Galinat, and S.S. Bang, *Microbiological precipitation of CaCO₃*. Soil Biology and Biochemistry, 1999. **31**(11): p. 1563-1571.
230. Ramachandran, S.K., V. Ramakrishnan, and S.S. Bang, *Remediation of concrete using microorganisms*. ACI Materials Journal, 2001. **98**(1): p. 3-9.
231. De Muynck, W., et al., *Bacterial carbonate precipitation improves the durability of cementitious materials*. Cement and Concrete Research, 2008. **38**(7): p. 1005-1014.
232. Jonkers, H.M. and E. Schlangen, *Crack Repair by Concrete-Immobilized Bacteria*, in *the First International Conference on Self Healing Materials*. 2007: Noordwijk aan Zee, The Netherlands.
233. Jonkers, H.M. and E. Schlangen. *A two component bacteria-based self-healing concrete*. 2009.
234. Dhami, N.K., S.M. Reddy, and A. Mukherjee, *Biofilm and Microbial Applications in Biomineralized Concrete*, in *Advanced Topics in Biomineralization*, D.J. Seto, Editor. 2012, InTech.
235. Jonkers, H.M., et al., *Application of bacteria as self-healing agent for the development of sustainable concrete*. Ecological Engineering, 2010. **36**(2): p. 230-235.
236. Andersen, C.B., *Understanding Carbonate Equilibria by Measuring Alkalinity in Experimental and Natural Systems*. Journal of Geoscience Education, 2002. **50**(4): p. 389 - 403.
237. Li, V.C. and E.-H. Yang, *Self Healing in Concrete Materials*, in *Self Healing Materials: An Alternative Approach to 20 Centuries of Materials Science*, S. van der Zwaag, Editor. 2007, Springer: Dordrecht, The Netherlands. p. 161-194.
238. Hannant, D.J. and J.G. Keer, *Autogenous healing of thin cement based sheets*. Cement and Concrete Research, 1983. **13**(3): p. 357-365.
239. Rodriguez-Navarro, C., et al., *Conservation of Ornamental Stone by Myxococcus xanthus-Induced Carbonate Biomineralization*. Applied and Environmental Microbiology, 2003. **69**(4): p. 2182-2193.
240. Lian, B., et al., *Carbonate biomineralization induced by soil bacterium Bacillus megaterium*. Geochimica et Cosmochimica Acta, 2006. **70**(22): p. 5522-5535.
241. Lesley A. Warren, P.A.M.N.P.F.G.F., *Microbially Mediated Calcium Carbonate Precipitation: Implications for Interpreting Calcite Precipitation and for Solid-Phase Capture of Inorganic Contaminants*. Geomicrobiology Journal, 2001. **18**(1): p. 93-115.
242. Astrom, K.J. and R.M. Murray, *Feedback Systems, An Introduction for Scientists and Engineers* 2008: Printon University Press.

Samenvatting

De hoge energieconsumptie, haar bijbehorende CO₂ uitstoot en financiële verliezen als gevolg van voortijdig falen zijn de dringende duurzaamheidskwesties die dienen te worden aangepakt door de betonindustrie werkzaam voor de infrastructuur. Verbetering van betonmaterialen en duurzaamheid van constructies (het ontwerpen van nieuwe infrastructurele werken voor langere levensduur) is een oplossing om het dilemma te overwinnen.

Beton is een pseudo-bros materiaal met eigenschappen die hoog zijn onder druk, maar zwak onder trekkracht, vandaar dat beton gevoelig is voor het ontstaan van scheuren. In het geval dat een continu netwerk van scheuren wordt gevormd, wordt de permeabiliteit van beton verhoogd en kunnen de wapeningsstaven worden blootgesteld aan de omringende atmosfeer. Deze opening biedt een eenvoudige manier voor agressieve stoffen om het beton binnen te dringen en de wapeningsstaaf te bereiken, die kan beginnen te corroderen. Daarnaast kunnen scheuren de dichtheid van kerende constructies bedreigen, bijvoorbeeld tankwanden van waterhoudende constructies, aquaducten, ondergrondse ruimtes, tunnels, enz., die op trek belast worden. In deze gevallen kunnen scheuren de stroming van vloeistoffen of gas vergemakkelijken naar en vanuit de constructies, wat de bruikbaarheid aanzienlijk verandert, leidt tot een ongezond milieu binnenin een constructie, en de *functionaliteit* reduceert. In het geval dat de container of het reservoir afval bevat, zeer giftige stoffen of radioactieve stoffen, is lekkage door het beton catastrofaal en onaanvaardbaar.

Een veelbelovend concept om *nieuwe betonnen constructies te ontwerpen voor het behalen van hogere duurzaamheid* is het inbouwen van zelfherstellende mechanismen uit de natuur in de cementgebonden materialen of het betonnen constructiedeel. Als onvermijdelijke scheuren als gevolg van intrinsieke brosheid in beton vanzelf gedicht/genezen/hersteld kunnen worden, kan beton zeker langer meegaan en meer duurzaam zijn, zowel op het gebied van levensduur als ecologisch.

Over het algemeen, in een poging om technische problemen op te lossen, kan men (altijd) inspiratie zoeken uit de biologie (natuur). Hoewel het lenen van ideeën uit de natuur om onze leefomgeving te verbeteren zo oud is als de mensheid, maakt de postindustriële technische inzichten het proces meer systematisch en weloverwogen, en maakt daarom gebruik van *biomimicry* om problemen op te lossen en innovatie te inspireren.

In het gebied van de biologie, zijn er verscheidene wond genezende mechanismen te vinden in de natuur: genezing van gesneden huid en botbreuk in mens en dier, en de reactie van planten op verwonding. Het huidige werk is geïnspireerd door studies op bot van hedendaagse zoogdieren en vogels en hun herstellende mechanisme. Twee van de toepasselijke principes die constructief kunnen zijn, zijn geïdentificeerd; (1) *botmorfologie* dat bestaat uit corticaal (vast) bot en trabeculair (sponsachtig) bot en (2) een *terugkoppelmecanisme* zijn aanwezig in het remodelleer- en genezingsproces.

Deze twee principes vormden de basis voor de ontwikkeling van een (zelf-)herstellend betonmateriaal en voor een methode voor (zelf-)herstel met herstellende middelen. Het idee hierachter is dat corticaal bot kan worden nagebootst met massief beton en trabeculair bot kan worden geïmiteerd door poreus beton. De combinatie van de twee types van beton lijkt op *Poreus Netwerk Beton*, een botachtig beton in staat is om zichzelf te herstellen door het mechanisme van de terugkoppeling. Dit zijn de punten behandeld in hoofdstuk 1, waarin het

succesverhaal van beton in het dienen van een samenleving en beschaving voor duizenden jaren, de huidige uitdaging om modern beton duurzamer te maken, en de bio-geïnspireerde oplossing van zelf-herstellend beton verkend worden.

Poreus Netwerk Beton (PNB) is een hybride systeem waarbij zeer permeabel poreus beton is ingebed in het inwendige of uitwendige van beton van normale dichtheid. De kern van poreus netwerk vormt een alternatieve manier voor het [1] transporteren van tijdelijke of permanente materialen om een dichte laag te vormen in een latere fase en [2] verspreiden van herstellend middel van het punt van injectie tot de scheuren in het betonnen hoofdlichaam. In hoofdstuk 2 wordt het concept van PNB uitgewerkt door het opzetten van criteria en gerealiseerd door het creëren van een fabricage procedure. Het productieproces – *het maken van het PNC* – volgt de huidige standaard voor zowel het hoofd als poreuze onderdeel en een ingewikkelde fabricage procedure is niet nodig. PNB karakterisering werd uitgevoerd om zijn porie en mechanische eigenschappen te bestuderen.

Het *autonome* herstelmechanisme in het PNB is ontworpen door het opnemen van het terugkoppelingmechanisme; zodra een bepaalde scheurwijdte wordt gedetecteerd, vindt een actie voor herstel plaats. Om het concept aan te tonen is, in hoofdstuk 3, een eenvoudige en intuïtieve benadering uitgevoerd om een terugkoppelingssysteem voor het zelf-herstellende mechanisme in PNB te ontwerpen. Wanneer een betonconstructie belasting opvangt en interne spanningen opbouwt, buigt, scheurt en vervormt het. Zodra de scheurmondopening een bepaalde voorgeschreven waarde bereikt wordt het herstellende middel automatisch geïnjecteerd. Het voorgestelde werkingsprincipe is geverifieerd door mechanische en lekkage (permeabiliteit, infiltratie) testen.

Het verhardingsproces van het zelf-herstellend middel is belangrijk en zelfs cruciaal voor het succes van de ontworpen herstelstrategie en het mechanisme. In plaats van het ontwikkelen van nieuw herstellend middel en onderzoek naar zijn gedrag, heeft deze huidige studie als doel om de effectiviteit en efficiëntie te onderzoeken van het herstelproces in het PNB met verschillende soorten van middelen. Drie groepen van herstellende middelen worden vervolgens bestudeerd en hun herstellende efficiëntie getest door lekkage en mechanische testen.

Het *eerste* type herstellend middel is een- en tweecomponenten chemisch product, dat meestal werkt door middel van polycondensatie of crosslink polymerisatie bij contact met de atmosfeer, betonmatrix of tussen de reactiecomponenten. In dit geval wordt epoxyhars gebruikt. Het *tweede* gebruikte herstellend middel is speciemateriaal gemaakt van een cementgebonden poedermengsel. Cementgebonden speciemateriaal kan worden gezien als het herstellende middel voor betonconstructies, omdat het functioneert als een scheurafdichtingsmiddel en vulstof voor de leegtes met als doelstelling constructieve integriteit te herstellen. Het gebruik en de herstelprestaties van PNB door beide herstellendmiddelen wordt besproken in hoofdstuk 4.

Het derde middel is een op bacteriën gebaseerd reparatievloeistof. Het bevat alkalifiele bacteriën die in staat zijn om bio-mineralisatie te vergemakkelijken, voedingsstoffen en transportoplossing. Het werd oorspronkelijk ontwikkeld als een bio-gebaseerd reparatiemiddel voor gescheurd beton. Dit wordt besproken in hoofdstuk 5.

Er is in dit proefschrift aangetoond dat het Poreuze Netwerk Beton een goede kans heeft om betonnen bouwelementen zelf-herstellend te maken. Dit is het afsluitende punt gepresenteerd in het laatste hoofdstuk. Een aantal aanbevelingen om het werk te verbeteren worden gepresenteerd, zoals; modelleerwerk, grotere en realistische experimentele series en verbeterde schadewaarneming.

Ringkasan

Konsumsi energi dalam jumlah tinggi, emisi CO₂ dan kerugian finansial akibat kegagalan bangunan sebelum akhir usia layan adalah masalah-masalah *sustainability* yang harus di hadapi dan tangani oleh industri konstruksi beton masa kini. Pengembangan kualitas material dan durabilitas struktur beton (perancangan struktur dengan usian layan yang lebih lama) adalah salah satu jawaban untuk mengatasi dilemma ini.

Beton adalah material semi-getas (*quasi-brittle*) yang memiliki sifat unik; kuat menerima tegangan tekan dan lemah menahan tegangan tarik. Sebagai akibatnya beton mudah retak. Ketika retakan membentuk jejaring yang berkesinambungan, permeabilitas beton akan meningkat dan tulangan beton menjadi terbuka terhadap pengaruh atmosfer luar. Retakan seperti ini menjadi jalan yang mudah bagi cairan agresif untuk masuk dan menyebabkan proses korosi pada tulangan. Retakan juga menurunkan kedekatan konstruksi beton penahan, semisal dinding tangki penampung cairan, talang air, ruang bawah tanah, terowongan, dsb., yang menerima gaya tarik. Dalam kasus seperti ini, fluida – cair atau gas – dapat berpindah masuk atau keluar. Hal ini akan mengurangi tingkat layan bangunan, membuat lingkungan menjadi tidak sehat dan mengganggu fungsi struktur. Pada kasus tumpungan limbah cair beracun dan material radioaktif, kebocoran akibat retakan beton akan berdampak bencana buruk yang sulit dapat diterima.

Konsep terkini yang cukup menjanjikan dalam perancangan struktur beton baru agar memiliki keawetan tinggi adalah integrasi mekanisme *self-healing* yang biasa ditemukan di alam kedalam material atau struktur beton. Jika retakan beton – yang memang tak dapat dihindari karena sifat alami beton yang getas – dapat ‘disembuhkan oleh dirinya sendiri’ (*self-healing*), beton tentu akan lebih awet, mampu memberikan usia layan yang lebih lama, dan berkelanjutan (*sustainable*).

Untuk memecahkan masalah rekayasa seperti ini, seseorang insinyur dapat menggali gagasan (inspirasi) dari ilmu hayati (biologi), atau secara umum, *dari alam*. Sekalipun proses mengambil ide dari alam untuk mengembangkan perkakas, peralatan, perikehidupan, dan lingkungan hidup manusiawi sudah setua usia manusia itu sendiri, kehadiran teknik rekayasa pasca revolusi industri membuat proses tersebut menjadi lebih sistematis. Proses tersebut seringkali disengaja dengan memanfaatkan *bio-mimicry* untuk memecahkan masalah dan mendorong pembaruan (inovasi).

Di alam (ranah ilmu hayati) dapat ditemukan beberapa contoh proses penyembuhan luka; semisal kulit yang tersayat, patah/retak tulang pada manusia dan hewan, dan getah yang keluar dari kulit pohon yang terkelupas. Tesis ini mengambil inspirasi dari bentuk tulang mamalia dan burung modern dan proses penyembuhannya. Dari proses abstraksi terhadap tulang diperoleh dua prinsip yang dianggap tepat guna yakni: [1] morfologi tulang yang terdiri dari bagian padat (*cortical*) dan bagian berpori (*trabecular*), dan [2] proses umpan-balik yang terjadi dalam proses *remodelling* dan penyembuhan patah tulang.

Dua prinsip ini membentuk dasar bagi pengembangan ide beton yang ‘dapat menyembuhkan’ retaknya sendiri dan metode ‘penyembuhannya’ (perbaikannya). Ide dibalik konsep ini adalah: bagian tulang *cortical* ditiru dengan *beton normal (padat)* dan tulang *trabecular* ditiru dengan *beton porous*. Kombinasi kedua tipe beton ini membentuk *Porous Network Concrete*; beton yang

menyerupai formasi tulang dan mampu memperbaiki diri secara otomatis dengan mekanisme umpan-balik. Topik ini dikaji secara lebih dalam pada bab 1. Bab ini juga mengeksplorasi kisah sukses beton sepanjang peradaban manusia ribuan tahun, tantangan untuk membuat beton modern lebih awet, dan solusi bio-inspiratif *self-healing concrete*.

Porous Network Concrete (PNC) adalah sistem *hibrida* dimana beton porous dengan permeabilitas tinggi ditanam pada bagian dalam (*interior*) atau bagian permukaan (*exterior*) beton normal yang menjadi struktur utama. Inti yang berpori-pori ini berfungsi menjadi sarana: [1] menyalurkan material sementara atau permanen untuk membentuk lapisan padat pada tahapan berikut di usia layan beton, dan [2] mendistribusikan material perbaikan beton dari titik injeksi ke retakan pada struktur utama beton. Pada bab 2, konsep PNC diejawantahkan dengan pertama-tama menetapkan syarat-syarat keberhasilan dan menyusun tata cara pembuatan PNC. Proses produksi PNC dikerjakan mengikuti bakuan (peraturan) yang berlaku saat ini. Prosedur yang dihasilkan dalam bab ini tidak rumit dan dapat dikerjakan dengan peralatan membuat beton yang umum digunakan. Selanjutnya, kajian material PNC dilakukan dengan mempelajari sifat-sifat pori dan mekaniknya.

Mekanisme perbaikan PNC secara otonom (otomatis) dirancang dengan menggunakan konsep umpan balik; setelah lebar retakan diketahui dari sensor, informasi ini diumpanbalikkan untuk aksi ‘penyembuhan’. Bab 3 membahas konsep dan desain purwarupa PNC. Konsep rancangan dapat digambarkan sebagai berikut; ketika struktur beton menerima beban, pada stuktur akan terjadi lendutan dan deformasi. Jika deformasi lebih besar dari kekuatan material, maka beton akan retak. Ketika lebar mulut retakan yang diindera oleh sensor mencapai nilai tertentu yang telah ditetapkan, material perbaikan disuntikkan secara otomatis. Verifikasi dengan uji mekanik dan uji kebocoran (permeabilitas, infiltrasi) dibahas lebih lanjut dalam bab ini.

Proses pemadatan material perbaikan (healing agent) amatlah penting untuk keberhasilan strategi dan mekanisme *self-healing* yang dirancang. Tesis ini tidak berusaha mengembangkan material perbaikan baru dan meneliti perilakunya, melainkan menilai efektivitas dan efisiensi proses ‘penyembuhan’ (perbaikan) PNC menggunakan beberapa jenis material perbaikan yang berbeda. Tiga kelompok material (dua tersedia di pasaran dan satu larutan dikembangkan oleh Wiktor dan Jonkers) dikaji dan diuji efisiensinya.

Jenis *pertama* adalah material kimiawi dengan komponen tunggal atau ganda yang bekerja dengan cara poli-kondensasi atau polimerisasi saat terpapar udara, beton atau dengan pelarut lain. Tesis ini menggunakan epoxy resin. Jenis material perbaikan *kedua* adalah material *grout* yang terdiri dari campuran partikel semen dan air yang mudah diinjeksikan karena cair. Jenis material seperti ini dapat dijadikan *healing agent* struktur beton karena saat ini digunakan dalam konstruksi dan berfungsi sebagai penutup retakan dan pengisi rongga untuk mempertahankan integritas struktur. Penggunaan kedua jenis material dan bagaimana kinerjanya dalam perbaikan PNC dikaji pada Bab 4.

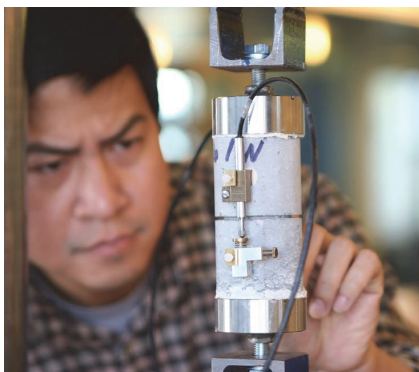
Material perbaikan ketiga adalah larutan berbasis bakteri. Larutan ini mengandung kombinasi: (1) bakteri *alkaliphilic* (dapat hidup di kondisi basa) yang mampu membantu proses biomineralisasi, (2) nutrisi untuk bakteri, dan (3) larutan penghantar. Larutan ini dikembangkan pada awalnya untuk material perbaikan struktur beton eksisting yang telah retak. Bab 5 mendiskusikan aspek-aspek kinerja larutan ini pada proses ‘penyembuhan’ PNC.

Secara umum, tesis ini mendemonstrasikan bahwa *Porous Network Concrete* memiliki prospek yang baik untuk membuat struktur beton mampu ‘menyembuhkan retaknya sendiri’. Ini adalah kesimpulan yang disajikan pada Bab akhir. Beberapa rekomendasi dibahas pula dalam bab ini antara lain; pemodelan optimasi sistem dengan komputer, uji eksperimental yang lebih realistis, dan penginderaan kerusakan yang lebih baik.

About the author

'The scientist does not study nature because it is useful to do so. He studies it because he takes pleasure in it, and he takes pleasure in it because it is beautiful. If nature were not beautiful it would not be worth knowing, and life would not be worth living. I am not speaking, of course, of the beauty which strikes the senses, of the beauty of qualities and appearances. I am far from despising this, but it has nothing to do with science. What I mean is that more intimate beauty which comes from the harmonious order of its parts, and which a pure intelligence can grasp.'

- Henri Poincare



Senot Sangadji was born in Banyuwangi, Indonesia. He received his elementary and secondary education in Malang, East Java, Indonesia. He graduated from Universitas Brawijaya, Malang, on 1997 with BSc in civil engineering. His final project was on *'finite element analysis of grid structures subjected to dynamic loading'*. On 2001 he received his master degree from Institut Teknologi Bandung (ITB) where he conducted research in *'design, production, and testing of aero-elastic model of long-span cable supported bridge'*.

He joined Civil Engineering Department, UNS, Indonesia as junior lecturer after received his master degree. There he taught and conducted research in structural analysis, structural dynamics, and earthquake engineering for 6 years. He also worked for professional and social service as independent evaluator for wind-bridge interaction design of one of long span bridge built in Indonesia, education quality improvement team leader and several management activities.

He was granted a scholarship by Directorate General of Higher Education, Ministry of National Education, the Government of Republic of Indonesia and joined Section of Materials and Environment, Faculty of Civil Engineering and Geosciences, Delft University of Technology. In 2010 and became a doctoral candidate under supervision of Prof. dr. ir. Erik Schlangen. His research concerns on self-healing mechanism and processes of cement-based materials. He particularly focuses on the development of *'porous network concrete, a bio-inspired component of to make concrete structures self-healing'*. He published several papers in peer-reviewed conferences, journal and scientific magazine. On November 2011 his innovation was chosen to be one of the finalists of Delft Innovation Award 2011.

He is married to Pungky Pramesti and they have a boy, Quanta A. Sangadji. He enjoys reading popular science and science fiction, playing jembe and guitar, cycling around the city, cooking *bakmi goreng*, and spending quality time with his family and friends.

Selected publications:

1. Sangadji, S. & Schlangen, E., *Feasibility and potential of prefabricated porous concrete as a component to make concrete structures self-healing*, In C Leung & KT Wan (Eds.), *Advances in construction materials through science and engineering* (pp. 121-131). Bagnex, France.
2. Sangadji, S. & Schlangen, E., *Porous Network Concrete: a new approach to make concrete structures self-healing using prefabricated porous layer*, The proceeding of the 3rd international conference self-healing materials (pp. 291-292). Bath, UK.
3. Schlangen, E. & Sangadji, S., *Addressing Infrastructure Durability and Sustainability by Self-Healing Mechanisms; Recent Advances in Self-Healing Concrete and Asphalt*, the 2nd International Conference on Rehabilitation and Maintenance in Civil Engineering, Solo, Indonesia, March 8th-10th, 2012.
4. Sangadji, S. & Schlangen, E., *Novel approach to make concrete structures self-healing using porous network concrete*, the 2nd International Conference on Microdurability, Amsterdam, 11 – 13 April 2012.
5. Sangadji, S. & Schlangen, E., *Porous network concrete: novel concept of healable concrete structures*, the 3rd International Conference on Concrete Repair, Rehabilitation and Retrofitting, Cape Town, South Africa, 3 – 5 September 2012, **Best Paper Award**.
6. Sangadji, S. & Schlangen, E., *Development of self-repairing concrete structures by means of porous network*, Intl IABSE Spring Conf, Rotterdam, 6-8 May 2013.
7. Senot Sangadji, Virginie Wiktor, Henk Jonkers, and Erik Schlangen, *Injecting a liquid bacteria-based repair system to make porous network concrete healed*, the 3rd International Conference on Self-Healing Materials, Ghent, 16-20 June 2013
8. Sangadji, S. & Schlangen, E., *Self-Healing of Concrete Structures, Novel Approach Using Porous Network Concrete*, JACT, Journal of Advanced Concrete Technology, Volume 10, (2012), pp. 185-194.
9. Sangadji, S & Schlangen, E, *Zelfreparerend beton met poreus network (in Dutch)*, Cement 2013/4 - IABSE-congres 2013, pp. 54-48. **Translated into Russian**.
10. Sangadji, S & Schlangen, E., *Mimicking Bone Healing Process to Self-Repair Concrete Structure; Novel Approach Using Porous Network Concrete*, Procedia Engineering, Volume 54, 2013., Pages 315–326.
11. Schlangen, E, & Sangadji, S, *Addressing Infrastructure Durability and Sustainability by Self-Healing Mechanisms; Recent Advances in Self-Healing Concrete and Asphalt*, Procedia Engineering, Volume 54, 2013, Pages 39–57.